ROLES OF BNIPXL IN REGULATING CELL GROWTH AND MORPHOLOGY

SOH JIM KIM, UNICE

NATIONAL UNIVERSITY OF SINGAPORE

2005

ROLES OF BNIPXL IN REGULATING CELL GROWTH AND MORPHOLOGY

SOH JIM KIM, UNICE

(B.Sc. Hons.)

A THESIS SUBMITTED
FOR THE DEGREE OF DOCTOR OF PHILOSOPHY
DEPARTMENT OF BIOLOGICAL SCIENCES
NATIONAL UNIVERSITY OF SINGAPORE
2005

Acknowledgments

I would like to express my deepest gratitude and appreciation to my supervisor, Dr. Low Boon Chuan, for his advice, criticisms, encouragement and countless discussions during the course of this dissertation.

My heartfelt thanks to fellow colleagues, Chew Li Li and Zhou Yiting for discussions and generous gifts of reagents. I would also like to extend a special thank you to all current and past members of the Cell Signaling and Developmental Biology Laboratory, for their help and friendship during the course of this work. Namely, Drs. Jan Paul Buschdorf and Liu Lihui; Lua Bee Leng; Zhu Shizhen; Tan Shui Shian; Soh Fu Ling and Zhong Dandan.

My deepest appreciation goes to Sumana Chandramouli for critical proof reading, generous gifts of DNA constructs, discussions and encouragement throughout the course of this work.

I would like to thank Lo Ting Ling and Chow Soah Yee for gifts of human cell lines and yeast strains; Toh Yi Er and Lee Kong Heng for their technical assistance at the confocal microscopy facility; Allan Tan and Liew Chye Fong for expert assistance with DNA sequencing; Lim Yun Ping and Luo Ming for technical assistance with the Vector NTI suite and bioinformatics analysis.

This work would not have been possible without support from the Academic Research Fund and Graduate Research Scholarship from the National University of Singapore.

Finally, I owe my dearest thanks to my parents, for their love, encouragement and kind understanding, always.

Unice Soh
2005

Table of Contents

Title Page	i
Acknowledgements	ii
Table of Contents	iii
Summary	x
List of Figures	xiii
List of Tables	xviii
List of Abbreviations	xix

Chapter 1 Introduction

1.1. The machinery of signal transduction	**1**
1.1.1. Molecular basis of signaling transduction	1
1.1.2. Components and mechanisms of signaling networks	3
1.1.3. Protein domains in signal transduction networks	6
1.2. Signaling networks of small monomeric G proteins	**9**
1.2.1. The Ras superfamily of small G proteins	9
1.2.2. The Rho subfamily of small G proteins	12
1.2.3. Regulators of Rho GTPase signaling	15
1.2.3.1. Rho family Guanine Nucleotide Exchange Factors (RhoGEFs)	15
1.2.3.1.1. Structure of RhoGEFs	16

1.2.3.1.2. Regulation of RhoGEFs 17

1.2.3.1.3. Physiological roles of RhoGEFs 23

1.2.3.2. Rho family GTPase-Activating Proteins (RhoGAPs) 24

1.2.3.2.1. Structure of RhoGAPs 25

1.2.3.2.2. Regulation of RhoGAPs 27

1.2.3.2.3. Roles of RhoGAPs in whole animal physiology 31

1.2.3.3. The Rho Guanine Nucleotide Dissociation Inhibitors (RhoGDIs) 32

1.2.3.3.1. Structural insights of GDI function 33

1.2.3.3.2. Mechanisms of GDI activity 36

1.2.3.4. Intracellular targeting of the Rho family GTPases 37

1.2.4. Structural aspects of Rho GTPase signaling: effector and regulator recognition motifs 38

1.2.4.1. Interaction with RhoGDIs 39

1.2.4.2. Interaction with RhoGEFs 39

1.2.4.3. Interaction with RhoGAPs 41

1.2.4.4. Effector-recognition sites 41

1.2.5. Deregulated Rho GTPase mutants: tools for functional studies 44

1.2.5.1. Constitutively active mutants 44

1.2.5.2. Dominant negative mutants 46

1.2.5.3. Defective effector-binding mutants 46

1.2.6. Functions of the Rho family GTPases 48

1.2.6.1. Reorganization of the actin cytoskeleton 51

1.2.6.1.1. Roles of Rho GTPases in cytoskeleton reorganization 52

1.2.6.1.2. Roles of Rho GTPases in microtubule regulation 59

1.2.6.2. Rho GTPases in cell dynamics and motility 63

1.2.6.2.1. Roles of Rho GTPases in cell migration 63

1.2.6.2.2. Roles of Rho GTPases in phagocytosis 67

1.2.6.3. Rho GTPases in cell proliferation, transformation and cancer development 68

1.2.6.3.1. Cell proliferation and cell cycle progression 68

1.2.6.3.2. Roles of Rho GTPases in gene expression 69

1.2.6.3.3. Role of Rho GTPases in cellular transformation and cancer 70

1.2.6.3.4. Convergence of Rho and Wnt signaling pathways during cancer development 72

1.3. The BNIP-2 and BPGAP protein families 75

1.3.1. The BNIP-2 and Cdc42GAP Homology (BCH) domain 75

1.3.2. Functions and classification of the BNIP-2 family members 75

1.3.3. BNIP-2: the prototypical BCH-domain containing protein 80

1.3.4. BNIP-S: mediator of cell apoptosis 83

1.3.5. BNIP-H: a tissue specific member of the BNIP-2 family 87

1.3.6. BPGAP1: a multi-domain intergrator of of GTPase signalling 88

1.4. Hypothesis and aims of study 93

Chapter 2 Material and Methods **95**

2.1. Bioinformatics analysis 95

2.2. DNA amplification and cloning of BNIPXL 95

2.3. Plasmid DNA isolation, restriction and sequencing analysis 97

2.4. Mammalian cell culture 100

2.5. Total RNA isolation and first strand cDNA synthesis 101

2.6. Semi-quantitative reverse transcription PCR 102

2.7. Mammalian cell transfection, lysis and immunoprecipitation 102

2.8. SDS-polyacrylamide gel electrophoresis and transfer 103

2.9. Western blot analyses 105

2.10. Yeast two-hybrid protein interaction assays 106

2.11. GST-fusion protein production 112

2.12. GST-fusion protein binding assays 112

2.13. *In vitro* direct protein binding assays 113

2.14. *In vitro* Rho activity assays 115

2.15. Confocal immunofluorescence microscopy 115

Chapter 3 Results

3.1. Investigating the roles of the BCH domain in novel proteins **118**

3.1.1. *In silico* identification of a novel BCH-domain containing protein 118

3.1.2. Sequence verification and bioinformatics analysis of BNIPXL 120

3.1.2.1. Genomic organization of BNIPXL 125

3.1.2.2. BNIPXLα and BNIPXLβ are novel members of the BNIP-2 family 125

3.1.2.3. Multiple sequence alignments of BCH domains 129

3.1.2.4. Phylogenetic analyses of the BNIP-2 family 129

3.2 Investigating the biochemical and cellular functions of BNIPXL 133

3.2.1 Expression profile of BNIPXL 133

3.2.1.1. Expression profile of BNIPXL in human tissues and cell lines 133

3.2.1.2. Expression profile of BNIPXL in murine tissues and cell lines 134

3.2.2 Domain architecture of BNIPXL constructs 140

3.2.3. BNIPXL contains a functional protein-protein interaction domain 143

3.2.3.1. BNIPXL isoforms form homophilic complexes via the BCH domain *in vivo* 143

3.2.3.2. BNIPXL associates with BNIP-2 and p50-RhoGAP *in vivo* 147

3.2.3.3. BNIPXL directly associates with its target proteins 147

3.2.4. BNIPXL induces morphological changes in HeLa cells via its BCH domain 150

3.3 Delineating the molecular mechanisms of BNIPXL-induced morphological changes 156

3.3.1 BNIPXL associates with RhoA *in vivo* 156

3.3.2. The BNIPXL BCH domain directly interacts with RhoA 158

3.3.3. Delineating the RhoA-binding region in BNIPXL 158

3.3.4. Domain architecture of BNIPXL deletion constructs 160

3.3.5. A full composite BCH domain is necessary for RhoA association 160

3.3.6. BNIPXL interacts with RhoA *in vitro* in a conformation-dependent manner 166

3.3.7. BNIPXL interacts with dominant negative RhoA *in vivo* 168

3.3.8. BNIPXL interacts with specific constituitive active RhoA mutants *in vivo* 170

3.3.9. BNIPXL reduces active wild-type RhoA and RhoA(F30L) *in vitro* 173

3.4 Investigating the effects of BNIPXL and RhoA *in vivo* 175

3.4.1. Loss of individual motifs within the BCH domain affects cell phenotype 175

3.4.2. BNIPXL potentiates protrusive phenotype during RhoA downregulation but is inhibited by constitutive active RhoA pathway 175

3.4.3. A requirement for active Cdc42/Rac1 signaling pathways in BNIPXL-induced morphological changes 182

Chapter 4 Discussion and Conclusions

4.1. BNIPXL: a novel member of the BNIP-2 family in cell dynamics control 184

4.1.1. Significance of the BNIPXL domain architecture and functional characterization 186

4.2. The role of BNIPXL in Rho GTPase signaling pathways 190

4.2.1. Significance of BNIPXL-RhoA associations 190

4.2.2. BNIPXL-induced cell shape changes require coordinate modulation of Rho GTPase signaling pathways 197

4.3 Implications of BNIPXL-induced cell shape changes and its multi-motif BCH domain 199

4.4. Conclusions and future work 201

Chapter 5 References 207

Appendices

Appendix I Genbank records of BNIPXLα and BNIPXLβ

Appendix II Oligonucleotide sequence of human, mouse and rat specific BNIPXL primer pairs used in RT-PCR

Summary

Cells undergo distinct morphological changes during cellular division, differentiation and migration, elicited mainly by the intricate network of activation and inactivation of Rho family small GTPases which function as molecular switches linking their immediate upstream regulators and downstream effectors. The BCH domain is a novel protein module first identified and characterized in this laboratory. This unique protein domain is about 145 amino acids in length and was initially known to be conserved in two proteins: BCL2/adenovirus E1B 19kDa interacting protein 2 (BNIP-2) and p50-RhoGAP. BNIP-2 is a potent inducer of membrane protrusions and exerts its function as a novel regulator of cell morphogenesis by specifically targeting Cdc42, a member of Rho GTPases via its BCH domain. In addition, it can form homo- and heterophilic complexes with itself or others via this domain.

To elucidate the functional significance of such a domain, we have identified and cloned the novel BCH-domain containing BNIPXL (for BNIP-2 Extra-Long) cDNAs from the human brain and kidney libraries. BNIPXL encompasses most of the prototypic BNIP-2 sequence at its distal carboxyl terminus with ~65% amino acid identity to the BCH domain of BNIP-2. BNIPXL exists as two alternatively spliced isoforms: BNIPXLα and BNIPXLβ. BNIPXLα is 769 amino-acid residues in length and is encoded by a 13-exon gene mapped to the human chromosome 9q21.2. Exon skipping results in the removal of exons 11 and 12 and introduces a premature stop codon in BNIPXLβ. This corresponds to a deletion of the last 36 amino acids of its BCH domain. Both isoforms are ubiquitously

expressed in most human tissues and cell lines examined, except for the HEK293T embryonic kidney epithelial cells which showed exclusive expression of the β-isoform. Interestingly, the expression profile of murine BNIPXL closely resembles that of BNIP-H/Caytaxin, whose loss-of-function is responsible for Cayman ataxia, a form of neurological disorder. Through the BCH domain, BNIPXL associates with itself and other BCH-domain containing proteins. However, unlike BNIP-2, the BCH domain of BNIPXL associates specifically with RhoA but not Cdc42 or Rac1. This is similar to that of BNIP-Sα, another BCH-domain containing homolog which targets RhoA for its activation in cell rounding during apoptosis.

Intriguingly, immunofluorescence microscopy indicates that the BNIPXL BCH domain is sufficient to elicit filopodia-like protrusions that is potentiated only by co-expression of the dominant negative RhoA(T19N), but inhibited by co-expression of the PAK-CRIB domain which sequesters endogenous active Cdc42. This indicates that BNIPXL promotes cell protrusions that involve inactivation of the RhoA pathway concomitant with the activation of the Cdc42/Rac pathways. Removal of the proximal region of the its BCH domain (residues 615-644), which resembles the Class I Rho-binding motifs (found in the RhoA effectors PKN, rhophilin and rhotekin) and other neighboring regions abolished both RhoA binding and cell protrusions. This suggests that, unlike BNIP-S, a full composite of the BCH domain, probably in a conformation-dependent manner, is required for both RhoA binding and cell morphological changes. These results suggest that the unique structural motifs in the BNIPXL BCH domain target different small GTPases to confer distinct mechanisms in cell morphogenesis.

Our present study indicates that BNIPXL functions differently from BNIP-2 and BNIP-S in mediating cell shape changes by directly promoting RhoA inactivation via its direct binding with the BCH domain while it indirectly activates Cdc42/Rac effector pathways necessary for the membrane protrusions. These findings highlight the plasticity of the BCH domain amidst increasing evidence supporting an emerging notion that the BCH domain is an important signaling module integrating diverse small GTPase pathways into coherent cellular responses.

List of Figures

Figure 1.1	The molecular basis of signal transduction	2
Figure 1.2	Cell signaling at the plasma membrane	5
Figure 1.3	Extensive cross-talk occurs between different signaling pathways	7
Figure 1.4	Dendrogram of the small G protein superfamily	10
Figure 1.5	The small G proteins have conserved structural folding	11
Figure 1.6	Rho GTPases are molecular switches	13
Figure 1.7	Ribbon plot of the DH domain	18
Figure 1.8	Coordinate regulation of Ras and Rac1 by Sos1	21
Figure 1.9	A model for Gα-mediated RhoA activation	22
Figure 1.10	Domain distribution of the RhoGAP family	28
Figure 1.11	Models for RhoGAP regulation	30
Figure 1.12	Domain layout of the RhoGDI family	34
Figure 1.13	Ribbon plots of GDP- and GTP-γS-bound RhoA	40
Figure 1.14	Structural motifs and intermolecular contact sites of RhoA	43
Figure 1.15	Strategies for dissecting Rho GTPase function	45
Figure 1.16	Schematic diagram of RhoA mutants and their effects	47
Figure 1.17	Rho GTPases participate in diverse cellular events downstream of receptor activation	49
Figure 1.18	Rho GTPase effector pathways	50
Figure 1.19a	Different actin filaments are generated by the activities of actin-binding proteins	53
Figure 1.19b	Rho GTPases regulate the induction of distinct actin structures	54
Figure 1.20	Rho GTPase effector pathways in actin cytoskeleton	55

remodelling
Figure 1.21 Rho GTPases signaling networks regulate microtubule organization 61
Figure 1.22 Cell migration requires the concerted efforts of Rho GTPases 64
Figure 1.23 Rho GTPases modulate different aspects necessary for cell motility 66
Figure 1.24 Convergence of Rho and Wnt signaling pathways 74
Figure 1.25 Domain organization of the prototypic BCH-domain containing proteins BNIP-2 and p50-RhoGAP 76
Figure 1.26 Classification of BCH domain-containing proteins 79
Figure 1.27 BNIP-2 modulates the Cdc42 signaling pathway via multiple motifs within its BCH domain 82
Figure 1.28 BNIP-S isoforms exert different cellular effects 84
Figure 1.29 BNIP-Sα exerts its pro-apoptotic effects via its intact BCH domain 86
Figure 1.30 BPGAP1 induces distinct pseudopodia via its BCH and GAP domains 90
Figure 1.31 Proposed model of BPGAP1 as a multi-domain integrator of Rho GTPase signaling 91
Figure 2.1 Schematic diagram of the pXJ40 vector map 98
Figure 2.2 The principles of immunoprecipitation 104
Figure 2.3 The modular nature of the yeast GAL4 transcription factor 109
Figure 2.4 Schematic diagram of the yeast-two hybrid protein interaction assay 111
Figure 2.5 Schematic diagram of a GST-fusion protein binding assay 114
Figure 2.6 Multi-color detection of cellular proteins using immuno-fluorescence confocal microscopy 117
Figure 3.1 Cloning of full-length human BNIPXL 119
Figure 3.2 Nucleotide and deduced amino acid sequence of human 121

BNIPXL
Figure 3.3 Genomic organization of human BNIPXL gene 126
Figure 3.4 The shorter BNIPXLβ isoforms is generated during exon skipping 127
Figure 3.5 Pairwise alignments of BNIP-XL with BNIP-2 and BNIP-H 131
Figure 3.6a Multiple sequence alignments of the BCH domains from the BNIP-2 family 132
Figure 3.6b Average distance trees showing phylogenetic relationships of the BNIP-2 family members 132
Figure 3.7 The expression profile of BNIPXL cDNAs in human tissues and cell lines 135
Figure 3.8 The expression profile of BNIPXLcDNAs in murine and rat tissues and cell lines 136
Figure 3.9 Pairwise alignments between BNIPXL, BMCC1 and KIAA0367 139
Figure 3.10 Schematic diagram of primers for diagnostic RT-PCR 141
Figure 3.11 Schematic diagram of BNIPXL fragments used in protein interaction studies. 142
Figure 3.12 Expression profiles of epitope-tagged BNIPXL expression constructs in mammalian cells 144
Figure 3.13 Co-immunoprecipitation of BNIPXLα with different BNIPXLα constructs 145
Figure 3.14 Co-immunoprecipitation of BNIPXLβ with different BNIPXLβ constructs 146
Figure 3.15 Co-immunoprecipitation of BNIP-2 with different BNIPXLα and BNIPXLβ constructs 148
Figure 3.16 Co-immunoprecipitation of p50-RhoGAP with different BNIPXLα and BNIPXLβ constructs 149
Figure 3.17 *In vivo* protein-protein interaction assay using yeast-two hybrid system 152

Figure 3.18	Confocal fluorescence microscopy of HeLa cells expressing BNIPXL constructs	153
Figure 3.19	Co-**i**mmunoprecipitation of BNIPXL with Rho GTPases	157
Figure 3.20	BNIPXL directly interacts with RhoA *in vitro*	159
Figure 3.21	Multiple sequence alignments of BNIPXL, BNIP-S and the Rho-binding motifs from the Class I Rho effectors	161
Figure 3.22	Secondary structure prediction of the BNIPXLβ BCH domain	162
Figure 3.23	Schematic diagram of BNIPXL deletion constructs	163
Figure 3.24	The full composite BCH domain is required for RhoA binding	164
Figure 3.25	BNIPXL deletion mutants are structurally intact	165
Figure 3.26	*In vitro* GTPase binding assays using GDP- and GTPγS loaded GST-RhoA	167
Figure 3.27	BNIPXL interacts with dominant negative RhoA(T19N) but not with constitutive active RhoA(G14V) *in vivo*	169
Figure 3.28	BNIPXL, interacts specifically with the RhoA(F30L) fast cycling mutant	171
Figure 3.29	The CBCH fragment of BNIPXL is responsible for RhoA interactions observed with full-length BNIPXL *in vivo*	172
Figure 3.30	BNIPXL reduces active wild-type RhoA and RhoA(F30L) levels *in vitro*	174
Figure 3.31	Confocal fluorescence microscopy of HeLa cells expressing wild-type and BNIPXL deletion mutants	176
Figure 3.32	Confocal fluorescence microscopy of MCF-7 cells co-expressing wild-type BNIPXL and RhoA mutants	178
Figure 3.33	Confocal fluorescence microscopy of MCF-7 cells expressing wild-type RhoA and mutants alone	181
Figure 3.34	Confocal fluorescence microscopy of MCF-7 cells expressing wild-type BNIPXL and the PAK-CRIB domain	183
Figure 4.1	Model for the effects of BNIPXL on cell shape	198

determination

Figure 4.2 Perspectives of future work and the potential roles of BNIPXL in cell dynamics control, physiology and development 206

List of Tables

Table 1	Combinations of Dropout (DO) supplements	108
Table 2	List of nucleotide polymorphisms between BNIPXL and the KIAA0367 gene	124
Table 3	Pairwise global alignments of full-length BNIP-2 family members	128
Table 4	Pairwise global alignments of the BCH domain of the BNIP-2 family members	130
Table 5	Tabulated results of *in vivo* protein-protein interaction assays using the yeast-two hybrid system	151

List of Abbreviatons

Chemicals and reagents

APS	Ammonium persulphate
$CaCl_2$	Calcium chloride
D-MEM	Dulbecco's modified Eagle's medium
DMSO	Dimethyl sulfoxide
dNTP	Deoxynucleoside triphosphate
DO	Dropout
DTT	Dithiothreitol
EDTA	Ethylenediaminetetraacetic acid
EGTA	Ethylene glycol-bis(baminoethylether)-*N*,*N*,*N*9,*N*9-tetraacetic acid
ETOH	Absolute ethanol
FCS	Bovine fetal calf serum
FDB	Fluorescence dilution buffer
FITC	Fluorescein isothiocyanate-conjugated
GDP	Guanosine 5'-diphosphate
GST	Glutathione S-transferase
GTP	Guanosine 5'-triphosphate
GTPγS	Guanosine 5'-O-3-thiotriphosphate
HEPES	*N*-2-hydroxyethylpiperazine-*N*9-2-ethanesulfonic acid
His	Histidine

LB	Luria bertani
Leu	Leucine
LiAc	Lithium acetate
Mg_2SO_4	Magnesium sulphate
$MgCl_2$	Magnesium chloride
$MgSO_4$	Magnesium sulphate
Na_2HPO_4	Disodium hydrogen phosphate
NaCl	Sodium chloride
NADPH	Nicotinamide adenine dinucleotide phosphate, reduced form
NaH_2PO_4,	Sodium dihydrogen phosphate
NEAA	Non-essential amino acids
NGF	Nerve growth factor
PBS	Phosphate-buffered saline
PEG	Polyethylene glycol
SD	Synthetic dropout
SDS	Sodium dodecylsulphate
TAE	Tris acetate EDTA
TEMED	N,N,N,N -tetramethyl-ethylenediamine
Tris	Tris(hydroymethyl)-aminomethane
TRITC	Tetramethylrhodamine isothiocyanate
Trp	Tryptophan
X-gal	5-bromo-4-chloro-3-indolyl-β-D-galactopyranoside

Units and Measurements

μM	micromoles per litre
bp	base pairs
g	grams
hr	hour
kbp	kilo base pair(s)
kDa	kilodalton(s)
M	moles per litre
mA	milliampere
min	minute
ml	millilitre
mM	millimoles per litre
nt	nucleotide(s)
O.D.	optical density
^{o}C	degree Celsius
rpm	revolutions per minute
UV	ultraviolet

Others

ABPs	Actin-binding proteins
ABR	Active BCR related
ACK	Cdc42-associated kinase

AD	Activation domain
AMV	Avian myeloblastosis virus
APC	Adenomatous polyposis coli
aPKC	atypical Protein kinase C
Arf	ADP-ribosylation factor
Arp2/3	Actin-related proteins 2 and 3
Asef	APC-stimulated guanine nucleotide exchange factor
BCH	BNIP-2 and Cdc42GAP homology
Bcl-2	B-cell CLL/lymphoma 2
BCR	Breakpoint cluster region
BH	Breakpoint cluster region homology
BMCC1	BCH motif-containing molecule at the carboxyl terminal region 1
BNIP-2	BCL2/adenovirus E1B 19kDa interacting protein 2
BNIP-H	BNIP-2-Homology
BNIP-S	BNIP-2-Similar
BNIPXL	BNIP-2-Extra long
BPGAP1	BCH domain-containing, Proline-rich and Cdc42GAP-like protein subtype-1
cAMP	cyclic adenosine monophosphate
CDART	Conserved Domain Architecture Retrieval Tool
Cdc42	Cell division cycle 42
CDKs	Cyclin-dependent kinases
cDNA	Complementary deoxyribonucleic acid

CE	Convergence and extension
CKIs	Cyclin-dependent kinase inhibitors
CLASPs	CLIP-115 and CLIP-170-associating proteins
CLIP	Corticotropin-like intermediate-lobe peptide
CMV	Cytomegalovirus
Dbl	Diffuse B-cell lymphoma
Dbs	Dbl's big sister
DH	Dbl homology
DNA	Deoxyribonucleic acid
DNA-BD	DNA-binding domain
Duo	Huntingtin-associated protein-interacting protein
Dvl	Dishevelled
ECM	Extracellular matrix
ER	Endoplasmic recticulum
ERM	Ezrin-radixin-moesin
EST	Expressed sequence tag
et al.	*et alter* (and others)
FAK	Focal adhesion kinase
FGFR	Fibroblast growth factor receptor
Fz	Frizzled
GAPDH	Glyceraldehyde-3-phosphate dehydrogenase
GAPs	GTPase activating proteins
GBD	GTPase-binding domain

GBDs	GTPase-binding domains
GDIs	Guanine nucleotide dissociation inhibitors
GEFs	Guanine nucleotide exchange factors
GFER	Augmenter of liver regeneration
GIT1	GRK Interactor I
Glu-MT	Glu-tubulin
GPCRs	G-protein coupled receptors
GSK-3β	Glycogen synthase kinase-3β
GTP	Guanosine triphosphate
GTPases	Guanosine triphosphatases
JNK	Jun N-terminal kinase
LARG	Leukemia-associated Rho GEF
Lbc	Lymphoid blast crisis
LIM	Lin11, Isl1 and Mec3
MALDI/IMS/TOF	Matrix-assisted laser desertion/Ionization mass spectrometry/Time of flight
MAP	Mitogen-activated protein
MAPs	Microtubule-associated proteins
MBS	Myosin Binding Subunit
mDia	Mammalian diaphanous
MIF	Macrophage migration Inhibitory Factor
Miro	Mitochondrial rho
MLCK	Myosin light chain kinase

MLCP	Myosin light chain phosphatase
MLKs	Mixed lineage kinases
MT	Microtubule
MTOC	Microtubule organizing center
NBL	Neuroblastoma
NF-1	Neurofibromatosis type 1
NF-κB	Nuclear factor-κB
N-WASP	Neuronal Wiskott-Aldrich syndrome protein
PAK	p21-activated kinase
PCR	Polymerase chain reaction
PDGF	Platelet-derived growth factor
PH	Pleckstrin homology
PI3K	Phosphatidylinositol 3-kinase
PIP5K	Phosphoinositol-4-phosphate 5 kinase
PIPs	Phosphoinositides
PIX	PAK-Interactive exchange factor
PKN	Protein kinase N
Rac	Ras-related C3 Botulinum toxin substrate
Ras	Retrovirus associated sequence
Rb	Retinoblastoma tumor suppressor
RBD	Rho binding domain
RBR	Rho binding region
RGS	Regulator of G protein Signaling

Rho	Ras homologous member A
Rif	Rho in filopodia
RNA	Ribonucleic acid
ROCK	Rho kinase
ROS	Reactive oxygen species
RTKs	Receptor tyrosine kinases
SH2	Src-homology 2
SH3	Src-homology 3
SMART	Simple Modular Architecture Research Tool
Sos1	Son of Sevenless 1
SPEC	Small protein effector of Cdc42
SRE	Serum response element
SRF	Serum response factor
TCF	T-cell factor
TCL	TC10-Like
TGF	Transforming growth factor
Tiam1	T-cell lymphoma invasion and metastasis 1
TTF/RhoH	Translocated three four
UAS	Upstream activating sequences
UTR	Untranslated region
WAVE	WASP-like Verprolin-homologous protein
WCL	Whole cell lysates
Wrch	Wnt-1 responsive Cdc42 homolog

Introduction

1. Introduction

1.1. The machinery of signal transduction

1.1.1. Molecular basis of signal transduction

Signal transduction is the transmission of extracellular signals via a network of intracellular protein cascades and allows the cell to elicit a specific response necessary for adaptation to changing physiological conditions. Cells respond to a diverse range of external stimuli such as light, hormones, neurotransmitters, growth factors and cytokines. This process is initiated when a signaling molecule or ligand is recognized by its cognate membrane-bound receptor which triggers a series of consecutive events that serve to amplify the initial signal within the cell interior. A subset of these signals is transmitted into the nucleus which results in changes in gene expression while others direct biochemical modifications of cytosolic proteins, formation of subcellular ternary signaling complexes or cytoskeletal rearrangements (**Figure 1.1**).

Signals can be propagated via multiple signaling pathways within the cytosol and beyond. While some are direct, others follow more complex routes which provide greater opportunities for cross-talk, diversification and modulation of the cellular response via a whole plethora of second messengers, accessory proteins and lipid complexes. This scheme allows for selective activation of several pathways downstream of receptor activation in both quantitative and qualitative terms. Furthermore, simultaneous activation of various linear pathways may result in the formation of molecular complexes comprising distinct combinations of proteins and/or lipids adding to signaling complexity and plasticity. Conversely, a single signaling complex may coordinate several diverse biochemical activities simultaneously. Such scaffold proteins are essential for recruitment

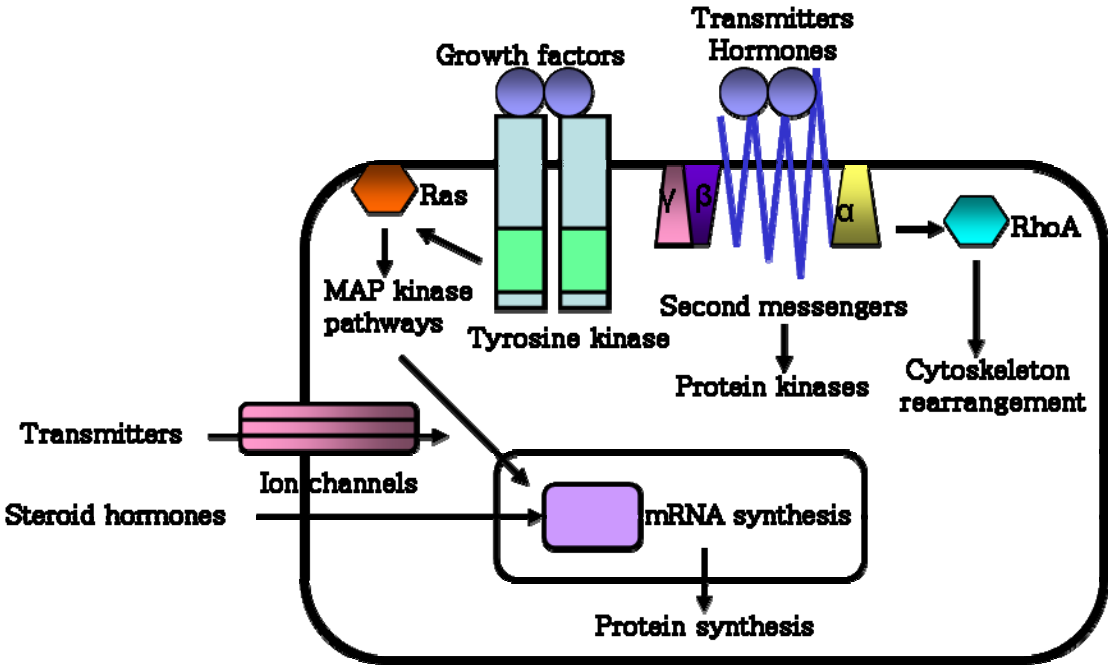

Figure 1.1. Signaling molecules can transmit signals to cells in a variety of ways. Growth factor receptors have tyrosine kinase activities whilst hormones interact with GPCRs to increase second messenger levels that serve to propagate the signals further. Cytosolic steroid hormone receptors translocate into the nucleus upon activation to direct gene transcription. Neurotransmitters bind to receptors that function as ion channels and may also direct second messenger production via GPCR coupling. Ras and Rho are small, monomeric G proteins that couple RTK and GPCR activation to cell growth and cell dynamics control. More detailed description on the involvement of Rho GTPases is given under **section 1.26, Figure 1.18**.

of a diverse repertoire of proteins allowing greater signaling specificity possibly, in a spatio-temporal manner. Taken together, these concerted events help mediate a coherent cell response in the face of multiple synergistic and/or antagonistic stimuli (reviewed in Pawson and Saxton, 1999).

1.1.2. Components and mechanisms of signaling networks

There are generally two types of signals: hydrophobic compounds like steroid hormones and metabolites that pass through the plasma membrane by diffusion or through specific membrane channels and hydrophilic molecules such as growth factors and hormones that cannot pass through the membrane, but instead bind to membrane receptors to activate signal transduction. Thus, the induction of a cellular response is dependent on ligand recognition by its cognate membrane bound receptors in target cells thereby defining downstream intracellular events in a cell-type specific manner.

There are several receptor families classified based on their structure and biochemical activities. Amongst them are the receptor tyrosine kinases (RTKs), the seven transmembrane G-protein coupled receptors (GPCRs) and the multi-chain cytokine receptors (reviewed in Hunter, 2000). Although varied in structure and function, all receptors operate via fundamentally similar mechanisms. Generally, receptor activation results in the generation of a variety of second messengers and effector proteins which serve to propagate and amplify the initial signal, causing changes in biochemical activities within the cell. At the core of these events, distinctive mechanisms provide coordinated response. The Ras superfamily of small, monomeric G proteins represents a point of convergence coupling RTK and GPCRs to a variety of cellular events like cell growth, cell

dynamics control, endocytosis and vesicular trafficking. Detailed description on the involvement of Rho GTPases is given under **section 1.26, Figure 1.18**.

The transmembrane segments of RTKs contain intrinsic protein kinase activity which participates in receptor autophophorylation thereby creating docking sites for downstream signaling molecules and the trans-activation of intracellular substrates (**Figure 1.2**). RTKs work in concert with adaptor proteins which participate in the recruitment of protein complexes required for specific pathways (reviewed in Pawson and Scott, 1997). Further information on their mode of action is discussed in **section 1.1.3**. Ligand stimulation results in RTK dimerization and activation, leading to phosphorylation of protein components in distinct mitogen-activated protein (MAP) kinase pathways leading to modulations in gene expression, cell proliferation, differentiation and survival (Furnari *et al*., 1998).

GPCRs function as guanine nucleotide exchange factors (GEFs) that coordinate ligand stimulation at the membrane with intracellular activation of heterotrimeric G-proteins (reviewed in Cabrera-Vera *et al*., 2003). Ligand binding results in conformational changes that promote GPCR-mediated GDP to GTP exchange on the G-protein α subunit. The subsequent dissociation of the Gα/Gβγ complex results in signal propagation through various downstream effectors and secondary messengers such as cyclic adenosine monophosphate (cAMP) and Ca^{2+} (**Figure 1.2**). There is also increasing evidence for extensive cross-talk between the different signaling pathways. For example, GPCR signaling has been linked to activation of the Ras superfamily of small GTPases (Sah *et al*., 2000; Marinissen and Gutkind, 2001). This may be via the classical second messenger-dependent protein kinases (reviewed in Takai *et al*., 2001) or through the transactivation

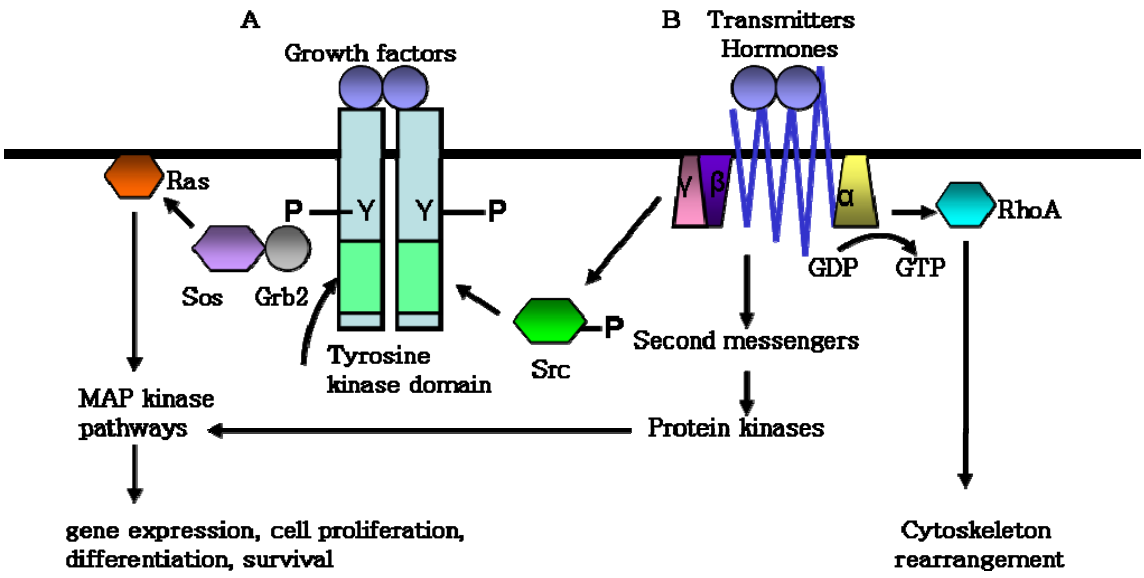

Figure 1.2. Schematic diagrams of cell signaling at the plasma membrane. (a) Ligand binding results in receptor dimerization and autophophorylation on tyrosine residues within the intracellular kinase domain which in turn phosphorylates cytosolic adaptors to turn on several MAPK phosphorylation cascades downstream. (b) Ligand binding to GPCRs result in the dissociation of the Gα subunit from the Gβγ subunits of the heterotrimeric G-protein complex enabling it to function as a molecular switch binding to effector proteins in a nucleotide dependent manner.

of receptor and non-receptor tyrosine kinases (Luttrell, 2002). Furthermore, GPCRs can influence actin cytoskeleton reorganization by mediating Rho activation through the $G\alpha_{q/11}$ and $G\alpha_{12/13}$ families of heterotrimeric G-proteins (**Figure 1.3**). The $G\alpha_{q/11}$ and $G\alpha_{12/13}$ families couple GPCR activation to small monomeric G-proteins via direct interactions with the RhoGEFs, lymphoid blast crisis (Lbc) (Sagi *et al*., 2001) and p115-RhoGEF, respectively. Detailed descriptions of which are provided under **section 1.2.3.1.2, Figure 1.10**. Conversely, the Arf and Rab subfamilies have been implicated in the modulation of GPCR signaling by regulating membrane trafficking events associated with receptor endocytosis and recycling (reviewed in Bhattacharya *et al*., 2004; Moolenaar *et al*., 2004).

1.1.3. Protein domains in signal transduction networks

Ligand stimulation and subsequent activation of membrane bound receptors result in activation of downstream signaling cascades. Signal transduction along these networks is dependent on faithful activation and amplification through post-translational modification, structural and biochemical activation of protein components (Pawson and Nash, 2000). Deregulated signaling could have potentially lethal effects and thus, several checks are in place in the cell to ensure spatial and temporal regulation. Cytosolic proteins are key players which orchestrate diverse cellular events and are thus candidates for regulation. Discrete polypeptide modules within these proteins serve as recognition sites which mediate specific protein–protein and protein–phospholipid interactions through tertiary folds. Signaling complexity is increased through homo- and heterodimerization or cooperation with different protein domains acting *in cis* or *tran*s (reviewed in Pawson *et al*., 2002; Pawson and Nash, 2003). These signaling modules can be subdivided into

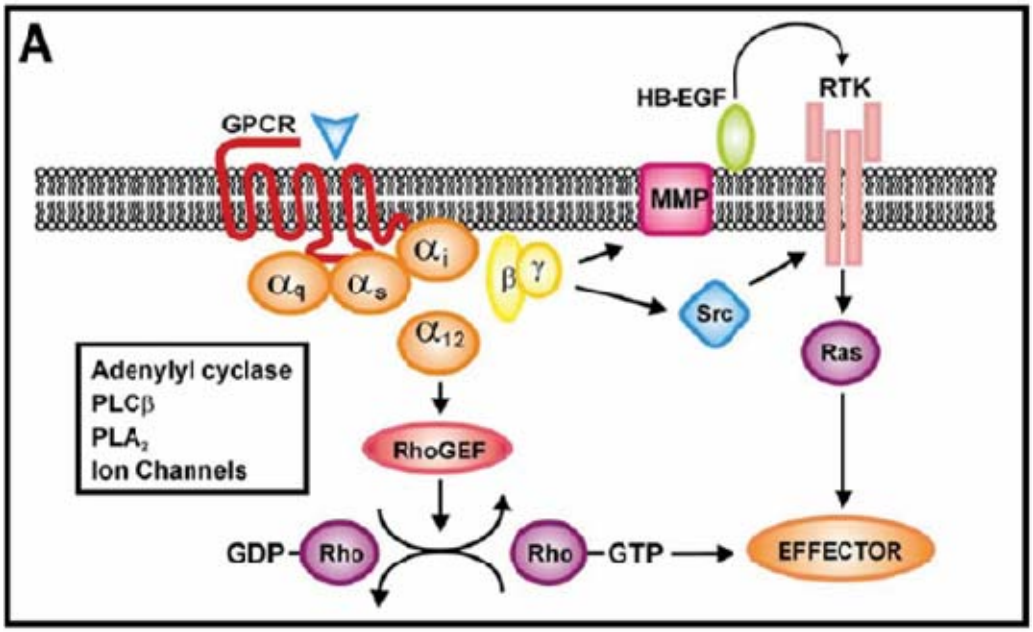

Figure 1.3. Ligand binding to the GPCR promotes GDP to GTP exchange on the G*α* subunit resulting in the dissociation of the G*α*/G*βγ* complex and activation of second messengers. In addition, GPCRs can also signal to Ras and Rho GTPases via G*βγ* and G_{12}/G_{13}, respectively. G*βγ* proteins also stimulate Src-dependent activation of metalloproteinases (MMPs) that release heparin-binding EGF (HB-EGF) for RTK and Ras activation. (Adapted from Bhattacharya *et al*., 2004).

different families based on structure-function relationships in which closely related members may participate in complementary pathways with specific targets. For example, the Src-homology 2 (SH2) domain recognizes phosphorylated tyrosines on their cognate binding partners which effectively limits their participation to RTK signaling (reviewed in Pawson, 2004). Alternatively, protein domains may also direct context-dependent interactions which increase signaling plasticity as in the case of the SH3 domain which directs proline-rich motif-dependent protein-protein interactions and are thus implicated in diverse cellular processes (reviewed in Zarrinpar *et al*., 2003).

Generally, protein domains contain recognition motifs made up of a core group of consensus residues with conserved flanking sequences that aid its function. The presence of multiple recognition motifs in tandem allows protein domains to modulate affinities and response to different targets. In addition, these motifs may bring different proteins together in a scaffold-complex thus exerting spatial control. Post-translational modifications are an integral part of protein-protein interactions. These covalent modifications include prenylation, acetylation, methylation, phosphorylation and ubiquitination. They enhance candidate recognition by protein domains by mediating structural changes that expose the complementary residues or subcellular localization. Furthermore, these modifications are often reversible, allowing temporal control over the signaling. Propagation of intracellular signals is thus the result of multiple sequential steps involving protein modification, recognition and activation. Multiple linear activation events often intersect one another with common components participating in different pathways and providing feedback and crosstalk mechanisms.

1.2 Signaling networks of small monomeric G proteins

1.2.1 The Ras superfamily of small G proteins

The extensive Ras superfamily of guanine nucleotide binding proteins comprises more than 100 individual eukaryotic proteins that are divided into 5 sub-families: Ras, Rho, Rab, Sar1/Arf and Ran (reviewed in Takai *et al*., 2001; Ridley *et al*., 2001; Aspenstrom, 2004) (**Figure 1.4**). Generally, these proteins have molecular masses of 20-40kDa and function as molecular switches cycling between an inactive GDP- and an active GTP-bound state. They posses an intrinsic GTP hydrolyzing activity and are thereby also referred to as GTPases. Structurally, these proteins share ~30% to 50% amino acid identity with conserved regions adopting similar conformations that present the switch I and II regions to different binding partners (**Figure 1.5**). In addition, a subset of the Ras superfamily (Ras, Rho, Rab and Arf) also undergoes post-translational modifications which are crucial for subcellular distribution and function.

Despite their structural and biochemical similarities, these small GTPase orchestrate a diverse range of signaling events. Typically, the Ras subfamily regulates gene expression while the Rho subfamily is involved in actin cytoskeleton organization and gene expression. The Rab and Sar1/Arf subfamilies regulate intracellular vesicle trafficking and the Ran subfamily is involved in nucleocytoplasmic transport crucial for cell cycle progression. These proteins direct different cellular activities through integration of upstream activating signals with the concomitant activation of downstream pathways via complex signaling cascades involving several families of effector proteins.

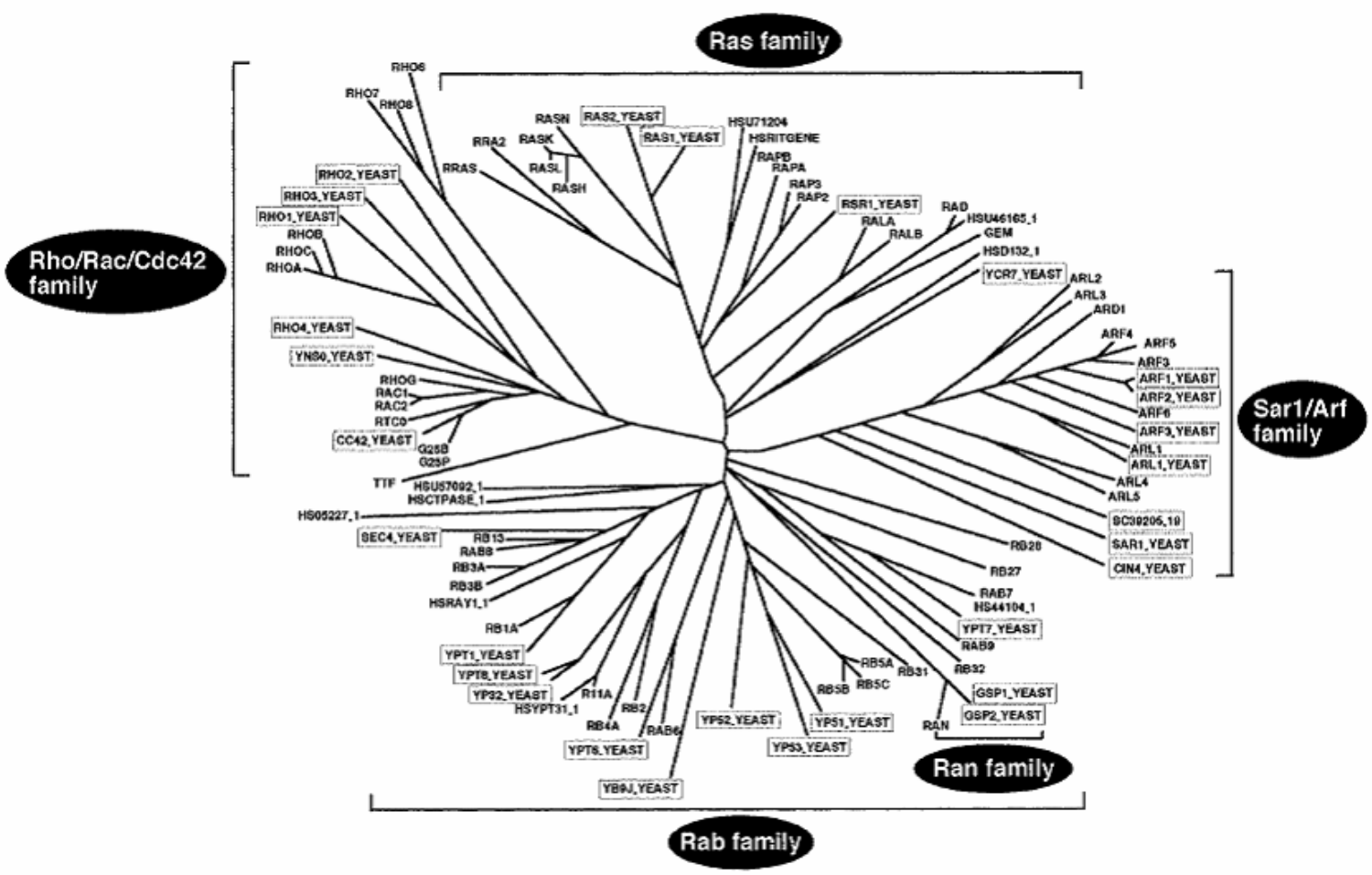

Figure 1.4. Dendrogram of the small G protein superfamily. (Adapted from Takai *et al*., 2001).

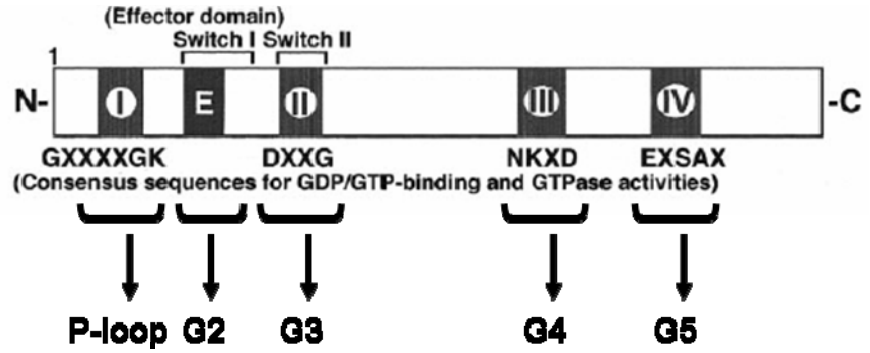

Figure 1.5. Small G proteins are made up of five α-helices and six β-strands joined by five highly conserved polypeptide loops (G1-G5). Consensus sequences indicate conserved regions amongst small G proteins for nucleotide binding, recognition and catalytic activities. The switch I region corresponds to the G2 loop and is the site for effector and GAP binding while switch II is formed by the G3 loop. The G1 or P-loop (phosphate-binding loop) binds to the α- and β-phosphate groups while the G2 (effector) loop provides a conserved Thr residue responsible for Mg^{2+} binding. The G3 loop contains a Gly residue in the DXXG sequence essential for orientation and folding of the switch II region. The consensus motifs in G4 and G5 loops provide residues that participate in nucleotide recognition and association. (Modified from Takai *et al*., 2001; Paduch *et al*., 2001).

1.2.2. The Rho subfamily of small G proteins

First identified as a homolog of the Ras gene in *Aplysia* (Madaule and Axel, 1985), the mammalian Rho family currently consists of 23 members, which can be further subdivided into 8 subgroups: Cdc42 (Cdc42, TC10, TCl, Chp, Wrch1), Rac (Rac1-3, RhoG), Rho (Rho A-C), Rnd (Rnd1-3), RhoD (RhoD and Rif), RhoH/TTF. RhoBTB (RhoBTB1-3) and Miro (Miro1-2) (Aspenstrom, 2004). RhoA, Rac and Cdc42 are the best characterized members and like their counterparts in other subfamilies, these Rho members carry out their physiological functions by cycling between the two interconvertible forms under the influence of three distinct classes of regulatory proteins that provide spatial and temporal regulation of RhoGTPases in a nucleotide-dependent manner (**Figure 1.6**).

The GEFs are positive regulators promoting GDP to GTP exchange. There are two classes of negative regulators: GTPase activating proteins (GAPs), which stimulate intrinsic GTPase activity by catalyzing the hydrolysis of GTP to GDP and guanine nucleotide dissociation inhibitors (GDIs), which prevent nucleotide exchange and sequester Rho from membranes. The GDIs represent a class of regulatory proteins found in the Rho and Rab subfamilies (reviewed in Pfeffer and Aivazian, 2004). While some regulatory proteins are specific for certain members of the Rho subfamily of G proteins, others have a larger substrate repertoire (Settleman *et al*., 1992). Active GTP-bound Rho GTPases adopt complementary conformations that promote effector binding enabling the propagation of signals to downstream signaling pathways. Rho GTPases can activate a common pool of effectors allowing for crosstalks necessary for coordination of signaling events (reviewed in Schwartz, 2004).

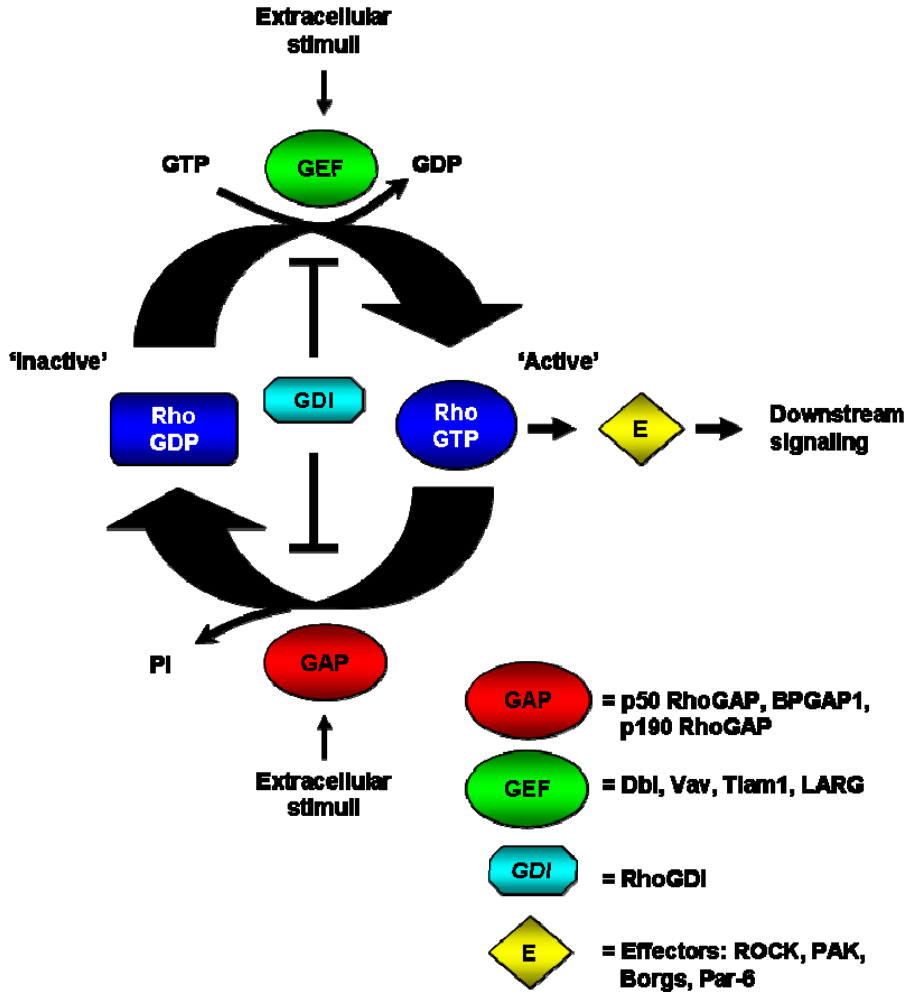

Figure 1.6. Rho GTPases are molecular switches, shuttling between the inactive GDP-bound and the active GTP-bound states. Activation is supported by guanine nucleotide exchange factors (GEFs) which promote GDP to GTP exchange. Downregulation is mediated by the GTPase activating proteins (GAPs) and guanine nucleotide dissociation inhibitors (GDIs). GAPs stimulate intrinsic GTPase activity resulting in hydrolysis of GTP to GDP while GDIs prevent nucleotide exchange and sequester Rho from membranes. Activated GTP-bound Rho binds to effectors (E) which mediate downstream signal propagation. Different Rho GTPases may regulate a common pool of effectors downstream of activating signals. Some examples of the regulators are indicated. (Modified from Karnoub and Der, 2004).

In addition to these classes of regulatory proteins, the subcellular distribution of GTP-binding proteins also determine their functions. Members of the Rho and Rab subfamilies translocate between the cell membrane and the cytosol while Ras proteins are found associated with the cytoplasmic side of the plasma membrane. Generally, these subfamilies undergo posttranslational modifications at their C-terminus CAAX (C, cysteine; A, aliphatic; X, any residue) motifs which facilitate membrane association. In Rho proteins, this involves the addition of geranylgeranyl and methyl moieties. The lipid moieties are expected to interact with the acyl moieties of the membrane phospholipids. In addition, a stretch of polybasic amino acids upstream of the CAAX motif contributes to membrane association by interacting with the polar head groups of the phospholipids. These regions have been classified into four groups: Cys-A-A-X, Cys-A-A-Leu/Phe, Cys-X-Cys and Cys-Cys based on amino acid composition (reviewed in Takai *et al*., 2001).

Recent work however suggests that post-prenylation C-terminus processing of Ras but not Rho proteins is required for membrane localization (Michaelson *et al*., 2005). These reactions are catalyzed by several enzymes including the geranylgeranylytransferases which catalyze the transfer of lipid moieties to the C-terminus CAAX motifs, a prenyl-CAAX-specific protease, Rce1 which mediates the subsequent proteolytic cleavage of the –AAX motif (Boyartchuk *et al*., 1997; Schmidt *et al*., 1998) and isoprenylcysteine-directed carboxyl methyltransferase which adds a methyl group to the cysteine residue (Dai *et al.,*, 1998). Further investigations should provide deeper insights into the roles of posttranslational modifications in Rho GTPase function.

1.2.3. Regulators of Rho GTPase signaling

1.2.3.1. Rho family Guanine Nucleotide Exchange Factors (RhoGEFs)

The prototypic mammalian GEF is the proto-oncogene diffuse B-cell lymphoma (Dbl) that was first isolated in foci formation assays (Eva and Aaronson, 1985). Interestingly, Dbl was found to share significant similarity to CDC24, a RhoGEF with activity toward Cdc42p, the yeast ortholog of Cdc42 (Bender and Pringle, 1989; Ron *et al*., 1991). Further investigations revealed that the conserved region in Dbl was responsible for nucleotide exchange activity on human Cdc42 (Hart *et al*., 1991; Hart *et al*., 1994). Subsequently, an increasing number of Dbl homology (DH) domain-containing proteins were isolated. In addition to the DH domain, these proteins also possessed a pleckstrin homology (PH) domain found in tandem and C-terminal to the DH domain. Generally, the DH/PH domain pair is considered the minimal module for nucleotide exchange activity.

To date, the RhoGEF protein family is estimated to contain forty-six members in eukaryotes sharing low homology limited to the tandem DH/PH domains (Venter *et al*., 2001). Although structurally diverse beyond the DH/PH domains, RhoGEFs have similar activities toward Rho GTPases. Biochemically, GEFs bind to the GDP-bound small GTPase destabilizing it in favor of a nucleotide-free reaction intermediate (Cherfils and Chardin, 1999). The released GDP is subsequently replaced with GTP due to high intracellular ratio of GTP to GDP. This effectively promotes effector recognition of the active small GTPase (reviewed in Schmidt and Hall, 2002; Rossman *et al*., 2005). Recent work suggests that GEFs may also stimulate GDP dissociation with the formation of a two nucleotide-one G-protein intermediate indicating that GEF activity may occur via

competitive displacement of GDP by GTP through this intermediate (Zhang *et al*., 2005). Mammalian GEFs can be identified by their ability to stimulate nucleotide exchange *in vitro* in GEF activity assays or by examining effects of overexpresion *in vivo*. Interestingly, some GEFs appear specific toward a single GTPase target like the p115RhoGEF for RhoA (Hart *et al*., 1996; Zheng *et al*., 1996) while others like Dbl and Vav1 have promiscuous affinities for multiple Rho proteins (Hart *et al*., 1994; Olson *et, al*., 1996).

More recently, there has been increasing evidence suggesting the existence of non-conventional RhoGEFs that utilize a novel DH-independent domain for catalysis (reviewed in Meller *et al.,* 2005; Rossman *et al.,* 2005). These atypical RhoGEFs are members of the Ced-5, DOCK180, Myoblast city (CDM)-zizimin homology (CZH) protein superfamily that are conserved throughout evolution with representatives from *Saccharomyces cerevisiae*, *Dictyostelium discoideum*, *Caenorhabditis elegans, Drosophila melanogaster, Arabidopsis thaliana* and *Homo sapiens* (Meller *et al*., 2005). CZH proteins share two conserved domains namely, CZH1 and CZH2. To date, the latter is known to confer GEF activity while the role of former remains elusive (Cote and Vuori, 2002; Brugnera *et al*., 2002). CZH proteins can be further classified into the CDM protein and zizimin1 sub-families based on their ability to activate Rac and Cdc42, respectively (Meller *et al*., 2005; Wu and Horvitz, 1998; Cote and Vuori, 2002; Brugnera *et al*., 2002).

1.2.3.1.1. Structure of RhoGEFs

All members of this protein family share a region of similarity spanning ~300 residues. This region can be further classified into two smaller domains, a ~200 residue DH domain and a ~100 residue PH domain. The DH domain contains three conserved

regions (CR1, CR2 and CR3) about ten to thirty residues in length. While the DH domain is specific to members of the RhoGEF family, the PH domain is a general protein domain that binds to phospholipids and is found in other signaling molecules (Rebecchi and Scarlata; 1998; Lemmon and Ferguson, 2000). In addition, RhoGEFs may also contain additional signaling modules like the SH2, SH3, kinase, PDZ RhoGAP, RasGEF and Regulator of G protein signaling (RGS) domains.

Structurally, the DH domain is folded into a flattened, elongated bundle of eleven α-helices (Aghazadeh *et al*., 1998; Liu *et al*., 1998; Soisson *et al*., 1998; Worthylake *et al*., 2000) and forms extensive interactions with the switch regions of Rho GTPases. Switch I interacts with the DH domain via the exposed CR1 and CR3 helices while the Switch II region contacts the CR3 and a C-terminal helix (α6). A conserved glutamate in CR1 and two other residues in CR3 mediate complex formation and nucleotide-exchange potential. Structural elements (β2 and β3 strands) between the switch regions mediate additional contacts with the DH domain that determine specificity for different Rho targets (**Figure 1.7**).

1.2.3.1.2. Regulation of RhoGEFs

Regulation of GEF activity is mediated via different interactions which modulate the conformation of the RhoGEF. Inactive RhoGEFs exist in a conformation in which the DH domain contacts the adjacent PH domain or distal regulatory sequences and blocks GEF activity through intramolecular interactions (Ron *et al*., 1989; Katzav *et al*., 1991; van Leeuwen *et al*., 1995; Bi *et al*., 2001). The PH domain can participate in the GTPase-binding interface and facilitate nucleotide exchange in concert with the DH domain

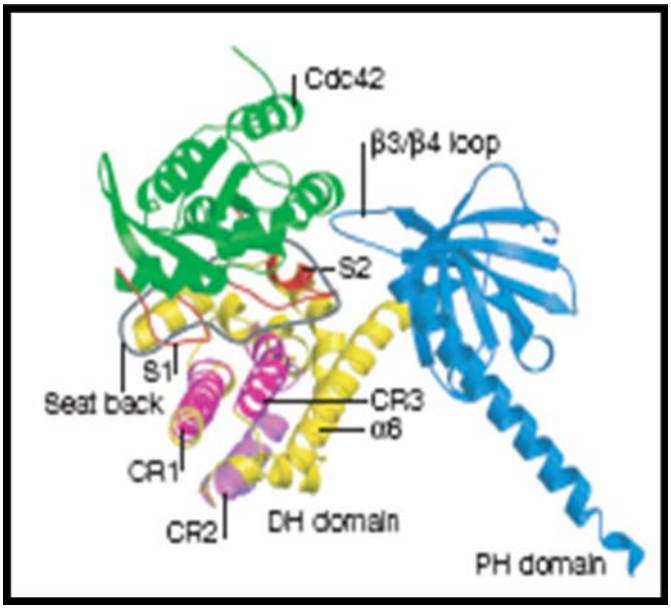

Figure 1.7. Ribbon plot of the DH domain (yellow) and PH domain (blue) of Dbs bound to Cdc42 (green) (available from http://www.rcsb.org/pdb/ under the PDB ID 1KZ7). CR1, CR3 (magenta) and α6 helix of the DH domain are primary contact sites with the switch I and II (S1 and S2, respectively) regions of Cdc42 (red). The β3-β4 loop of the Dbs PH domain makes contacts with switch II of Cdc42, essential for catalysis of nucleotide exchange. The 'seat back' region (grey outline) of the Dbs DH domain forms a complementary interface with β1-β3 strands of Rho GTPases. (Adapted from Rossman *et al*., 2002). PIP_2 to PIP_3 results in exposure of the Rac binding site (Das *et al*., 2000) which is necessary for phosphorylation (Hart *et a*l., 1998).

(Rossman *et al*., 2002). Alternatively, they could help target GEFs to the appropriate intracellular location through associations with phosphoinositides (PIPs) (Rebecchi and Scarlata; 1998; Lemmon and Ferguson, 2000; Bi *et al*., 2001). Recent work indicate that PH domains provide docking sites for proteins associated with a common Rho signaling pathway as seen in the Dbl PH domain with ezrin (Vanni *et al*., 2004). Collectively, these activities suggest that the PH domain plays crucial roles in regulating GEF activity.

In addition, the diversity of domain combinations found in RhoGEFs provides the basis for modulating GEF activity through synergistic activities of different signaling molecules. These include phosphoinositides, protein kinases, heterotrimeric G proteins and small GTPases. In Vav, autoinhibitory constraints imposed by the DH/PH domain can be relieved by activation of phosphatidylinositol 3-kinase (PI3K) and tyrosine phosphorylation (Bustelo, 2000; Crespo *et al*., 1997). The subsequent conversion of PIP_2 to PIP_3 results in exposure of the Rac binding site (Das *et al*., 2000) which is necessary for phosphorylation (Hart *et a*l., 1998).

Members of the RhoGEF family have been known to regulate several small GTPase targets via coordinating GEF activities toward two targets. For example, the RasGEF Son of Sevenless 1 (Sos1) can stimulate guanine nucleotide exchange on Ras and Rho proteins, thus providing a mechanism for sequential activation of GTPase signaling pathways. Investigations reveal that Sos1 stimulates guanine nucleotide exchange on Rac1 in a PI3K-dependent manner. Activation of PI3K is associated with upstream activation of Ras which is mediated through Sos1 (Nimnual *et al*., 1998). Thus, Sos1 utilizes structurally distinct domains to mediate its biochemical activities on Ras and Rac which can be regulated by PIP_3 binding to the PH domain (Das *et al.*, 2000). A schematic diagram

of coordinated regulation of Ras and Rac by Sos1 is illustrated (**Figure 1.8**). Upon ligand binding and receptor activation, Sos1 is recruited to the membrane resulting in Ras activation through the Sos1 RasGRF domain. This in turns activates PI3K which promotes conversion of PIP_2 to PIP_3 through phosphorylation, leading to conformational changes that relieve the Sos1 DH domain from intramolecular interactions, thus promoting guanine nucleotide exchange on Rac.

Regulation of GEF activity by regions other than the conserved DH/PH domains are likely to involve upstream receptors and signaling molecules like the heterotrimeric G proteins which coordinate conversion of extracellular stimuli and intracellular events (Whitehead *et al*., 2001). p115RhoGEF, PDZ-RhoGEF and leukemia-associated Rho GEF (LARG) form a subgroup of RhoGEFs containing the RGS domain which may serve to couple cellular changes accompanying heterotrimeric G protein activation with small GTPase signaling. Almost all RGS domain-containing proteins can function as GAPs for Gα subunits by accelerating GTP hydrolysis on the Gα (Hollinger and Hepler, 2002). p115RhoGEF is a RhoA-specific exchange factor (Hart *et al*., 1996; Kozasa *et al*., 1998) (**Figure 1.9**). Interestingly, the recruitment of $G\alpha_{13}$ but not $G\alpha_{12}$ to the p115RhoGEF RGS domain allows coupling of $G\alpha_{13}$ deactivation with $G\alpha_{13}$-induced RhoA activation, thus allowing tight control of G protein signaling through an in-built feedback mechanism (Hart *et al*., 1998; Mao *et al*., 1998). Recent work indicates distinct residues within the RGS domain may be responsible for the dual activities of $G\alpha_{13}$/p115RhoGEF complex (Grabocka and Wedegaertner, 2005). In addition to temporal regulation of GEF activity, subcellular sequestration of Dbl proteins provide spatial regulation of Rho GTPase activation in response to different stimuli as evidenced by T-cell lymphoma invasion and

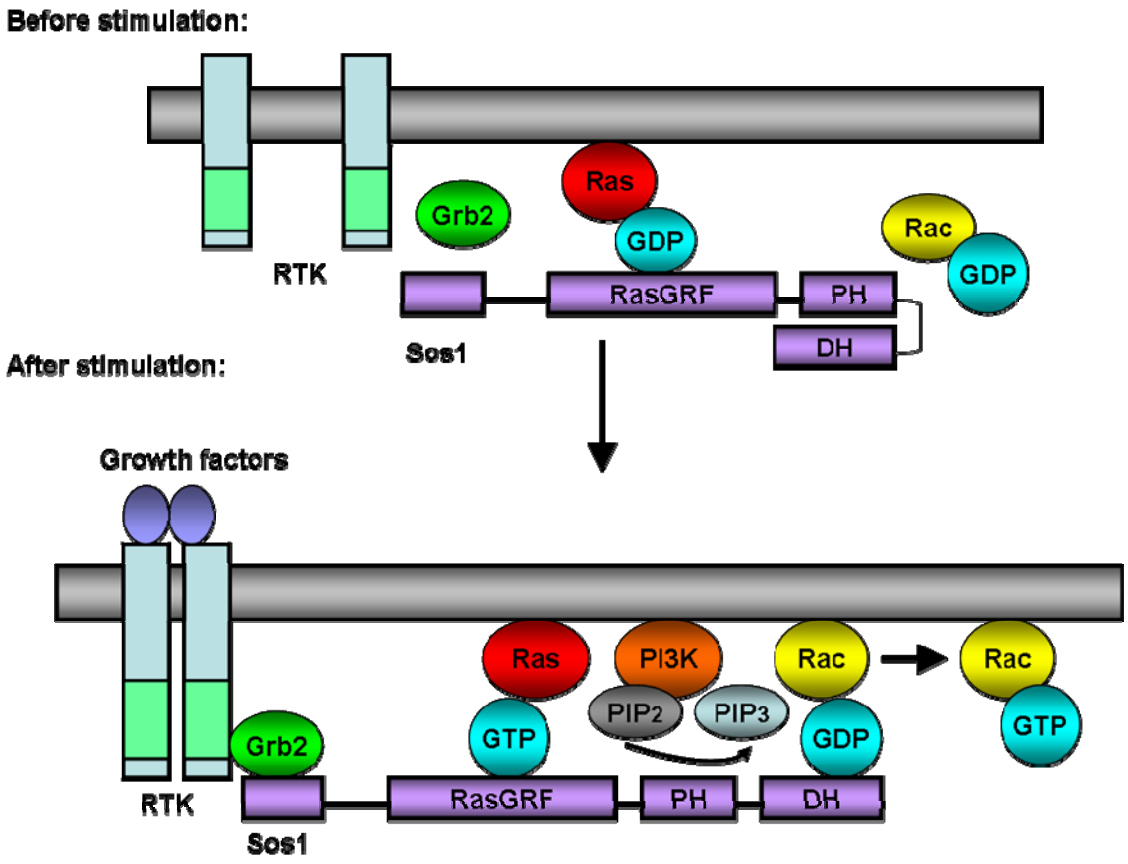

Figure 1.8. Coordinate regulation of Ras and Rac1 by Sos1. Recrutiment of the Grb/Sos1 complex to the membrane following ligand stimulation of RTK results in activation of membrane-bound Ras which in turn interacts with PI3K which converts PH-domain bound PIP_2 to PIP_3. Conformational changes allow Rac1 access to the catalytic DH domain.

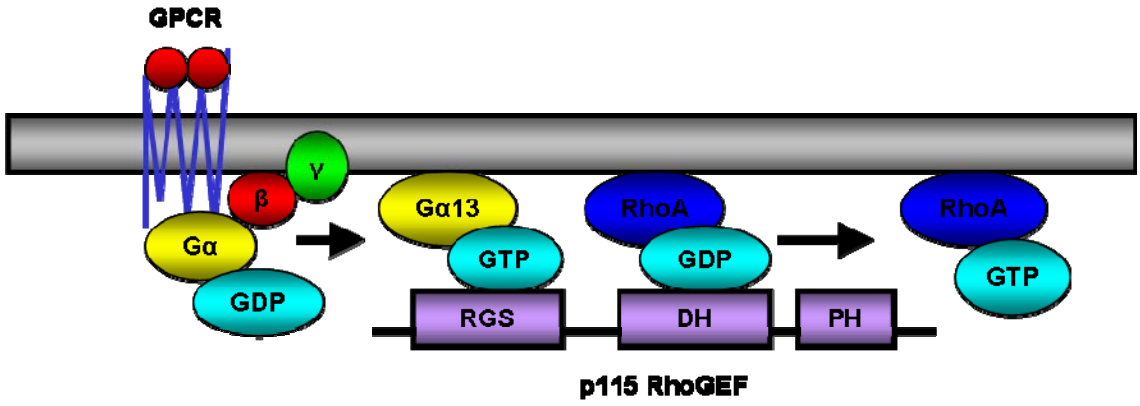

Figure 1.9. A model for Gα-subunit mediated RhoA activation. Ligand binding to the GPCR results in a sequential cascade that activates RhoA through the conversion of Gα-subunit to the GTP-bound state, its dissociation from the Gβγ dimer and binding to the N-terminus RGS domain of p115RhoGEF. Subsequent conformational changes provide the mechanism for coordinate regulation of small GTPase activation via GPCRs.

metastasis 1 (Tiam1)-dependent Rac activation, where redistribution of Tiam1 from the cytoplasm to the membrane follows serum (Michiels *et al*., 1997) or platelet-derived growth factor (PDGF) (Buchanan *et al*., 2000) stimulation.

1.2.3.1.3. Physiological roles of RhoGEFs

GEF participation in diverse physiological processes is associated with actin cytoskeleton remodeling. The ability to influence the guanine nucleotide binding status of small GTPases implicates RhoGEFs in diverse Rho-mediated cellular events including regulation of transcription and cell cycle progression. Interestingly, a recent survey of the human genome indicates that RhoGEFs far exceed the number of Rho GTPases (Venter *et al*., 2001). It is possible that multiple GEFs increases signaling plasticity linking several receptor classes to downstream Rho activation (Bustelo, 2000).

The most well-known RhoGEF function is its role in oncogenic transformation as most GEFs were first identified in NIH3T3 foci formation assays. Overexpression of RhoGEFs result in distinct phenotypes such as anchorage independent cell growth and tumorigenesis in animal models (Whitehead *et al*., 1997; Cerione and Zheng, 1996). The transforming effects of RhoGEFs are mainly attributed to truncation mutants that relieve intramolecular interactions leading to constitutive GEF activity and chronic stimulation of GTPase targets. Several reports confirm the absolute requirement of the DH domain for transformation (Ron *et al*., 1991; Horii *et al*., 1994; Whitehead *et al*., 1995). However, other lines of evidence indicate a requirement for the PH domain for full transforming potential (Hart *et al*., 1994; Whitehead *et al*., 1999; Ron *et al*., 1991). Thus, transformation appears to require concerted coordination of catalytic GEF activity and subcellular

localization conferred by the DH and PH domains, respectively. Many RhoA effector proteins like protein kinase N (PKN) and Rho kinase (ROCK) have been implicated in the propagation of signals for deregulated growth as the GEF mutant phenotypes closely resemble those exhibited by constitutive active GTPase mutants (Marinissen *et al*., 2001; Sahai *et al*., 1999; Tran *et al*., 2000). In addition, mutations and chromosomal rearrangements that affect RhoGEF gene expression have been associated with leukemias and human developmental disorders linking these clinical etiologies to deregulated Rho GTPase signaling.

1.2.3.2. Rho family GTPase-Activating Proteins (RhoGAPs)

The first GAP to be identified was the p50-RhoGAP which was isolated from human spleen extracts and was found to have intrinsic activity toward Rho, Rac and Cdc42 (Garrett *et al*., 1989). Sequence analyses indicate that p50-RhoGAP shares a region of homology with the breakpoint cluster region (BCR) and N-chimaerin which have GAP activity towards Rac1 and Cdc42 (Diekmann *et al.,* 1991). Subsequent investigations determined that the conserved ~140 residue region was responsible for the catalytic activity of these proteins and was designated the RhoGAP domain (Zheng *et al.,* 1993).

Generally, members of the RhoGAP family possess a catalytic RhoGAP domain with at least 20% amino acid identity while retaining the ability to catalyze the conversion of GTP to GDP by stimulating the intrinsic GTPase activity of their cognate targets. To date, the RhoGAP family is estimated to consist of 40 distinct proteins from prokaryotes and eukaryotes. In addition, *in silico* analyses by SMART (Simple Modular Architecture Research Tool) has identified another ~220 potential members in the non-redundant

protein database (Ponting *et al*., 1999). Sequence alignment of the various RhoGAP domains provide insights into the phylogenetic relationships of the different members, suggesting that this domain has undergone frequent duplication with entire genes coding these domains (Peck *et al*., 2002).

Although the RhoGEF and RhoGAP families have essentially antagonistic biochemical functions, several common themes exist between them. It is evident that the number of RhoGEFs and RhoGAPs far outnumber the current 23 members of the Rho GTPase family. The large repertoire of regulatory proteins provides a means for regulating common substrates through substrate specificity in different signaling complexes (Ahmed *et al*., 1990; Ahmed *et al*., 1991; Ahmed *et al*., 1993; McGlade *et al*., 1993); Ren *et al*., 2001; Jenna *et al*., 2002). Conversely, both GEFs and GAPs can show specificity towards multiple targets within a branch of the Ras superfamily providing plasticity to Rho signaling networks. For example, the human active BCR related (ABR) and BCR proteins are known to stimulate GTPase activity of Rac1, Rac2 and Cdc42 but not RhoA (Chuang *et al*., 1995).

1.2.3.2.1. Structure of RhoGAPs

Much of the structural information on RhoGAPs is derived from p50-RhoGAP, the smallest member (499 residues) of the RhoGAP family. This protein contains an N-terminus Sec14-like domain which we previously identified as the BNIP-2 and Cdc42GAP Homology (BCH) domain (Low *et al*., 2000a) and a C-terminus RhoGAP domain which has activity toward RhoA and Cdc42 (Ridley *et al*., 1993; Barfod *et al*., 1993; Lancaster *et al*., 1994). The Sec14 domain is speculated to bind PIP_3 providing a mode of regulation for

GAP activity via recruitment to the plasmas membrane and/or conformational changes (Krugmann *et al*., 2002). Interestingly, recent work implicates the Sec14-like domain of p50-RhoGAP in mediating auto-inhibitory conformations that block access to its catalytic GAP domain which may be relieved by lipid modification of its Rho targets (Moskwa *et al*., 2005).

Sequence analysis of the RhoGAP domain indicates the presence of three blocks of conserved residues (Zheng *et al*., 1993; Mussacchio *et al*., 1996) while crystal structures of the human p50-RhoGAP and p85α subunit of PI3K reveal that RhoGAP domains share similar tertiary folds and GTPase-activating mechanisms with that of RasGAP (Bax, 1998; Rittinger *et al*., 1998) even though their primary sequence may vary. Structural information from GAP domain complexes with RhoA (Rittinger *et al*., 1997b) and Cdc42 (Nassar *et al*., 1998; Rittinger *et* al., 1997a) provide greater insights into the mechanisms underlying RhoGAP-mediated GTP hydrolysis. The RhoGAP domain is composed of 9 α-helices and a highly conserved arginine residue presented in a loop structure (Gamblin and Smerdon, 1998). It interacts with the switch regions and the P-loop of Rho GTPases and participates in GTP hydrolysis by contributing an arginine residue (Arg85) to the active site of the Rho GTPase. During hydrolysis, a glutamine residue (Gln63 in RhoA) positions a water molecule necessary for the reaction. Thus, stabilizing this residue with the GAP domain arginine finger motif restricts the water molecule and reduces energy barrier for GTP hydrolysis (Nassar *et al*., 1998).

Substrate specificity of RhoGAPs is mediated by interactions with residues that lie outside the P-loop and switch regions of Rho GTPases (Li *et al*., 1997; Longenecker *et al.*, 2000; Dvorsky and Ahmadian, 2004). Interestingly, although the RhoGAP domain is

distinguishable from the GAP modules of other GTPase classes (Ras, Ran or ARF), the involvement of multiple residues for RhoGAP specificity prevents clear distinction of structure-function relationships amongst the Rho subfamily members. Consistent with these observations, site-directed mutational analyses indicate that RhoGAP association with their cognate targets is independent of GAP activity thus, providing an additional level of complexity in RhoGAP-mediated regulation (Ahmed *et al*., 1994). The RhoGAP domain of the p85 regulatory subunit of PI3K is one such example, having the ability to associate with Rho GTPases even though it lacks GAP activity (Lamarche and Hall, 1994; Musacchio *et al*., 1996; Barrett *et al*., 1997).

1.2.3.2.2. Regulation of RhoGAPs

Like the RhoGEF family, a number of RhoGAPs have multiple Rho substrates. The multi-domain architecture of many RhoGAPs provides additional regulatory motifs for tight regulation preventing spurious activity of their cellular substrates (reviewed in Bernards, 2003; Bernards and Settleman, 2004) (**Figure 1.10**). These motifs may facilitate RhoGAP recruitment to protein complexes in a spatio-temporal manner (Lamarche and Hall, 1994). For example, RhoA inactivation by the p190A-RhoGAP occurs in a spatio-temporal manner in fibroblasts upon integrin engagement which promotes cell movement (Arthur *et al*., 2000).

Interestingly, a common repertoire of protein or lipid-binding domains directs conformational changes and localization in RhoGEF and RhoGAP proteins. Phosphorylation by protein kinases provides a mode of RhoGAP regulation as evidenced by Src-mediated p190 RhoGAP activity (Roof *et al*., 1998; Hu and Settleman, 1997). Src activation results in phosphorylation of p190RhoGAP. This promotes p120RasGAP

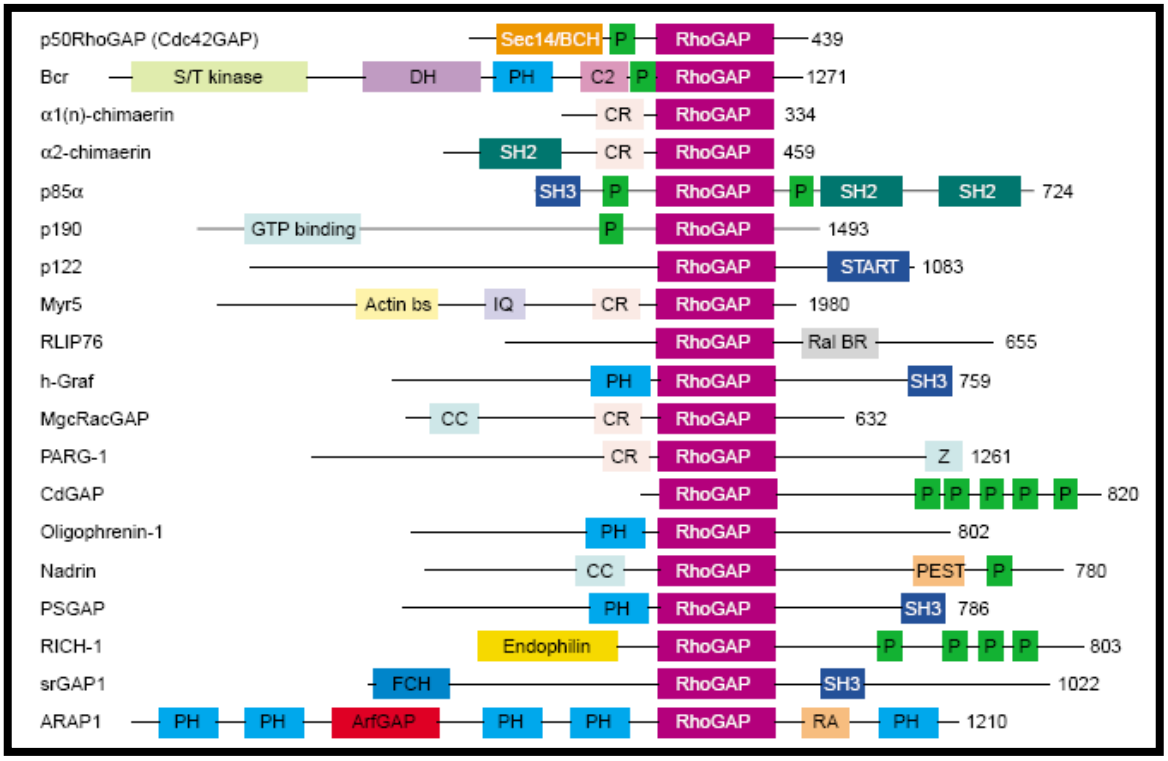

Figure 1.10. Domain distribution of the RhoGAP family. A recent survey of the RhoGAP proteins indicates an increasingly diverse combinations of protein domain(s) exist with the canonical RhoGAP domains. Abbreviations: Actin bs, actin filament binding site; C2, calcium-dependent lipid binding; CC, coiled coil; CR, cysteine rich, zinc butterfly motif, binds diacylglycerol and phorbol ester; DH, Dbl homology; Endophilin, Endophilin homology domain; FCH, Fes/CIP4 homology domain; IQ, calmodulin binding; PH, pleckstrin homology; P, proline-rich SH3 binding motif; PEST, amino acids P-, E-, S- and T-rich degradation motif; RA, Ras-associating (also known as ralGDS/AF-6) domain; Ral BR, Ral GTPase binding region; Rho GAP, Rho GTPase-activating protein motif; Sec14/BCH, Sec14 homology/BNIP2 and Cdc42 GAP homology; SH2, Src homology 2; SH3, Src homology 3; S/T kinase, serine and threonine kinase; START; Star-related lipid transport domain; Z, PDZ binding region. (Adapted from Moon and Zheng, 2003).

recruitment to the p190RhoGAP complex via a SH2 domain-phosphotyrosine interaction leading to subsequent activation of Rho-specific p190RhoGAP activity. In addition, auto-inhibitory intra- or intermolecular interactions is another common mechanism that contributes to GAP regulation as evidenced in p190 RhoGAP and p50-RhoGAP (Tatsis *et al*., 1998; Moskwa *et al*., 2005). A variation of this mechanism is observed in the RacGAP chimaerin, whose activity is regulated by a cysteine-rich CR domain. The CR domain has been speculated to mediate spatial regulation of chimaerin through association with membrane components (Caloca *et al*., 1997). In addition, GEFs can coordinately down-regulate GAPs and promote activation of nucleotide exchange. The scaffold protein intersectin, is a Cdc42-specific GEF that can regulate the RhoGAP activity of CdGAP through SH3 domain interactions with the proline-rich C-terminus of CdGAP. This promotes an unfavorable conformation that reduces its intrinsic RhoGAP activity (Jenna *et al*., 2002). Recruitment of additional factors to this complex mediates concerted regulation of the actin cytoskeleton (O'Bryan *et al*., 2001). Collectively, these observations demonstrate that GAP regulation is mediated by diverse mechanisms orchestrated by the various resident domains acting *in cis*- and *trans* (**Figure 1.11**).

Although RhoGAPs are known to be specific for Rho family GTPases, a subset can interact with targets outside the Rho subfamily. The human IQGAP1 and IQGAP2 interacts with Cdc42 and Rac1 via their RasGAP-related domains resulting in the inhibition of intrinsic and RhoGAP-stimulated GTPase activity (Hart *et al*., 1996; Brill *et al.* 1996). Similarly, the RhoGAP domain of the p85α regulatory subunit of PI3K may structurally resemble the p50-RhoGAP (Musacchio *et al*., 1996) and interact with activated Cdc42 and Rac1 but it does not exhibit any GAP activity towards Rho family members

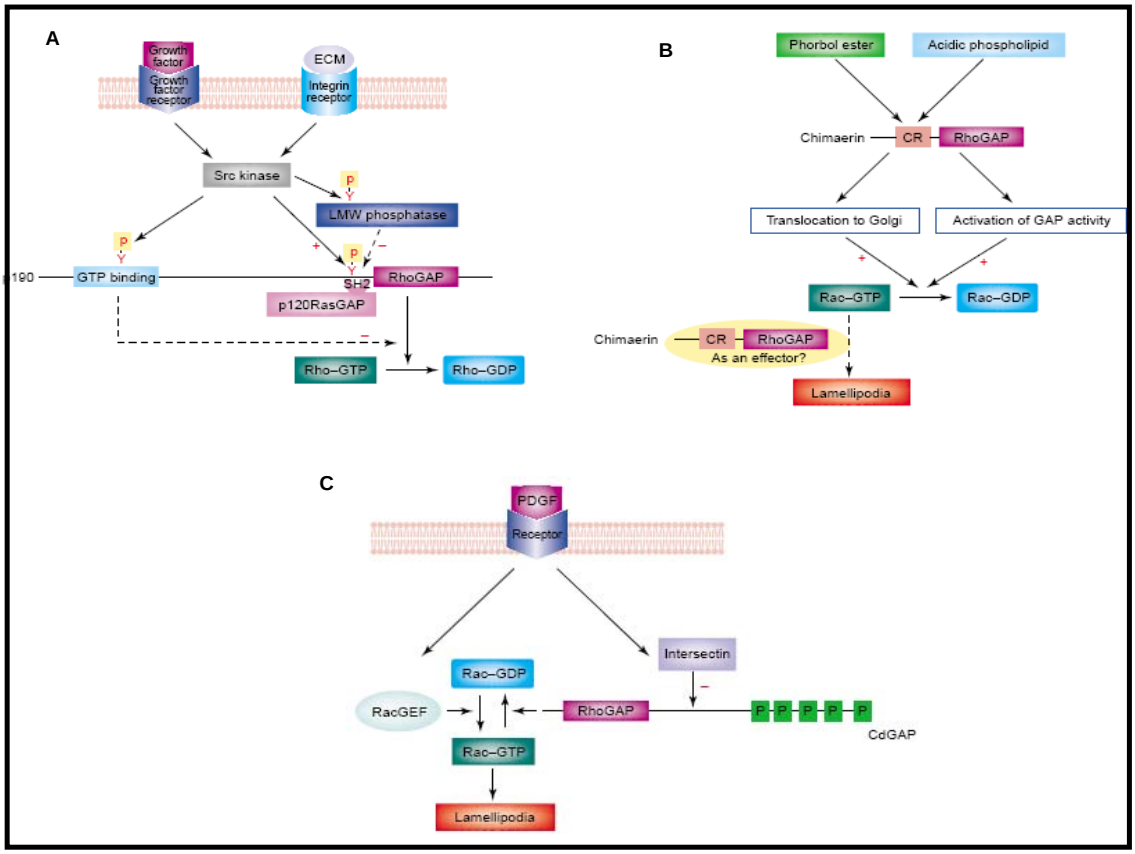

Figure 1.11. Models for RhoGAP regulation. (a) Phosphorylation of p190 RhoGAP by Src family tyrosine kinases downstream of PDGF receptor activation initiates association with p120 RasGAP, membrane translocation and activation of GAP activity. (b) Proposed lipid mediated regulation of n-chimaerin. (c) Regulation of CdGAP via protein complex formation with intersectin. (Adapted from Moon and Zheng, 2003).

(Zheng *et al*., 1994). Recently, our group identified that the BCL2/adenovirus E1B 19kDa interacting protein 2 (BNIP-2) can function as a non-canonical RhoGAP via its BCH/Sec14-like domain which resembles the noncatalytic domain of p50-RhoGAP (Low *et al*., 2000a, Low *et al*., 2000b). We also showed that the BCH domain of the BCH domain-containing, Proline-rich and Cdc42GAP-like protein subtype-1 (BPGAP1) regulates cell protrusion necessary for migration (Shang *et al*., 2003) and Erk1/2 activation (Lua and Low, 2005b). It remains to be seen how the BCH domain coordinates the activities of the GAP domain.

1.2.3.2.3. Roles of RhoGAPs in whole animal physiology

Insights into the normal *in vivo* functions of RhoGAP domain-containing proteins has been obtained using knockout mouse models of p190A RhoGAP (Billuart *et al*., 2001) and p190B RhoGAP (Sordella *et al*., 2002). The null mice for p190B RhoGAP exhibited reduced body size and developmental defects. Embryonic fibroblasts had high levels of RhoA activity and defective insulin signaling pathways indicating that p190B RhoGAP functions in glucose metabolism, cell growth and animal size determination during embryogenesis. Chromosomal rearrangements that affect the RhoGAP oligophrenin-1 has been implicated in X-linked mental retardation (Billuart *et al*., 1998). Further investigations using RNA interference assays and targeted knock-ins will aid the elucidation of the physiological functions of the RhoGAPs.

1.2.3.3. The Rho Guanine Nucleotide Dissociation Inhibitors (RhoGDIs)

The third class of Rho GTPase regulatory proteins is the RhoGDI proteins. As the name suggests, these proteins have a negative regulatory effect on Rho GTPase signaling pathways (reviewed in Sasaki and Takai, 1998; Olofsson, 1999; Hoffman and Cerione, 2004). The GDI proteins were first isolated based on their ability to block RhoGEF mediated nucleotide exchange by associating with the inactive GDP-bound form of Rho GTPases (Ueda *et al*., 1990; Leonard *et al*., 1992; Fukumoto *et al*., 1990). Subsequent investigations demonstrate that the RhoGDI could also bind to the GTP-bound form of Cdc42, inhibiting its intrinsic and RhoGAP-mediated GTP hydrolysis (Hart *et al*., 1992). In addition, it could also extract Cdc42 from cellular membranes, retaining it in cytosolic RhoGDI-Cdc42 complexes (Isomura *et al*., 1991; Nomanbhoy *et al*., 1999). The RhoGDI family represents a unique class of proteins with the ability to mediate both spatial and temporal regulation of Rho proteins by influencing the cellular localization and nucleotide binding states of their cognate targets, respectively. To date, only three members of the RhoGDI family have been identified unlike the extensive RhoGEF and RhoGAP protein families

The first Rho-specific GDI was isolated from bovine brain cytosol extracts and designated RhoGDI (also known as GDI1 or αGDI) (Ueda *et al*., 1990; Leonard *et al*., 1992; Fukumoto *et al*., 1990) and is involved in Cdc42-mediated cellular transformation (Lin *et al*., 2003) as well as Rac1-mediated regulation of the NADPH oxidase system in neutrophils (Di-Poi *et al*., 2001). Subsequently, another member of this family with 75% sequence identity to RhoGDI was identified by two groups (Adra *et al*., 1993; Lelias *et al*.,

1993; Scherle *et al*., 1993). The Ly- or D4-GDI (also known as GDI2 or βGDI) is preferentially expressed in hematopoietic cells and has a lower affinity for Cdc42 than RhoGDI. The third RhoGDI designated GDI3 (or γGDI), was found to be enriched in the brain and has high affinities for RhoB- and RhoG binding, weakly to Cdc42 and RhoA, but not Rac (Adra *et al*., 1997; Zalcman *et al*., 1996). Interestingly, GDI3 has a different subcellular distribution compared to the other cytosolic members. The N-terminus amphipathic alpha-helix appears to mediate its association with vesicular structures in the vicinity of the endoplasmic recticulum (ER). Functionally, RhoGDI3 specifically sequesters RhoG at the Golgi (Brunet *et al*., 2002), inhibiting translocation to cell periphery and induction of lamellipodia and membrane ruffles (Gauthier-Rouviere *et al*., 1998; Blangy *et al*., 2000). Regardless of structural differences and biochemical affinities, the conserved primary sequences of the RhoGDIs suggest that a common mode of interaction exists amongst members of this family (**Figure 1.12**).

1.2.3.3.1. Structural insights of GDI function

Understanding the structural basis of RhoGDI-GTPase interactions has provided insights into the mechanisms underlying its biochemical activities and cellular functions. Rho proteins can stably associate with the plasma membrane via a series of post-translational modifications at their C-terminus CAAX motif (Clarke, 1992). RhoGDIs bind specifically to the prenylated forms of Rho, thereby sequestering it from the membrane to form soluble cytosolic GDI-GTPase complexes. Mechanisms underlying RhoGDI functions are based on Cdc42/RhoGDI (Hoffman *et al*., 2000), Rac1/GDI2 (Scheffzek *et al*., 2000) and Rac2/RhoGDI (Grizot *et al*., 2001; Di-Poi *et al*., 2001) complexes. RhoGDI

Figure 1.12. Domain layout of the three members of the RhoGDI family. Each member shares high level of amino acid identity (values indicated as percentage identity). Generally, members are composed of an N-terminus regulatory domain and a C-terminus immunoglobulin-like domain with the exception of GDI3, which contains a unique amphipathic helix. (Adapted from Hoffman and Cerione, 2004).

is composed of two distinct domains: a well-ordered C-terminus and a more flexible N-terminus. The former adopts a conformation comprising two anti-parallel β-sheets forming a β-sandwich (Gosser *et al*., 1997; Keep *et al*., 1997) which provides a hydrophobic immunoglobulin-like fold for binding the geranylgeranyl moiety while the latter has a well-ordered helix-loop-helix conformation. In the absence of Cdc42, the binding pocket is too small to accommodate the lipid but RhoGDI-Cdc42 complex formation results in expansion that permits insertion of the lipid moiety. Sequestration of this moiety within the hydrophobic cavity results in the release of the GTPase from the plasma membranes. Analysis of the Rac1/GDI2 complex demonstrate that a hydrophobic isoleucine residues at position 177 stabilizes lipid sequestration and its substitution to a polar asparagine residue explains the differential affinities of RhoGDI and GDI2 for Cdc42 (Platko *et al*., 1995).

The N-terminus regulatory arm of RhoGDI is responsible for mediating interactions with the switch I and II regions of Rho proteins. RhoGDIs exist in two conformations in which the N-terminus exists either in a random coil or a helical structure (Lian *et al*., 2000; Nomanbhoy and Cerione, 1996; Golovanov *et al*., 2001a). The latter is stabilized against the immunoglobulin-like domain (Hoffman *et al*., 2000) by an invariant arginine residue in the switch II (Arg66 in Cdc42) region. In this conformation, residues 45-60 mediate GTPase binding and inhibit guanine nucleotide dissociation and hydrolysis (Nomanbhoy and Cerione, 1996; Golovanov *et al*., 2001b) while residues 10-15 participate in lipid moiety sequestration.

1.2.3.3.2. Mechanisms of GDI activity

A proposed model for GDI-mediated membrane release involves the acidic residues of the C-terminus binding pocket and the phospholipid headgroups of the membrane bilayer. Competition for the lipid moiety at the polybasic tail of the Rho protein results in its extraction from the membrane. In addition, extensive contacts between the RhoGDI N-terminus regulatory arm and the switch II region enable the GDI to bind GTPases regardless of their nucleotide states (Nomanbhoy *et al*., 1996). GDIs inhibit GEF and GAP activities by competing for a common set of residues necessary for Rho GTPase interaction. High affinity nucleotide associations with the switch regions are stabilized by a Mg^{2+} ion which neutralizes the negative charge on the phosphate groups. Generally, GEFs and GDIs regulate nucleotide binding by influencing Mg^{2+} ion coordination (Wei *et al*., 1997). While GEFs form favorable interactions that promote the release of the bound nucleotide, GDIs achieve an opposite effect by stabilizing Mg^{2+} ion coordination to promote a switch II conformation that locks the nucleotide in the binding pocket. GAP proteins on the other hand, contribute an arginine finger motif to the active site to stabilize the conformation of the invariant glutamine (Gln63 in RhoA) residue to facilitate GTP hydrolysis through the formation of a catalytically active transition state. As no structural data is currently available, GDI binding is proposed to maintain the Rho-GTP bound conformation by influencing the formation of this transition state based on structural insights from RhoGAPs in complex with active small GTPases (Hoffman and Cerione, 2004).

1.2.3.4. Intracellular targeting of the Rho family GTPases

The diversity of cellular distribution of Rho family members may aid Rho involvement in different cellular events. As described previously, nascent cytosolic Rho proteins undergo a series of posttranslational modifications which attach a hydrophobic group to the C-terminus CAAX motif, necessary for its subcellular localization. However, this modification is only sufficient for targeting to endomembranes (Choy *et al.*, 1999). The distribution of Rho proteins to different cellular compartments including the cytosol (Abo *et al*., 1991), plasma membranes (Boivin and Beliveau, 1995), Golgi (Erickson *et al*., 1996), endosomes (Murphy *et al*., 1996) and the nucleus (Baldassare *et al*., 1997) involves a second signal provided by the 20-amino acid hypervariable region found upstream of the CAAX motif. However, recent works demonstrate a contradicting view suggesting that post-prenylation CAAX motif processing is not essential for Rho GTPase localization and function unlike the farnesylated Ras proteins (Michaelson *et al*., 2005). The hypervariable region consists of a series of basic amino acids or cysteine residues that are sites for palmitoylation (Hancock *et al*., 1990; Choy *et al*., 1999; Michaelson *et al*., 2001). Previous work indicates that Rho proteins lacking this second motif are retained in the endomembrane and exhibit defective subcelluar localization (Michaelson *et al*., 2001). Thus, RhoGDI-mediated intracellular targeting involves coordinate regulation by the CAAX motif and the hypervariable region. This enables cytosolic sequestration of Rho in the absence of stimuli and the translocation of Rho proteins to suitable compartments upon activation. Sequence comparisons of the hypervariable regions of Rho and Ras proteins demonstrate the existence of 4 different classes based on the number of positively charged

residues corresponding to distinct intracellular compartmentalization (Michaelson *et al*., 2005).

1.2.4. Structural aspects of Rho GTPase signaling: effector and regulator recognition motifs

The complexities of Rho signaling cascades can be attributed to its ability to interact with a diverse repertoire of protein targets. These include the different classes of regulatory proteins previously discussed as well as downstream effectors which serve to direct distinct cellular response. The cross-utilization of common effectors by the Rho GTPases contribute to increasingly complex signaling cascades. Emerging data on the structural characteristics of these interactions provide further insights into the underlying mechanisms that direct the biochemical activities of these molecular switches (Vetter and Wittinghofer, 2001; Corbett and Alber, 2001).

Interestingly, the monomeric small G proteins share common mechanisms that direct protein-protein interaction with diverse auxiliary proteins. Generally, these protein targets bind the small GTPase in a nucleotide-dependent manner. Discrimination of the GTP- or GDP-bound state is mediated by three segments that border the nucleotide-binding site. The switch I and II regions undergo conformational changes in response to the GTP binding while the P-loop motif (**G**XXXX**GK**[**S/T**]) commonly found in adenine and guanine nucleotide-binding proteins makes contact with a phosphate group of the bound nucleotide and coordinates a Mg^{2+} ion for stabilizing nucleotide binding (Saraste *et al*., 1990; Wittinghofer, 2000). Recent analyses of the Rho family GTPase-protein complex interface indicates that the consensus binding site responsible for mediating interactions

with various effectors, activators and inhibitors in RhoA correspond to residues 29-42 (switch I) and 62-68 (switch II) (Dvorsky and Ahmadian, 2004) (**Figure 1.13**).

1.2.4.1. Interaction with RhoGDIs

RhoGDIs sequester the prenyl moiety at the COOH-terminus of the small GTPase inside an immunogloubulin-like domain (Hoffman *et al*., 2000). This effectively blocks the hydrophobic tail from the aqueous environment and extracts the Rho GTPase from membrane compartments. Structural data also indicate that GDIs form extensive contacts with their cognate Rho targets involving residues beyond the switch I and II regions which results in high-affinity interactions that inhibit GDP dissociation and GTP hydrolysis (Hoffman *et al*., 2000; Scheffzek *et al*., 2000)

1.2.4.2. Interaction with RhoGEFs

The Dbl family of RhoGEFs catalyze nucleotide exchange by disrupting Mg^{2+}-ion coordination and favourable interactions for high affinity nucleotide binding (Worthylake *et al*., 2000; Buchwald *et al*., 2002; Rossman *et al*., 2002; Snyder *et al*., 2002). This is achieved through the DH domain which promotes conformational changes in the switch regions by insertion of residues in close proximity to the P-loop and the Mg^{2+}-binding area resulting in nucleotide ejection (Vetter and Wittinghofer, 2001).

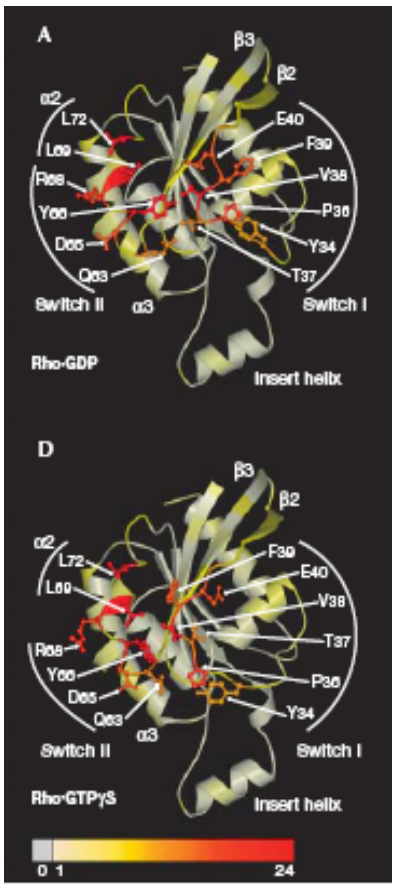

Figure 1.13. Ribbon plots of GDP- and GTPγS-bound RhoA (upper and lower panels, respectively) with the switch region coloured from yellow (corresponding to one contact) to red (corresponding to a maximal number of 24 contacts). Grey indicates the residues that are not involved in any interactions. Conserved residues frequently used for interactions with GDIs, GEFs, GAPs and effectors are depicted in a ball-and-stick configuration. (Adapted from Dvorsky and Ahmadian, 2004).

1.2.4.3. Interaction with RhoGAPs

The canonical GAP domain found in RhoGAPs catalyzes GTPase binding and GTP hydrolysis (Moon and Zheng, 2003). Interestingly, these RhoGAP activities have been found to be independent of one another (Ahmadian *et al*., 1997; Leonard *et al*., 1998; Graham *et al*., 1999). Structurally, RhoGAPs serve to promote the transistion state of GTP-hydrolysis reaction by insertion of an arginine residue into the active site and by stabilizing the glutamine residue (Gln63) in the switch II region in a conformation promoting nucleophilic attack crucial for GTP hydrolysis (Gamblin and Smerdon, 1998; Scheffzek *et al*., 1998; Kosloff and Selinger, 2001; Vetter and Wittinghofer, 2001).

1.2.4.4. Effector-recognition sites

Effector proteins are molecules that associate with small GTPases in a conformation-dependent manner but unlike the regulatory proteins, they act downstream of GTPase activation. Generally, effector activation involves the relief of intramolecular auto-inhibitory conformations that allow greater access to its functional domains. Although little is known about the mechanisms underlying effector activation, the conserved leucine residues (Leu69 and Leu72) in RhoA switch II region have been suggested to mediate hydrophobic contacts necessary for activation of Cdc42/Rac-interactive binding (CRIB)-motif-containing proteins including activated Cdc42-associated kinase (ACK) and p21-activated kinase (PAK) (Morreale *et al*., 2000). In addition, Cdc42-effector complexes demonstrate that CRIB-motif-containing proteins make extensive contacts around the small GTPase (Hoffman and Cerione, 2000). Structural data on the GTPase-binding

domains (GBDs) of a subset of RhoA effectors including PKN and ROCK indicate that these effectors form multiple contact points with regions outside the classical RhoA switch domains (Blumenstein and Ahmadian, 2004). Thus, despite their structural differences and affinities, these groups of Rho effectors employ a strategy that utilizes a core binding interface with additional associations that provide target specificity.

Current reviews provide insights into the structural basis underlying versatility in Rho GTPase signaling pathways and provide greater understanding of the dynamics of RhoGTPase interactions. In summary, two invariant leucines in the α2-helix and twelve residues in the switch regions mediate GTPase interactions with all binding partners in a nucleotide-independent manner. In addition, different partners also interact with additional regions on the small GTPase to enhance recognition specificity. For example, all regulatory proteins associate with the α3-helix while the GDIs sequester the hydrophobic C-terminus and the GAPs make contact with the insert region of Rho GTPases. Effector proteins on the other hand bind to the N-terminus of the small GTPase or the α5-helix region (**Figure 1.14**).

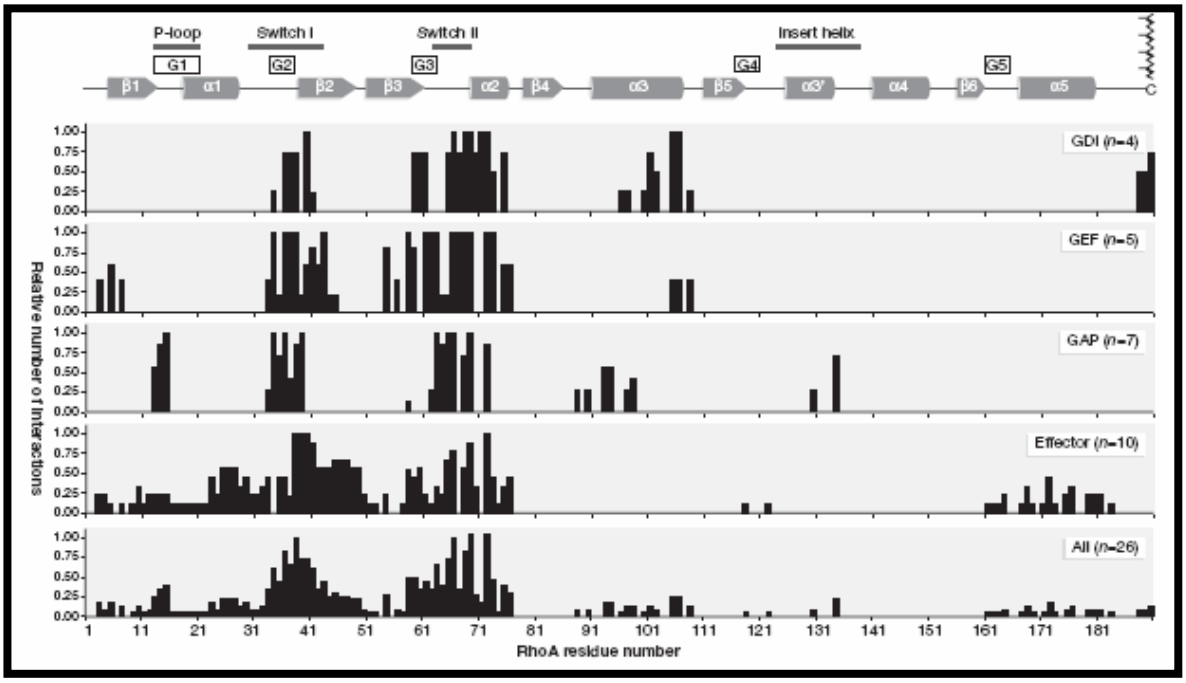

Figure 1.14. Structural motifs and intermolecular contact sites of RhoA. Structural elements (α-helices are represented as cylinders and β-strands as arrows), the guanine nucleotide-binding peptide loops (G1−G5), the conserved sequence motifs and the isoprenylation site at the C-terminus of RhoA are highlighted on the top according to Ihara *et al* (1998). The frequencies of intermolecular contacts of interacting partners with Rho GTPases are shown as histograms. (Adapted from Dvorsky and Ahmadian, 2004).

1.2.5. Deregulated Rho GTPase mutants: tools for functional studies

Structural data presented here demonstrate the importance of conformational folds in mediating Rho GTPase interactions and has helped identify a series of residues that are crucial for these associations. Thus, it is not surprising that alteration of these specific residues through mutations occurring naturally or by molecular manipulations *in vitro* can lead to development of aberrant signaling and mutant phenotypes *in vivo*. Substitution of crucial residues within the switch regions and the C-terminus usually result in the gain of transforming activity and oncogenesis. Nevertheless, these mutants provide an opportunity for the genetic manipulation of Rho binding with its plethora of protein targets and the dissection of small GTPase signaling networks. Depending on the residue, different mutant forms of a small GTPase can be generated. Generally, these mutants are classified into three functional classes: dominant active, dominant negative or inactive. Amongst these, the dominant active and negative mutants have proven to be useful in evaluating the different biological functions of Rho GTPases (**Figure 1.15**).

1.2.5.1. Constitutively active mutants

The constitutively active (G12V, Q63L) mutants have amino acid substitutions that interefere with the intrinsic GTP hydrolysis resulting in a GAP-insensistive mutant protein that is always in the GTP-bound active conformation (Rittinger *et al*., 1997a; Ihara *et al*., 1998). Another subset of activated mutants are the 'fast-cycling' variants based on the Ras(F28L) mutant. The corresponding versions in the Rho proteins are spontaneously activated and exhibit rapid GDP to GTP exchange while retaining normal GTP hydrolysis

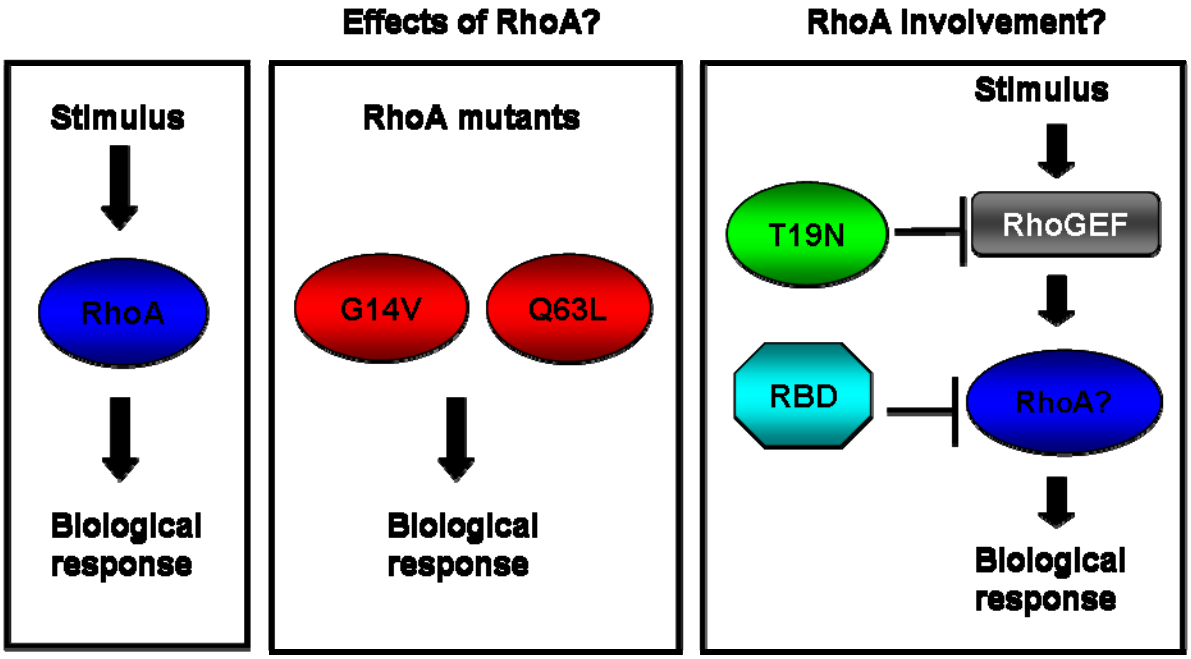

Figure 1.15. Strategies for dissecting Rho GTPase function. The RhoA constitutive active (G14V, Q63L) mutant is GAP-insensistive and is used to characterize different cellular functions of wild-type Rho proteins. The dominant negative (T19N) mutant inhibits RhoGEF function via sequestration and has been used to assess Rho involvement in various signaling pathways. The T19N mutants can sequester several GEFs and thus, have broader inhibitory effects on other Rho GTPases. In addition, peptide fragments consisting of the GTP-dependent Rho binding domain (RBDs) or p21 binding domains (PBDs) of specific effectors have been used as selective dominant negative versions of specific Rho proteins. (Adapted from Karnoub and Channing, 2004).

(Reinstein *et al*., 1991).

1.2.5.2. Dominant negative mutants

These mutants have helped establish the roles of Rho GTPases in oncogenesis (Feig, 1999). Introduction of an aspargine at position 19 in RhoA (T19N) results in increased affinity for RhoGEFs, corresponding to impaired nucleotide exchange and decreased affinity for GTP (Seasholtz *et a*l., 1999). Thus, when introduced into cells, this mutant exerts its effects through RhoGEF sequestration which in turn affects GEF turnover and the subsequent inhibition of endogenous GTPase activation.

1.2.5.3. Defective effector-binding mutants

The third functional class of GTPase mutants have impaired effector recognition and activation. Most effector interactions involve the switch I and II regions. Selected mutations in these regions can affect effector binding and thus aid assessment of the effector function downstream of a specific Rho GTPase pathway (Westwick *et al*., 1997; Sahai *et al*., 1998). A summary of residue substitutions and their effects is represented in **Figure 1.16**.

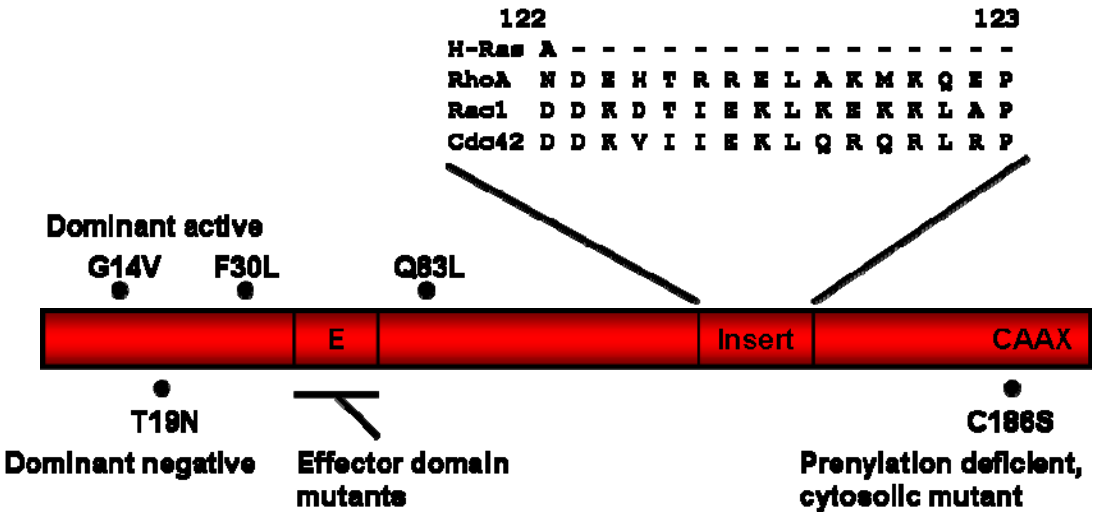

Figure 1.16. Schematic diagram of dominant active (G14V, F30L, Q63L) and dominant negative (T19N) RhoA mutants. Site directed mutagenesis and effector domain swap studies have delineated functionally important residues within the effector domain. Mutations in the CAAX motif result in defective GTPase membrane targeting due to lack of prenyl group addition during post-translational modifications. The insert regions have been implicated in effector activation. (Adapted from Karnoub and Channing, 2004).

1.2.6. Functions of the Rho family GTPases

Earlier studies demonstrate that impaired Rho expression resulted in defective budding in S. *cerevisiae*, indicating that they may mediate actin reorganization during division (Lelias *et al*., 1993; Yamochi *et al*., 1994). Further insights into the cellular functions of the Rho subfamily have been derived from studies utilizing the C3 exoenzyme of *Clostridium botulinum*. The C3 exoenzyme modifies specific residues within the effector binding region in Rho proteins by ADP-ribosylation, thus inhibiting Rho-effector interactions and subsequent propagation of downstream signaling pathways (reviewed in Bishop and Hall, 2000).

These studies indicate that Rho proteins are the main regulators of actin cytoskeleton remodeling that forms the basis of various cellular events such as cell shape change, cell motility and cell adhesion. This in turn influences basic developmental processes such as cell migration, cytokinesis and axon guidance. In addition, Rho proteins also participate in other cellular events such as gene transcription, cell proliferation and cell cycle progression and vesicular transport (reviewed in Ridley, 2001; Symons and Settleman, 2000; Takai *et al*., 2001) (**Figure 1.17**). Recent reviews indicate that several major families of effector proteins and feedback regulatory proteins act downstream of activated Rho GTPase (reviewed in Schwartz, 2004) (**Figure 1.18**). A subset of these effectors will be reviewed with respect to their functions in cell motility, phagocytosis and cell cycle progression.

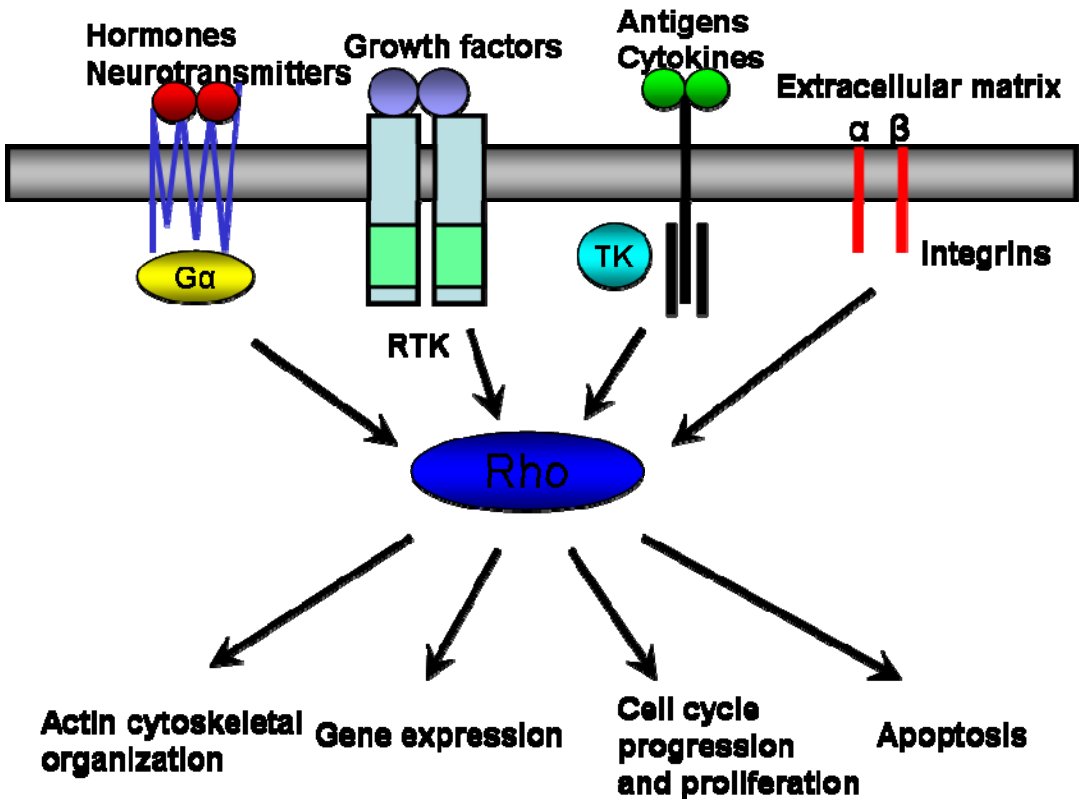

Figure 1.17. Rho GTPases participate in a plethora of cellular events and represent a point of convergence downstream of receptor activation.

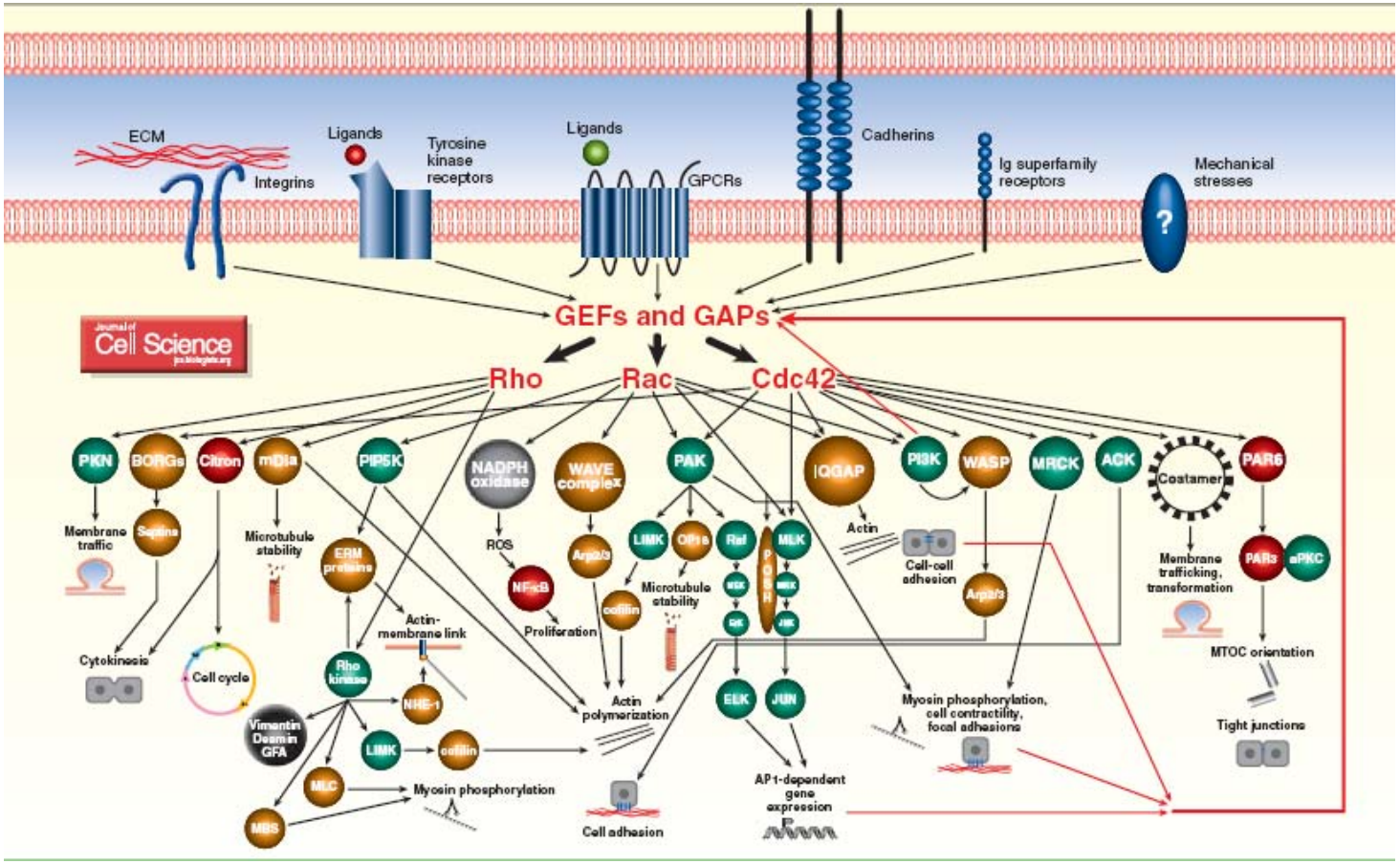

Figure 1.18. Rho GTPase effector pathways. (Adapted from Schwartz, 2004).

1.2.6.1. Reorganization of the actin cytoskeleton

In addition to its primary role in cell shape maintenance, the actin cytoskeleton provides an environment in which various biochemical and cellular activities take place. The cytoskeleton is composed of a network of different protein filaments namely actin, microtubule and intermediate filaments (reviewed in Chang and Goldman, 2004). Actin filaments are made up of filamentous actin bound to accessory proteins designated actin-binding proteins (ABPs). These include gelsolin, profilin, cofilin and villin and mediate a dynamic process known as treadmilling in which actin monomers continually undergo a series of polymerization and depolymerization reactions to form F-actin filaments (reviewed in Revenu *et al*., 2004). A balance between these antagonistic reactions results in a dynamic state of equilibrium and stabilization of filament lengths. Perturbation of this steady state in response to upstream activating signals allow the cells to modify the composition and architecture of the actin cytoskeleton network for cell motility, migration or other cellular events like organogenesis and wound repair.

Generally, these filaments are organized into discrete structures that are divided into three distinct classes. Actin stress fibers are actin filament bundles that traverse the cell with its ends anchored to the extracellular matrix via distinct contact points known as focal adhesions. Lamellipodia or membrane ruffles are protrusive actin sheets found at the leading edge of migratory cells while filopodia are long, thin cellular processes that are organized by a bundle of polarized actin filaments found mainly in motile cells. Different structures can be generated by modulating the capping activity at the barbed ends of the actin filaments (**Figure 1.19a**). These structures are maintained by the underlying actin

cytoskeleton in concert with co-factors that regulate the activity of the ABPs via posttranslational modifications which cause conformational changes or compete with actin filaments for these actin binding proteins (reviewed in Wear and Cooper, 2004). In this respect, the Rho GTPases participate in regulation of these co-factors in a guanine nucleotide-dependent manner. Generally, Rho proteins induce stress fiber formation (Mura *et al*., 1993; Ridley and Hall, 1992), while Rac proteins regulate membrane ruffles and lamellipodia formation (Ridley *et al*., 1992), and Cdc42 mediates filopodia formation (Kozma *et al*., 1995; Nobes and Hall, 1995) (**Figure 1.19b**).

1.2.6.1.1. Roles of Rho GTPases in cytoskeleton reorganization

Rho GTPases act as transducers that relay extracellular stimuli to activate several downstream signaling pathways leading to cytoskeleton remodeling. In fibroblasts, Rac induces lamellipodia and membrane ruffles followed by subsequent stress fiber formation (Ridley *et al*., 1992) while Cdc42 induces filopodia at the cell periphery prior to lamellipodia and membrane ruffles formation (Kozma *et al*., 1995; Nobes and Hall, 1995). These reports are an indication that members of the Rho family modulate the dynamics of actin remodeling through a series of sequential and coordinated events. **Figure 1.20** summarizes the main Rho effector pathways involved in regulation of actin cytoskeleton.

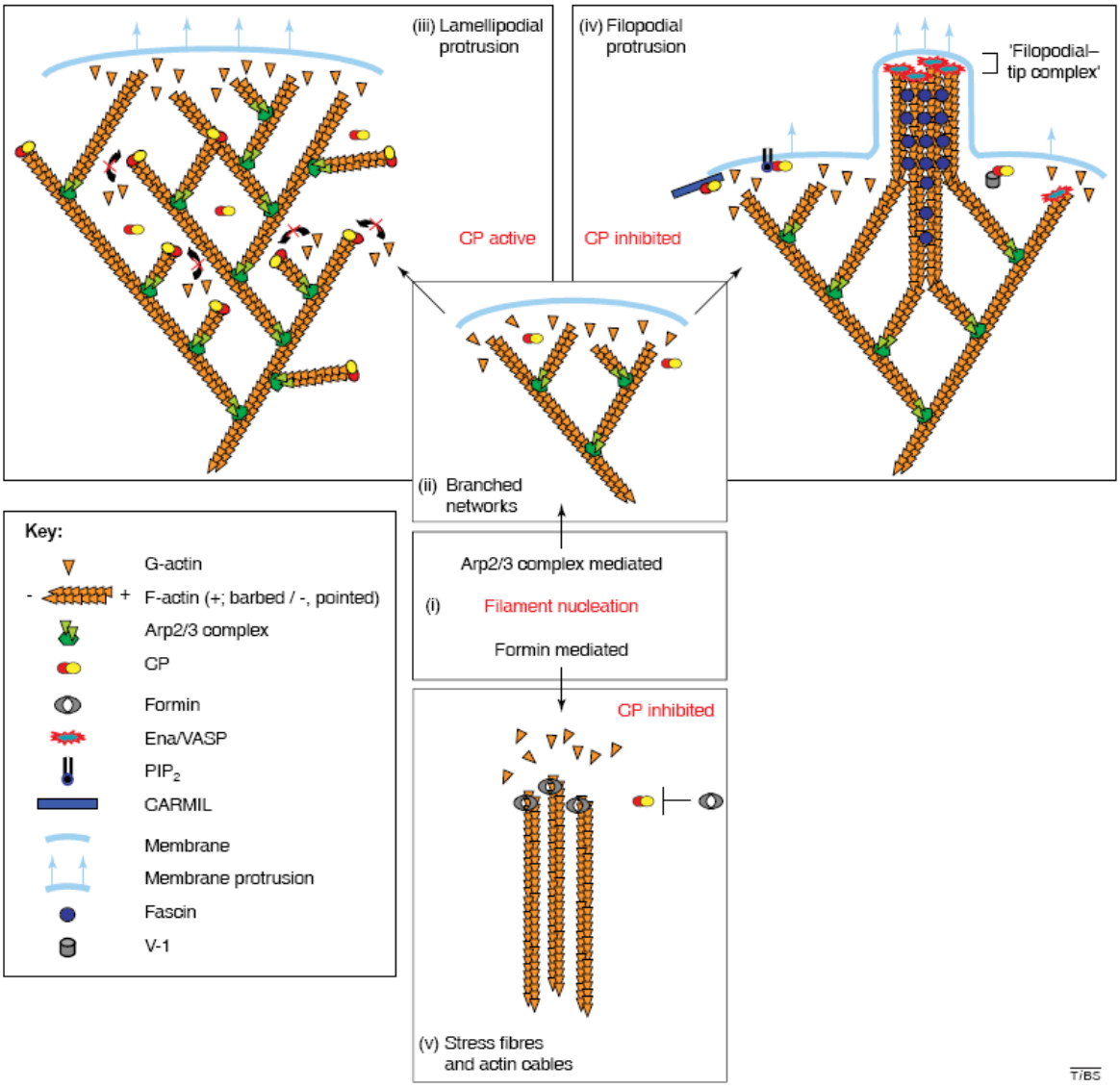

Figure 1.19a. Generation of different actin filament architectures by modulating the activities of actin-binding proteins. (Adapted from Wear and Cooper, 2004).

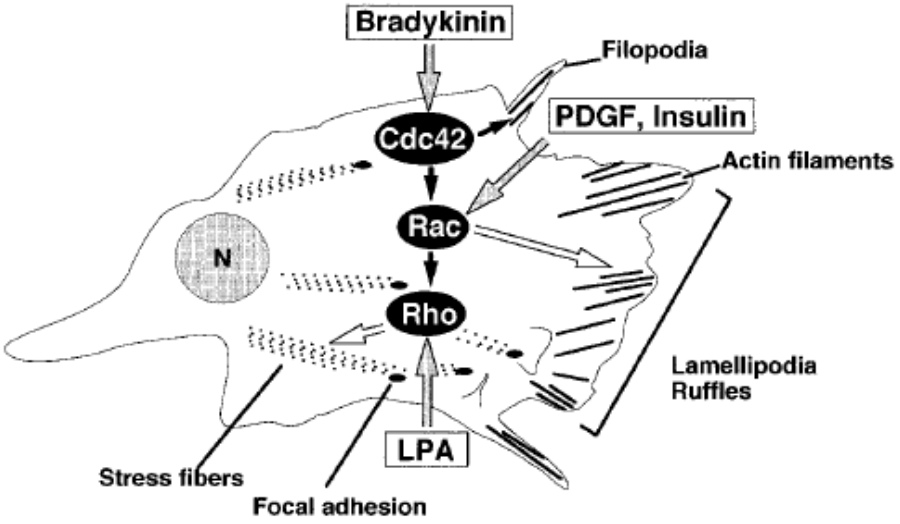

Figure 1.19b. Rho GTPase proteins regulate the actin cytoskeleton organization through the induction of distinct actin structures. GTPase activity can be stimulated in the presence of different ligands bradykinin (Cdc42), PDGF or insulin (Rac) and LPA (Rho). LPA, lysophosphatidic acid. (Adapted from Takai *et al*., 2001).

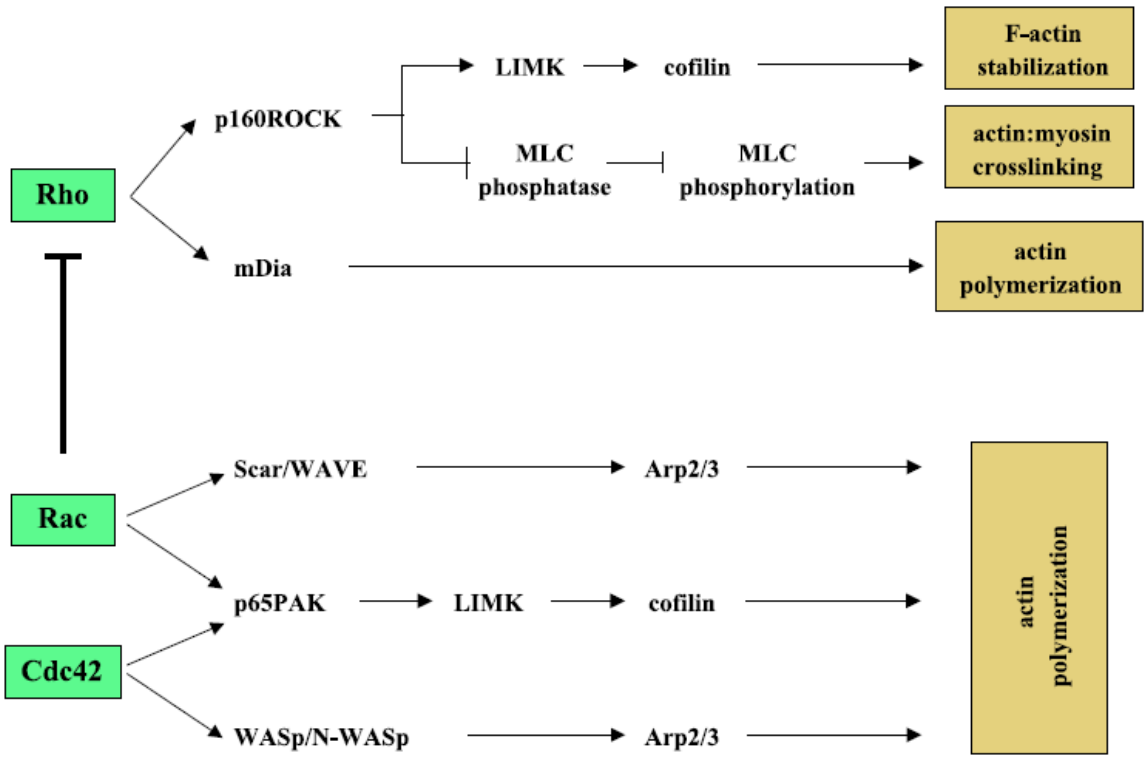

Figure 1.20. Rho GTPase effector pathways in actin cytoskeleton remodeling. (Adapted from Raftopoulou and Hall, 2004).

Amongst the Rho effector families, the Rho-associated coiled-coil kinase (ROCKs) are ~160kDa protein serine/threonine kinases of that play important roles in induction of Rho-induced stress fibers and focal adhesions by regulating the phosphorylation states of different candidate proteins downstream (reviewed in Riento and Ridley, 2003). Phosphorylation of the myosin light chain promotes F-actin bundling, stress fiber and focal adhesion formation thus, enhancing cell contractility. This is regulated by the antagonistic activities of myosin light chain kinase (MLCK) and myosin light chain phosphatase (MLCP). Activated ROCK negatively regulates the activities of MLCP by phosphorylation of its myosin binding subunit (MBS) resulting in upregulated MLCK actvity which in turn promotes the cell contractility and stress fiber induction (Gong *et al*., 1996; Noda *et al*., 1995). ROCK cooperates with mammalian Diaphanous (mDia), a member of the formin-homology containing protein family in RhoA-induced stress fiber formation and actin cytoskeleton remodeling (Watanabe *et al*., 1999). mDia can bind to profilin, an actin-binding protein via its FH1 domain to enhance actin polymerization (Watanabe *et al*., 1997). Alternatively, it could directly stimulate actin polymerization (Pruyne and Bretscher, 2000) and stabilize microtubules assembly during cell migration (Palazzo *et al*., 2001).

ROCK can also function via an alternative cascade involving LIM (Lin11, Isl1 and Mec3) kinase, a serine/threonine kinase that participates in regulation of actin-filament assembly via a series of phosphorylation events initiated by Rho activation (reviewed in Riento and Ridley, 2003). The Rho-ROCK-LIM kinase pathway promotes actin filament assembly by negative regulation of cofilin, an actin-depolymerizing protein that regulates the turnover of actin filaments (Maekawa *et al*., 1999). Conversely, LIM kinase is also

targeted by PAK. This family of serine/threonine kinases serve as important regulators of cytoskeletal dynamics and cell motility downstream of Rac and Cdc42 activation (reviewed in Zhao and Manser, 2005). In addition to LIM kinase, PAKs also mediate the activities of myosin light chain in actin filament assembly. All PAKs contain an 18-amino acid Cdc42/Rac interactive binding (CRIB) motif that mediates its interactions with Rac and Cdc42 proteins while different regions designated the Rho-binding domain (RBD) on Rho effectors mediate their interactions with Rho. These effectors have been subdivided into three distinct classes based on their Rho-binding motifs (Fujisawa *et al*., 1998). Class I and III effectors bind to RhoA between residues 75-92 and 23-40, corresponding to the switch II and switch I regions, respectively. Class II effectors utilize both these regions for RhoA associations.

The ERM (ezrin-radixin-moesin) proteins are adaptors that translocate between the cytosol and the plasma membrane. These proteins are common targets downstream of Rho, Rac and Cdc42 activation. ROCKs can phosphorylate ERM proteins resulting in translocation to cell protrusions (Shaw *et al*., 1998) while the Cdc42/Rac effector, myotonic-dystrophy-kinase-related Cdc42-binding subunit (MRCK) enhances Cdc42-induced filopodia and activation of ERM proteins by serine/threonine phosphorylation (reviewed in Zhao and Manser, 2005).

In addition to PAKs, several other Rac and Cdc42 effectors participate in actin cytoskeletal remodeling. This includes the partner of Rac (POR1) which interacts with Rac in a GTP-dependent manner and has been implicated in Rac-dependent membrane ruffles (van Aelst *et al.*, 1996). Within the cell, the Arp2/3 complex functions as a major regulator of actin polymerization that nucleates actin filament assembly in a unidirectional manner

initiating the growth of protrusive actin filaments at the leading edge. Rac and Cdc42 target the WASP family verprolin homologous (WAVE) and the neuronal Wiskott-Aldrich syndrome protein (N-WASP) complexes, respectively. These in turn direct the activation of the Arp2/3 complex in a spatio-temporal manner. Rac activation causes the recruitment of the WAVE multiprotein complex to the membrane. The subsequent dissociation of WAVE from the complex promotes the formation of a WAVE-Arp2/3 complex which positively regulates actin polymerization in lamellipodia. Conversely, active Cdc42 recruits N-WASP to the membrane, subsequent PIP_2 binding relieves autoinhibitory conformations exposing binding sites for actin and Arp2/3 complex which promotes filopodia induction. These events link actin polymerization to extracellullar stimuli received at the plasma membrane. The multidomain architecture of N-WASP includes a PH and CRIB domain that allows Cdc42 and PIP_2 to coordinately activate N-WASP by stabilizing an active, open conformation (reviewed in Bompard and Caron, 2004).

Both Rac and Cdc42 also participate in IQGAP activities at membrane ruffles and at cell-cell adhesions (Kuroda *et al*., 1998). This multidomain protein functions as a scaffold linking Cdc42 activation with various components of the cytoskeleton (reviewed in Briggs and Sacks, 2003). Several motifs such as the WW domain, a SH3-binding motif, a calmodulin-binding domain, and a Ras GAP-like motif help orchestrate diverse activities such as cytoskeleton reorganization, cell adhesion, polarity and motility (Kuroda *et al*., 1998; Li *et al*., 1999; Watanabe *et al*., 2004). Interestingly, IQGAP does not function as a GAP but instead inhibits the intrinsic Cdc42 GTPase activity (Brill *et al*., 1996; Hart *et al*., 1996; Ho *et al*., 1999) and the maintenance of active Cdc42 for filopodia induction (Swart-Mataraza *et al*., 2002).

Rho GTPases can also mediate actin cytoskeleton remodeling via influencing lipid signaling pathways mainly via activation of the lipid kinases, PI3K and phosphoinositol-4-phosphate 5 kinase (PIP5K) (reviewed in Janmey and Lindberg, 2004). These enzymes catalyze the production of second messenger PIP_2 which regulates actin cytoskeletal dynamics by modifying ABPs, influencing their activities in actin filament assembly. Increased cellular PIP_2 levels usually correspond to increased actin assembly. Besides acting downstream of Rac and Cdc42 activation which contributes to actin polymerization via the activities of N-WASP, profilin and other actin-capping proteins, Rho-mediated activation of PIP5K influences downstream activation of ERM proteins via ROCK. Arf6 has been implicated in Rac-mediated membrane ruffling downstream of PIP_2. Thus, phosphoinositide signaling integrates different upstream stimuli and allows for concerted regulation of growth factor and G protein signaling.

1.2.6.1.2. Roles of Rho GTPases in microtubule regulation

In addition to actin cytoskeleton remodeling, the Rho family GTPases can utilize different subsets of these effectors to direct other cellular events. Microtubules (MTs) are a major component of the cytoskeleton essential for cell polarization, cell division, cell migration, and vesicular transport (reviewed in Watanabe *et al*., 2005). MTs are composed of 13 protofilaments made up of α- and β-tubulin dimers. Generally, MTs nucleate at their minus ends which are localized at the microtubule organizing center (MTOC) while their plus ends adopt a state of dynamic instability, continually growing and shrinking. Selective stabilization of these MTs at their growing ends enables the MTOC to maintain an asymmetrical polarized MT array important for cell shape maintenance. This is supported

by the activities of microtubule-associated proteins (MAPs) that bind to the plus ends of microtubules (reviewed in Revenu *et al*., 2004)

Although Rho GTPases are known more as regulators of the actin cytoskeleton, some of those effectors also participate in the temporal regulation of MT dynamics in response to signals that induce cytoskeleton reorganization (**Figure 1.21**). A concerted model for MT organization involves Rac activation which induces the formation of microtubules at the leading edge while RhoA activation induces the assembly of posttranslationally modified tubulin subunits, Glu-tubulin (Glu-MT) into stable microtubule filaments. Cdc42 signaling reorients the MTOC towards direction of the stimuli. This is mediated by the Cdc42 effectors dynein and dynactin which form motor complexes that redirects the minus end of microtubules.

Stable microtubules are the result of the polymerization of Glu-MT. RhoA and its downstream effector mDia have been implicated in the formation of Glu-MT. In addition, integrin-mediated activation of focal adhesion kinase (FAK) may enhance the formation of Glu-MT by targeting RhoA and mDia to lipid rafts localized in the leading edges effectively bringing about site specific RhoA activation of mDia. Alternatively, Rho and mDia can also facilitate integrin-FAK signaling via interactions with the tumour suppressor adenomatous polyposis coli (APC) and the EB1 proteins which are MAPs that promote MT bundling and stabilization. In addition, ROCKs may target MAPs (MAP-2 and tau) and work in concert with mDia in directing the dynamics of MT formation downstream of Rho activation.

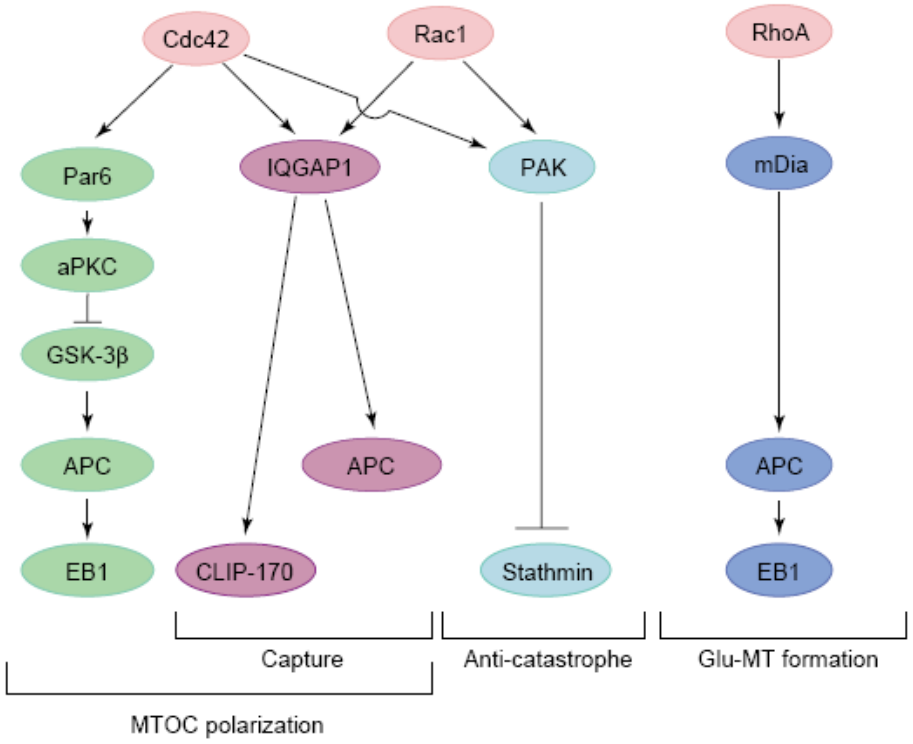

Figure 1.21. Signaling networks of Rho GTPases in microtubule organization. (Adapted from Watanabe *et al*., 2005).

APC is a major regulator of MT organization and directs MT stability under the influence of various upstream activators. Besides Rho, Rac and Cdc42 also play crucial roles in MT organization via the activation of various downstream effectors at the leading edge of cells. Cdc42 promotes APC-mediated MT stability at the leading edge and influence the subsequent establishment of cell polarity by regulating the MTOC through Par6. Substratum adhesion results in integrin-FAK activation which promotes atypical protein kinase C (aPKC) activity via Cdc42 and Par6. This results in the phosphorylation and inactivation of glycogen synthase kinase-3β (GSK-3β) which relieves APC inhibition at the leading edges of cell.

In addition, Cdc42 and Rac enhance IQGAP and CLIP-170 associations which form docking sites for MT plus ends at the cell cortex thereby, enhancing MT stability. Taken together, this suggests that the IQGAP-CLIP-170 complex functions in the recruitment and anchorage of APC-mediated microtubules plus ends to specific points at the cell cortex under the influence of Rac and Cdc42. APC association with the Rac-specific GEF, Asef promotes Rac activation which influences both MT and actin filament assembly creating a positive feedback mechanism necessary for sustained cytoskeleton reorganization involving both the actin and microtubule components.

Besides APC, Rho family effectors also regulate the functions of other MAPs. The MT destabilizing protein, stathmin (Op18) is downregulated by PAK phosphorylation downstream of Rac activation. The asymmetrical distribution of CLIP-115 and CLIP-170-associating proteins (CLASPs) direct polarized growth of MT arrays toward the leading edge. These proteins are regulated by PI3K and GSK-3β allowing the regulation of directional MT growth in response to extracellular cues upstream of Cdc42 and Rac

activation.

1.2.6.2. Rho GTPases in cell dynamics and motility

1.2.6.2.1. Roles of Rho GTPases in cell migration

Cell migration is essential for various physiological processes like wound repair, chemotaxis, angiogenesis and development. Cells may respond to various extra- or intra-cellular cues that influence the cell shape, polarity and location. Migration requires the coordinated movement of different parts of the cell which is regulated by dynamic cytoskeleton remodeling within the cell involving both the actin and microtubule filament networks (reviewed in Raftopoulou and Hall, 2004). Polarized protrusions at the leading edge are stabilized by cell adhesions followed by cell body contraction and detachment of cell adhesions at the trailing end to produce a net forward movement (**Figure 1.22**).

Different members of the Rho GTPase family are spatially regulated with distinct sites of localized activation. Rac and Cdc42 may shuttle between the cytosol and different membrane sites while RhoA remains mainly cytosolic. During cell migration, Cdc42 regulates the MTOC via activating the Par proteins and aPKC in determining cell polarity (Etienne-Manneville and Hall, 2003). In addition, Cdc42 also localizes to the Golgi apparatus to direct transport pathways to the leading edge for sustained migration. Recent work also indicates that Cdc42 mediates Arp2/3 complex and F-actin dynamics at the Golgi downstream of Arf1 activation (Dubois *et al*., 2005). At the forefront of the cell, both Rac and Cdc42 work in concert with their effectors to induce actin assembly leading to membrane ruffling and filopodia, respectively. Rac is localized immediately behind the leading edge while Cdc42 is found mostly at the tips of the

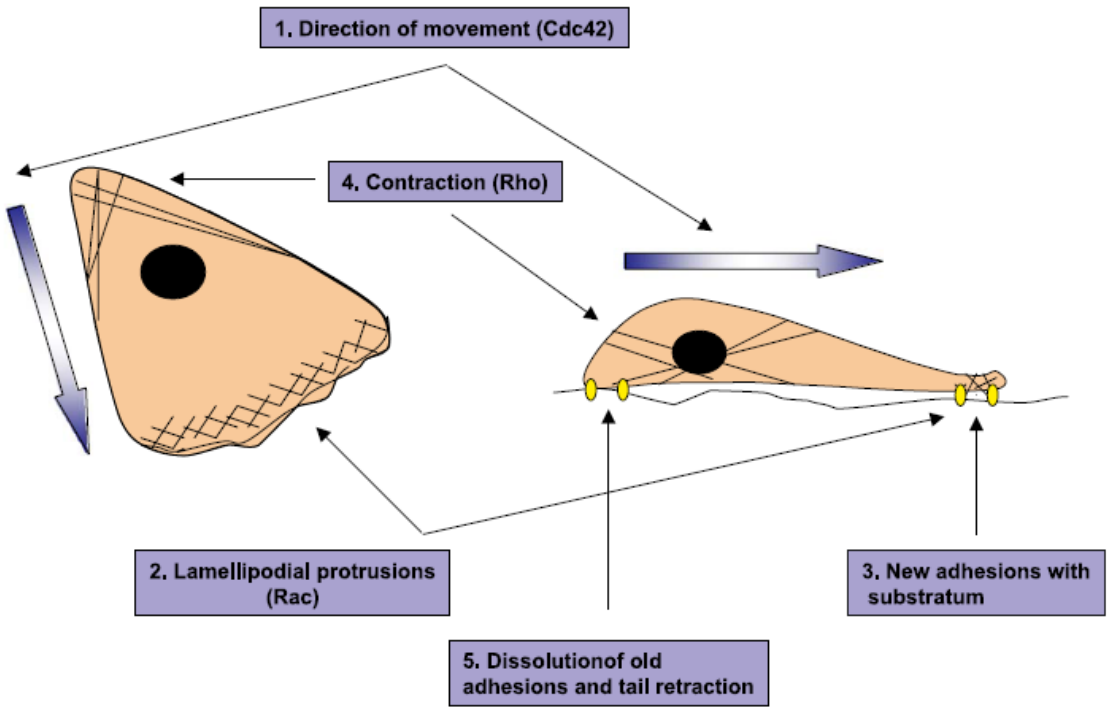

Figure 1.22. Cell migration requires the concerted efforts controlled by distinct members of the Rho GTPases. (Adapted from Raftopoulou and Hall, 2004).

leading edge. Rac may also promote microtubule stabilization through PAK-dependent inactivation of stathmin. Subsequent APC activation promotes microtubule assembly and stabilization at the leading edge. APC binding to Asef allows feedback up-regulation of Rac signaling and coordination of Cdc42-mediated microtubule organization and cell polarization with Rac-mediated actin polymerization at the leading edge. This allows for the actin cytoskeleton to assist in guiding microtubule assembly.

The membrane protrusions are then stabilized by cell adhesions induced by integrin and FAK activation. This in turn activates Rac and Cdc42 in a positive feedback loop. In addition, PAK can act in concert with PAK-interactive exchange factor (PIX) and GRK interactor I (GIT1) to regulate focal adhesion turnover necessary for actin organization and recycling of components. This results in sustained protrusion at the front and retraction at the rear of the cell providing traction for cell movement (Manabe Ri *et al*., 2002; Obermeier *et al*., 1998). Rho could promote microtubule stability via mDia by targeting microtubules to focal adhesions (Ishizaki *et al*., 2001; Palazzo *et al*., 2001) and inducing the maturation of focal adhesions behind the leading edge while participating in the dissociation of focal adhesions and regulation of actin–myosin contractility at the rear (**Figure 1.23**).

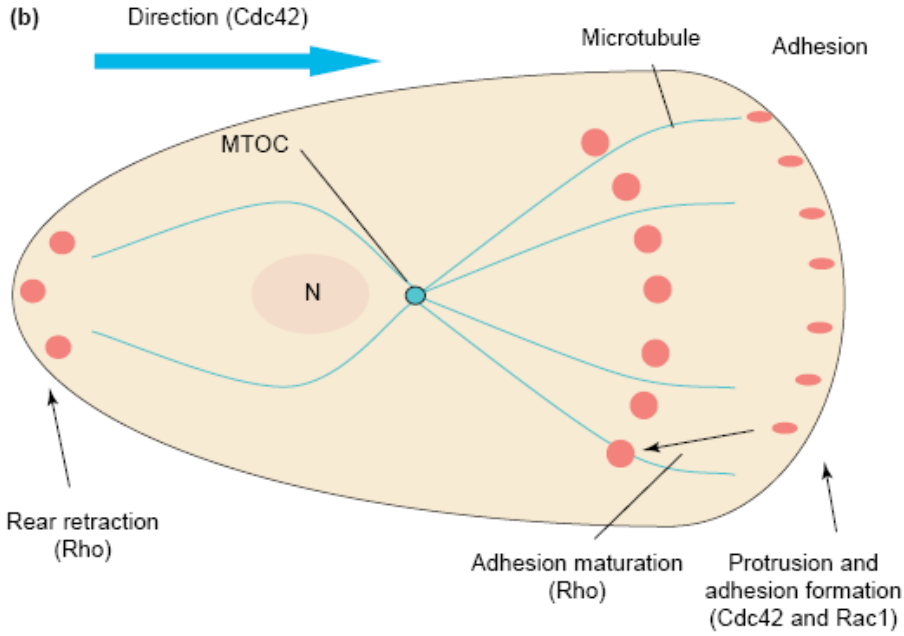

Figure 1.23. The roles of Rho GTPases in cell migration. The Cdc42/Par/aPKC complex is involved in establishment of cell polarity. At the front of the cell, Rac1 and Cdc42 work in concert with their effectors to regulate membrane ruffles and filopodia induction, respectively. These protrusions are stabilized by the formation of focal adhesions which involves integrin activation and the recruitment of structural and signaling components to the nascent adhesions. This in turn, positively regulates Rac1 and Cdc42 activation. RhoA is thought to be involved in retraction at the rear of the cell through the regulation of actin–myosin contractility. RhoA activation also induces the maturation of focal adhesions behind leading edges. (Adapted from Watanabe *et al*., 2005).

1.2.6.2.2. Roles of Rho GTPases in phagocytosis

Rac is a regulator of the NADPH oxidase complex which participates in the killing internalized foreign bodies during phagocytosis. In neutrophils, Rac can directly associate with the phox protein complex (p67, p47 and p40) via direct binding to the cytosolic p67phox which results in the subsequent membrane recruitment of the complex. Activation of the NADPH oxidase results in the generation of reactive oxygen species (ROS). This mechanism has been proposed to act in concert with Rac-mediated lamellipodia formation to direct phagocytosis (reviewed in Ridley, 2001). Rac mediates actin polymerization via activation of the WAVE-Arp2/3 complex which results in engulfment of foreign particles into phagosomes. Subsequent Rac dissociation from the WAVE-Arp2/3 complex promotes its interaction with the phox protein complex, bringing the phox proteins in close proximity to NADPH oxidase in the vicinity of the membrane thereby generating free radical ions within the phagosome. This biochemical activity allows the degradation of the internalized particle after phagocytosis.

1.2.6.3. Rho GTPases in cell proliferation, transformation and cancer development

1.2.6.3.1. Cell proliferation and cell cycle progression

Cell proliferation is a tightly regulated event associated with cell cycle progression and is dependent on stimulation from mitogenic growth factors and integrin-extracellular matrix adhesion. Deregulation often leads to defective nuclear signaling resulting in anchorage and growth factor independent growth, one of the hallmarks of cellular transformation. Cell cycle progression is mediated by complexes of cyclins and cyclin-dependent kinases (CDKs) which phosphorylate retinoblastoma (Rb) tumor suppressor proteins thereby relieving its inhibition on cell-cycle progression. The D- and E-type cyclins (D1, D2, D3, E1, E2) form active complexes with CDK4/CDK6 and CDK2, respectively. CDKs are in turn regulated by two groups of cyclin-dependent kinase inhibitors (CKIs). These include the INK4 proteins (p16INK4a, p15INK4b, p18INK4c, and p19INK4d) which specifically inhibit CDK4/6 and the Cip/Kip family ($p21^{cip1}$, $p27^{kip1}$ and $p57^{kip2}$) which activate cyclin-D-CDK4 and cyclin-D-CDK6 but inactivate cyclin-E-CDK2 complexes upon association. The relative balance of cyclin and CKIs determine CDK activity and G_1 progression. Cells can remain in the quiescent G_0 phase until growth factor stimulation which activates the cyclin-CDK complexes leading to G_1 progression and transcription of E2F-regulated genes necessary for entry into S phase. G_1 progression is considered the 'restriction point' beyond which the cell is committed to division and serves as a point for integration of growth factor stimulation with the integrin-extracellular matrix (ECM) signaling pathway (Assoian, 1997). This effectively coordinates events downstream of the RTK and integrin signaling leading to Ras/Raf/MAPK/ERK activation

(Assoian and Schwartz, 2001). Thus, normal cell proliferation involves cell adhesion in the presence of growth factors which then promote G_1 progression by upregulating cyclin D1 expression allowing the inhibition of Rb as well as the formation of cyclin-D1-CDK4/6 complexes which compete with cyclin-E-CDK2 for p21/p27 resulting in concomitant activation of both cyclin-D1-CDK4/6 and cyclin-E-CDK2 complexes (reviewed in Coleman *et al*., 2004; Sherr and Roberts, 1999).

1.2.6.3.2. Roles of Rho GTPases in gene expression

Several studies have established roles of Rho family effectors in Ras signaling pathways linking them to gene expression control. PAK activation downstream of Rac signaling stimulates the phosphorylation of Raf-1 and MEK1 which are intermediates of the Ras/Raf/MAPK pathways leading to Erk activation. Furthermore, PAKs can also mediate the activation of the stress-activated kinases, Jun N-terminal kinase (JNK) and p38MAPK via the activation of the mixed lineage kinases (MLKs), thereby stimulating AP-1 dependent gene expression. Genetic analysis of dorsal closure in *Drosophila* indicates that Rac participates in JNK regulation (Glise and Noselli, 1997). Recent work has established a link between ROCK-dependent JNK activation via MEKK1 in induction of Rho-mediated stress fibers downstream of transforming growth factor (TGF)-β signaling (Zhang *et al*., 2005).

The serum response factor (SRF) is a nuclear protein that binds to the serum response element (SRE) found upstream of immediate early genes in skeletal and smooth muscle. The Rho GTPases can activate gene transcription via the SRF in a temporal manner. In addition, RhoA and ROCK have been shown to provide spatial regulation of

gene transcription by influencing SRF subcellular localization (Hill *et al.,* 1995; Liu *et al*., 2003). The active N-WASP has been shown to translocate into the nucleus implicating it in the modulation of gene expression (reviewed in Bompard and Caron, 2004).

1.2.6.3.3. Role of Rho GTPases in cellular transformation and cancer

Dysfunctional regulation of signaling cascades often results in deregulated cell growth, proliferation and survival leading to cellular transformation and oncogenesis. Cancer development is usually associated with gene mutations that create dominant active oncogenes or defective tumour suppressor proteins. Alternatively, changes in protein expression and biochemical activity of regulatory and effector proteins also contributes to transformation (Ridley, 2004, Boettner and van Aelst, 2002). Unlike the Ras oncogenes, members of the Rho family do not exhibit gene mutations but instead show altered gene expression that influence protein signaling cascades (Lin and van Golen, 2004). Thus, Rho-dependent pathways are thought to contribute to oncogenic Ras transformation (Perona *et al*., 1993; van Leeuwen *et al*., 1995). In addition, mutations within GEFs often result in constitutive activation of their cognate Rho targets and contribute to cellular transformation (Ron *et al*., 1991).

The ability of Rho GTPases to target components of the MAP kinase pathway allows Rho-mediated apoptosis to reduce survival of transformed cells. When deregulated, cells become resistant to apoptosis leading to transformation. Rho GTPases also serve as key regulators of cytoskeletal remodeling and cell adhesion, prerequisites for anchorage-independent cell growth. Their participation in cell migration indicates further involvement

in cellular transformation and metastasis. As previously discussed, Rho GTPases can act downstream of integrin-FAK signaling leading to actin and microtubule reorganization.

Rho GTPases can direct cell cycle progression through regulation of cyclins and CKIs (reviewed in Coleman *et al*., 2004). Rac activation stimulates ERK-dependent cyclin D1 expression (Westwick *et al*., 1997; Gille *et al*., 1999; Welsh *et al*., 2001), subsequent Rb phosphorylation and E2F promoter activity in a positive feedback loop (Gjoerup *et al*., 1998). Interestingly, cyclin D1 upregulation may also be induced by Rac-dependent ROS generation via NADPH oxidase and the allosteric activation of the cyclin D1 promoter by nuclear factor-κB (NF-κB) (Joyce *et al*., 1999). In addition, PI3K may mediate Rac activation downstream of α5β1 integrin (fibronectin) receptor (Mettouchi *et al*., 2001). Conversely, Rho controls a parallel pathway that regulates the timing of ERK-dependent cyclin D1 expression through sustained ERK activation (Page *et al*., 1999).

Rho GTPases have also been implicated in downregulating $p21^{cip1}$ and $p27^{kip1}$ induction which contributes to cell cycle progression and oncogenic Ras-mediated transformation (reviewed in Welsh, 2004), the mechanisms of which require further clarifications. It has been proposed that Rho promotes G_1 progression by downregulating $p21^{cip1}$ expression during the mid- to late G1 phase. Upon growth factor stimulation, $p21^{cip1}$ undergoes an initial ERK-dependent induction which activates the cyclin-D-CDK4/6 complexes in early G_1 phase. Cell adhesions subsequently activates RhoA which in turn downregulates $p21^{cip1}$ expression through an ERK- and p53-independent mechanism (Bottazzi *et al*., 1999).

In addition, Rho activation downstream of growth factor stimulation is proposed to stimulate cyclin-E-CDK2 activation which directs $p27^{kip1}$ for degradation by

phosphorylation during the late G_1,S,G_2 phase (Sheaff *et al*., 1997). Alternatively, Rho may inhibit $p27^{kip1}$ protein synthesis by regulating translation via a Rho-responsive element at the 3' untranslated region (UTR) in the $p27^{kip1}$ mRNA (Vidal *et al*., 2002). Recent work suggests that RhoA conveys cell shape-dependent control of the F-box protein, Skp2 and is required for ubiquitination-dependent degradation of $p27^{kip1}$. This in turn promotes G_1 progression and implicates ROCK and mDia in mediating cell growth by coupling cell shape with cell cycle progression (Mammoto *et al*., 2004).

1.2.6.3.4. Convergence of Rho and Wnt signaling pathways during cancer development

Mutations in components of Wnt signaling result in defective Wnt/β-catenin/T cell factor (TCF) signaling and have been implicated in tumourigenesis (reviewed in Malliri and Collard, 2003). The axin/APC/GSK-3β complex regulates the phopshorylation state of β-catenin downstream of Wnt signaling. β-catenin phosphorylation by GSK-3β targets it for ubiquitination and subsequent proteolytic degradation. Upon stimulation by Wnt factors, the Frizzled (Fz) receptors downregulate GSK-3β through an adaptor protein, Dishevelled (Dvl) resulting in the stabilization of β-catenin which translocates to the nucleus to direct transcription in concert with the TCF family of DNA-binding proteins. Subsequent constitutive transcriptional activation and overexpression of Wnt-responsive genes result in cell proliferation and oncogenic transformation. In addition, Dvl can also mediate Wnt-Fz activation of Rac and Rho signaling pathways to promote morphogenetic movements during vertebrate gastrulation (Habas *et al*., 2003). Other components of the Wnt signaling can also participate in the Rho signaling pathways. Wnt/Fz can regulate the

expression of several components of Rho signaling like the Rac-specific GEF, Tiam1 and a Cdc42-like GTPase, Wrch-1 (Tao *et al*., 2001). As previously discussed, APC can bind and enhance the GEF activity of the Rac-specific Asef thus enhancing microtubule assembly while downregulating E-cadherin-mediated cell-cell adhesions. In addition, downregulation of GSK-3β through the Par6-aPKC complex promotes microtubule stability that aids the establishment of cell polarity downstream of Cdc42 activation. Collectively, the multiple activities of Dvl, APC and GSK-3β in the Wnt/Rho signaling pathways contribute to cell movements in development and deregulated cell proliferation and motility in cancer development (**Figure 1.24**).

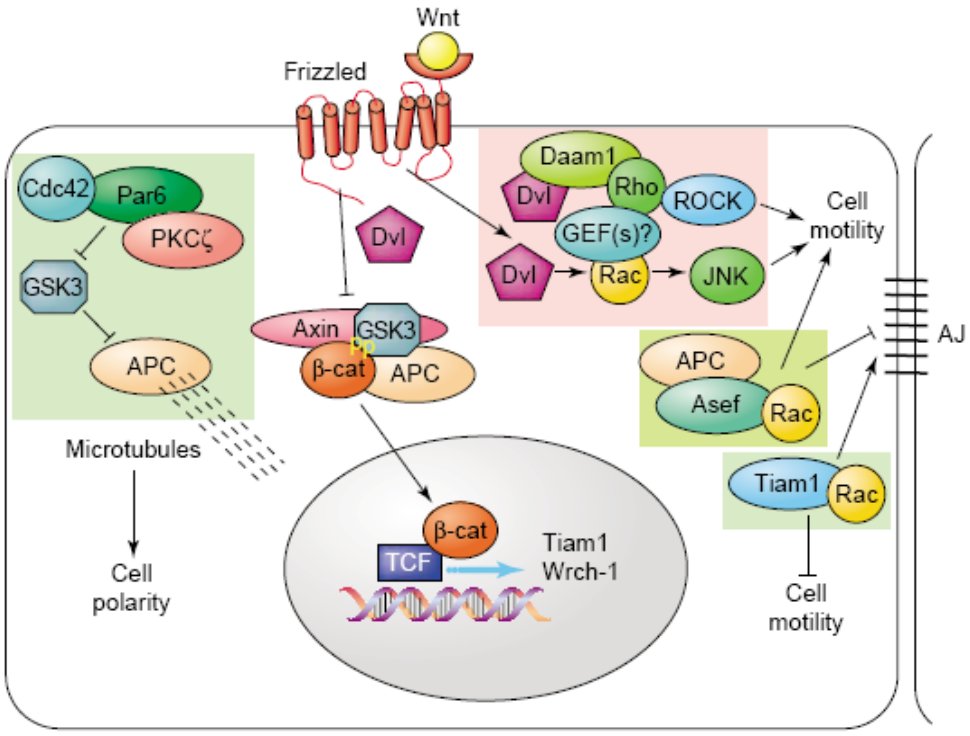

Figure 1.24. Convergence of Rho and Wnt signaling pathways. Dvl, APC and GSK-3β participate in multiple pathways which contribute to cell movements during development, cell proliferation and motility in cancer development. (Adatped from Malliri and Collard, 2004).

1.3. The BNIP-2 and BPGAP protein families

1.3.1. The BNIP-2 and Cdc42GAP Homology (BCH) domain

The BCH domain is a novel protein module first identified and characterized in this laboratory (Low *et al*., 1999; Low *et al*., 2000a; Low *et al*., 2000b). This unique protein domain is about 145 amino acids in length and was initially known to be conserved in two proteins: BCL2/adenovirus E1B 19kDa interacting protein 2 (BNIP-2) and p50-RhoGAP. We reported that a region in the C-terminus of BNIP-2 shares a significant level of homology to the non-catalytic domain of p50-RhoGAP (**Figure 1.25**). Interestingly, this region of p50-RhoGAP could bind Cdc42 but did not possess any GAP activity unlike its counterpart in BNIP-2. This led to the hypothesis that the BCH domain may represent a novel protein interaction domain regulating the functions of p50-RhoGAP and BNIP-2 via recruitment of different candidate proteins. In line with these findings, bioinformatics analyses indicate that this protein domain is highly conserved throughout evolution with representatives from *Saccharomyces cerevisiae*, *Plasmodium falciparum*, *Arabidopsis thaliana*, *Caenorhabditis elegans,* and *Homo sapiens* (Low *et al*., 2000b).

1.3.2. Functions and classification of the BCH domain-containing proteins

A previous survey of uncharacterized globular proteins including BNIP-2 and several GAPs and GEFs like the Neurofibromatosis type 1 (NF1) protein neurofibromin (White and O'Connell, 1991), Dbl's big sister (Dbs), Duo/Kalirin (Alam *et al*., 1997; Colomar *et al*., 1997) and Trio (Debant *et al*., 1996) revealed that these proteins contained regions that shared sequence similarity that was subtle yet statistically significant to the

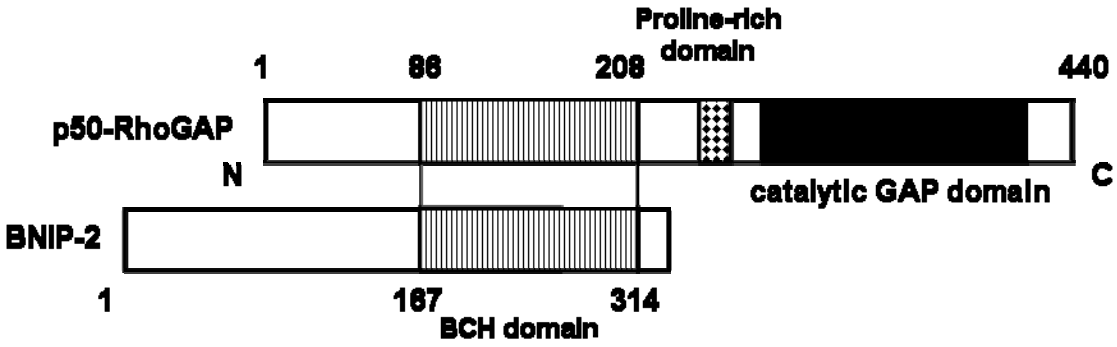

Figure 1.25. The BCH domain is involved in protein-protein interactions. Schematic diagram of homologous BCH domains in p50-RhoGAP and BNIP-2. (Adapted from Low *et al*., 1999).

lipid-binding domain of the *S. cerevisiae* phosphatidylinositol transfer protein, Sec14p (Aravind *et al*., 1999). Sequence analysis indicates that BNIP-2 shares ~17% sequence homology to Sec14p. These findings indicate possible lipid regulation of Ras and Rho GTPases. However, these properties have yet to be confirmed.

The *S. cerevisiae* Sec14p mediates phospholipid transfer between phosphatidylinositol and phosphatidylcholine in membrane lipid bilayers (Bankaitis *et al*., 1990). The Sec14p crystal structure was solved in a complex with *n*-octyl-β-D-glucopyranoside, a detergent molecule that is a putative analogue of endogenous substrates phosphatidylcholine and phosphatidylinositol (Sha *et al*., 1998). The Sec14p structure consists of an amino-terminus α-helical domain and a carboxyl terminus lipid-interacting α/β domain. Attempts to derive a functional interpretation of the relationships between the different subsets of Sec14p-like domain containing sequences were based on multiple alignments of the carboxyl terminus which indicate that the conserved β sheet may constitute a lipid-binding surface by directing lipid interactions through several key hydrophobic residues. The prevalence of a highly divergent amino-terminal α-helical domain led the conclusion that these proteins may have retained their ability to bind lipids but may lack phospholipid-transfer properties (Aravind *et al*., 1999).

Subsequent investigations have provided further insights into their biochemical functions. Genetic mapping of several neurofibromatosis-related mutations to a region corresponding to that of the *NF1* gene (Upadhyaya *et al*., 1997; Tassabehji *et al*., 1993) underscores the functional importance of the Sec14p-like region in the manifestation of a clinical phenotype. Aberrant neurofibromin has been attributed to tumour development in the nervous system and associated learning disabilities (Ozonoff, 1999). In addition, the

presence of Sec14p-like domains in Rho specific GAPs (p50-RhoGAP) and GEFs (Dbl, Duo and Trio) indicate lipid-mediated regulation of their catalytic activities and subcellular localization.

Consistent with this hypothesis, recent reports demonstrated that p50-RhoGAP undergoes an auto-inhibitory regulation of its activity through intra-molecular interactions involving its Sec14p-like/BCH domain (Moskwa *et al*., 2005). Furthermore, the Sec14p-like domain has been implicated in regulating the cellular distribution and transforming activity of Dbs (Kostenko *et al*., 2005) in addition to directing the subcellular localization of Dbl and Ost isoforms and their substrate Cdc42 (Ueda *et al.,* 2004). These findings provide insights into the role(s) of the Sec14p-like domain in directing RhoGEF-mediated spatial regulation of substrate activation. Taken together, it appears that the BCH domain is a lipid and/or protein interaction domain and represents a subset of the *S. cerevisiae* Sec14p lipid-binding domain whose function has diverged during evolution.

Given the diversity of BCH domain-containing proteins and other subsets of Sec14p-like domains, understanding the domain organization of these protein repertoires will provide greater insights into the functions of their homologous Sec14p-like domains. PFAM analyses of the protein database revealed that the subset of BCH domain-containing proteins can be divided into two distinct groups based on the position and distribution of the BCH domain (Low *et al.,* 2000b). We observed that Type I proteins contain a conserved C-terminus BCH domain while Type II proteins on the other hand contain a classical catalytic GAP domain distal to the N-terminus BCH domain (**Figure 1.26**). Systematic characterization of these proteins will provide greater insights into the function of the BCH domain in different contexts. Currently, this laboratory has identified and

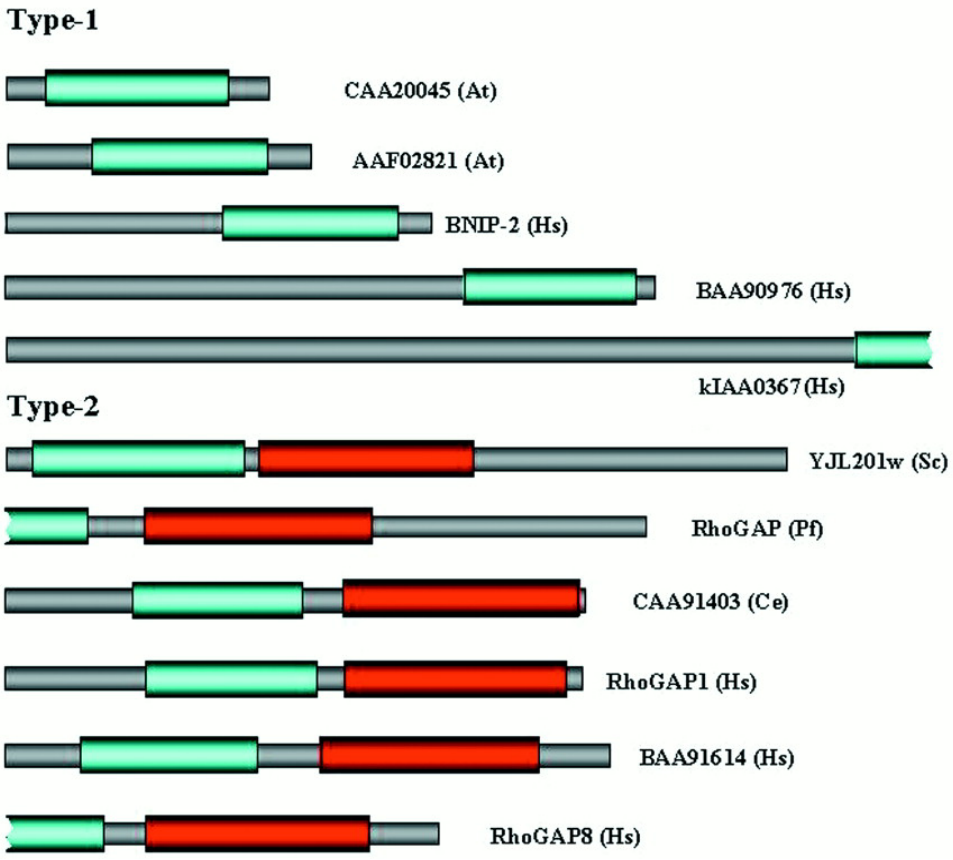

Figure 1.26. Domain organization of BCH domain-containing candidate genes and classification based on BCH domain location. The BCH and RhoGAP catalytic domains are indicated as green and red, respectively. Species abbreviations used are: Sc, *S. cerevisiae*; Pf, *P. falciparum*; Ce, *C. elegans*; At, *A. thaliana*; and Hs, *H. sapiens*. (Adapted from Low *et al*., 2000b).

characterized several Type I members including BNIP-2 and BNIP-S as well as a Type II member, BPGAP1 as described below.

1.3.3. BNIP-2: the prototypical BCH-domain containing protein

The cellular roles of BCH-domain containing proteins have been extensively delineated in BNIP-2. First identified in a yeast two-hybrid screen as a cellular target of the adenoviral E1B 19kDa protein and the B-cell CLL/lymphoma 2 (Bcl-2) protein, BNIP-2 was proposed to be involved in cell survival in line with the anti-apoptotic functions of E1B 19kDa and Bcl-2 (Boyd *et al*., 1994). Interestingly, BNIP-2 overexpression was found to induce cell death that could be rescued by Bcl-2 (Garnier *et al*., 1997) leading to speculations that BNIP-2 exerts its pro-apoptotic effects by functioning as a cysteine protease. Alternatively, changes to the equilibrium of BNIP-2 and Bcl-2 levels may trigger apoptosis (Belcredito *et al*., 2000; Meda *et al*., 2000). In addition, BNIP-2 gene expression has been shown to be negatively regulated by estradiol stimulation in different cell types (Garnier *et al*., 1997; Vegeto *et al*., 1999; Belcredito *et al*., 2000; Meda *et al*., 2000) and during murine brain development and maturation (Belcredito *et al*., 2001). These studies indicate the involvement of BNIP-2 in neural cell apoptosis and its correlation to neurodegenerative diseases such as Alzheimer's disease. BNIP-2 has also been implicated in coxsackievirus B3 (CVB3)-induced myocarditis (Yang *et al*., 1999). Further investigations suggest that BNIP-2 induces caspase-dependent apoptosis which inhibits CVB3 replication (Zhang *et al*., 2001). More recently, a survey of gene expression profiles indicates that BNIP-2 is downregulated during mouse lung tumor progression (Bonner *et a*l., 2004).

BNIP-2 was identified by our group as a putative substrate of the fibroblast growth factor receptor (FGFR) and is tyrosine phosphorylated upon growth factor stimulation (Low *et al*., 1999). Furthermore, BNIP-2 could directly bind p50-RhoGAP and mutually compete for Cdc42 binding. Interestingly, we showed that BNIP-2 could function biochemically as a weak GAP, stimulating the intrinsic GTPase activity of Cdc42 albeit at a much lower level compared to conventional GAPs. These activities of BNIP-2 were found to be negatively regulated by tyrosine phosphorylation. Taken together, these results suggest that BNIP-2 may mediate novel mechanisms coordinating RTK signaling, small monomeric G proteins and cellular events like apoptosis.

Further investigations to delineate the mechanisms underlying BNIP-2 GAP activity revealed that its BCH domain could function as a non-canonical GAP domain with a novel arginine finger motif, (235)RRLRK(239) and targeting Cdc42 through a separate motif, (288)EYV(290) found adjacent to the catalytic motif (Low *et al*., 2000a). In addition, we observed that BNIP-2 and p50-RhoGAP could form homo- and heterophilic interactions via their conserved BCH domains which negatively regulate the GAP activity of both proteins (Low *et al*., 2000b). Deletion studies revealed that a third motif, (217)RRKMP(221) was responsible for homodimer formation independent of its intrinsic GAP activity and ability to bind Cdc42. In line with these findings, an extended region flanking the Cdc42 binding motif within the BCH domain was recently identified to mediate both BNIP-2/Cdc42 interaction and elicit BNIP-2 induced cell morphological changes (Zhou *et al*., 2005a) (**Figure 1.27**). These results demonstrate that the BCH domain contains multiple recognition motifs.

Transient expression of the BNIP-2 BCH domain was sufficient to elicit membrane

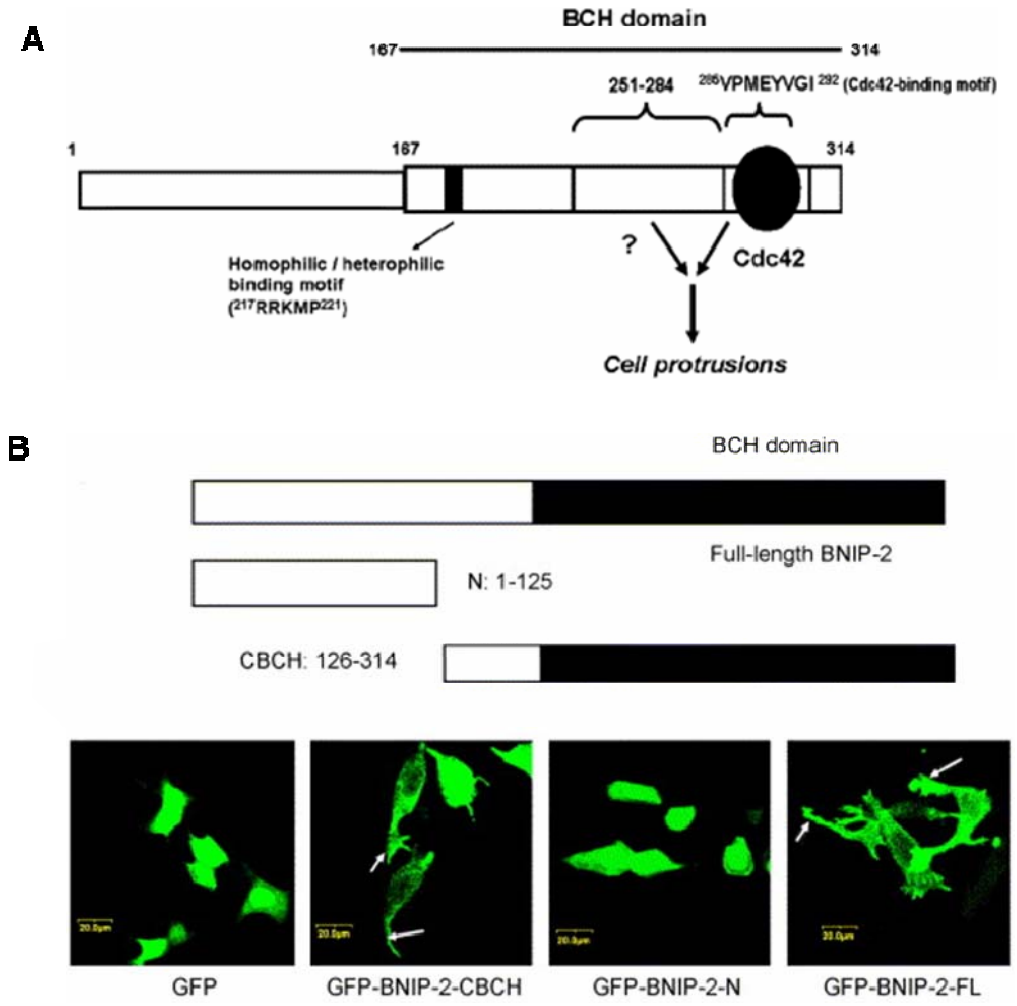

Figure 1.27. The BNIP-2 BCH domain contains multiple signalling motifs to mediate different cellular effects. (a) Schematic diagram of motifs important for homo- and heterodimer formation, Cdc42 binding. (b) The BNIP-2 BCH domain is sufficient to elicit membrane protrusions and cell elongation. (Adapted from Zhou *et al*., 2005a).

protrusions and cell elongation with BNIP-2 localized in punctate vesicles and concentrated at the protrusive ends of extensions (**Figure 1.27**). Interestingly, these morphological effects could be inhibited by the isolated PAK-CRIB domain suggesting that the recruitment of Cdc42 via the BCH domain is necessary for the activation of Cdc42 effector pathways. Taken together, these results indicate that BNIP-2 utilizes different motifs within its BCH domain to exert its roles in modulating and activating Cdc42 signaling pathways.

1.3.4. BNIP-S: a mediator of cell apoptosis

Two alternatively spliced isoforms of BNIP-2-Similar (BNIP-S) was identified based on their homology to BNIP-2 (Zhou *et al.,* 2002). The two protein isoforms were designated BNIP-Sα and BNIP-Sβ with the latter lacking an intact BCH domain at its C-terminus (**Figure 1.28**). Genome analysis revealed that the abrupt loss of the C-terminus was due to the introduction of a nonsense intron during RNA splicing in BNIP-Sβ. Semi-quantitative RT-PCR in established cell lines indicates that both BNIP-S isoforms have differential expression profiles where high expression of one is accompanied by the weak expression of the other. In addition, weak expression of BNIP-Sα and not BNIP-Sβ was detected in mouse organs with elevated levels in the penis. These findings are in contrast to that of BNIP-2 which is ubiquitously expressed and suggest that BNIP-S isoforms may have different cellular functions. Interestingly, when introduced into cells, BNIP-Sα but not BNIP-Sβ induced extensive cellular apoptosis, exhibiting the hallmark cell rounding phenotype. Further investigations include Hoeschst dye staining for nuclear condensation and annexin V detection of externalized phosphatidylyserine to the cell surface. These

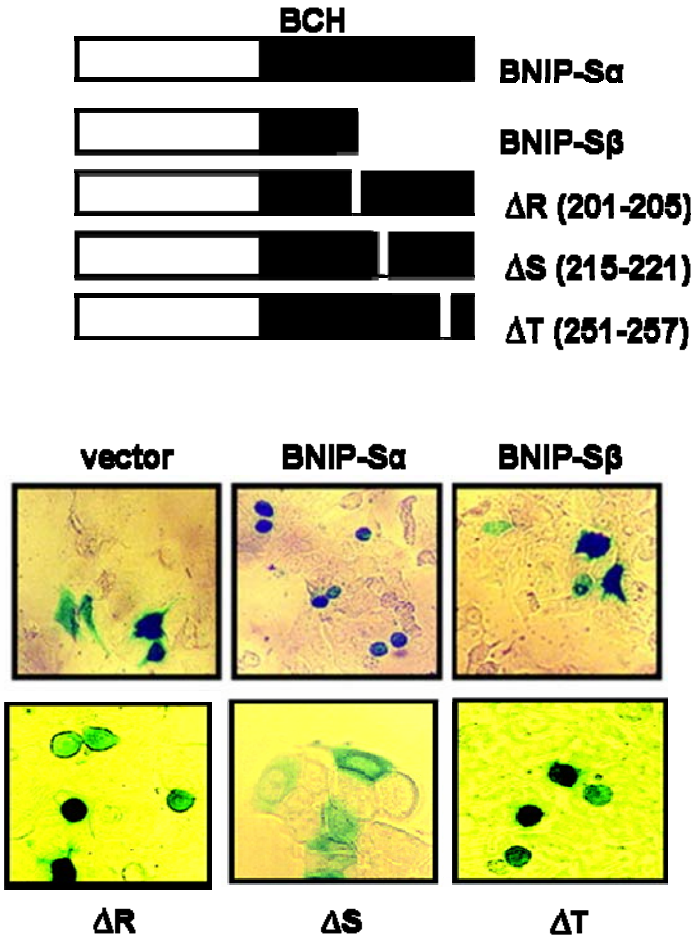

Figure 1.28. Differential cellular effects of BNIP-S isoforms. (a) Schematic diagram of BNIP-Sα, BNIP-Sβ and the BCH domain deletion mutants. (b) BNIP-Sα induces cell rounding phenotype in β-galactosidase marker assays via an apoptosis-inducing motif in its BCH domain. Deletion of this region (ΔS) aborogates BNIP-Sα-mediated apopotosis. (Adapted from Zhou *et al*., 2002).

indicators associate with events early in the apoptotic pathways, confirming the role of BNIP- Sα as a mediator of cellular apoptosis (**Figure 1.29**). Furthermore, these results also indicate that the lack of a complete, functional BCH domain in BNIP-Sβ abrogated the pro-apoptotic effects seen in BNIP-Sα.

In addition, we demonstrated that the pro-apoptotic effects of BNIP-Sα can be attributed to its BCH domain alone and delineated an apoptosis-inducing motif within the BCH domain of BNIP-Sα (**Figure 1.28**). As expected, this motif lies in a region of the BCH domain that is absent in BNIP-Sβ. In addition, we demonstrated the involvement of this motif in BNIP-Sα homodimer formation. Taken together, these results indicate a requirement for BCH domain-mediated homo- and heterophilic interactions in pro-apoptotic events. Interestingly, BNIP-Sα does not associate with or inhibit the effects of the pro-survival Bcl-2 and Bcl-xL indicating that BNIP-Sα promotes apoptosis through caspase-independent pathways. Furthermore, an alternatively spliced variant designated BNIPL-2 which differs from BNIP-Sα at its N-terminus has been speculated to mediate apoptosis via its interactions with Bcl-2 and p50-RhoGAP unlike BNIP-Sα (Qin *et al*., 2003). In addition, overexpression of BNIPL-2 in Hep3B hepatocellular carcinoma cells was found to induce the differential expression of genes involved in cell growth, proliferation, differentiation and apoptosis (Xie *et al*., 2004).

In an attempt to elucidate the mechanisms underlying BNIP-Sα function, our group has recently delineated a region in the proximal part of the BCH domain that mediates exclusive binding to RhoA (Zhou e*t al*., 2005b). Interestingly, this region also encompasses the p50-RhoGAP binding motif. Further investigations indicate that RhoA and p50-RhoGAP can mutually compete for BNIP-Sα binding. In line with these findings,

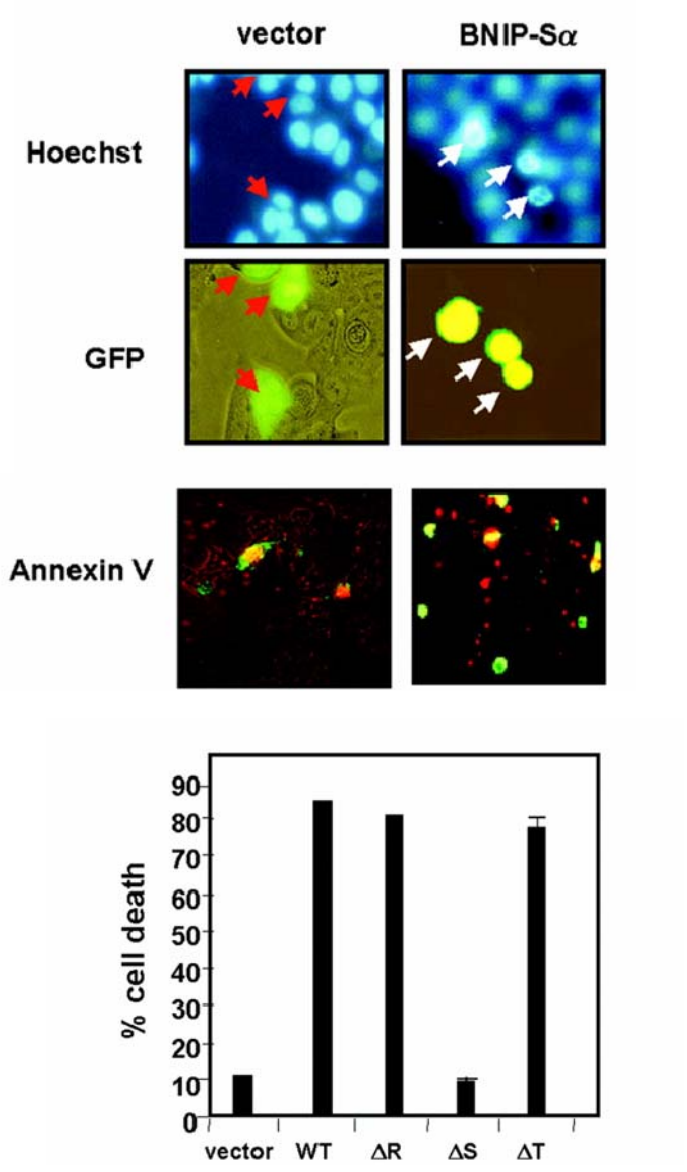

Figure 1.29. Pro-apoptotic effects of BNIP-Sα. (a) Hoeschst dye staining showing nuclear condensation and annexin V staining on cell membrane confirm BNIP- Sα expressing cells are undergoing apoptosis. (b) Deletion of S-region within the BCH domain abrogates the apoptotic effects of BNIP- Sα. (Adapted from Zhou *et al*., 2002).

BNIP-Sα mutants lacking motifs for RhoA and/or p50-RhoGAP binding failed to elicit the cell rounding phenotype suggesting that the pro-apoptotic effects of BNIP-S is mediated by RhoA activation. It was proposed that different pools of BNIP-S may work in concert for RhoA binding and p50-RhoGAP sequestration. Taken together, these results suggest that multiple motifs within the BNIP-Sα BCH domain act cooperatively to promote pro-apoptotic events by activating RhoA pathway necessary for cell rounding. In addition, yeast-two hybrid library screening has identified the Macrophage Migration Inhibitory Factor (MIF) and the Augmenter of liver regeneration (GFER) as novel BNIP-Sα interacting partners (Shen *et al*., 2003) suggesting that BNIP-Sα may regulate cell proliferation through apoptosis in concert with these cytokines.

1.3.5. BNIP-H: a tissue specific member of the BNIP-2 family

BNIP-2-Homology (BNIP-H) or Caytaxin is a tissue-specific member of the BNIP-2 family first identified in this laboratory. Unlike currently known members, BNIP-H/Caytaxin is exclusively expressed in the brain (Zhou and Low, unpublished results). Consistent with these findings, genetic studies indicate BNIP-H/Caytaxin expression is neuron-specific and mutations at the locus on 19p13.3 results in the development of a congenital form of ataxia found distinctively in the Grand Cayman Islands (Bomar *et al*., 2003). Interestingly, the authors also suggest that the phenotype of Cayman ataxia correspond to that of the recessive ataxic mouse mutant, '*jittery*'. Work is currently in progress in our group to delineate the function of this novel protein and the roles of the BCH domain in neuronal development. Unlike BNIP-2 and BNIP-Sα which target Cdc42 and RhoA, respectively, BNIP-H does not interact with Cdc42, RhoA or Rac1 and its

GTPase target currently remains elusive.

1.3.6. BPGAP1: a multi-domain integrator of GTPase signaling

As its name suggests, this novel ubiquitously expressed RhoGAP protein, BCH domain-containing, Proline-rich and Cdc42GAP-like protein subtype-1 (BPGAP1) maps to the same locus as human ARHGAP8 on band 22q13.31 and harbors a BCH/Sec14p-like domain at its N-terminus. Besides this, it also possesses a classical catalytic GAP domain with a highly conserved 'arginine finger' motif and a proline-rich sequence that lies between these two domains (Shang *et al*., 2003). Co-workers in our group demonstrate that besides enhancing the GTPase activity of RhoA both *in vivo* and *in vitro*, BPGAP1 also targets Cdc42 and Rac1. The introduction of a mutation at R232A abrogates its ability to catalyse GTP hydrolysis, consistent with previous reports that the 'arginine finger' confers the catalytic activity of other functional GAPs (Nassar *et al*., 1998; Gamblin and Smerdon, 1998; Fidyk and Cerione, 2002). More recently, alternatively spliced variants of ARHGAP8 which differ in their BCH domains have been shown to be differentially upregulated in colorectal tumors (Johnstone *et al*., 2004) suggesting a possible link between GAP activity and the regulation of cancer progression.

The multidomain architecture of BPGAP1 suggests that it could coordinate multiple cellular events via selective interactions with target proteins through these domains. This raises the possibility that BPGAP1 could regulate the activities of Cdc42 and Rac1 even though they are not its substrates. Consistent with this hypothesis, we provide evidence that dominant negative mutants of Cdc42 and Rac1 could inhibit BPGAP1-induced pseudopodia formation. Conversely, RhoA activation inhibits the

formation of long pseudopodia while Cdc42 and Rac1 activation potentiates the appearance of drastic neurite-like extensions consistent with morphological changes associated with BPGAP1. Interestingly, the isolated BCH and GAP domains initiated the formation of short and long pseudopodia, respectively (**Figure 1.30**). Further analysis revealed a requirement for the central proline-rich region for initiation of cell migration. In this regard, we raised the possibility that BPGAP1 could function in recruiting Cdc42, Rac1 and other signaling components necessary for the activation and propagation of Cdc42 and/or Rac1 mediated pathways.

To elucidate the molecular mechanisms underlying BPGAP1 function, matrix-assisted laser desertion/ionization mass spectrometry/time of flight (MALDI/IMS/TOF) identified cortactin as a novel BPGAP1 interacting partner (Lua and Low, 2004). Like BPGAP1, cortactin is a multi-domain protein and has been implicated as a key regulator of actin rearrangments especially through binding of multiple protein targets at its C-terminus SH3 domain (reviewed in Lua and Low, 2005a; Bershadsky, 2004; Daly, 2004). Progressive deletion studies demonstrate the involvement of the BPGAP1 proline-rich region for binding to the SH3 domain in cortactin. The authors also show that BPGAP1 facilitates cortactin translocation to the periphery coupled with enhanced cell migration. Taken together, these results provide evidence that BPGAP1 promotes efficient cell migration through its interactions with protein components of the cytoskeletal network. **Figure 1.31** is a schematic diagram of a model outlining the roles of BPGAP1 in cell dynamics. More recently, co-workers demonstrate that BPGAP1 also targets the SH3 domain of EEN/endophilin-II through the same proline-rich region and collaborate with its GAP domain to regulate endocytosis whereby co-expression of BPGAP1 and EEN

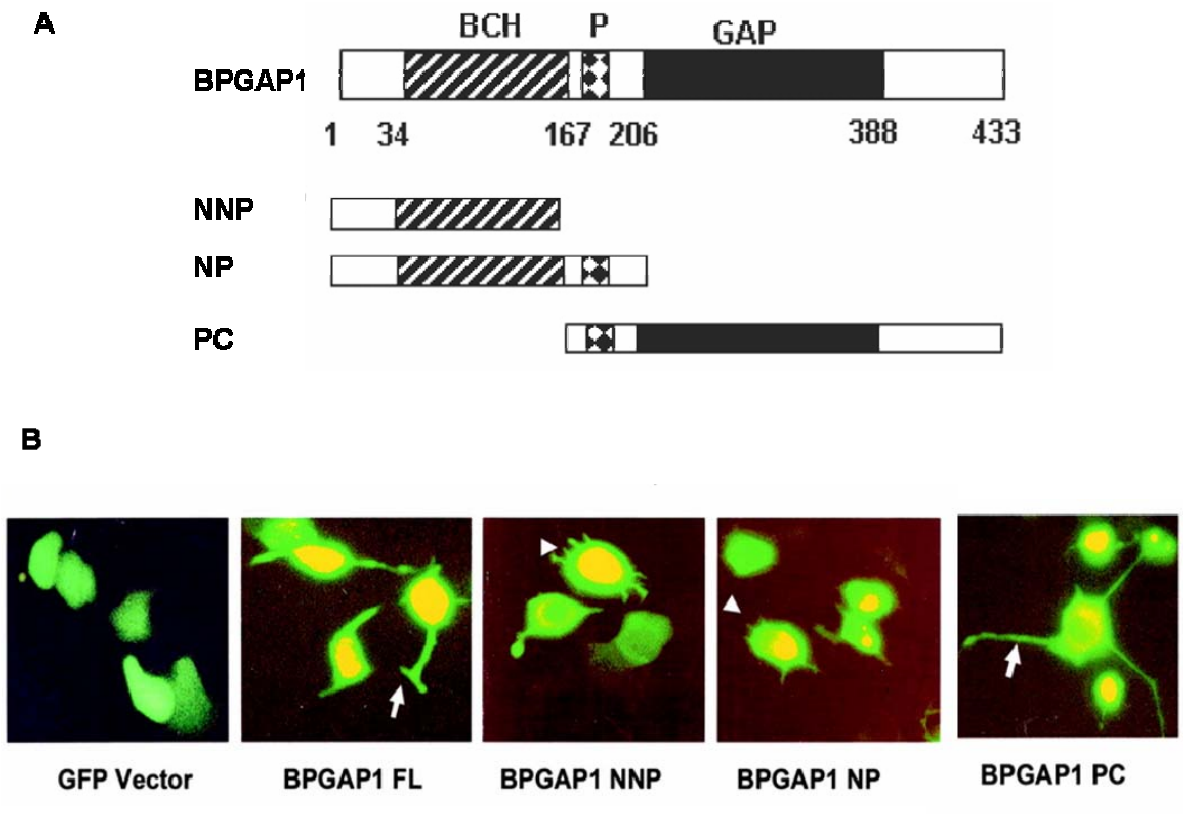

Figure 1.30. BPGAP1 induces unique pseudopodia via its BCH and GAP domains. (a) Schematic diagram of the domain layout of BPGAP1. (b) MCF7 cells were transfected with different fragments of BPGAP1 and visualized by direct fluorescence microscopy 16 h post transfection. (Adapted from Shang *et al*., 2003).

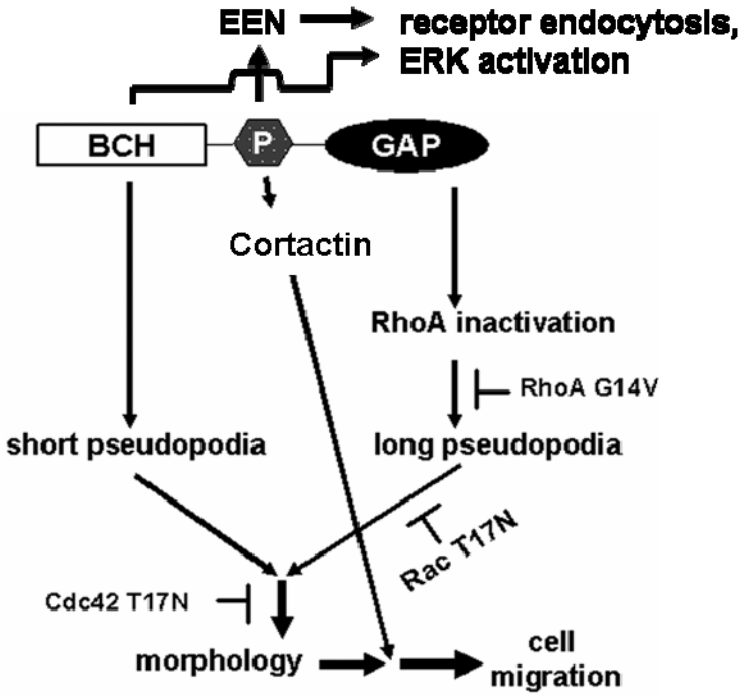

Figure 1.31. BPGAP1 is a multi-domain integrator of Rho GTPase signaling. Proposed model of BPGAP1 function in cell dynamics regulation. (Adapted from Shang *et al*., 2003; Lua and Low, 2004; Lua and Low; 2005b).

enhanced EGF-stimulated receptor endocytosis and ERK1/2 activation (Lua and Low, 2005b). These findings indicate that BPGAP1 plays multiple roles in regulating distinct GTPase signalling pathways linking the cytoskeletal network to endocytic trafficking and the Ras/MAPK signaling pathways.

1.4. Hypothesis and aims of study

The current review indicates that BCH domain-containing proteins can mediate diverse effects on cell morphology, motility and cell survival in association with Rho GTPase-mediated actin cytoskeleton remodelling. These proteins have been divided into two groups on the basis of their domain architecture. The Type I family currently consists of three members closely related to the prototypic BNIP-2 at amino acid level while BPGAP1 and p50-RhoGAP are the main Type II members containing other domains and motifs in addition to the BCH domain. Interestingly, while the regions encompassing the BCH domain remain conserved during evolution, they appear to mediate different aspects of cell dynamics when present in different proteins.

BNIP-2 targets Cdc42 producing characteristic protrusive phenotypes whilst BNIP-S isoforms direct their pro-apoptotic effects via associations with RhoA. Both however, mediate these cell morphological changes through the Rho family GTPases. Thus, we asked the question: what are the implicit differences amongst these BCH domains that allow specificity to GTPase binding and the implication of this relationship to actin cytoskeletal dynamics? Intriguingly, the BCH domain of BNIP-2 also functions as a non-canonical GAP for downregulating Cdc42. Furthermore, deletion studies have mapped the GTPase binding and GAP activity to individual motifs within the BCH. Studies in BPGAP1 also indicate that the BCH domain can coordinate adjacent signaling domains to induce distinct cellular phenotypes which are prerequisites for cell motility. This is further supported by recent findings that the BCH domains of BPGAP1 (Shang *et al*., 2003) and p50-RhoGAP (Moskwa *et al*., 2005) can form intramolecular interactions that limit their activities Thus, it would seem possible that the BCH domain location directs the

recognition of different binding partners and exerts its effects in concert with flanking sequences.

Identification of novel BCH-domain containing proteins is expected to provide further insights into the function and mechanisms that govern the activities of this protein module and the evolutionary implications of these functional differences in comparison to the Sec14p-lipid binding domain. Both share sequence similarity (~17%) and may have diverged from a common ancestor in response to cellular needs. Aberrant Rho GTPase signaling has been implicated in cancer development and neurological disorders. The identification of BNIP-H gene mutations and its association with the onset of Cayman ataxia indicates the involvement of BCH domain-containing proteins in developmental events and disease progression.

Here, we hypothesize that novel BNIP-2 family members could confer certain aspects of cell morphogenesis by targeting selective GTPases. The mechanism of which will be elucidated here. Specifically, we aim to:

- identify novel BCH domain-containing proteins *in silico*;
- clone and express BNIPXL full length cDNA that codes for a novel BCH protein;
- determine the mRNA expression profile of BNIPXL and the possible existence of splicing variants in various human cell lines and tissues;
- investigate the nature of protein-protein interactions of BNIPXL with its target(s) *in vitro* and *in vivo*;
- delineate regions responsible for such interactions;
- examine the cellular effects of BNIPXL; and
- elucidate the potential function and mechanisms underlying these effects.

Materials and Methods

2. Material and Methods

Reagents used were of analytical grade, and standard protocols for molecular manipulations and media preparation were as described previously (Sambrook and Russell, 2001).

2.1. Bioinformatics analyses

Novel proteins that contain homologous BCH domains were identified by position-specific iterative BLAST (PSI-BLAST) (Altschul *et al*., 1997) search against the current non-redundant sequence database and human expressed sequence tag (EST) database at the National Center for Biotechnology Information (http://www.ncbi.nlm.nih.gov/blast) as described previously (Low *et al.,* 2000b). Multiple sequence alignments and phylogenetic analyses were generated using Vector NTI Suite while pairwise global alignments were generated using the Stretcher program from EMBOSS (available at mirror site: http://sbcr.bii.a-star.edu.sg/emboss/). Genome analysis was generated using the Human Genome BLAST (http://www.ncbi.nlm.nih.gov/genome/seq/HsBlast.html).

2.2. DNA amplification and cloning of BNIPXL

Full length BNIPXL cDNA was amplified by polymerase chain reaction (PCR) using the Expand Long Template PCR System (Roche Molecular Biochemicals) from BD Marathon Ready adult human brain and kidney cDNA libraries (CLONTECH, Palo Alto, CA) using the forward primer (5'-ATGGCTTTGTTTGATGGTGATCC-3') and reverse primer (5' CTTCTTCCAGCATGGCCAACTAAGGC-3') with *Xho*I (forward) and *Not*I (reverse) restriction sites to facilitate subsequent cloning. A 50µL reaction mix containing 10X Expand Long Template Buffer 2, 10mM dNTP mix, 3.75U Expand Long Template

enzyme mix, 1μL cDNA library and 5mM forward and reverse primers were subjected to the following PCR conditions: initial denaturation at 94 °C, 4 min; annealing at 55°C, 30 s; extension at 68 °C, 4 min; subsequent cycling (30 cycles) at 94 °C, 40 s; annealing at 55 °C, 30 s; extension at 68 °C, 4 min; and final extension at 68 °C, 10 min. BNIPXL fragments were generated from the full-length template using various combinations of PCR primers with *Xho*I (forward) and *Not*I (reverse) sites with the same cycling conditions. In addition, BNIPXL deletion mutants were generated by outward PCR using primers incorporating *Nhe*I sites flanking the region to be excluded. The PCR products were separated by gel electrophoresis.

DNA gels were cast using regular ultra-pure electrophoresis-grade agarose (Invitrogen Corp., San Diego, CA). 1%-1.5% (w/v) agarose was dissolved in Tris acetate EDTA (TAE) buffer (0.04M Tris acetate, 1mM EDTA) supplemented with ethidium bromide (0.5μg/mL). Samples were mixed with a suitable amount of a 6X DNA gel loading dye (1X TAE, 30% (w/v) glycerol, 0.25% (w/v) bromophenol blue, 0.25% (w/v) xylene cyanol FF) and loaded alongside GeneRuler™ 1kb DNA Ladder (Fermentas UAB, Vilnius, Lithuania). Routine DNA gel electrophoresis was performed in the same buffer and the gels were viewed using a ultraviolet transilluminator (UVItec Limited, Cambridge, UK) and documented using a thermal printer (Mitsubishi Corp., Tokyo, Japan).

Fragments of the expected size were excised and purified using the QIAquick Gel Extraction Kit (QIAGEN GmbH, Germany) according to manufacturer instructions. The PCR products were cloned into the pXJ40-FLAG or pXJ40-HA and pXJ40-GFP mammalian expression vectors containing the cytomegalovirus (CMV) enhancer and promoter, the Kozak initiation and N-terminus FLAG or HA epitopes, respectively (**Figure**

2.1, courtesy of Dr. E. Manser, Glaxo-IMCB Laboratory, Institute of Molecular and Cell Biology, Singapore). A 10μL ligation mix containing 10X T4 ligase buffer, 1U of T4 ligase (New England BioLabs, Beverly, MA), 20ng of insert DNA and 50ng of vector was incubated overnight at room temperature and transformed into competent *Escherichia coli* strains, XL1-blue or DH5α.

Prior to transformation, competent cells were prepared according to Sambrook and Russell, 2001. A single colony was selected and cultured overnight at 37°C in 5mL Luria Bertani (LB) nutrient broth medium (5g/L NaCl, 10g/L tryptone, 5g/L yeast extract). The overnight culture was diluted (1:6000) in fresh LB medium and grown at 37°C until log phase ($O.D._{600}$ = 0.3-0.6). The bacterial pellet was collected by centrifugation at 3,500g for 10 min at 4°C and reconstituted in 1:20 volume of ice-cold sterile TSS (LB broth [pH 6.5], 10% (v/v) PEG 3,350, 5%(v/v) DMSO, 10mM $MgCl_2$, 10mM $MgSO_4$). Aliquots were stored at -70°C for subsequent use. For transformation, 5μL of the ligation mixture was incubated with 30μL each of KCM (100mM KCl, 30mM $CaCl_2$, 50mM $MgCl_2$) and competent cells on ice for 1 h and plated onto LB-agar supplemented with 100mg/L of ampicillin. Plates were incubated overnight at 37°C and single colonies selected for further analysis.

2.3. Plasmid DNA isolation, restriction and sequencing analysis

Plasmid DNA was isolated using the QIAprep Spin Miniprep Kit (QIAGEN) according to manufacturer instructions. The protocol is based on the alkaline lysis method originally described by Birnboim and Doly, 1979. Sodium dodecyl sulphate (SDS) and

A

>>>CMV enhancer/ Promoter/β-globin intron (non-coding)/T7/Epitope tag /Mulitple cloning sites/Polyadenylation signal sequence >>>

B

/*EcoR*I/ …….....HA epitope tag……./*BamH*I

T7 GAATTC ACC ATG GTC CCA TAC GAC GTG CCA GAC TAC GCA GGA TCC
Kozac M V P Y D V P D Y A G S

/ *Hind*III / *Xho*I / *Not*I / *Sma* I / *Pst*I / *Sac*I / KpnI / *Bgl* II

AAG CTT CTC GAG GCG GCC GCC CCG GGC TGC AGG AGC TCG GTA CC AGATCT
K L L E A A A P G C R S S V P D

C

ATG GAC TAC AAG GAC GAC GAT GAT AAG GGC
M D Y K D D D D K G

Figure 2.1. (a) Schematic diagram of the pXJ40 vector map. Transcription is driven by CMV enhancer/promoter and Kozak initiation upstream of a non-coding β-globin intron followed by an epitope tag, multiple cloning site (MCS) and a SV40 polyadenylation signal sequence. (b) Multiple cloning sites of the pXJ40 vector series constructed from parent plasmid (Xiao *et al.,* 1991). The *Sac*I site is not unique to the polylinker (Manser *et al.,* 1997). (c) The FLAG epitope tag sequence in the pXJ40-FLAG vector.

NaOH was used in denaturation of bacterial cell wall proteins, choromomal and plasmid DNA. Addition of potassium acetate results in neutralization and preferential annealing of covalently closed plasmid DNA whilst chromosomal DNA and bacterial proteins precipitate with SDS and potassium to form a complex which is removed by centrifugation. Plasmid DNA is then recovered through a cationic affinity chromatography column, purified and eluted. In brief, 5mL overnight cultures of recombinant colonies were pelleted by centrifugation and re-suspended in the cell resuspension solution (50mM Tris [pH 7.5], 10mM EDTA, 100μg/mL RNase A). The cell lysis solution (0.2M NaOH, 1% (w/v) SDS) was added and the suspension mixed by inversion. Neutralisation solution (1.32M KOAc) was added to the suspension, mixed gently and centrifuged at 13,000g to remove cell debris. The cleared lysate was applied to the QIAprep spin column and briefly centrifuged to aid passage of lysate through the column. The column was washed with PE buffer (80mM potassium acetate, 8.3mM Tris-Cl [pH 7.5], 40μM EDTA, 55% (v/v) ETOH). Excess PE buffer was removed by further centrifugation. The plasmid DNA was then eluted from the resin with 50μL of sterile water. Plasmid concentrations were calculated at O.D. $_{260}$ for use in subsequent experiments and the purified DNA was stored at -20° C.

Putative clones were identified using restriction enzyme digestion and verified through bi-directional DNA sequencing using the ABI PRISM BigDye Terminators v 3.0 (Applied Biosystems, Foster City, CA). A 5μL reaction mixture containing 70ng of plasmid DNA and 1.6mM of primer was subjected to the following PCR conditions (25 cycles): denaturation at 96°C, 30 s; annealing at 50°C, 15 s and extension at 60°C, 4 min. The amplified products were precipitated for 15 min at room temperature with 80μL of

ethanol/sodium acetate solution (3μL of 3M NaOAc [pH 4.6], 75% (v/v) ETOH). The mixture was centrifuged for 10 min at 13,000g and the supernatant aspirated. The pellet was washed with 500μL of 75% (v/v) ETOH, centrifuged for 5 min, supernatant aspirated and the pellet was air dried. DNA samples were re-suspended in 11μL of HI DI formamide, denatured for 2 min at 95°C and cooled on ice before loading. Sequencing was performed using the ABI PRISM™ 3100 DNA Sequencer (Applied Biosystems). Positive clones were propagated in *E. coli* and plasmids were purified using HiSpeed Plasmid Midi Kit (QIAGEN) according to manufacturer instructions.

2.4. Mammalian cell culture

HEK293T human embryonic kidney epithelial cells are a clonal derivative of the HEK293 adherent cell line stably expressing the SV40 large T antigen. This cell line is frequently used for production of recombinant proteins owing to its ease of transfection. HeLa is a human cervical cancer cell line. MCF-7, SK-BR3 and MDA-MB-231 are human epithelial breast cancer cell lines. All are mammary adenocarcinomas established from pleural effusions. MCF-7 are non-motile and exhibit morphologies resembling epithelial cells found in monolayers and are thus, excellent candidates for studying subcellular structures using fluorescence microscopy. SK-BR3 lacks E-cadherin expression while overexpressing the HER2/c-erb-2 gene product and are weakly invasive while the MDA-MB-231 is highly metastatic. These cell lines have been used in expression profiling studies to determine the significance of gene expression with their metastatic potential (Zajchowski *et al*., 2004).

HEK293T and MCF-7 (ATCC, Manassas, VA) and SK-BR3 human breast carcinoma cells (courtesy of T.L. Lo, Institute of Molecular and Cell Biology, Singapore) were maintained in RPMI-1640 (Hyclone, Logan, UT) medium supplemented with 10% (v/v) fetal calf serum (FCS) (Invitrogen Corp., San Diego, CA), 2mM L-Glutamine, 100U/ml penicillin and 100μg/ml streptomycin (Hyclone), and grown at 37°C in a 5% CO_2 atmosphere whereas HeLa was grown in high glucose Dulbecco's modified Eagle's medium (D-MEM) and MDA-MB-231 was maintained in D-MEM supplemented with 0.1mM non-essential amino acids (NEAA) and 1mM sodium pyruvate (Invitrogen Corp.). Cells were split to 80% confluence one day prior to subsequent manipulations.

2.5. Total RNA isolation and first strand cDNA synthesis

Cells were rinsed with cold phosphate-buffered saline (PBS) buffer (1.3M NaCl, 70mM Na_2HPO_4, 30mM NaH_2PO_4 [pH 7.4]) and total RNA isolated using the RNeasy Mini Kit (QIAGEN) according to manufacturer instructions. Briefly, cells were lysed in 600μL of buffer RLT supplemented with 1% (v/v) β-mercaptoethanol, aspirated several times through a sterile syringe and the total RNA was precipitated with 70% (v/v) ETOH before application to the RNeasy mini spin column. Column was centrifuged to aid passage of lysate followed by addition of buffer RWl and subsequent centrifugation. The bound RNA was washed twice with buffer RPE before elution in 30μL of RNase-free water. Total RNA (3μg) was denatured for 10 min at 80 °C and added to a reaction mix containing 32U avian myeloblastosis virus (AMV) reverse transcriptase, 5U RNAsin and 10mM dNTPs (Promega Corp., Madison, WI). First strand cDNA synthesis was primed

with oligo(dT) (Operon Biotechnologies, Inc. Alameda, CA) for 1 h at 42 °C and the cDNA was stored at -20° C for subsequent use.

2.6. Semi-quantitative reverse transcription PCR

Equal amounts of single-stranded cDNA was then subjected to PCR amplification with high fidelity, long-template DyNAzyme (Finnzymes Oy, Espoo, Finland) using the respective primers indicated. The glyceraldehyde-3-phosphate dehydrogenase (GAPDH) housekeeping gene was used to normalize the level of loading. PCR products were separated by electrophoresis using 1.5% (w/v) agarose gels and results were verified in at least two independent experiments with varying numbers of PCR cycles to ensure near-linear amplification.

2.7. Mammalian cell transfection, lysis and immunoprecipitation

Transient transfection was performed using FuGENE 6 transfection reagent (Roche Molecular Biochemicals) or LIPOFECTAMINE™ 2000 transfection Reagent (Invitrogen Corp.) according to manufacturer instructions. In brief, FuGENE 6 was diluted (1:30) in serum-free growth medium, mixed well and incubated for 5 min at room temperature. DNA plasmids were added to the cationic lipid mixture in the ratio of 2:3 (µg: vol), mixed well and incubated at room temperature for 15 min. The DNA-lipid complex was incubated with cells in serum-free medium at 37°C for 3 h followed by supplementation with 10% (v/v) serum. The cells were then incubated for 48 h before lysis. For transfections with LIPOFECTAMINE™ 2000, 2 µg of DNA plasmid and 5 µL of transfection reagent was diluted separately with 125 µL each of Opti-MEM® I reduced

serum medium (Invitrogen Corp.) for 5 min at room temperature. The mixtures were then combined and incubated for 20 min before addition to cells maintained in antibiotic-free, 10% (v/v) serum-containing growth medium for 48 h before lysis. Cells were lysed in cold lysis buffer (50 mM HEPES [pH 7.4], 150 mM sodium chloride, 1.5 mM magnesium chloride, 5 mM EGTA, 10% (v/v) glycerol, 1% (v/v) Triton X-100, 5 mM sodium orthovanadate, and a mixture of protease inhibitors) (Roche Molecular Biochemicals) and centrifuged at 13,000g for 10 min at 4°C. The supernatant was retained and used for subsequent experiments.

For immunoprecipitations, aliquots of cell extracts were analyzed as whole-cell lysates (25 μg) for protein expression or used in affinity precipitation experiments (500 μg) with anti-FLAG®M2 Affinity Gel (Sigma-Aldrich). 5μL of anti-FLAG antibody conjugate was added to each sample of cell extracts and incubated overnight at 4°C with rotation. The beads were spun down and washed three times with cold lysis buffer. The samples were then vortexed to release bound proteins and denatured at 95°C for 5 min in suitable amounts of 6X SDS-PAGE loading buffer (125mM Tris-HCL [pH 6.8], 15% (w/v) glycerol, 7.5% (v/v) β-mercapthoethanol, 0.15% (w/v) bromophenol blue) and separated by gel electrophoresis (**Figure 2.2**).

2.8. SDS-polyacrylamide gel electrophoresis and transfer

Polyacrylamide gels (10%-12.5%) were cast using 30% acrylamide/bis (37:5:1) solutions, N,N,N,N-tetramethyl-ethylenediamine (TEMED) as the accelerator (all from BioRad Laboratories, Hercules, CA) and 10% (w/v) ammonium persulphate (APS) (Invitrogen Corp.) as the polymerization catalyst. The top of the resolving gel was made

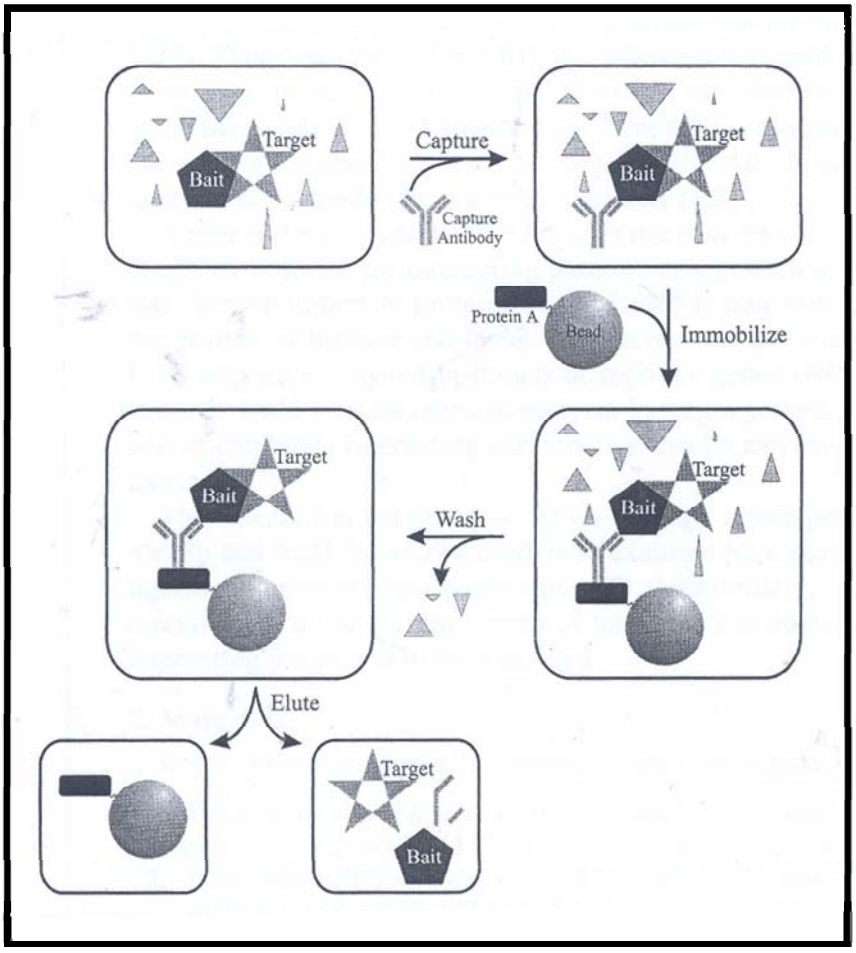

Figure 2.2. Schematic diagram of immunoprecipitation. Cell lysates serve as a source of target protein complexes and may contain non-specific proteins (small triangles). The bait complexes are captured using a specific antibody and the antibody-bait-target assembly is immobilized onto Protein A/G covalently attached to Sepharose beads. The beads are then washed to remove non-specific proteins and the antibody-bait-target conjugate is eluted by boiling in SDS-PAGE loading buffer. (Adapted from Masters, 2004).

even by layering with butanol and left to polymerize at room temperature for 45 min. The butanol was discarded and the resolving gel rinsed with water before addition of the stacking gel. The stacking gel with its large pore size has very little sieving effect, allowing the proteins to migrate and form a narrow band at the stacking/resolving gel interface (Johnstone and Thorpe, 1987; Hames, 1988). Samples were loaded alongside Precision Plus protein pre-stained standards (BioRad Laboratories) and gel electrophoresis performed using the Mini-PROTEAN 3 Electrophoresis System (Bio-Rad Laboratories) in Tris-glycine buffer (25mM Tris, 145mM glycine, 0.1% (v/v) SDS). A constant current of 40 mA per gel was applied until the dye front reached the bottom of the gel. Following electrophoresis, the size-fractionated proteins were transferred onto nitrocellulose membranes using a Trans-Blot cell (all from Bio-Rad Laboratories) in transfer buffer (25mM Tris, 195mM glycine, 0.1% (w/v) SDS, 20% (v/v) methanol). The membranes were pre-soaked in methanol and then rinsed in transfer buffer. The gel was sandwiched between one pre-equilibrated membrane and Whatman 3MM filters (Whatman plc., Middlesex, UK), assembled in the Trans-Blot cell and transferred at 100V for 90 min in 4° C.

2.9. Western blot analyses

Membranes were equilibrated in PBS-T buffer (1XPBS, 0.1% (v/v) Tween-20) and incubated in blocking buffer (PBS-T, 1% (w/v) bovine serum albumin [BSA]) either 1 h at room temperature or overnight at 4° C on an orbital shaker. Primary antibodies were diluted in sterile blocking buffer and incubated with the membranes for 90 min at room temperature on an orbital shaker. Primary antibodies used were anti-FLAG (monoclonal

and polyclonal; Sigma-Aldrich), polyclonal anti-HA (Zymed Laboratories, Inc., South San Francisco, CA), monoclonal anti-MYC (Roche Molecular Biochemicals), polyclonal anti-RhoA and monoclonal anti-Rac (Upstate Biotechnology, Inc., Lake Placid, NY), polyclonal anti-Cdc42 and polyclonal anti-GFP (both Santa Cruz Biotechnology, Inc., Santa Cruz, CA). All were diluted 1:1000 except for the anti-FLAG polyclonal antibody (1:10,000). The antibody solution was then removed, filter-sterilized and stored at 4° C for re-use.

The membranes were washed three times, 10 min each at room temperature with PBS-T buffer before incubation with the appropriate goat anti-mouse or anti-rabbit horseradish peroxidase-conjugated secondary antibodies (1:2000 dilution in PBS-T) (Sigma-Aldrich) for 1 h at room temperature with agitation. The membranes was then subjected to three additional, 10 min wash in PBS-T buffer. Membranes were incubated in enhanced chemiluminescence reagents (Pierce Biotechnology, Inc., Rockford, IL), according to manufacturer instructions and placed between transparency sheets. Signal detection was performed by exposure to X-ray film (Fuji Photo Film, Tokyo, Japan) and developed in a RP X-OMAT Processor (Eastman Kodak Co., Rochester, NY).

2.10. Yeast two-hybrid protein interaction assays

Full length BNIPXLα and BNIPXLβ were subcloned into the yeast GAL4 Activation Domain (AD) vector, pACT2 and the GAL4 DNA-binding domain (DNA-BD) vector, pAS2-1 (CLONTECH). The clones were verified by restriction analysis and sequencing for use in subsequent experiments. The *Saccharomyces cerevisiae* AH109 host stain (courtesy of S.Y. Chow, Institute of Molecular and Cell Biology, Singapore) was

obtained and working stocks were streaked on YPD agar medium supplemented with 0.003% (w/v) adenine hemisulphate (YPDA). Phenotype testing was performed on minimal Synthetic Dropout (SD) agar base supplemented with the appropriate Dropout (DO) supplement shown in **Table I**. The AH109 strain contains three reporter genes (ADE2, HIS3 and lacZ) under tight control from GAL4 upstream activating sequences (UASs) and TATA boxes which help reduce false positives ADE2 and HIS3 reporters provide strong nutritional selection to adenine and histidine, respectively. lacZ reporter encodes for β-galactosidase allowing for assay for transcriptional activation of gene expression (**Figure 2.3**).

Yeast transformations were performed using the Yeastmaker™ Yeast Transformation System 2 (CLONTECH), according to manufacturer instructions. Prior to lithium acetate (LiAc)-mediated transformation, competent yeast cells were prepared according to manufacturer instructions. Fresh yeast colonies were dispersed in 50mL of YPDA liquid medium and cultured overnight at 30°C. The overnight culture was diluted (1:10) in fresh YPDA liquid medium and grown at 30°C until mid-log phase ($O.D._{600}$ = 0.4-0.6). The yeast pellet was collected by centrifugation at 1,000g for 5 min at room temperature, washed once with sterile 1XTE (10mM Tris-HCl, 1mM EDTA [pH 7.5]) buffer and the pellet reconstituted in 1.5mL of sterile TE/LiAc (1XTE, 100mM lithium acetate [pH 7.5]) solution.

For simultaneous cotransformation, 0.1 µg of each plasmid DNA was incubated with 0.1 mg of pre-denatured herring testes carrier DNA, 100µL of competent yeast cells and 600µL of sterile PEG/LiAc (40% (v/v) PEG 4,000, TE/LiAc) solution. The mixture was vortexed and incubated for 30 min at 30°C followed by addition of 70µL of DMSO

Table I. Combinations of minimal Synthetic Dropout (SD) agar base supplemented with the Dropout (DO) supplements.

	Dropout (DO) supplements
Single	-Leu
	-Trp
	-His
Double	-Leu/-Trp
	-Leu/-His
	-Trp/-His
Triple	-Leu/-Trp/-His

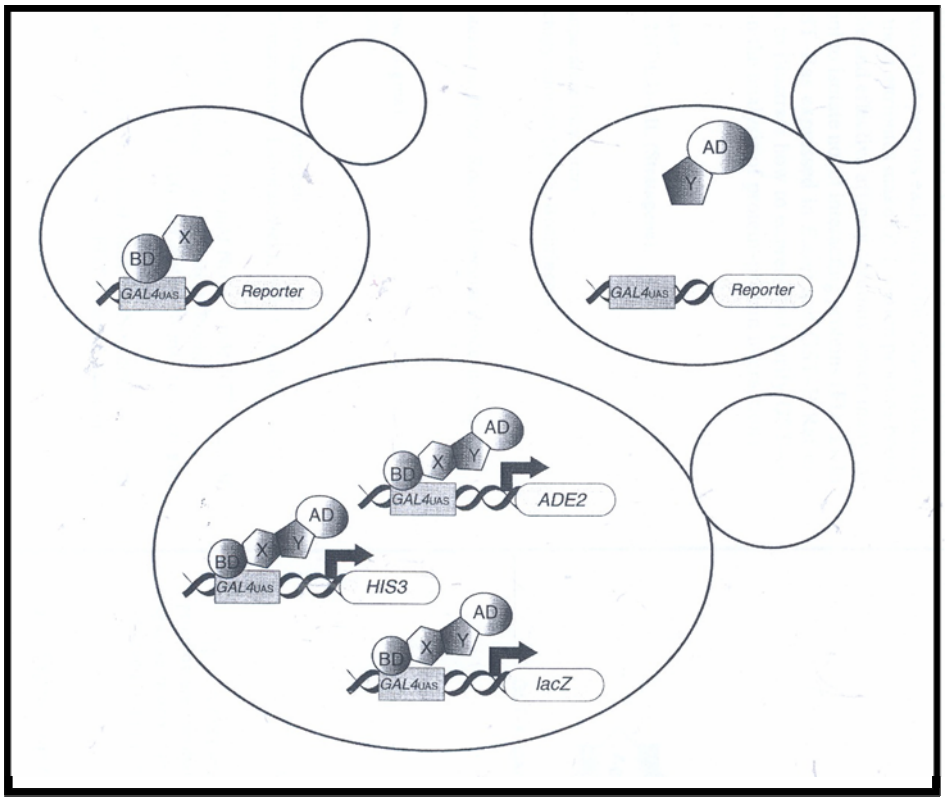

Figure 2.3. Schematic diagram illustrating the modular nature of the yeast GAL4 transcription factor and the regulation of downstream reporter genes for ADE2, HIS3 and lacZ. (Adapted from Miller and Stagljar, 2004).

and gentle inversion. The samples were then heat shocked for 15 min at 42°C, chilled on ice and centrifuged at 13,000g for 5 s at room temperature. The supernatant was discarded and the pellet resuspended in 100µL sterile 1X TE buffer. 20µL each of diluted samples was (1:10, 1:100) plated on each type of SD agar plate in **Table I** and incubated at 30 °C for 2 days. Transformation efficiency and potential lethality of constructs was determined by selection on -Trp, -Leu or -His agar plates while plating on -Trp/-His and -Leu/-His SD allows determination of spurious self-activation of HIS reporter by the individual constructs. Dual transformants were selected on Trp/Leu-free SD agar plates while plating on Trp/Leu/His-free SD agar gave indication of direct protein-protein interaction. Colonies that survived the HIS3 growth selection were re-streaked on fresh Trp/Leu/His-free agar, grown at 30 °C for 2 days and subjected to β-galactosidase colony lift filter assays according to the manufacturer's protocol (CLONTECH). A schematic diagram illustrates an overview of the assay (**Figure 2.4**).

To measure β-galactosidase activity, sterile Whatman filters were pre-soaked in Z buffer/X-gal solution (Z-buffer: $Na_2HPO_4 \bullet 7H_2O$, $NaH_2PO_4 \bullet H_2O$, KCl, $MgSO_4 \bullet 7H_2O$ [pH 7.0], 33.4% (w/v) X-gal, 0.27% (v/v) β-mercaptoethanol). The colonies were blotted onto dry sterile Whatman filters and submerged in liquid nitrogen for 10 s and left to thaw at room temperature for cell permeablization. The filter is then placed colony side up onto the pre-soaked filters and incubated at 30 °C. Positive interactions were scored for the appearance of blue colonies in less than 8 h according to the protocol. In all experiments, however, the appearance of blue colonies was apparent within 3 h.

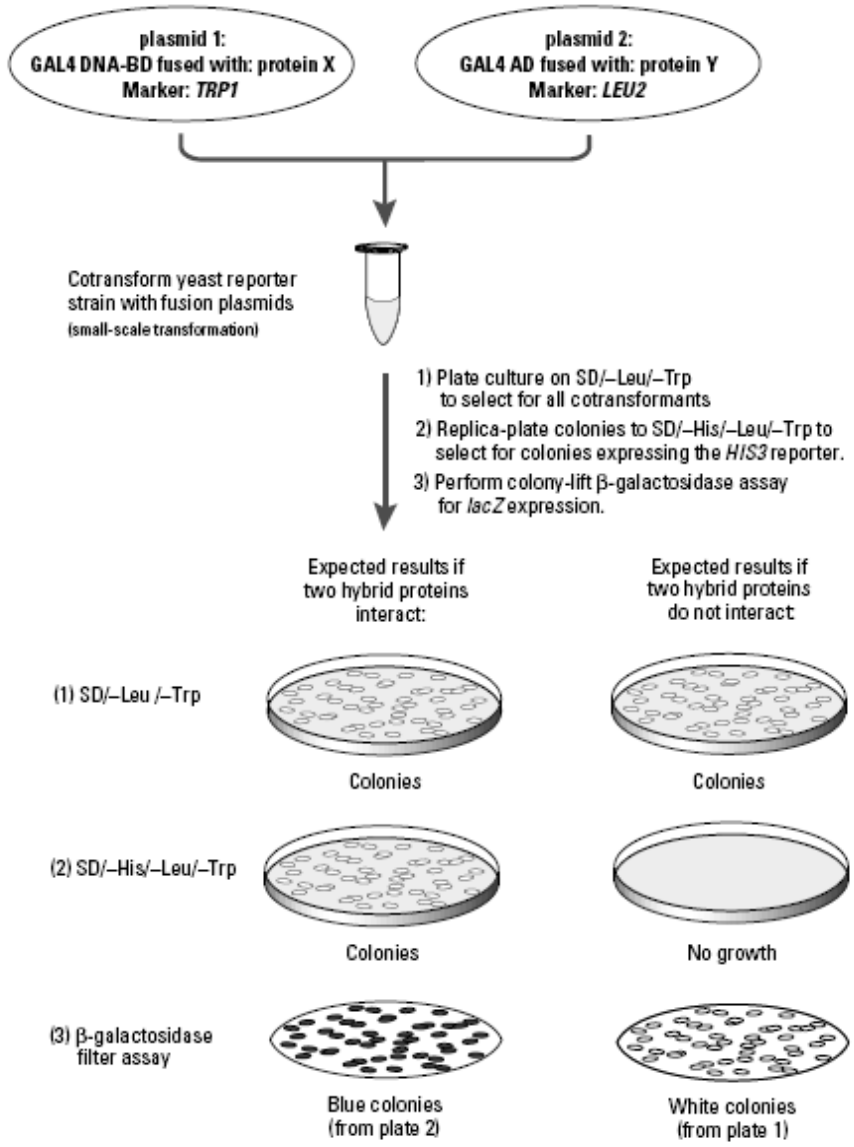

Figure 2.4. Schematic diagram for yeast two-hybrid protein interaction assay (CLONTECH).

2.11. GST-fusion protein production

Glutathione S-transferase (GST) fusion proteins were produced in *E. coli* BL21 strain carrying pGEX vectors (Amersham Pharmacia Biosciences, Piscataway, NJ). An overnight culture was diluted (1:200) in fresh LB medium and grown at 37°C until log phase ($O.D._{600}$ = 0.3-0.6). The bacterial pellet was collected by centrifugation at 3,500g for 10 min at 4°C and stored at -70° C. Pellets were thawed and reconstituted in 5mL of GST lysis buffer (1XPBS, 1% (v/v) Triton X-100 and 1mM dithiothreitol [DTT]) and a mixture of protease inhibitors (Roche Molecular Biochemicals). The mixture was sonicated for 3 min at 20% amplitude and centrifuged at 3,500g for 1 h (Vilber Lourmat, Marne la Vallée Cedex, France). The supernatant was incubated with 150µL of glutathione sepharose 4B beads (Amersham Pharmacia Biosciences) for 1 h at 4°C. Beads were washed five times in cold PBS buffer supplemented with 1% (v/v) Triton X-100 and stored at 4°C as a 50% slurry for up to 2 weeks. A second round of capture was performed with the supernantant overnight at 4°C, if necessary.

2.12. GST-fusion protein binding assays

For *in vitro* binding assays, aliquots of the suspensions (10ug) were washed twice with 500µL of cold pre-binding buffer (50mM Tris HCl [pH 7.4], 50mM NaCl, 5mM $MgCl_2$, 1mM DTT, and a mixture of protease inhibitors). The beads were then loaded with water, GDP or guanosine 5'-*O*-3-thiotriphosphate (GTPγS) (Sigma) in 39µL of binding buffer (25 mM NaCl, 20 mM Tris HCl [pH 7.5], 0.1 mM dithiothreitol), 50 mM EDTA, and 10 mM GDP or GTPγS at 30°C for 10 min. The reaction with stopped by addition of

$MgCl_2$ to final concentration of 20mM. The beads were subsequently incubated with whole cell lysates (500 µg) at 4°C in GAP lysis buffer (50 mM HEPES [pH 7.4], 150 mM NaCl, 1.5 mM $MgCl_2$, 5 mM EGTA, 10% (v/v) glycerol, 1% (v/v) Triton X-100), 5 mM sodium orthovanadate and a mixture of protease inhibitors (Roche Molecular Biochemicals), collected by centrifugation, and washed three times with 1 ml of IP wash buffer (20 mM HEPES [pH 7.4], 150 mM NaCl, 10mM $MgCl_2$, 10% (v/v) glycerol, 0.1% (v/v) Triton X-100). Bound proteins were eluted and heat denatured in suitable amounts of 6X SDS-PAGE loading buffer, separated by SDS-PAGE and analyzed by Western blot analyses (**Figure 2.5**).

2.13. *In vitro* direct protein binding assays

For direct binding assays, *in vitro* transcribed and translated epitope-tagged proteins were synthesized using the TNT® Quick Coupled Transcription/Translation System (Promega Corp.), according to manufacturer's instructions. Briefly, 1 µg of DNA plasmid template was incubated with 20 µL of TNT® Quick Master Mix and 1µL of the T7 TNT® PCR Enhancer in a 25 µL reaction volume at 30°C for 90 min. 2 µL of the TNT product was analyzed by SDS-PAGE while the remaining product was incubated with 10 µg of GST fusion proteins immobilized on glutathione-sepharose beads overnight at 4°C. The mixture was then diluted with 100 µL of cold lysis buffer and allowed to incubate for 1 h at 4°C. Beads were collected by centrifugation and washed three times with 200 µL of lysis buffer. Bound proteins were eluted and heat denatured in suitable amounts of 6X SDS-PAGE loading buffer, separated by SDS-PAGE and analyzed by Western blot analyses.

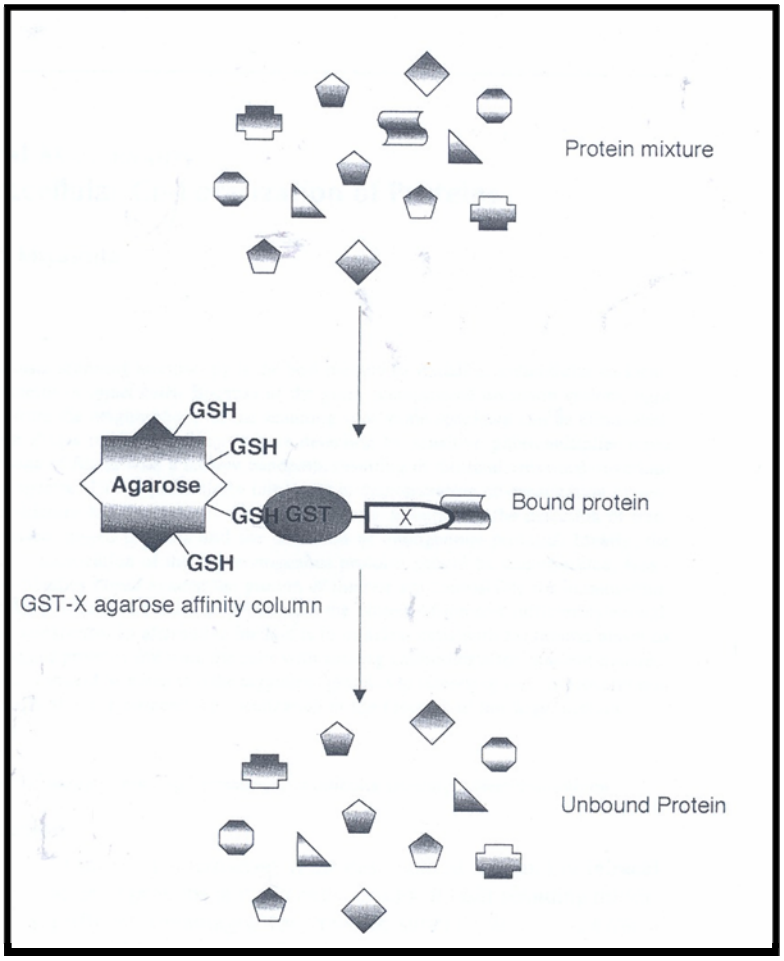

Figure 2.5. A schematic diagram illustrating a GST-fusion protein binding assay. Cell lysates are incubated with the bait, GST-fusion protein bound to gluthathione (GSH)-agarose matrix. Only proteins that interact with the fusion protein in the X region will be 'pull-down'. (Adapted from Vikis and Guan, 2004).

2.14. *In vitro* Rho activity assays

For GST-RBD pull-down assays, cells were lysed with ice-cold lysis buffer (50 mM Tris-HCl [pH 7.4], 2 mM magnesium chloride, 1% (v/v) Triton X-100, 10% (v/v) glycerol, 100 mM sodium chloride, supplemented with 1 mM dithiothreitol and a mixture of protease inhibitors). Lysates were centrifuged at 14,000 rpm for 10 min at 4°C. The cleared lysates were diluted five times with lysis buffer and incubated for 45 min at 4°C with 20µL of GST fusion of Rhotekin-RBD bound to glutathione sepharose 4B beads (plasmid courtesy of Dr Simone Schoenwaelder, Monash University, Australia). The beads were subsequently collected by centrifugation and washed three times with 750µL of lysis buffer. Bound proteins were eluted and heat denatured in suitable amounts of 6X SDS-PAGE loading buffer, separated by SDS-PAGE and analyzed by Western blot analyses.

2.15. Confocal immunofluorescence microscopy

MCF-7 and HeLa cells were seeded on glass coverslips in 6-well plates at 30% confluency and transfected with various constructs. 24 h post-transfection, the cells were washed with cold PBS buffer supplemented with 10mM $CaCl_2$ and 10mM $MgCl_2$ (PBSCM) and fixed in 4% (w/v) paraformaldehyde for 30 min at 4°C. Fixed cells were washed twice with PBSCM, twice with PBSCM containing 50mM NH_4Cl, and twice again with PBSCM, followed by permeabilization with 0.1% (w/v) saponin (Sigma-Aldrich) in PBSCM for 15 min at room temperature. Coverslips were incubated in fluorescence dilution buffer (FDB) (PBSCM, 7% (v/v) fetal bovine serum [FBS], 2% (w/v) BSA) for 30 min and then with monoclonal FLAG and/or polyclonal HA antibodies diluted

(1μg:100μL) in FDB for 1 h at room temperature. The coverslips were washed three times, 2 min each in PBSCM supplemented with 0.1% (w/v) saponin before incubation with secondary antibodies diluted (1:200) in FDB for 1 h at room temperature in the dark. Secondary antibodies used were fluorescein isothiocyanate-conjugated (FITC) goat anti-rabbit IgG (Jackson ImmunoResearch Laboratories, West Grove, PA) or Pacific Blue-conjugated goat anti-rabbit IgG (Molecular Probes, Eugene, OR). F-actin staining was performed using TRITC-conjugated phalloidin (Sigma-Aldrich) (**Figure 2.6**). Coverslips were washed five times in PBSCM supplemented with 0.1% (w/v) saponin and mounted with FluorSave (Calbiochem, San Diego, CA). Confocal microscopy was performed with an Olympus Fluoview confocal microscope (Olympus Corporation, Tokyo, Japan) attached to an Olympus 1 X 81 inverted fluorescent microscope equipped with a 60X oil immersion lens. Digitalized images were captured using Fluoview software version 4.3 (Olympus Corp.)

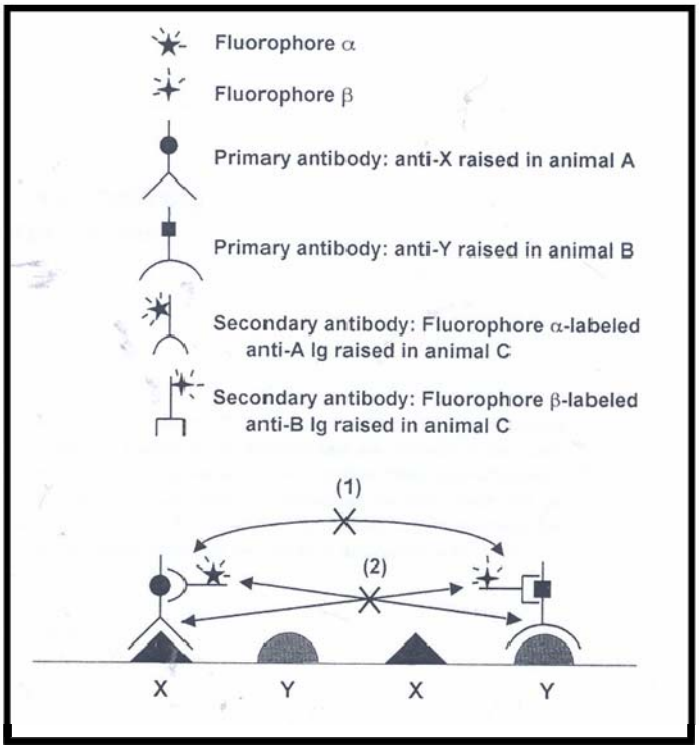

Figure 2.6. The schematic diagram illustrates the multicolor detection of cellular proteins. Primary antibodies are used to detected individual proteins (shaded triangles and semi-circle). Subsequent incubation with fluorophore-conjugated secondary antibody allows signal amplification and detection. (Adapted from Miyashita, 2004).

Results

3. Results

3.1. Investigating the roles of the BCH domain in novel proteins

3.1.1. *In silico* identification of a novel BCH domain-containing protein

To investigate the functional diversity of the novel BNIP-2 family proteins and the possibility that homologous BCH domains may exert distinct roles in targeting specific GTPases for cell morphogenesis, we set out to identify novel BCH domain-containing proteins using a bioinformatics approach. BCH domain homologues were identified using the BLASTN and PSI-BLAST (http://www.ncbi.nlm.nih.gov/BLAST/) programs as described in "Materials and Methods". All BCH domains were identified without iteration using unfiltered query sequences. Using the full-length human BNIP-2 and its BCH domain (residues 167-303) with an *E*-value of 0.001, we identified *in silico* a partial coding sequence for a putative human mRNA (GenBank™ accession number AB002365) with an extensive 3' untranslated region (UTR) encoding for the KIAA0367 gene (Nagase *et al.,* 1997). Several conserved primers were designed based on the predicted open reading frame and used in reverse-transcription-based PCR to isolate the full-length cDNA from human brain and kidney cDNA libraries. Following PCR, an expected 2500-bp DNA fragment was isolated (**Figure 3.1**) and cloned into epitope-tagged pXJ40 mammalian expression vectors for subsequent propagation in XL1-blue and DH5α *Escherichia coli* host strains. Antibiotic resistant colonies harboring DNA fragments of the expected size that was released by *Xho*I/*Not*I double restriction digest was selected for bi-directional DNA sequencing using T7 and a series of gene coding region-specific primers.

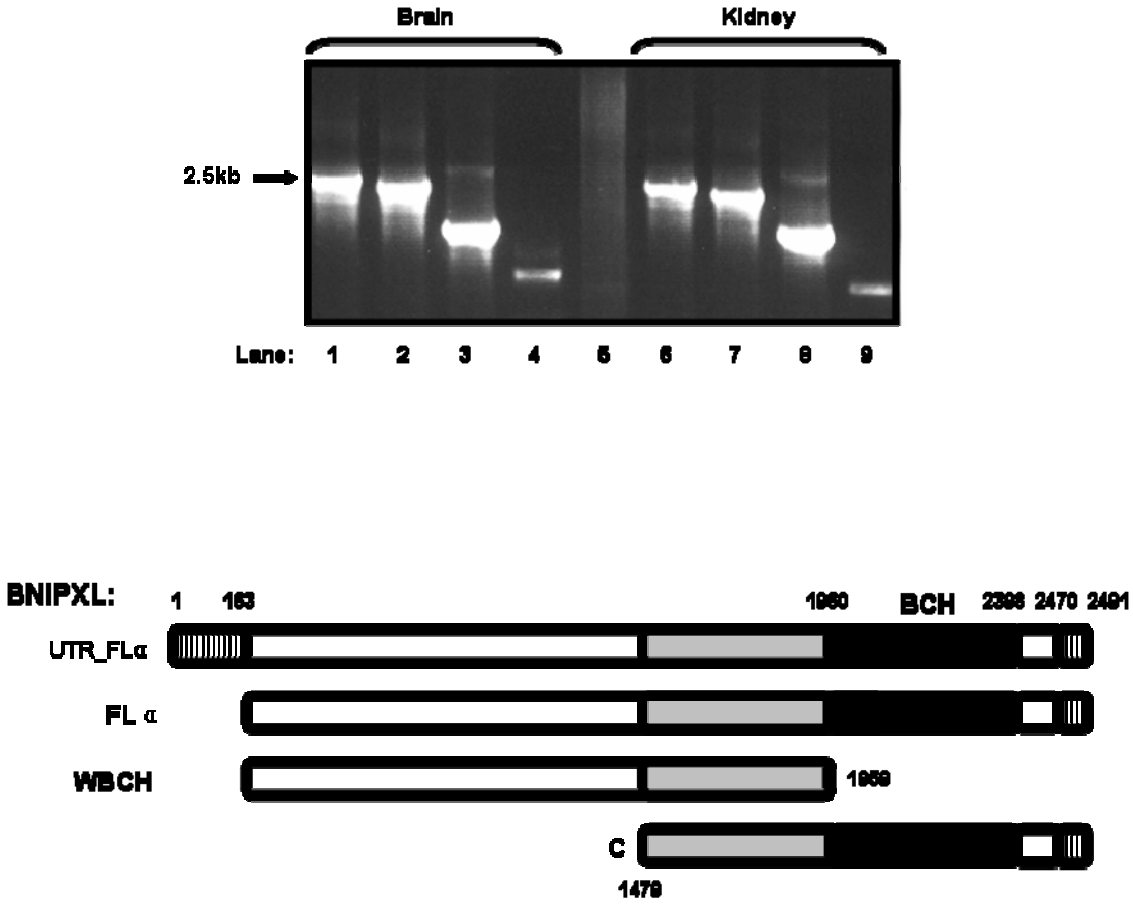

Figure 3.1. Cloning of full-length BNIPXL. PCR amplification from human brain and kidney libraries were performed using the cycling conditions described in 'Materials and Methods' (*upper panel*). From left to right, lanes 1, 6: 5' untranslated region and full length (UTR_FL); lanes 2, 7: full length; lanes 3, 8: N-terminus lacking BCH domain (WBCH); lanes 4, 9: C-terminus. Different primer pairs were used for amplification of BNIPXL fragments as indicated (*lower panel*). The BNIPXL coding sequence is from nucleotides 163-2470. In addition to the BCH domain, the region with significant homology to BNIP-2 is shaded in gray. Numbers indicate nucleotide base pairs.

3.1.2. Sequence verification and bioinformatics analyses of BNIPXL

Bi-directional sequencing using vector and gene specific primers repeatedly identified two unique cDNA sequences (**Figure 3.2**) in several clones that had 99% identity to the KIAA0367 gene (GenBank™ accession number AB002365). The KIAA0367 cDNA was originally isolated from size-fractionated human brain cDNA libraries (Nagase *et. al*., 1997). This cDNA generated a protein corresponding to an ORF of 716 amino acid residues in the *in vitro* transcription and translation system. The authors could not locate an in-frame termination codon in the 5'-untranslated region (5'UTR) suggesting that KIAA0367 could either be truncated at its N-terminal or that internal translation initiation sites within the existing cDNA clone could be induced.

We observed that several nucleotide polymorphisms (**Table 2**) had resulted in silent mutations and amino acid substitutions when compared to the KIAA0367 gene. These single nucleotide polymorphisms were consistently found in several clones of the two cDNA sequenced. Similar observations were noted for nucleotide insertions corresponding to the three amino acids residues (588)GLR(590). The three residue insertion is likely to be the result of polymorphism as BLAST results of the cDNA sequences against the human EST database indicates the presence of several ESTs from lung (GenBank™ accession number DB229725), brain (GenBank™ accession numbers DA216136, DA194357 and DA406210) and liver (GenBank™ accession number CB146736) that have similar insertions corresponding to three residues in the same region.

```
gctttgtttgatggtgatccacatttatccacagagaatcctgccttggttcctgatgct      60

ttgctagcctcagacacttgtctggatataagcgaagctgccctttgaccacagtttcagc     120

gatgcctcaggtctcaacacatccacgggaacaatagatgacatgagtaaactgacatta     180
                                            M  S  K  L  T  L       6

tccgaaggccatccggaaacgccagttgatggggacctagggaagcaagatatctgctca     240
 S  E  G  H  P  E  T  P  V  D  G  D  L  G  K  Q  D  I  C  S      26

tctgaagcctcgtggggtgattttgaatatgatgtaatgggccagaatatcgatgaagat     300
 S  E  A  S  W  G  D  F  E  Y  D  V  M  G  Q  N  I  D  E  D      46

ttactgagagagcctgaacacttcctgtatggtggtgaccctcctttggaggaagattct     360
 L  L  R  E  P  E  H  F  L  Y  G  G  D  P  P  L  E  E  D  S      66

ctgaagcagtcgctggcaccgtacacacctccctttgatttgtcttatatcacagaacct     420
 L  K  Q  S  L  A  P  Y  T  P  P  F  D  L  S  Y  I  T  E  P      86

gcccagagtgctgaaacaatagaggaagctgggtctccagaggatgaatctctgggatgc     480
 A  Q  S  A  E  T  I  E  E  A  G  S  P  E  D  E  S  L  G  C      106

agagcagcagagatagtgctttctgcacttcctgatcgaagaagtgagggaaaccaggct     540
 R  A  A  E  I  V  L  S  A  L  P  D  R  R  S  E  G  N  Q  A      126

gagaccaaaaacagactgcctggatcccagctggctgtgctgcatattcgtgaagaccct     600
 E  T  K  N  R  L  P  G  S  Q  L  A  V  L  H  I  R  E  D  P      146

gagtccgtttatttgccggtaggagcaggctccaacattttgtctccatcaaacgttgac     660
 E  S  V  Y  L  P  V  G  A  G  S  N  I  L  S  P  S  N  V  D      166

tgggaagtagaaacagataattctgatttaccagcaggtggagacataggaccaccaaat     720
 W  E  V  E  T  D  N  S  D  L  P  A  G  G  D  I  G  P  P  N      186

ggtgccagcaaggaaatatcagaattggaagaagaaaaaacaattcctaccaaagagcct     780
 G  A  S  K  E  I  S  E  L  E  E  E  K  T  I  P  T  K  E  P      206

gagcagataaaatcagaatacaaggaagaaagatgtacagagaagaatgaagatcgtcat     840
 E  Q  I  K  S  E  Y  K  E  E  R  C  T  E  K  N  E  D  R  H      226

gcactacacatggattacatacttgtaaaccgtgaagaaaattcacactcaaagccagag     900
 A  L  H  M  D  Y  I  L  V  N  R  E  E  N  S  H  S  K  P  E      246

acctgtgaagaaagagaaagcatagctgaattagaattgtatgtaggttccaaagaaaca     960
 T  C  E  E  R  E  S  I  A  E  L  E  L  Y  V  G  S  K  E  T      266

gggctgcagggaactcagttagcaagcttcccagacacatgtcagccagcctccttaaat    1020
 G  L  Q  G  T  Q  L  A  S  F  P  D  T  C  Q  P  A  S  L  N      286

gaaagaaaaggtctctctgcagagaaaatgtcttctaaaagcgatacgagatcatctttt    1080
 E  R  K  G  L  S  A  E  K  M  S  S  K  S  D  T  R  S  S  F      306

gaaagccctgcacaagaccagagttggatgttcttgggccatagtgaggttggtgatcca    1140
 E  S  P  A  Q  D  Q  S  W  M  F  L  G  H  S  E  V  G  D  P      326
```

```
tcactggatgccagggactcagggcctgggtggtccggcaagactgtggagccgttctct      1200
 S  L  D  A  R  D  S  G  P  G  W  S  G  K  T  V  E  P  F  S       346

gaactcggcttgggtgagggtccccagctgcagattctggaagaaatgaagcctctagaa      1260
 E  L  G  L  G  E  G  P  Q  L  Q  I  L  E  E  M  K  P  L  E       366

tctttagcactagaggaagcctctggtccagtcagccaatcacagaagagtaagagccga      1320
 S  L  A  L  E  E  A  S  G  P  V  S  Q  S  Q  K  S  K  S  R       386

ggcagggctggcccggatgcagttacccatgacaatgaatgggaaatgctttcaccacag      1380
 G  R  A  G  P  D  A  V  T  H  D  N  E  W  E  M  L  S  P  Q       406

cctgttcagaaaaacatgatccctgacacggaaatggaggaggagacagagttccttgag      1440
 P  V  Q  K  N  M  I  P  D  T  E  M  E  E  E  T  E  F  L  E       426

ctcggaaccaggatatcaagaccaaatggactactgtcagaggatgtaggaatggacatc      1500
 L  G  T  R  I  S  R  P  N  G  L  L  S  E  D  V  G  M  D  I       446

ccctttgaagagggcgtgctgagtcccagtgctgcagacatgaggcctgaacctcctaat      1560
 P  F  E  E  G  V  L  S  P  S  A  A  D  M  R  P  E  P  P  N       466

tctctggatcttaatgacactcatcctcggagaatcaagctcacagccccaaatatcaat      1620
 S  L  D  L  N  D  T  H  P  R  R  I  K  L  T  A  P  N  I  N       486

ctttctctggaccaaagtgaaggatctattctctctgatgataacttggacagcccagat      1680
 L  S  L  D  Q  S  E  G  S  I  L  S  D  D  N  L  D  S  P  D       506

gaaattgacatcaatgtggatgaacttgataccccgatgaagcagattcttttgagtac      1740
 E  I  D  I  N  V  D  E  L  D  T  P  D  E  A  D  S  F  E  Y       526

actggccatgaagatcccacagccaccaaagattctggccaagagtcagagtctattcca      1800
 T  G  H  E  D  P  T  A  T  K  D  S  G  Q  E  S  E  S  I  P       546

gaatatacggccgaagaggaacgggaggacaaccggctttggaggacagtggtcattgga      1860
 E  Y  T  A  E  E  E  R  E  D  N  R  L  W  R  T  V  V  I  G       566

gaccaagagcagcgcattgacatgaaggtcatcgagccctacaggagagtcatttctcac      1920
 D  Q  E  Q  R  I  D  M  K  V  I  E  P  Y  R  R  V  I  S  H       586

ggaggacttagaggatactatggggacggtctaaatgccatcattgtgtttgccgcctgt      1980
 G  G  L  R  G  Y  Y  G  D  G  L  N  A  I  I  V  F  A  A  C       606

tttctgccagacagcagtcgggcggattaccactatgtcatggaaaatcttttcctatat      2040
 F  L  P  D  S  S  R  A  D  Y  H  Y  V  M  E  N  L  F  L  Y       626

gtaataagtactttagagttgatggtagctgaagactatatgattgtgtacttgaatggt      2100
 V  I  S  T  L  E  L  M  V  A  E  D  Y  M  I  V  Y  L  N  G       646

gcaaccccaagaaggaggatgccagggctaggctggatgaagaaatgctaccagatgatt      2160
 A  T  P  R  R  R  M  P  G  L  G  W  M  K  K  C  Y  Q  M  I       666

gacagacggttgaggaagaatttgaaatcattcatcattgttcatccatcttggttcatc      2220
 D  R  R  L  R  K  N  L  K  S  F  I  I  V  H  P  S  W  F  I       686

agaacaatccttgctgtgacacgacctttataagttcaaaattcagcagtaaaattaaa      2280
 R  T  I  L  A  V  T  R  P  F  I  S  S  K  F  S  S  K  I  K       706
```

Figure 3.2. Nucleotide and deduced amino acid sequences of human BNIPXL gene. The human BNIPXLα and BNIPXLβ cDNAs encode for a 769- and 732 amino acid proteins, respectively. The BCH domain is underlined while the region excluded from the BNIPXLβ splice variant is in **bold**. Double lines indicate the Walker A motif (334)GPGWSGKT (341) identified by the NCBI Conserved Domain (CD) database search program (http://www.ncbi.nlm.nih.gov/Structure/cdd/wrpsb.cgi) while the three amino acid insertion (588)GLR(590) is highlighted in **red**. The forward and reverse arrows define the region corresponding to the BCH domain amplified during diagnostic RT-PCR experiments (**Figure 3.7**). Residues highlighted in **blue** indicate primers used for BMCC1 RT-PCR (**Section 3.2.1.2**)

Table 2. List of nucleotide polymorphisms compared to the KIAA0367 gene and its effect at amino acid level in the BNIPXL gene.

Nucleotide substitutions	Amino acid mutations
C409A	Leu83Ile
C739T	Pro193Ser
C816T	Cys218 (silent)
G1059A	Gly300Ser
T1175C	Ser338 (silent)
G1355A	Ser398Asn
T1402C	Ser414Pro
T1674C	Ser504 (silent)
A1763C	Asn535Thr
A1863C	Glu567Asp

3.1.2.1. Genomic organization of BNIPXL

Genome analysis using the Human Genome BLAST (http://www.ncbi.nlm.nih.gov/genome/seq/HsBlast.html) mapped both cDNAs to the human chromosome band 9q21.2 (**Figure 3.3**) indicating that they are products of alternative RNA splicing. Further analyses indicate that this gene spans 13 exons over a distance of ~86 kbp. The exclusion of two exons (exons 11 and 12) during exon skipping resulted in the introduction of an in-frame stop codon corresponding to a deletion of 86 nucleotides at the C-terminus of the shorter splice variant resulting in the lost of 28 amino acids (**Figure 3.4**).

3.1.2.2. BNIPXLα and BNIPXLβ are novel members of the BNIP-2 family

The predicted open reading frame of the novel cDNAs encode for a 769- and 732 amino acid proteins which had 25% amino acid identity to full-length human BNIP-2 and shares 68% identity at the C-terminus to the BNIP-2 BCH domain. Thus, we named them BNIPXLα and BNIPXLβ, extra-long members of the BNIP-2 family, with BNIPXLβ being the shorter splice variant. The complete sequences of human BNIPXLα and BNIPXLβ have been deposited in the GenBank™ under the accession numbers AY439213 and AY439214, respectively. Pairwise sequence alignments of full length BNIPXL with BNIP-2 family members indicate that BNIPXL shares ~18-25% amino acid identity over the entire cDNA sequence (**Table 3**) while pairwise alignments of the BCH domains demonstrates that BNIPXL and the BNIP-2 family share ~50-70% amino acid identity at their BCH domains. The BNIP-H BCH domain being the most similar (72% identity)

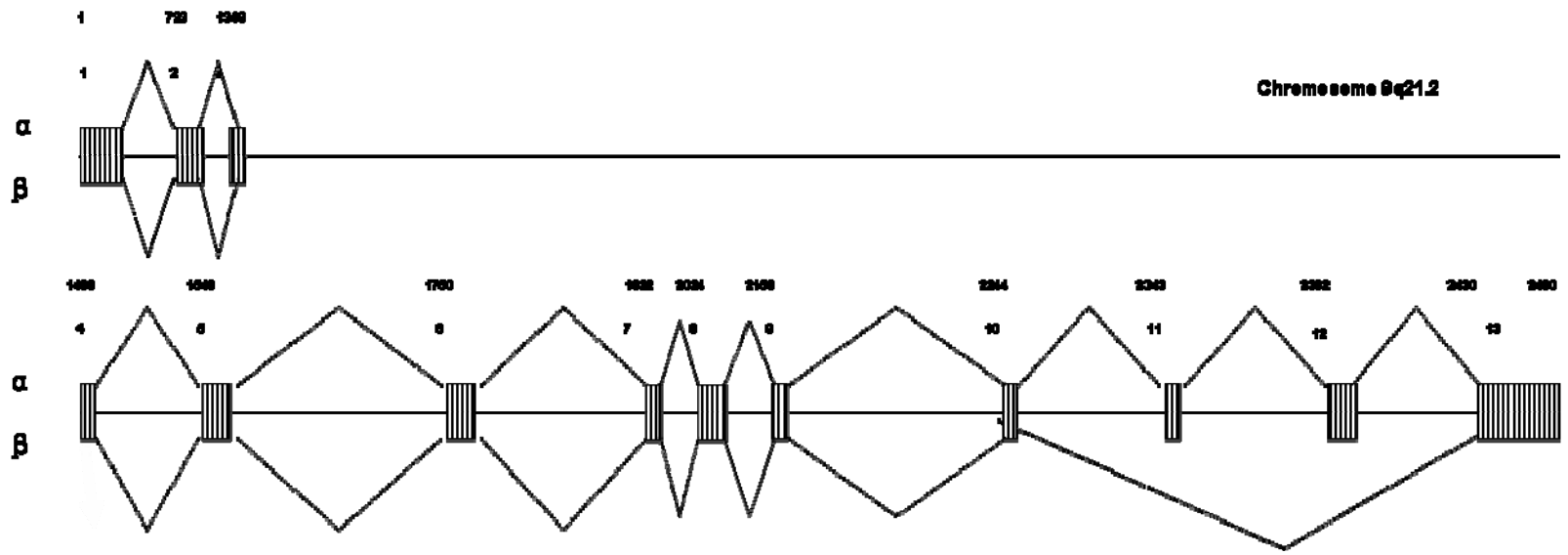

Figure 3.3. The genomic organization of the human BNIPXL gene. Both BNIPXLα and BNIPXLβ map onto the human chromosome 9q21.2, spanning a distance of ~86 kbp and are products of alternative RNA splicing with BNIPXLβ being shorter by 86 bp. Dotted lines indicate exons included in BNIPXLα (upper) and BNIPXLβ (lower) isoforms, respectively. Nucleotide base pairs and their corresponding exon numbers are indicated.

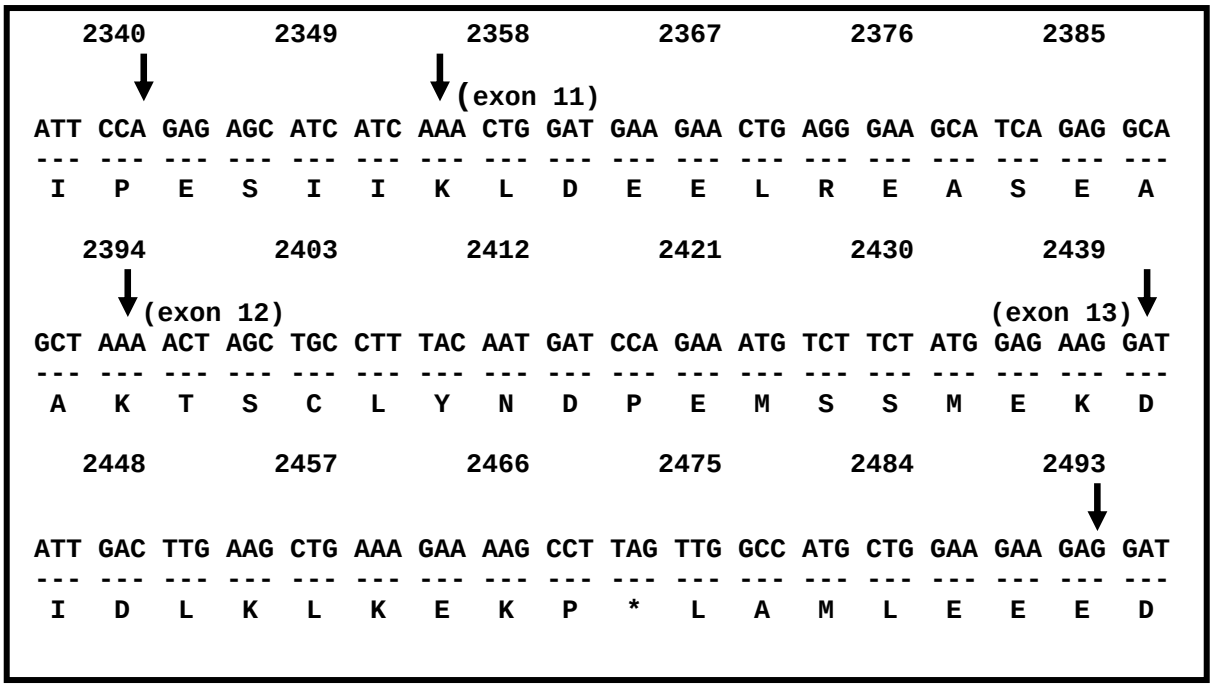

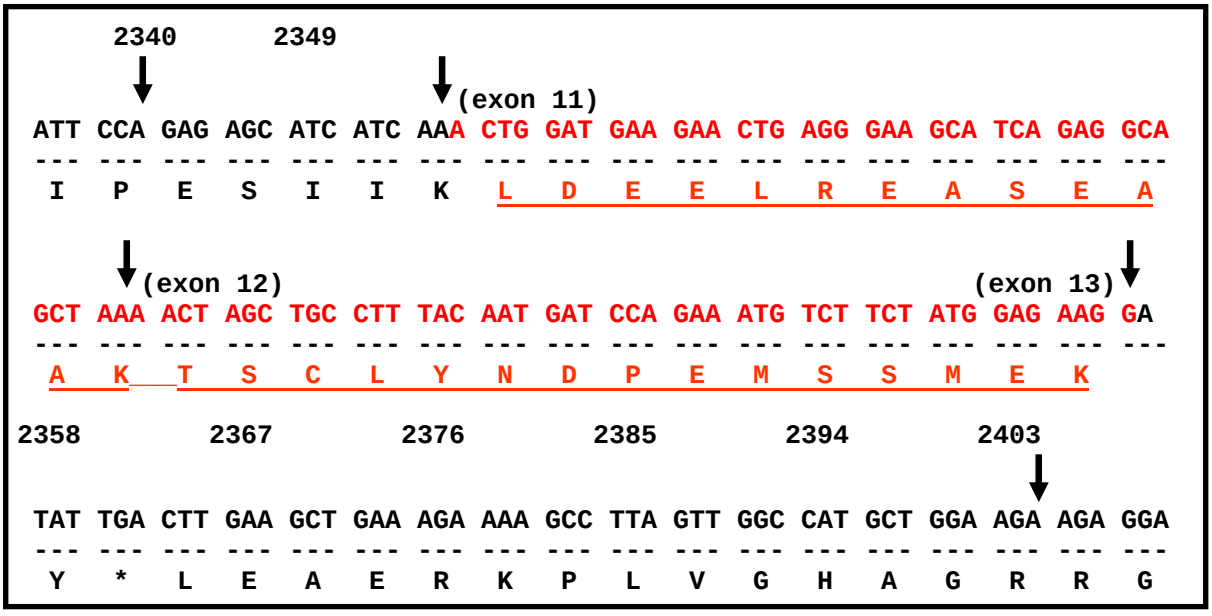

Figure 3.4. BNIPXLα spans 13 exons (upper panel) while exon skipping (exons 11 and 12, highlighted in red) results in the deletion of 86 nucleotides from BNIPXLβ with the introduction of an in-frame stop codon (lower panel). (*) indicates the stop codon. The boundaries of the exons are denoted by arrows.

Table 3. Pairwise global alignments of **full-length** BNIP-2 family members. Values are represented as percentage amino acid identity obtained using the Stretcher program at (http://sbcr.bii.a-star.edu.sg/emboss/).

	BNIPXLα	**BNIPXLβ**	**BNIP-2**	**BNIP-H**	**BNIP-Sα**
BNIPXLα	100	95.1	24.2	26.3	18.5
BNIPXLβ	95.1	100	24.9	25.3	18.7
BNIP-2	24.2	24.9	100	48.3	41.1
BNIP-H	26.3	25.3	48.3	100	32.8
BNIP-Sα	18.5	18.7	41.1	32.8	100

while BNIP-S the least similar (47% identity) (Table 4). In addition, the flanking regions of BNIP-H and BNIP-2 also share ~45% amino acid identity with BNIPXL (**Figure 3.5**).

3.1.2.3. Multiple sequence alignments of BCH domains

Conserved Domain Architecture Retrieval Tool (CDART) analyses using the full-length polypeptides as query sequence and multiple sequence alignments of the BCH domains of BNIPXLα and BNIPXLβ with other BNIP-2 family members revealed that the distal region of BNIPXL and the BCH domains of BNIP-2 family members were highly conserved. This confirms the presence of a BCH domain (**Figure 3.6**). Based on the classification derived from our previous survey of the GenBank (Low *et al*., 2000b), BNIPXLα and BNIPXLβ are now classified as novel Type I members where the BCH domain is present at the C-terminus.

3.1.2.4. Phylogenetic analyses of the BNIP-2 family

Phylogenetic trees were generated using the BCH domains and full length amino acid sequences of Type I family members. Tree topologies indicate that BNIPXL and BNIP-H share the closest relative ancestry followed by BNIP-2, with BNIP-S being more evolutionarily distant (**Figure 3.6**).

Table 4. Pairwise global alignments of the **BCH domains** of BNIP-2 family. Values are represented as percentage amino acid identity obtained using the Stretcher program at (http://sbcr.bii.a-star.edu.sg/emboss/).

	BNIPXLα_BCH	**BNIPXLβ_BCH**	**BNIP-2_BCH**	**BNIP-H_BCH**	**BNIP-Sα_BCH**
BNIPXLα_BCH	100	90.4	66.9	72.1	47.9
BNIPXLβ_BCH	90.4	100	64.2	72.7	50.0
BNIP-2_BCH	66.9	64.2	100	64.4	48.6
BNIP-H_BCH	72.1	72.7	64.4	100	47.6
BNIP-Sα_BCH	47.9	50.0	48.6	47.6	100

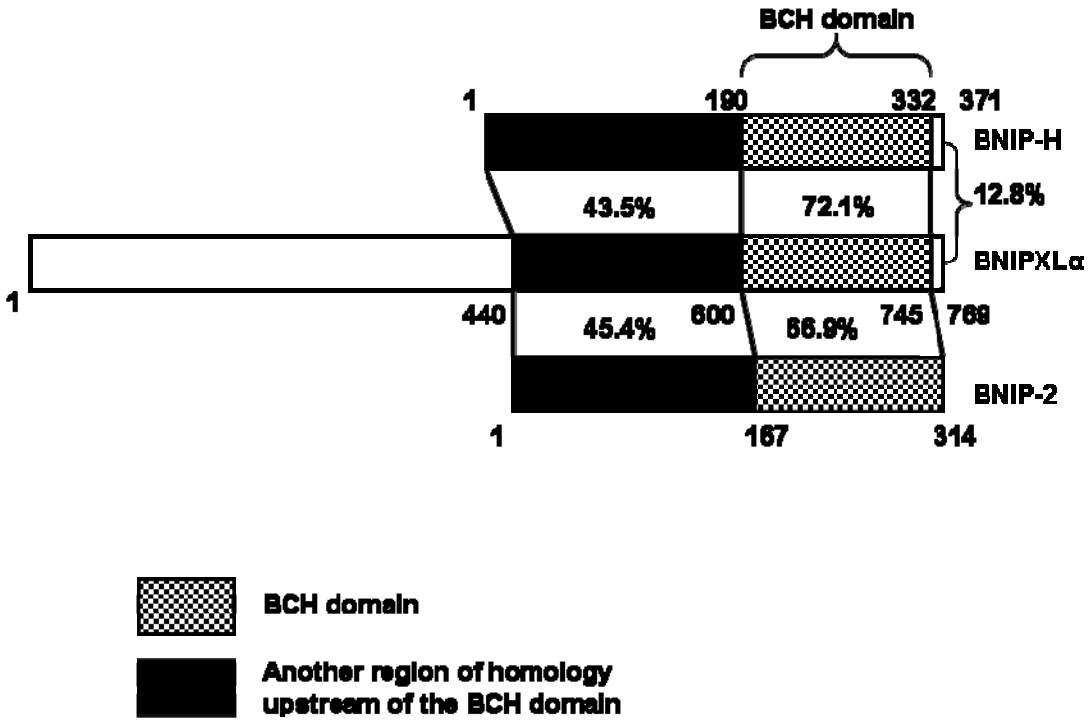

Figure 3.5. Schematic diagram showing pairwise alignments between the different regions of BNIP-2 and BNIP-H with BNIPXLα. Values are represented as percentage amino acid identity.

A

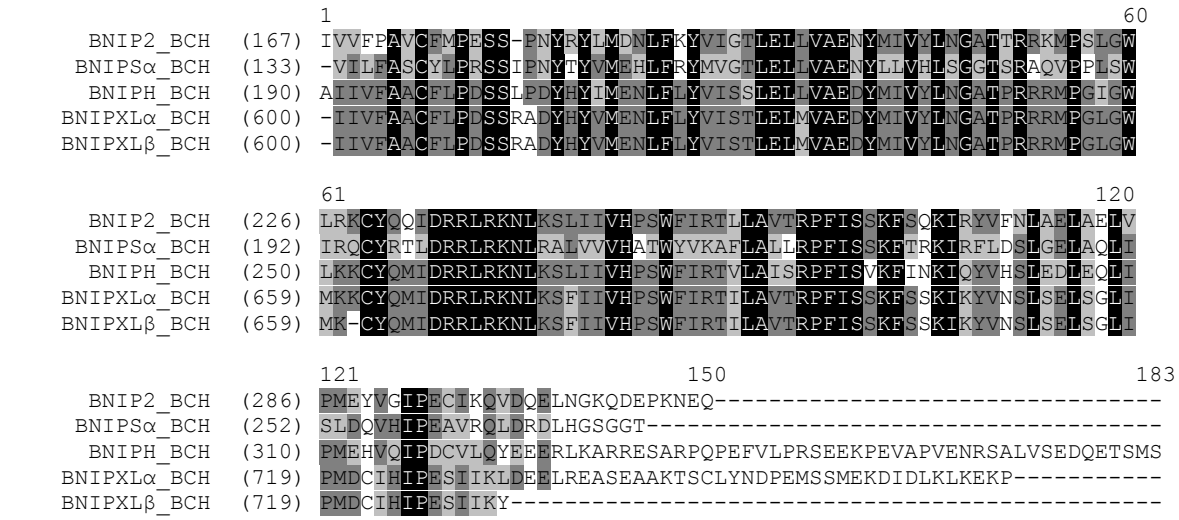

B

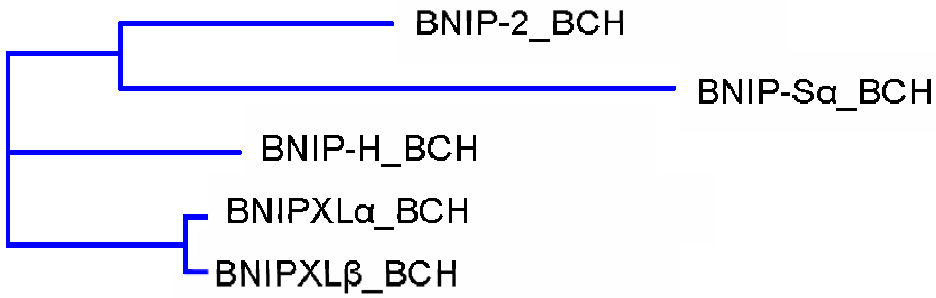

Figure 3.6. (a) Multiple sequence alignments of BCH domains of the BNIP-2 family using Vector NTI suite. Residues that are identical in all members are shaded *black*, those that are conserved in most of the members are in *dark gray* while the significant but least conserved ones are in *light gray* shading. (b) Average distance trees generated using the Vector NTI Suite showing the relative evolutionary relationships of the BCH domain from different BNIP-2 family members.

3.2. Investigating the biochemical and cellular functions of BNIPXL

3.2.1 Expression profile of BNIPXL

3.2.1.1. Expression profile of BNIPXL in human tissues and cell lines

To determine the expression profile of BNIPXL in human tissues and cell lines, we employed semi-quantitative RT-PCR instead of Northern analyses. This will allow different isoforms to be distinguished using diagnostic primers. In addition, their significant homology to BNIP-2 and other BCH domain-containing proteins could potentially result in cross-hybridization in Northern analyses. To ensure greater specificity, we utilized an RT-PCR strategy with specific primers for amplification of both full-length and the BCH domain cDNA. The latter would effectively allow unambiguous distinction of BNIPXLα and BNIPXLβ mRNA transcripts. Amplification of BNIPXL plasmid controls were used for size comparision while a conserved fragment of the glyceraldehyde 3-phosphate dehydrogenase (GAPDH) housekeeping gene was included for normalization of samples. Results are representative of at least two separate determinations.

Human brain, kidney and liver cDNA libraries and total RNA isolated from a panel of transformed human epithelial cell lines grown in appropriate serum-containing medium were used in semi-quantitative RT-PCR as described in 'Material and Methods'. MCF-7, SK-BR3 and MDA-MB-231 are human mammary adenocarcinomas established from pleural effusions. The HER2/c-erb-2 gene product is highly expressed in the weakly invasive SK-BR3 while MDA-MB-231 is an aggressive and highly metastatic breast cancer cell line which overexpresses RhoA and RhoC and exhibits constitutive activation of Ras (Kozma *et al*., 1987) and RhoA (Fritz *et al*., 1999). MCF-7 is a non-motile cell line

that exhibits morphologies resembling that of epithelial cells found in monolayers while HeLa is a human cervical carcinoma cell line that adopts a regular cuboidal shape. Both are excellent candidates for studying subcellular structures using fluorescence microscopy. The human embryonic kidney epithelial cell line HEK293T, is a clonal derivative of HEK293 stably expressing the SV40 large T antigen and was used in subsequent experiments for expression of epitope-tagged recombinant proteins. These studies were carried out to provide insights into the distinct characteristics of these cell lines in relation to BNIPXL expression. In all tissues and cell lines examined, both transcripts were present with the exception of the human embryonic kidney epithelial cells, HEK293T where only the BNIPXLβ isoform was expressed (**Figure 3.7**).

3.2.1.2. Expression profile of BNIPXL in murine tissues and cell lines

To better understand the spatial and temporal expression of BNIPXL, we examined a series of murine tissues and cell lines (**Figure 3.8**). Neuro2a is a mouse neuroblastoma cell line while PC12 is a well-characterized rat adrenal pheochromocytoma cell line that differentiates into neuron-like cells in response to nerve growth factor stimulation. Our earlier attempts to amplify murine BNIPXL using the human-specific forward and reverse primers were unsuccessful, suggesting that the murine BNIPXL sequence may have diverged from its human ortholog at its N-terminus and/or C-terminus end. Mouse and rat-specific BNIPXL primers were then designed based on partial nucleotide sequences from overlapping cosmid clones of the mouse and rat genome. Semi-quantitative RT-PCR produced a band of the expected size in the various mouse organs and indicates that murine BNIPXL is highly expressed in the brain and absent in all other organs except the

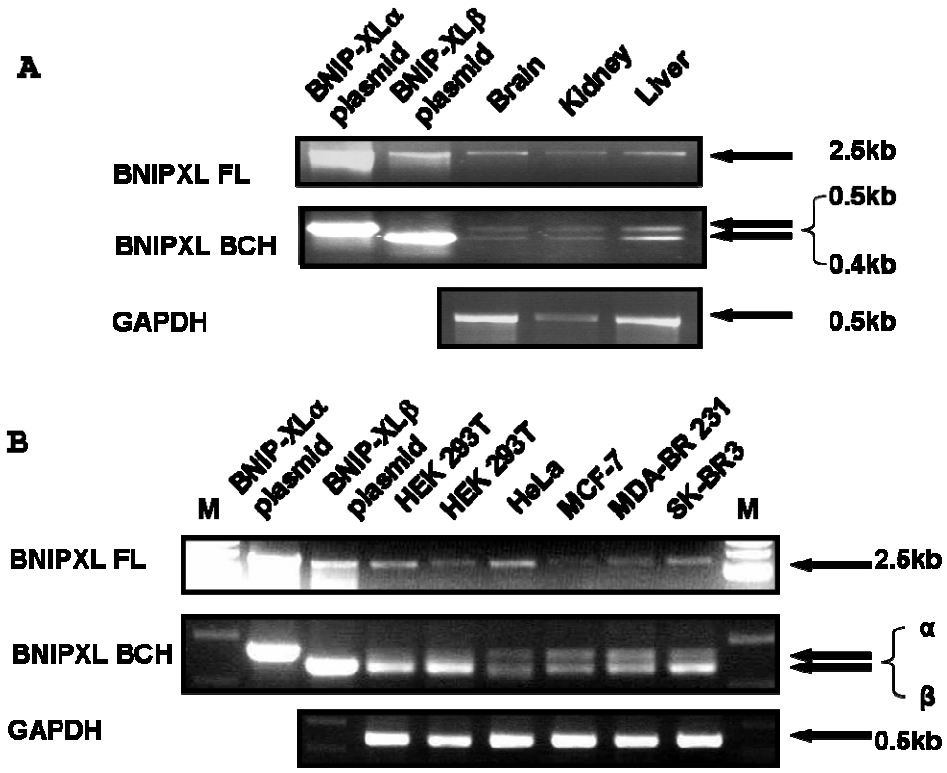

Figure 3.7. (a) The distribution of BNIPXL isoforms in adult human brain, kidney and liver cDNA libraries and (b) various human cell lines was examined by semi-quantitative PCR using primers pairs to amplify full-length (first panel) and BCH domain (second panel), as indicated by the forward (F) and reverse (R) arrows in **Figure 3.2**. BNIPXL plasmid controls and GAPDH expression was analyzed for size comparison and sample normalization, respectively. *M,* markers.

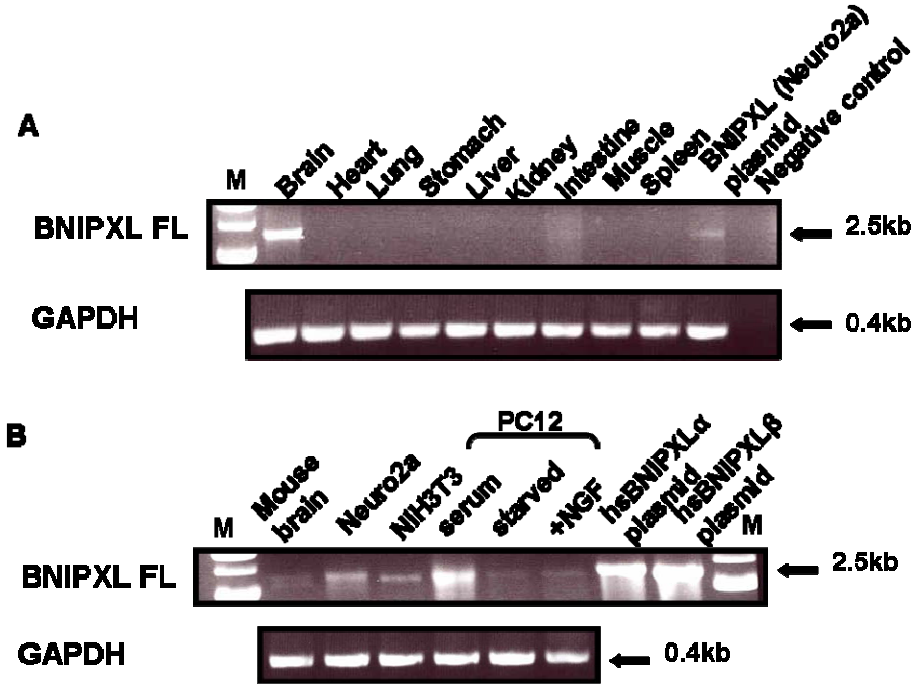

Figure 3.8. (a) The distribution of BNIPXL in (a) mouse organs and (b) various murine or rat cell lines was examined by semi-quantitative PCR using mouse- and rat specific primers pairs for full-length BNIPXL amplification. PC12 cells were maintained in serum, starved for 16 h in 0.5% serum-containing growth media or stimulated for 4 h with 50ng/ml NGF following starvation. BNIPXL plasmid controls and GAPDH expression was analyzed for size comparison and sample normalization, respectively. *M,* markers.

intestines where a weak band was detected (**Figure 3.8a**). The mouse brain fragment were cloned into pGEMT-Easy vector and partial sequencing performed in both directions to confirm its identity. Sequence analyses confirm that the N- and C-terminus of murine BNIPXL are significantly different from human BNIPXL while pairwise alignments of mouse and rat BNIPXL indicate sequence homology at their C-terminus but not at the N-terminus.

The expression profile of mouse BNIPXL is unlike that of human BNIPXL which is detected in various tissues. Similarly, the RT-PCR expression profile of KIAA0367 in various human tissues (http://www.kazusa.or.jp/huge/gfimage/rt-pcr/html/KIAA0367.html) using primers corresponding to the 3'UTR region indicates that KIAA0367 is expressed in most of the human tissues examined except the heart, pancreas, spleen and thymus which show low or no detectable levels of expression. This suggests that expression of this gene locus in mouse may be differentially regulated in contrast to its human orthologs. An indication that mouse BNIPXL may be subjected to alternative RNA splicing comes from the observation of doublet bands in the mouse brain sample (**Figure 3.8b**). BNIPXL was highly expressed in Neuro2a and PC12 cells and to a lesser extent, in the mouse fibroblast cell line, NIH3T3. We note BNIPXL expression in PC12 is highest when maintained in serum as compared to starved cells whilst nerve growth factor (NGF) induction alone is not sufficient to restore its expression to comparative levels.

During the course of thesis amendments, an article reporting the isolation and characterization of another novel BCH domain-containing protein designated BCH motif-containing molecule at the carboxyl terminal region 1 (BMCC1) was published (Machida *et al.,* 2005). Intriguingly, real-time RT-PCR indicates that favorable primary

neuroblastomas (NBL) exhibit increased expression of BMCC1. In addition, the authors observe increased apoptosis in the superior cervical (SCG) neurons derived from BMCC1 transgenic mice upon the withdrawal of nerve growth factor (NGF) stimulation. Collectively, these findings led the authors to conclude that increased expression of the pro-apoptotic BMCC1 correlates to favorable prognosis in childhood NBLs.

Interestingly, full-length BNIPXL shares 98.6% amino acid identity to BMCC1 at its C-terminus suggesting that BMCC1 may be an extended isoform of BNIPXL and a product of alternative RNA splicing (**Figure 3.9**). Alternatively, this also suggests that BNIPXL may be a severely truncated form of BMCC1 since we are unable to identify an in-frame stop codon upstream of the BNIPXL translation initiation start site. Furthermore, Northern blot analysis indicates the expression of a 12kb mRNA transcript in human fetal brain which correlates to an expected size of 350kDa for BMCC1 (Machida *et al*., 2005).

However, the authors have not addressed if this 12kb species is also the only transcript present in other human organs. We note that the BMCC1-specific antibodies used in the paper failed to detect endogenous BMCC1 in the human embryonic kidney epithelial (HEK293) cell line while expression profiling of BMCC1 in multiple human tissues indicates that it is expressed in almost all the tissues surveyed including the kidney. Closer examination revealed that the primers used for amplification lie in the N-terminal region of the BNIPXL nucleotide sequence suggesting that different tissues may express various splicing isoforms of this gene that may or may not be recognized by the BMCC1-specific peptide antibodies (**Figure 3.2**). Furthermore, the *in vitro* assembly of individual PCR- amplified exons into a full-length BMCC1 cDNA construct masks any potential alternative RNA splicing mechanisms that may regulate endogenous expression. In order

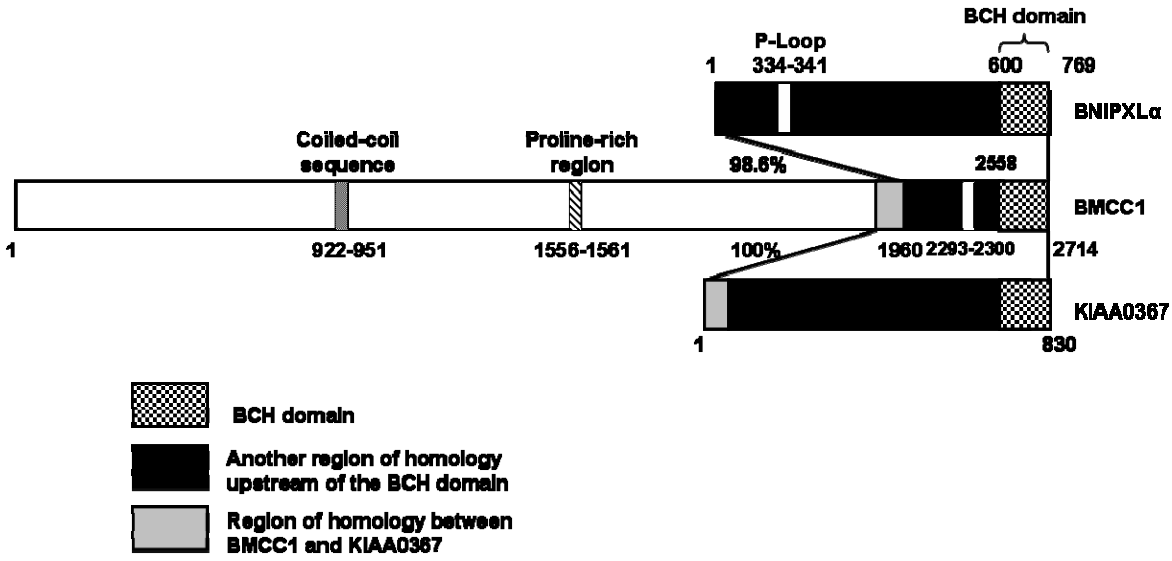

Figure 3.9. Schematic diagram showing pairwise alignments between BNIPXL, BMCC1 and KIAA0367. Values are represented as percentage amino acid identity.

to address these questions, we sought to determine if BNIPXL is indeed an independent isoform using antibodies raised against BMCC1 in endogenous western blot analyses. However, the N- and C-terminus BMCC1 antibodies used in the paper correspond to residues 993-1022 and 1378-1402, respectively and are absent in BNIPXL. At the time of thesis re-submission, we are still waiting for the distal C-terminus BMCC1 antibodies corresponding to residues 2180-2209 and 2693-2714. In the absence of appropriate BMCC1 antibodies, we have utilized the designated primers for diagnostic RT-PCR in an attempt to clarify these discrepancies at the cDNA level (**Figure 3.10**). We were able to amplify the overlapping ~2.4kb fragments flanked by the XFL-1/XR (**lanes 9, 14**) and BMCCHF2/BMCC1R1 primers (**lanes 10, 15**) in HEK293T and HeLa cDNA but failed to amplify the ~4kb fragment flanked by the BMCCHF2/XR primers in HeLa (**lane 16**). Interestingly, we did not detect the ~4kb fragment in the BMCC1 plasmid control (**lane 3**). In addition, we observed a faint ~4kb fragment amplified in the HEK293T sample. We are currently sequencing the BMCC1 plasmid and cloning the ~4kb fragment for further clarification. Our results suggest that different splicing isoforms may be present in the two cDNA samples used.

3.2.2. Domain architecture of BNIPXL constructs

To characterize the well-conserved BCH domain of this novel BNIP-2 family member, a series of BNIPXL fragments comprising the full-length, N-terminus and C-terminus protein fragments (**Figure 3.11**) was FLAG epitope-tagged and transiently expressed in HEK293T cells. The C-terminus fragments starting from residue 440 encompass most of the BNIP-2 sequence having ~67% amino acid identity. Western blot

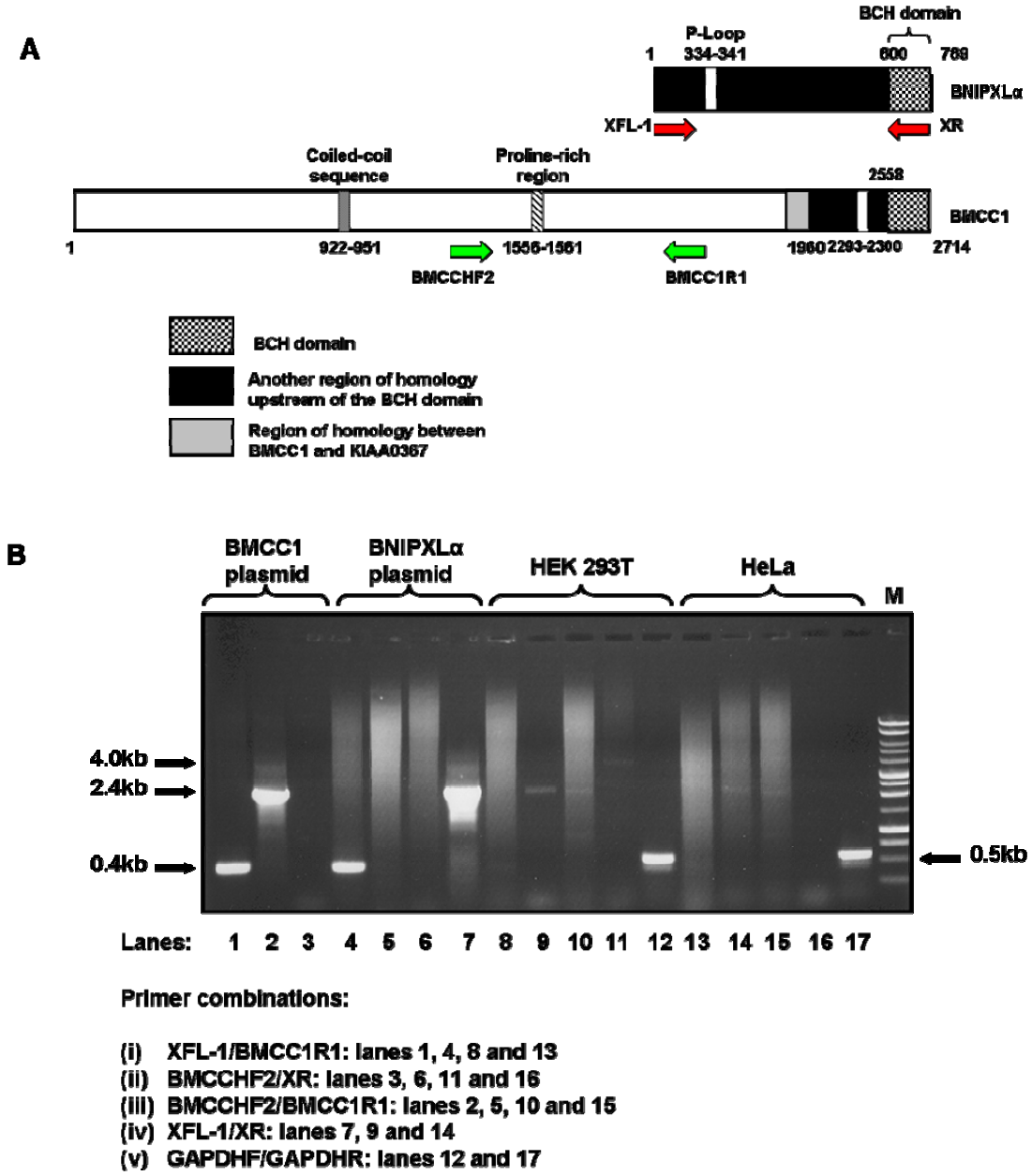

Figure 3.10. (a) Location of various primers used for diagnostic RT-PCR on BNIPXL and BMCC1. (b) Diagnostic RT-PCR using primers pairs as indicated. Plasmid controls and GAPDH expression was analyzed for size comparison and sample normalization, respectively. *M,* markers.

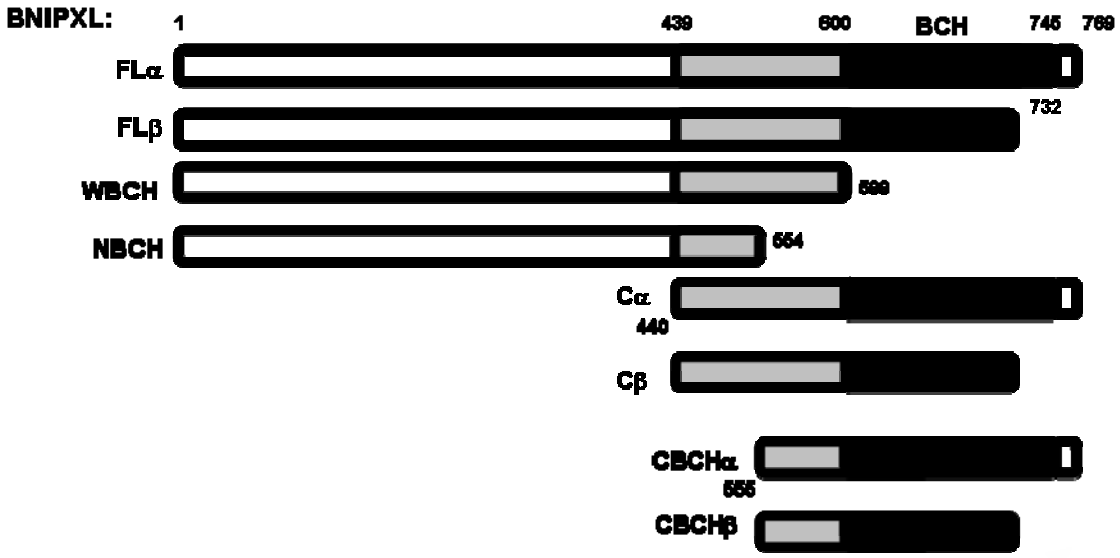

Figure 3.11. Schematic diagram of BNIPXL fragments used in subsequent protein interaction studies. FLα and FLβ (full length, residues 1-769 and 1-732, respectively); WBCH (N-terminus without BCH, residues 1-599); NBCH (N-terminus without CBCH, residues 1-554); Cα and Cβ (C-terminus, residues 440-769 and 440-732, respectively); CBCHα and CBCHβ (C-terminus containing BCH, residues 555-769 and 555-732, respectively). The BCH domain is shaded *black* (66.9% identity with BNIP-2) while the region shaded *gray* is conserved in BNIP-2 (45.4% identity with BNIP-2). All numbers are inclusive.

analyses revealed that each construct was well-expressed as a fusion protein, but each was larger than the expected size with the size disparity more augmented in the N-terminal constructs (**Figure 3.12**). Full length BNIPXL is expected to yield a protein of ~ 80kDa. However, it co-migrates with the 120kDa band on the protein ladder indicating that BNIPXL may undergo post-translational modifications that contribute to this disparity in size or that this could be due to abnormal charge distribution. It was also noted that the larger full-length and N-terminus constructs were susceptible to proteolytic degradation in the course of sample processing as observed by the non-specific bands in **Figure 3.12** (lanes 1-4, red arrow). Since these bands (~45kDa) were detected by the FLAG antibody, this suggests that the region susceptible to cleavage lies near the N-terminus of BNIPXL.

3.2.3. BNIPXL contains a functional protein-protein interaction domain

In light of our previous reports that demonstrate the importance of the BCH domain in mediating protein-protein interactions in the BNIP-2 family, we investigated the functions of the BCH domain in BNIPXL *in vivo* and *in vitro*.

3.2.3.1. BNIPXL isoforms form homophilic complexes via the BCH domain *in vivo*

HEK293T cell lysates co-expressing various HA epitope-tagged BNIPXL fragments and FLAG epitope-tagged full-length BNIPXL were subjected to immunopreicitation with mouse anti-FLAG®M2 beads. Bound proteins were resolved in SDS-PAGE and subjected to western blot analyses as described under 'Materials and Methods'. Both BNIPXL isoforms can form homophilic complexes requiring their respective BCH domains (**Figures 3.13 and 3.14**). It was observed that only fragments

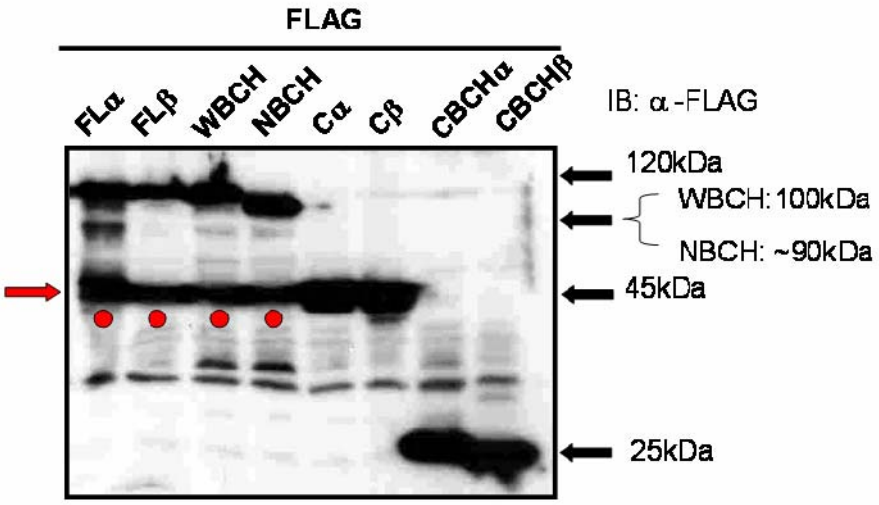

Figure 3.12. Various FLAG epitope-tagged BNIPXL fragments were transfected into HEK293T cells and analyzed for their expression by anti-FLAG immunoblot (IB) analysis. The size of the protein fragments are indicated on the left. The larger BNIPXL fragments are susceptible to degradation (lanes 1-4, red arrow). A series of HA epitope-tagged fragments were also tested for use in subsequent experiments.

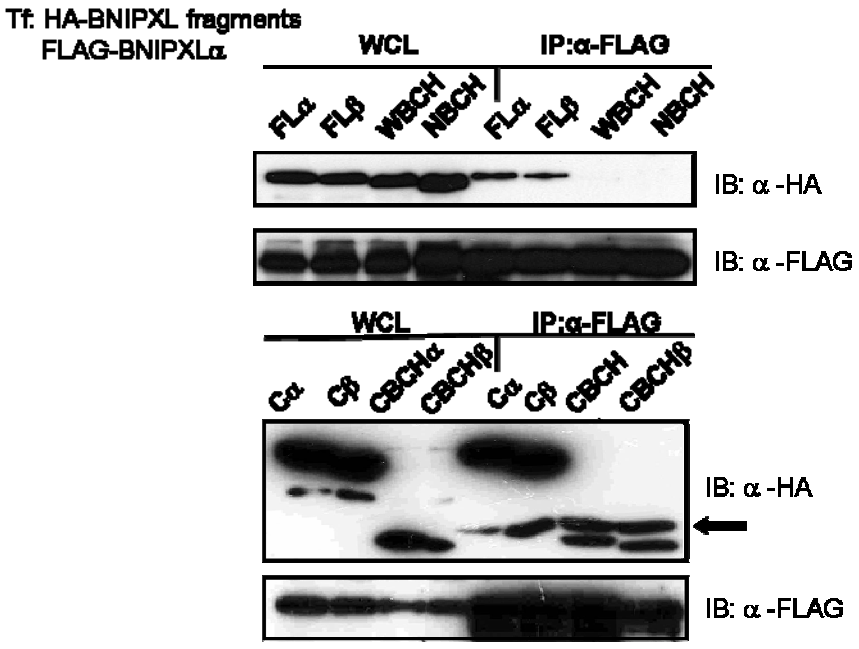

Figure 3.13. BNIPXLα forms homophilic associations with itself via the BCH domain. HEK293T cell lysates expressing both FLAG-tagged full-length BNIPXLα and HA-tagged BNIPXL fragments were immunoprecipitated (IP) with anti-FLAG antibody beads conjugate. Bound proteins were detected with anti-HA immunoblot (IB) (lanes 5-8; first and third panels). Expression of transfected proteins was verified by anti-HA (lanes 1-4; first and third panels) or anti-FLAG (lanes 1-4; second and fourth panels) western analyses of whole cell lysates (WCL), respectively. Blots was stripped and re-probed with anti-FLAG antibody to show amounts of precipitated proteins (lanes 5-8; second and fourth panels). Arrows indicate non-specific bands.

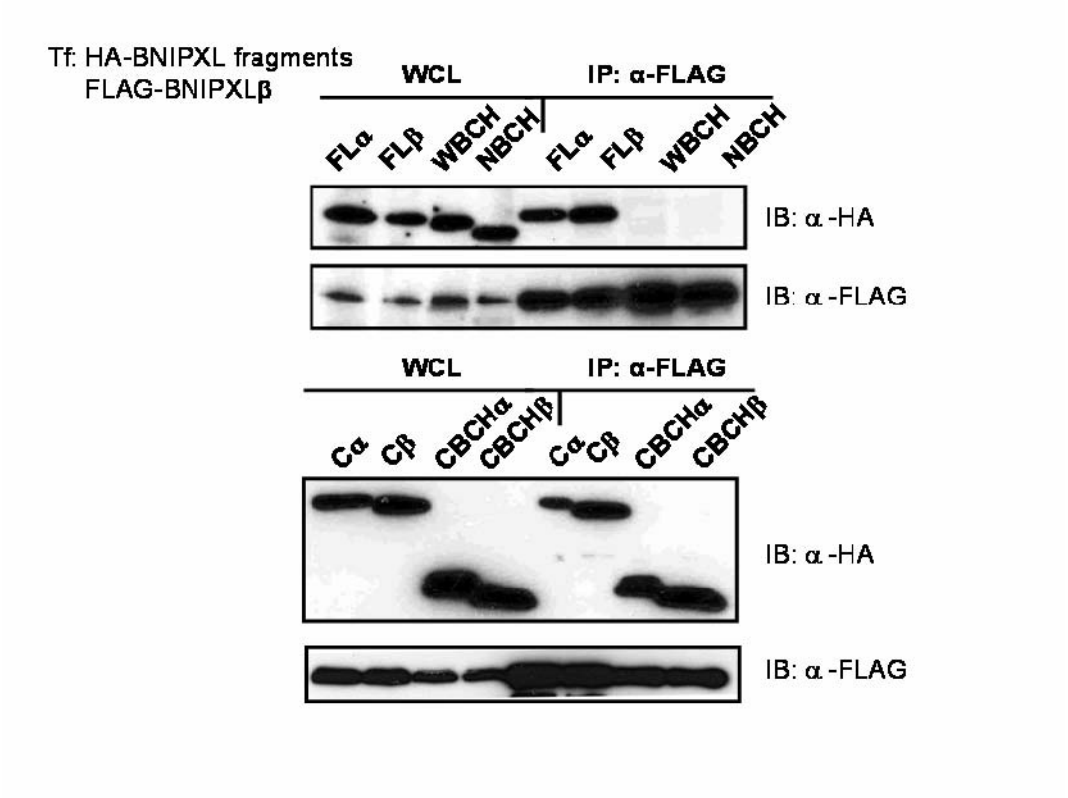

Figure 3.14. BNIPXLβ forms homophilic associations with itself via the BCH domain. Immunoprecipitation of HEK293T cell lysates expressing both FLAG-tagged full-length BNIPXLβ and HA-tagged BNIPXL fragments with anti-FLAG antibody beads conjugate. Bound proteins were detected with anti-HA immunoblot (lanes 5-8; first and third panels). Expression of transfected proteins was verified by anti-HA (lanes 1-4; first and third panels) or anti-FLAG (lanes 1-4; second and fourth panels) western analyses of whole cell lysates (WCL), respectively. Blots was stripped and re-probed with anti-FLAG antibody to show amounts of precipitated proteins (lanes 5-8; second and fourth panels).

containing the BCH domain could be detected in the IP lanes. Results from these initial binding experiments strongly indicate that BNIPXL may also bind other BCH domain-containing proteins in a similar manner forming heterophilic complexes.

3.2.3.2.BNIPXL associates with BNIP-2 and p50-RhoGAP *in vivo*

To test our hypothesis that BNIPXL may form heterophilic complexes with other BCH domain-containing proteins, FLAG epitope-tagged BNIP-2 or p50-RhoGAP was co-expressed with HA epitope-tagged BNIPXL fragments in HEK293T cells and lysates were subjected to immunoprecipitation as previously described (**Figures 3.15 and 3.16**). We demonstrate that full-length BNIP-2 and p50-RhoGAP can precipitate full-length BNIPXL *in vivo* and this was primarily mediated by the C-terminus BCH domain of BNIPXL and not by the other regions of the protein. The apparent homophilic and heterophilic interactions between BNIPXL with itself, BNIP-2 or p50-RhoGAP was mediated by the BCH domain and is deemed specific because all other BNIPXL fragments without the BCH domain failed to bind to these protein targets under the experimental conditions. These findings are therefore consistent with previous observations that the BCH domain mediates target protein binding in other BCH domain-containing BNIP-2 family members (Low *et al.,* 2000a; Zhou *et al.,* 2002), and the BPGAP family proteins (Shang *et al*., 2003).

3.2.3.3.BNIPXL directly associates with its target proteins

For all binding experiments described previously, both BNIPXL and the candidate protein were overexpressed in lysates where both proteins partners and/or fragments were

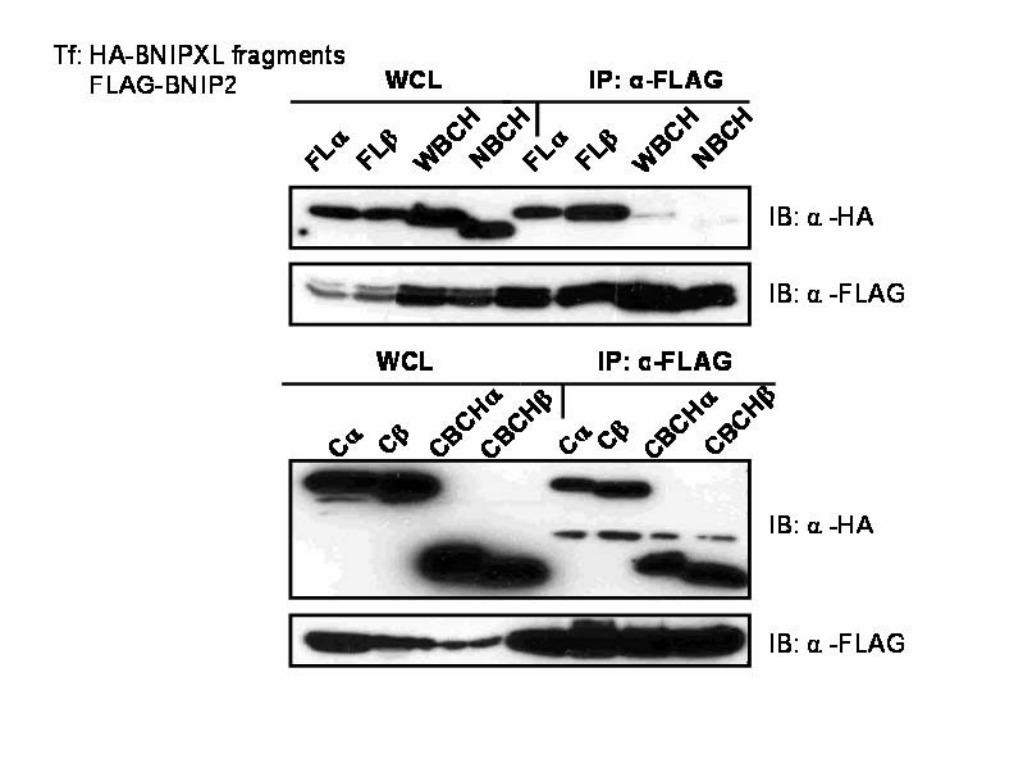

Figure 3.15. The BNIPXL BCH domain mediates protein-protein interaction with other BCH domain-containing proteins *in vivo*. FLAG-tagged BNIP-2 and HA-tagged BNIPXL fragments were immunoprecipitated with anti-FLAG antibody beads conjugate. Bound proteins were detected with anti-HA immunoblot (lanes 5-8; first and third panels). Expression of transfected proteins was verified by anti-HA (lanes 1-4; first and third panels) or anti-FLAG (lanes 1-4; second and fourth panels) western analyses of whole cell lysates (WCL), respectively. Blots was stripped and re-probed with anti-FLAG antibody to show amounts of precipitated proteins (lanes 5-8; second and fourth panels).

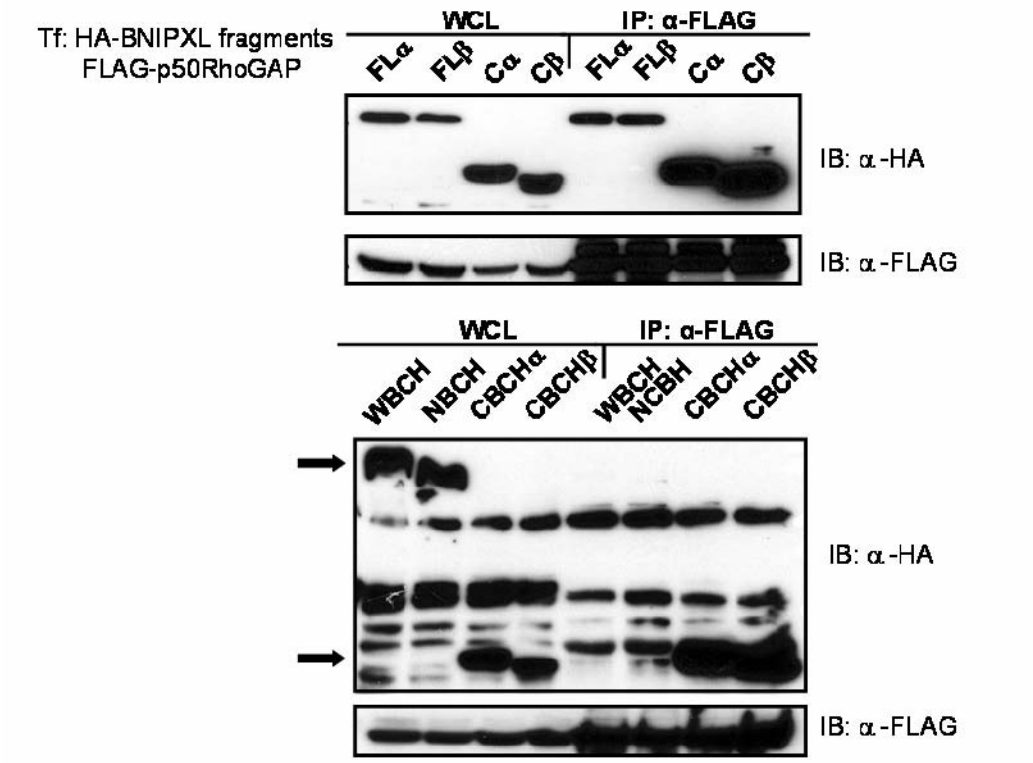

Figure 3.16. BNIPXL forms heteromeric complexes with p50-RhoGAP via the BCH domain. HEK293T cell lysates expressing FLAG-tagged p50-RhoGAP and various HA epitope-tagged BNIPXL domains were immunoprecipitated with anti-FLAG antibody beads conjugate. Bound proteins were detected with anti-HA immunoblot (lanes 5-8; first and third panels). Expression of transfected proteins was verified by anti-HA (lanes 1-4; first and third panels) or anti-FLAG (lanes 1-4; second and fourth panels) western analyses of whole cell lysates (WCL), respectively. Blots was stripped and re-probed with anti-FLAG antibody to show amounts of precipitated proteins (lanes 5-8; second and fourth panels). Arrows indicate non-specific bands.

present in great excess. Associations between these molecules are most likely to be direct since large protein amounts were precipitated indicating that there are no limiting third parties. To verify the direct involvement of BNIPXL in homo- and heterophilic complexes *in vivo* we employed the yeast-two hybrid system. BNIPXLα and BNIPXLβ were fused to the yeast GAL4 DNA-binding and activation domains and tested against itself, p50-RhoGAP and BNIP-2 (**Table 5**). pAS- BNIP-2 and pACT-p50-RhoGAP binding was used as a positive control (Low *et al.,* 2000a). Standard β-galactosidase assays confirmed that BNIPXL can directly form homo- and heterodimers *in vivo* (**Figure 3.17**). Collectively, these results demonstrate that BNIPXL can directly form homo- and heterophilic complexes that are mediated by its BCH domain in vivo confirming the notion that the BCH domain functions as a protein-protein interaction module within different protein contexts.

3.2.4. BNIPXL induces morphological changes in HeLa cells via its BCH domain

BNIP-2 and other BCH domain-containing proteins have been shown to elicit cell morphological changes by targeting different members of the Rho GTPases. To investigate the cellular effects of BNIPXL, full length and various fragments of FLAG-epitope tagged BNIPXL were transiently expressed and examined in HeLa, a human cervical carcinoma cells using confocal fluorescence microscopy (**Figure 3.18).** Full-length and fragments containing the BCH domain exhibited phenotypes distinct from the surrounding non-transfected cells and were localized in cytosolic punctate structures; inducing varying cell morphological changes dependent on the level of protein expression (**Figures 3.18a, 3.18b, 3.18d, 3.18e**). Generally, full-length BNIPXL expression results in cell elongation

Table 5. BNIPXL forms direct homophilic and heterophillic interactions with itself and other BCH-domain containing proteins. The AH109 yeast strain was transformed, growth/X-gal selection and β-galactosidase assays were performed as described under "Materials and Methods". Gal4 activation domain fusion proteins in the pACT vector included: BNIPXLα, BNIPXLβ, and p50-RhoGAP. Gal4 DNA-binding domain fusion proteins in the pAS vector included: BNIPXLα, BNIPXLβ, and BNIP-2. *O* denotes vector alone. A positive interaction (+) is scored by colonies that turned blue within 3 h; (-) indicates a negative interaction.

pACT / pAS	O	BNIPXL-FLα	BNIPXL-FLβ	p50-RhoGAP
O	-	-	-	-
BNIPXL-FLα	-	+	+	+
BNIPXL-FLβ	-	+	+	+
BNIP-2	-	+	+	+

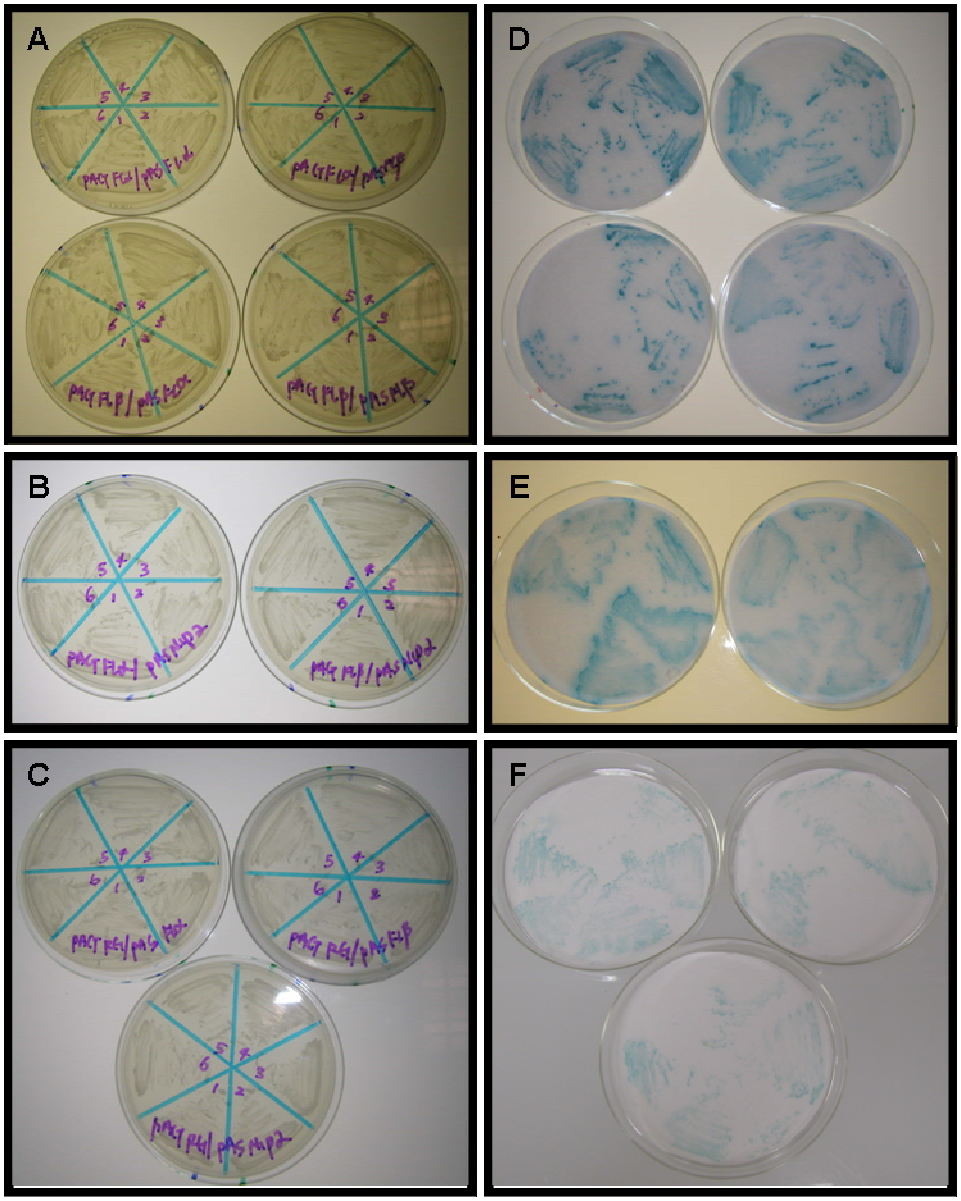

Figure 3.17. The *S. cerevisiae* AH109 strain was co-transformed with (a) pACT-FLα/pAS-FLα, pACT-FLα/pAS-FLβ, pACT-FLβ/pAS-FLα and pACT -FLβ/pAS-FLβ constructs; (b) pACT-FLα/pAS-BNIP-2 and pACT-FLβ/pAS-BNIP-2 constructs; (c) pAS-FLα/pACT-p50-RhoGAP, pAS-FLβ/pACT-p50-RhoGAP and pAS-BNIP-2/pACT-p50-RhoGAP as positive control. Selection was performed on –Leu/-Trp SD agar and five individual colonies were re-streaked on –Leu/-Trp/-His SD agar. The corresponding colony lifts for β-galactosidase expression demonstrate direct associations between target proteins (d-f).

BNIPXL:

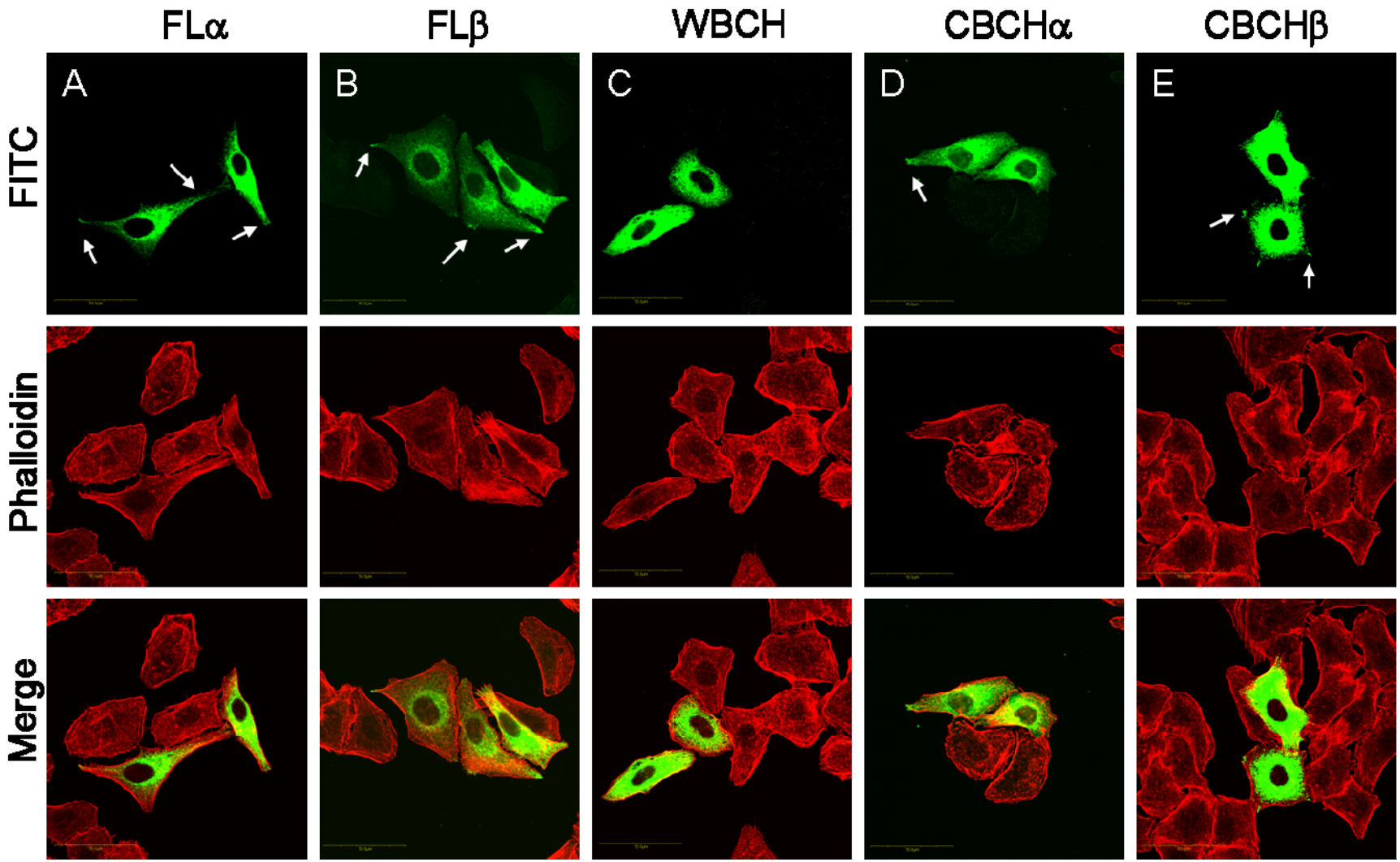

Figure 3.18. (a-e) BNIPXL induces cell morphological changes via its BCH domain. HeLa cells expressing FLAG-tagged BNIPXL fragments were fixed 24 h post-transfection, permeabilized and stained. FLAG-tagged constructs were detected with a mouse monoclonal anti-FLAG antibody followed by FITC-conjugated goat anti-mouse secondary antibody. F-actin was detected using TRITC-conjugated phalloidin and visualized by confocal fluorescence microscopy. Arrows indicate membrane protrusions and concentration of protein at the tips of these protrusions. Scale bars, 50μm.

coupled with membrane protrusions with BNIPXL concentrated at the leading edge of these protrusions while CBCH fragments exhibited similar protrusions and localization to the tips of these protrusions but without marked cell elongation. Conversely, the WBCH fragment lacking the BCH domain presented a uniform cytosolic distribution with no obvious perturbations in cell morphology when compared to control cells (**Figure 3.18c**). This was confirmed by co-staining transfected cells with TRITC-conjugated phalloidin for F-actin which demarcates the intact cuboidal cell border. These phenotypes observed is consistent with previous observations that transiently expressed full length BNIP-2 and BPGAP1 can induce similar cell morphological changes in MCF-7 cells (Zhou *et al.,* 2005a; Shang *et al.,* 2003). In contrast, BNIP-Sα transfected cells exhibited cell rounding, a typical hallmark of apoptosis (Zhou *et al.,* 2002). Taken together, these results suggest that the BCH domain is necessary for BNIPXL-induced cell morphological changes and that homologous BCH domains can cause distinct cell shape perturbations.

3.3. Delineating the molecular mechanisms of BNIPXL-induced morphological changes

3.3.1. BNIPXL associates with RhoA *in vivo*

To further delineate the molecular mechanisms underlying the BNIPXL-induced cell shape changes, we next sought to understand which other proteins it might associate with. Our recent reports demonstrate the involvement of BNIP-2 in the modulation of Cdc42 signaling pathways via its BCH domain (Zhou *et al.,* 2005a). To this end, we attempted to verify the possible involvement of the Rho family small GTPases in the observed cell phenotype based on the hypothesis that perturbations in cell shape are likely to be the result of actin cytoskeletal remodeling in which Rho GTPases are known to play important regulatory roles. Thus, we first determined if BNIPXL could specifically associate with members of the Rho GTPase family and then verified if this interaction(s) could affect BNIPXL-induced cell shape changes and membrane protrusions in any manner. Cells were cotransfected with HA-tagged wild-type RhoA, Cdc42 or Rac1 together with either FLAG-tagged-BNIPXLα or BNIPXLβ and immunoprecipitations performed as described in 'Materials and Methods' (**Figure 3.19**). Both isoforms of BNIPXL were found to interact specifically with RhoA but not to Cdc42 or Rac1 *in vivo*. However, we did not readily detect the presence of endogenous RhoA in the complex. This implies that their binding may be transient and/or weak. Due to the similar binding profiles of both isoforms to candidate proteins tested so far, we decided to utilize BNIPXLβ, the shorter variant in all our subsequent experiments.

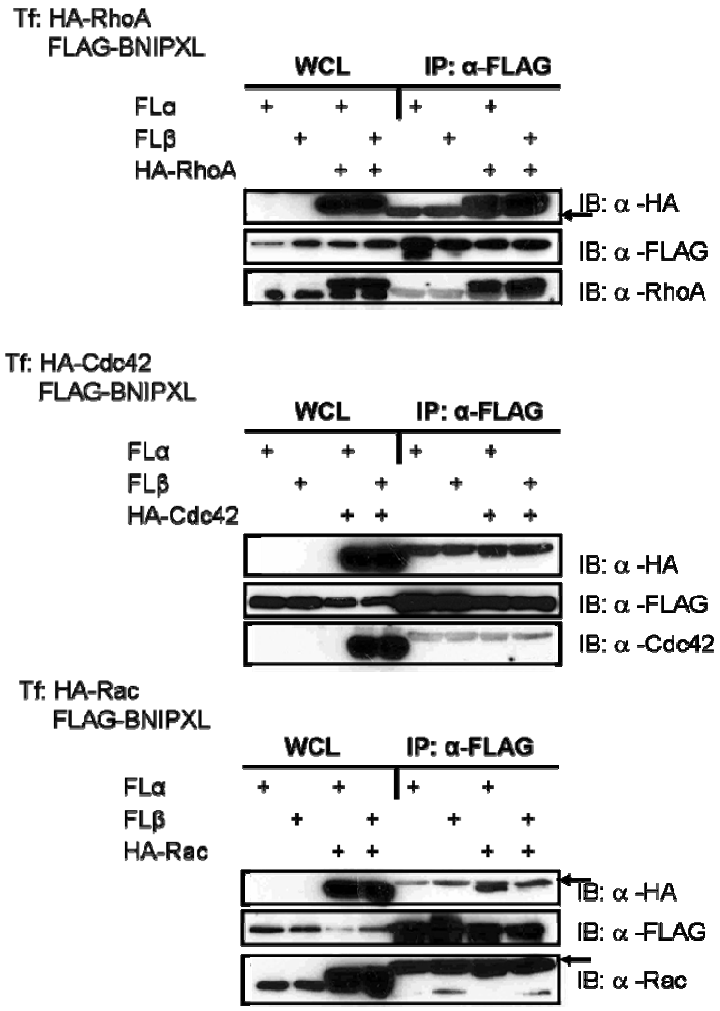

Figure 3.19. BNIPXL interacts specifically with RhoA *in vivo***.** Co-expression of FLAG-tagged BNIPXL with vector control or HA-tagged RhoA, Cdc42 or Rac1 were subjected to immunoprecipitation and bound proteins detected in anti-HA westerns (lanes 5-8, upper panels). Expression of transfected proteins was verified by westerns using anti-HA for GTPases (lanes 1-4, upper panels) or anti-FLAG for BNIPXL (lanes 1-4, middle panels) Blots were stripped and re-probed with anti-Rho GTPase antibody (lanes 5-8, lower panels) and re-probed with anti-FLAG antibody to show the amounts of precipitated proteins (lanes 5-8, middle panel). Arrows indicate light chain from antibody.

3.3.2. The BNIPXL BCH domain directly interacts with RhoA

To verify that BNIPXL-RhoA associations *in vivo* are direct, we subjected *in vitro* transcribed and translated FLAG-tagged BNIPXL to *in vitro* GST-fusion pull down assays with GST-RhoA. FLAG-tagged BNIPXL fragments produced *in vitro* was incubated with equal amounts of bacterially-produced GST or GST-RhoA and the bound proteins were then subjected to western blot analyses. Our results indicate that the CBCH fragment forms direct and strong interactions with RhoA (**Figure 3.20**). The requirement for longer exposure times is indicative that full-length BNIPXL-RhoA interactions may occur at much lower relative affinities *in vitro*. However, this claim has yet to be substantiated by quantitative measurements. These observations suggest that the presence of the N-terminus in full-length BNIPXL interferes with BNIPXL-RhoA interactions mediated by the CBCH domain.

3.3.3. Delineating the RhoA-binding region in BNIPXL

Our next question was whether RhoA binding had any influence on BNIPXL-induced cell shape changes. To answer this, we had to define the region that was responsible for mediating RhoA binding. Our recent finding indicates that BNIP-Sα contains a RhoA Binding Region (RBR) from residues 133-177 which lie within its BCH domain (Zhou *et al.,* 2005b). Consistent with these findings, multiple sequence alignments of class I Rho-binding motifs found in several RhoA effectors (Fujisawa *et al.,* 1998) and the BNIP-S Rho binding domain (RBD) (residues 148-177) suggests that the proximal region of the BNIPXL BCH domain (residues 615-644) could also be a putative RBR

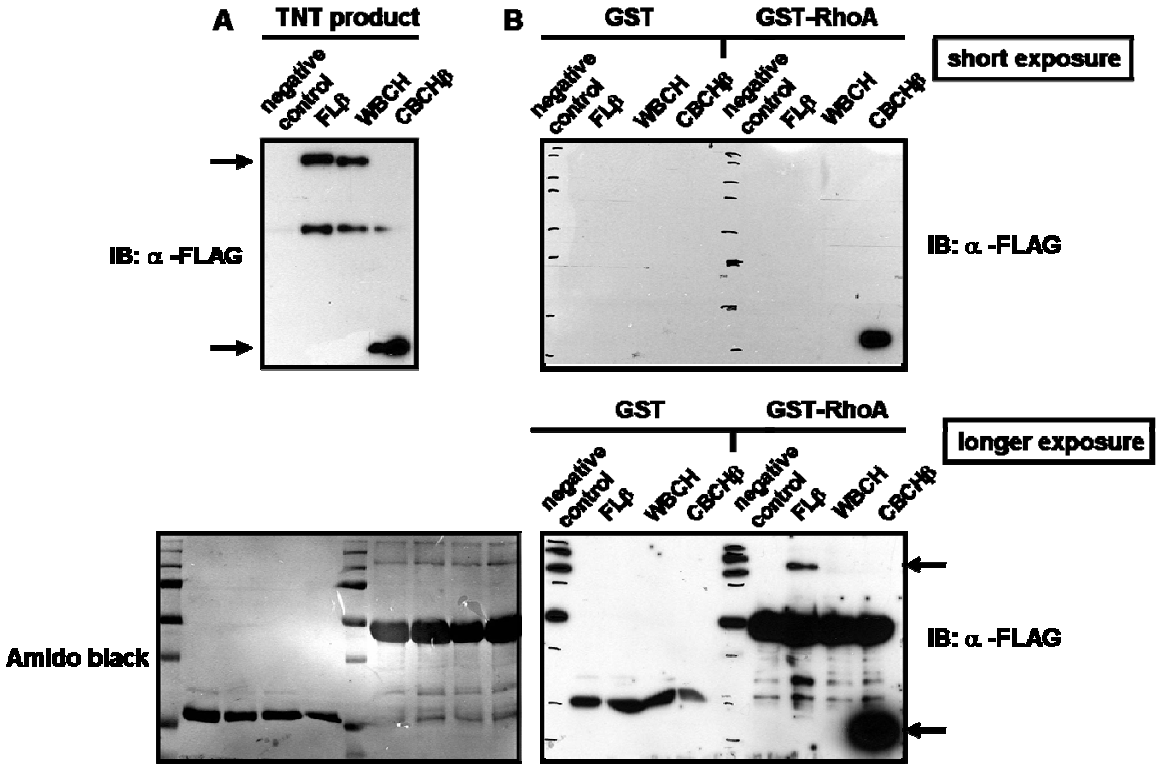

Figure 3.20. BNIPXL directly interacts with RhoA. *In vitro* transcribed and translated FLAG-tagged BNIPXL fragments (a) were incubated with equal amounts of bacterially-produced GST or GST-RhoA and the bound proteins were then subjected to western blot analyses using anti-FLAG antibody (b). Membranes were subjected to short (30 secs) and longer exposure (1 hr) times. Blots were then stained with amido-black to ascertain equal loading of GST fusion proteins in the *in vitro* pull-down assay. The integrity of GST fusion proteins was previously affirmed by checking their migration profiles on Commassie-blue stained gels. Arrows indicate expected bands.

(**Figure 3.21**).

3.3.4. Domain architecture of BNIPXL deletion constructs

Having identified the potential region for RhoA binding *in silico*, a sequential series of internal deletions within the BCH domain was generated based on the predicted secondary structure of the BNIPXLβ BCH domain. Using Jpred (http://www.compbio.dundee.ac.uk/~www-jpred/), residues outside the putative α-helices were chosen to define the different deletion regions to minimize the possibility of disrupting the BNIPXL conformational folds (**Figure 3.22**). The FLAG-epitope tagged deletion mutants were designated: △0, △1, △2, △3 and △4 was used in subsequent experiments (**Figure 3.23**).

3.3.5. A full composite BCH domain is necessary for RhoA association

Cells were co-transfected with the FLAG-tagged BNIPXLβ deletions and HA-tagged wild-type RhoA and subjected to immunoprecipitation as described previously (**Figure 3.24**). Interestingly, all five deletions failed to interact with wild-type RhoA suggesting that multiple motifs within the BCH domain are required for RhoA binding. We argued that deleting these regions within the BCH domain could have potentially destroyed the structural integrity of the protein. To confirm the structural integrity of the BNIPXLβ deletion mutants, the FLAG-tagged constructs were subjected to similar immunoprecipitation experiments with wild-type HA-tagged BNIPXLα and BNIPXLβ (**Figure 3.25**). All constructs retained their ability to associate with both wild-type BNIPXLα and BNIPXLβ *in vivo*. Collectively, the evidence suggests that the deletion

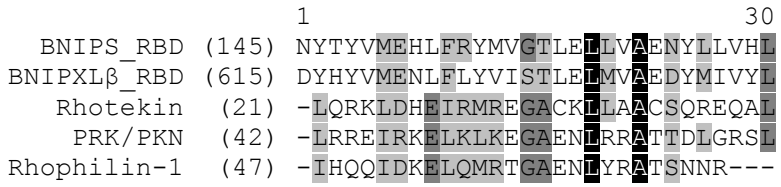

Figure 3.21. Multiple sequence alignments of BNIPXLβ, the BNIP-Sα RBR and Class I Rho binding motifs from RhoA effectors proteins using the Vector NTI Suite. Residues that are identical in all members are shaded *black*, those that are conserved in most of the members are in *dark gray* while the significant but least conserved ones are in *light gray* shading.

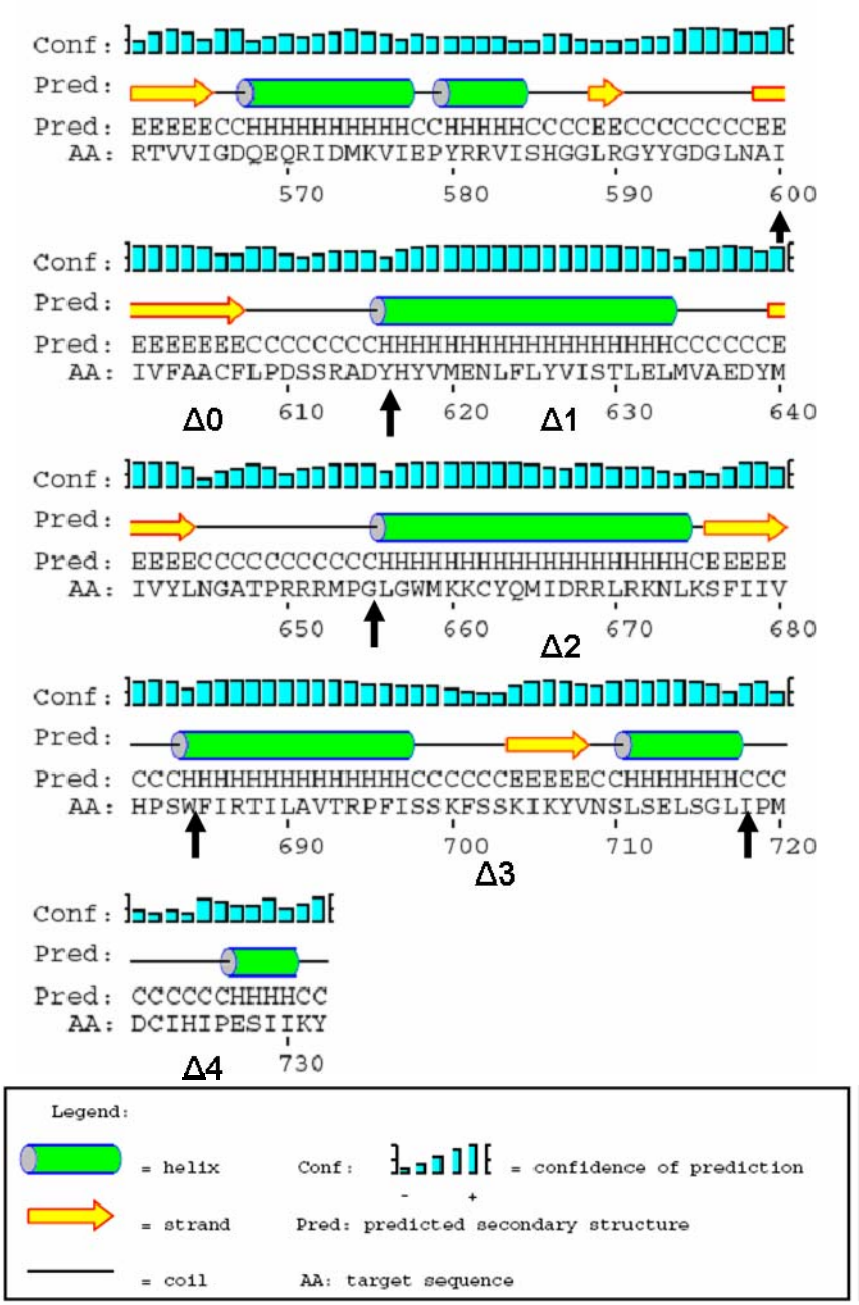

Figure 3.22. Secondary structure prediction of the BNIPXLβ BCH domain using Jpred (http://www.compbio.dundee.ac.uk/~www-jpred/). Arrows indicate the boundaries of the deletions.

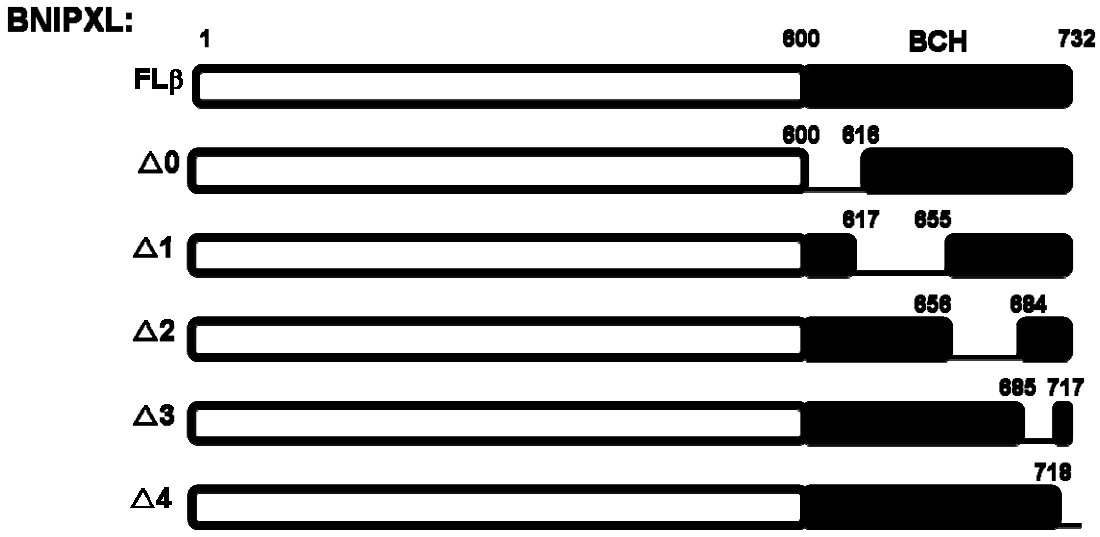

Figure 3.23. Schematic diagram of BNIPXLβ deletion mutants constructs: BNIPXLβ△0 (△600-616 amino acids), BNIPXLβ△1 (△617-655 amino acids), BNIPXLβ△2 (△656-684 amino acids), BNIPXLβ△3 (△685-717 amino acids) and BNIPXLβ△4 (△718-△732 amino acids); were all tagged with FLAG-epitope for subsequent experiments. All numbers are inclusive.

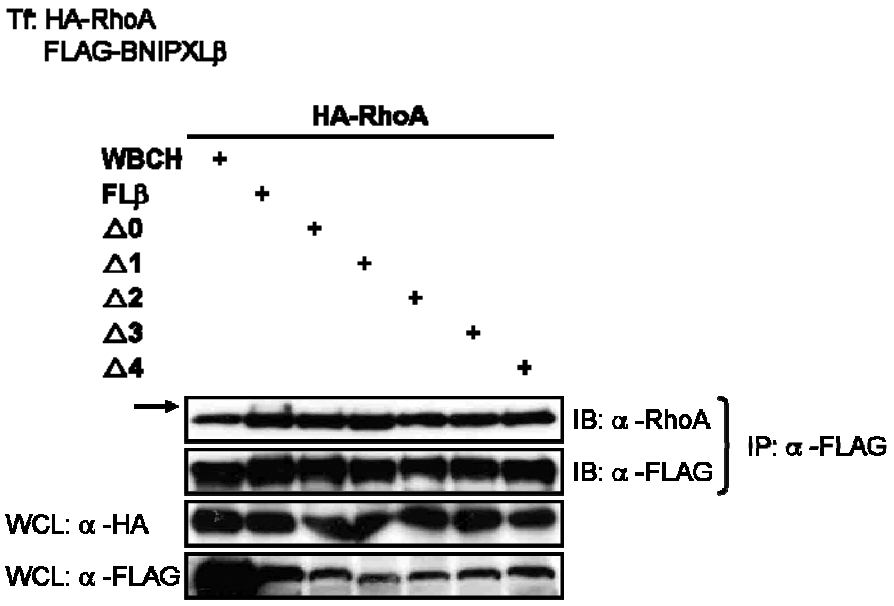

Figure 3.24. The full composite BCH domain is required for RhoA binding. HEK293T lysates expressing HA-tagged wild type RhoA and different FLAG-BNIPXL fragments were subjected to immunoprecipitation and processed as previously described. Expression of transfected proteins was verified by anti-HA (third panel) or anti-FLAG (fourth panel) western analyses of whole cell lysates (WCL), respectively. Blots were probed with polyclonal anti-RhoA antibody (first panel); stripped and probed with anti-FLAG antibody to show amounts of precipitated proteins (second panel). Arrow indicates the expected band.

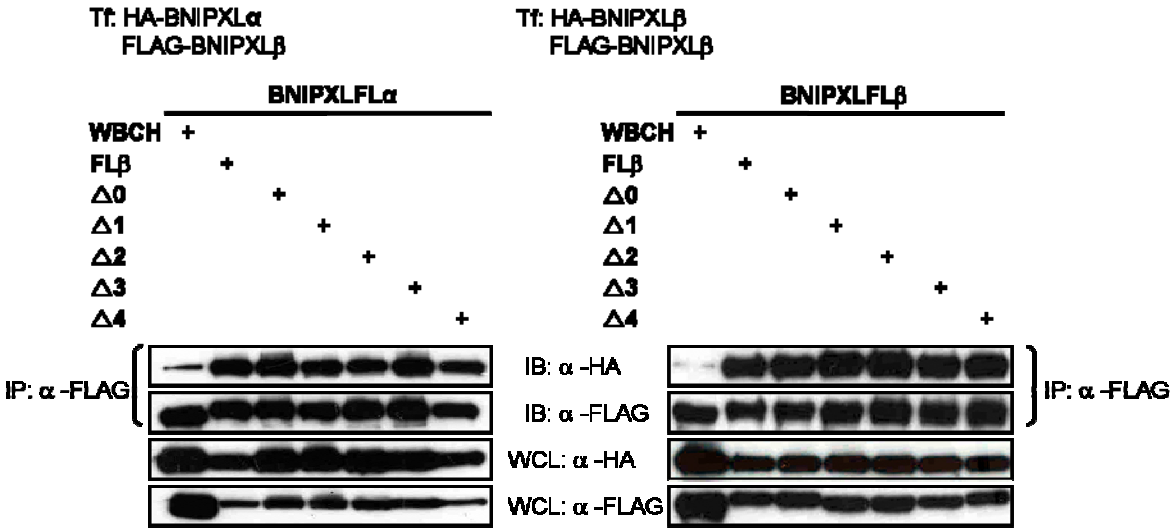

Figure 3.25. The BNIPXL deletion mutants are structurally intact. HEK293T lysates expressing HA-tagged wild type BNIPXLα or BNIPXLβ and different FLAG-BNIPXL fragments were subjected to immunoprecipitation and processed as previously described. Expression of transfected proteins was verified by anti-HA (third panel) or anti-FLAG (fourth panel) western analyses of whole cell lysates (WCL), respectively. Blots were probed with polyclonal anti-HA antibody (first panel); stripped and probed with anti-FLAG antibody to show amounts of precipitated proteins (second panel).

mutants possess an intact conformation and indicates that a full composite BCH domain is essential for RhoA association *in vivo.* The results also demonstrate that BNIPXL utilizes multiple regions within its BCH domain for homo- and heterophilic interactions unlike BNIP-2 and BNIP-S.

3.3.6. BNIPXL interacts with RhoA *in vitro* in a conformation-dependent manner

To investigate the nature of BNIPXL associations with RhoA, we employed an *in vitro* GST-fusion pull down assays. Our aim was to determine if BNIPXL had any binding preference to RhoA in a nucleotide-dependent manner. Cells were transiently transfected with various fragments of FLAG-tagged BNIPXLβ or Myc-tagged p160ROCK. The p160ROCK, first purified as a GTP-RhoA binding protein using a ligand overlay assay (Ishizaki *et al.,* 1996), was used as the positive control for GST-RhoA nucleotide loading as previously described (Peck *et al.,* 2002). Lysates were pooled and then divided into three equal portions and subjected to a pull-down experiment with equal amounts of GST-RhoA that was either preloaded with GDP or GTPγS (a nonhydrolyzable analogue of GTP) or not loaded with either nucleotide. The bound proteins were then subjected to western blot analyses.

Our results indicate that GST-RhoA binds to the CBCH fragment but failed to precipitate full length BNIPXL and the WBCH fragments *in vitro* (**Figure 3.26**)**.** This is similar to that observed in the direct binding assays. Comparatively, the CBCH fragment preferentially binds to nucleotide-free and GTPγS-RhoA but weakly to GDP-bound RhoA. These results indicate that BNIPXL can interact with RhoA regardless of its guanine nucleotide binding status although its apparent preference for GTPγS-RhoA over GDP-

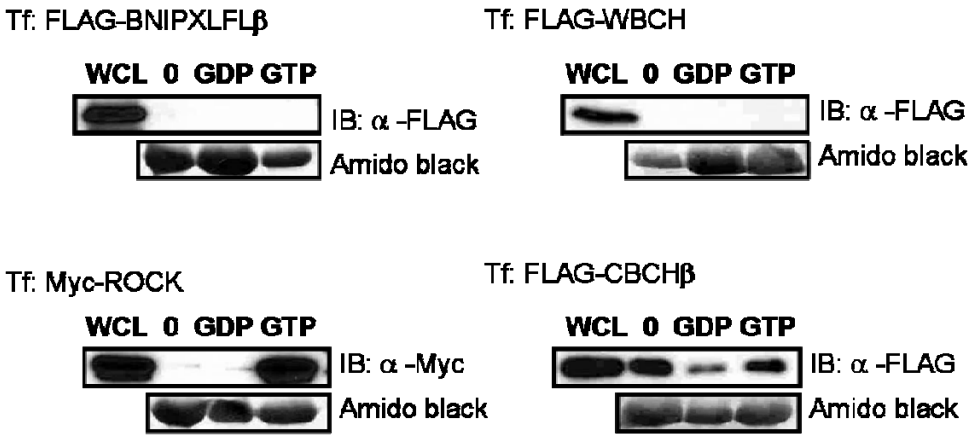

Figure 3.26. BNIPXLβ interacts with RhoA independent of its nucleotide-binding status. HEK293T lysates expressing FLAG-tagged BNIPXL fragments were incubated with GST-RhoA, RhoA preloaded with GDP or GTPγS as indicated. Bound proteins and whole cell lysate input were analyzed by immunoblotting with anti-FLAG polyclonal or anti-Myc monoclonal antibodies followed by Amido-black staining to ascertain equal loading of GST fusion proteins used for the *in vitro* pull-down assay. The integrity of GST fusion proteins was previously affirmed by checking their migration profiles on Commassie-blue stained gels.

RhoA suggests that BNIPXL may exert a regulatory effect on RhoA.

3.3.7. BNIPXL interacts with dominant negative RhoA *in vivo*

To understand the implications of the BNIPXL-RhoA interactions *in vivo*, we examined BNIPXL interactions with the RhoA(G14V) (constitutive active) and RhoA(T19N) (dominant negative) P-loop mutants. Interestingly, our results indicate that BNIPXL preferentially binds to wild-type RhoA compared to the RhoA(T19N) mutant while BNIPXL-RhoA interactions were completely abolished with the RhoA(G14V) mutant (**Figure 3.27**). This appears to contradict our previous *in vitro* results which indicate BNIPXL preferences for unloaded and GTP-bound RhoA. However, it could also be an indication that the glycine residue and the P-loop region of RhoA are important for its association with BNIPXL. A recent survey of the RhoA structural motifs indicate that the P-loop region (residues 12-19) may mediate effector binding in addition to GAP recognition (Dvorsky and Ahmadian, 2004). These results suggest that BNIPXL could regulate RhoA/effector interactions via its ability to discriminate conformational changes associated with nucleotide binding.

In addition, we note that RhoA(G14V) and RhoA(T19N) appear to have different migratory profiles compared to wild-type RhoA. To ensure that this migratory pattern is not the result of spontaneous nucleotide mutations, we have sequenced and confirmed the integrity of all three constructs. This indicates that the differential migratory profile is likely to be an intrinsic anomaly arising from post-translational modifications of these mutants. Similarly, such differential migratory patterns have been observed in other RhoA mutants with single amino acid substitutions in the effector loop (residues 37-42) (Sahai *et*

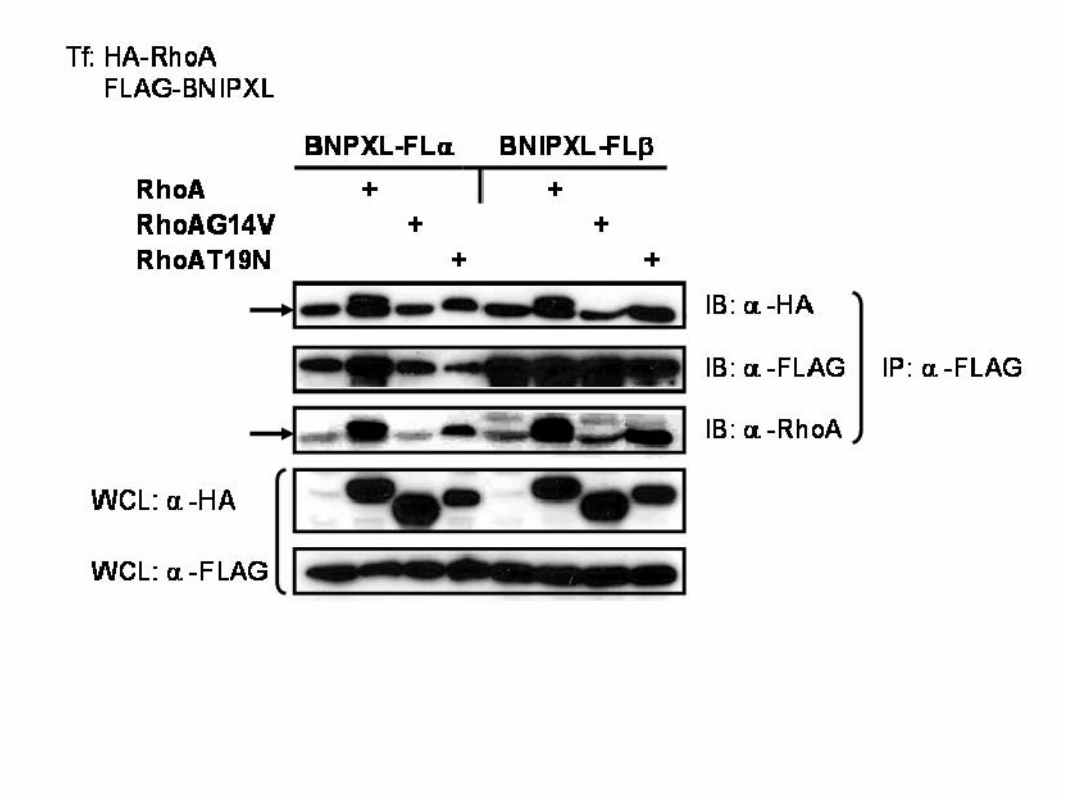

Figure 3.27. BNIPXL interacts with dominant negative RhoA (T19N) but not with constitutive active RhoA(G14V) *in vivo*. Co-expression of FLAG-tagged BNIPXL with vector control (lanes 1 and 5) or HA-tagged RhoA wild-type, dominant active (G14V) or negative (T19N) mutants were subjected to immunoprecipitation and bound proteins detected in anti-HA westerns (first panel). Blots were re-probed with anti-RhoA antibody (second panel) and re-probed with anti-FLAG antibody to show the amounts of precipitated proteins (third panel). Expression of transfected proteins was verified using anti-HA for RhoA (fourth panel) or anti-FLAG for BNIPXL (fifth panel). Arrows indicate light chain from antibody.

al., 1998).

3.3.8. BNIPXL interacts with specific constitutive active RhoA mutants *in vivo*

To further investigate the nature of BNIPXL-RhoA interactions *in vivo*, we examined BNIPXL interactions with other RhoA constitutive active mutants. The RhoA(F30L) and RhoA(Q63L) mutants have single amino acid substitutions in the switch I (residues 29-42) and switch II (residues 62-68) regions, respectively. Like the RhoA(G14V) mutant, these mutants result in a net increase of active RhoA when introduced into cells. However, these phenotypes are the result of distinct mechanisms. The RhoA(F30L) mutant is spontaneously activated and exhibits enhanced intrinsic guanine nucleotide exchange from GDP to GTP while retaining normal GTP hydrolysis rates catalyzed by GAP proteins (Lin *et al.,* 1999). RhoA(G14V) and (Q63L) are mutants locked in the GTP-bound active conformation as the residues necessary for GAP recognition have been mutated (Khosravi-Far *et a*l., 1995).

Interestingly, our results indicate that BNIPXL associates with the 'fast-cycling' RhoA(F30L) mutant but fails to bind RhoA(Q63L) (**Figure 3.28a**). The binding profile is similar when the CBCH fragment is utilized in co-immunoprecipitation studies (**Figure 3.29a**). In contrast, the WBCH fragment of BNIPXL fails to associate with any RhoA constructs (**Figure 3.29b**). Collectively, these results demonstrate that BNIPXL exhibits selective preference for different RhoA mutants via its CBCH fragment and suggests that the RhoA glycine14 and glutamine63 residues may be important for BNIPXL-RhoA association. To clarify the apparent size difference between wild-type RhoA and RhoA(G14V) observed previously (**Figure 3.27**), alternative sources of RhoA(G14V) and

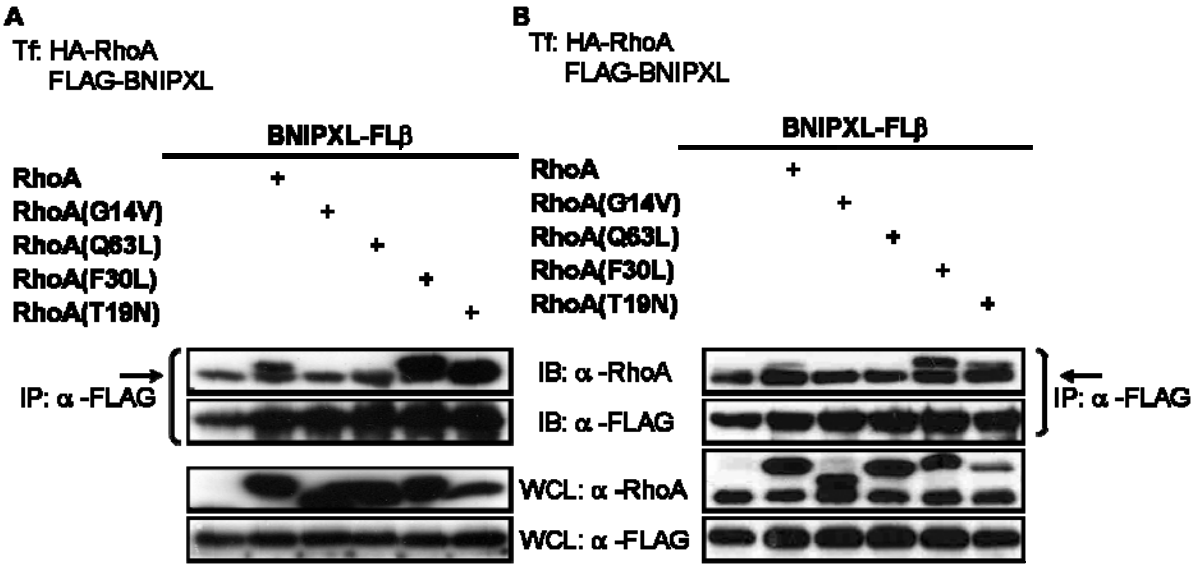

Figure 3.28. BNIPXL interacts specifically with the RhoA(F30L) fast-cycling mutant but not with other constitutive active mutants *in vivo*. Lysates co-expressing FLAG-tagged full-length BNIPXL fragments (a) with vector control or HA-tagged RhoA wild-type, dominant active (G14V), (Q63L) and (F30L) and dominant negative (T19N) mutants were subjected to immunoprecipitation and bound proteins detected in anti-RhoA westerns (first panel). Blots were re-probed with anti-FLAG antibody to show the amounts of precipitated proteins (second panel). Expression of transfected proteins was verified using anti-RhoA for RhoA (third panel) or anti-FLAG for BNIPXL (fourth panel). Arrows indicate light chain from antibody. (b) same as (a) with the exception that HA-tagged dominant active (G14V) and dominant negative (T19N) mutants were gifts from Prof. Thomas Leung, IMCB, Singapore.

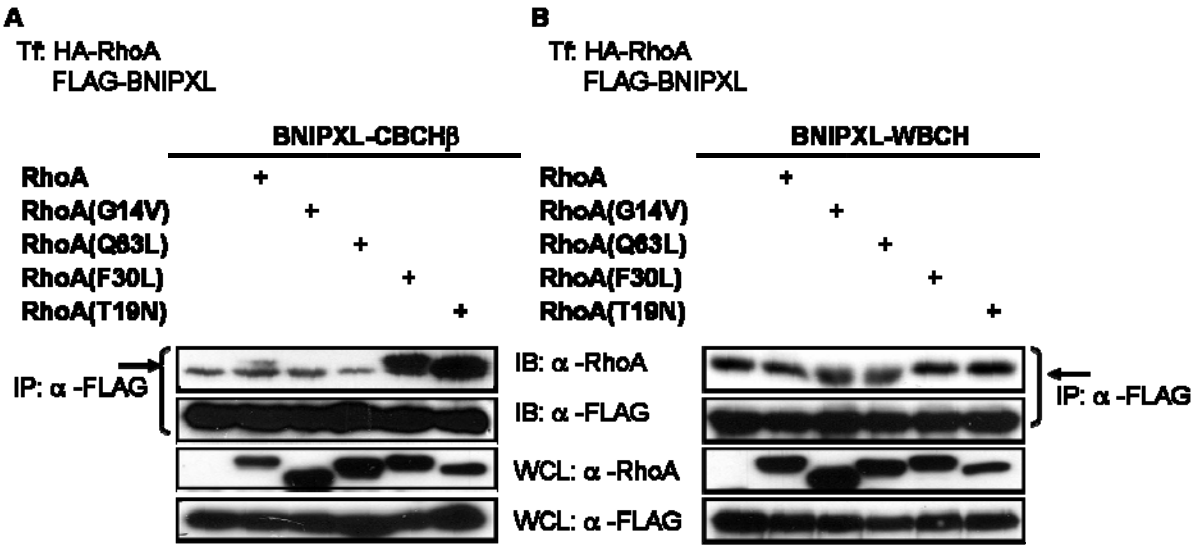

Figure 3.29. The BNIPXL CBCH fragment is responsible for RhoA interactions observed with full-length BNIPXL *in vivo*. Lysates co-expressing FLAG-tagged BNIPXL (a) CBCH and (b) WBCH fragments with vector control or HA-tagged RhoA wild-type, dominant active (G14V), (Q63L) and (F30L) and dominant negative (T19N) mutants were subjected to immunoprecipitation and bound proteins detected in anti-RhoA westerns (first panel). Blots were re-probed with anti-FLAG antibody to show the amounts of precipitated proteins (second panel). Expression of transfected proteins was verified using anti-RhoA for RhoA (third panel) or anti-FLAG for BNIPXL (fourth panel). Arrows indicate light chain from antibody.

(T19N) mutants were used for immunoprecipitation with BNIPXL (**Figure 3.28b**). Our results indicate that these RhoA mutants exhibit a similar migratory and binding profile with BNIPXL.

3.3.9. BNIPXL reduces active wild-type RhoA and RhoA(F30L) levels *in vitro*

To examine the effects of BNIPXL-RhoA interactions *in vivo*, we performed *in vitro* Rho activity assays with GST fusion of Rhotekin-RBD to determine the levels of active RhoA (**Figure 3.30**). Our results indicate that full-length BNIPXL could effectively reduce the levels of active wild-type RhoA *in vitro* whereas BNIPXL deletion mutants that fail to associate with RhoA has no apparent effect. A similar reduction was observed for cells co-expressing BNIPXL and RhoA(F30L) albeit to a lesser extent. This is in contrast to cells co-expressing BNIPXL and RhoA(Q63L) where wild-type or mutant BNIPXL had no apparent effect on active RhoA levels *in vitro*. Taken together, these results indicate that BNIPXL downregulates RhoA activity.

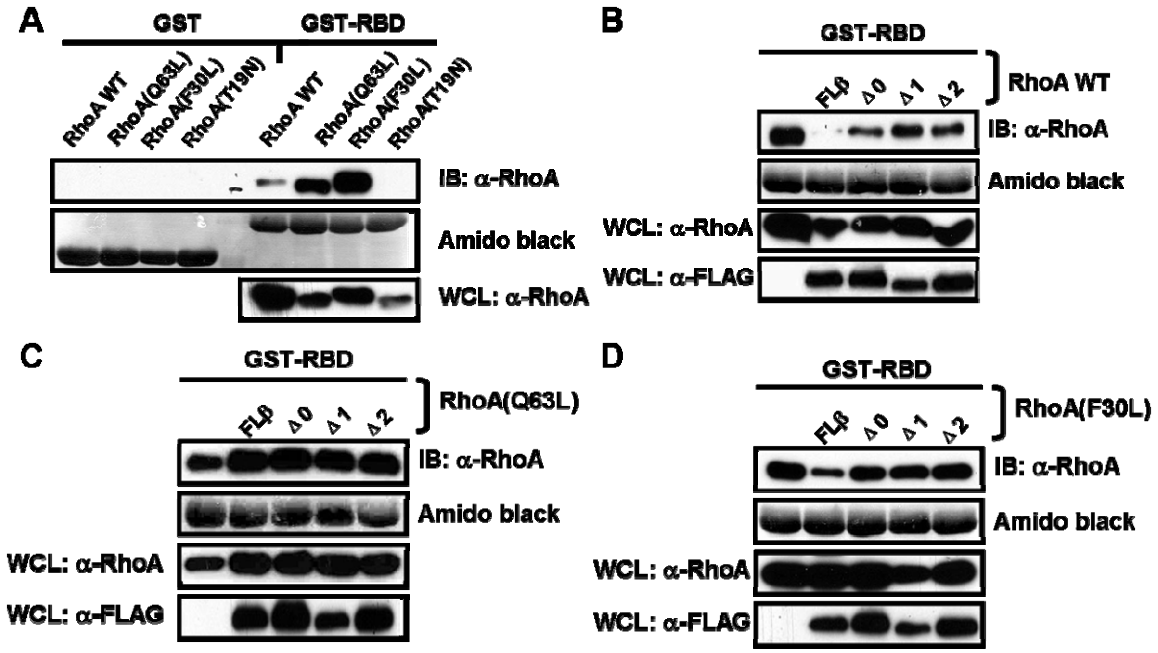

Figure 3.30. BNIPXL reduces active wild-type RhoA and RhoA(F30L) levels *in vitro.* Lysates expressing wildtype RhoA, RhoA(Q63L), RhoA(F30L) and RhoA(T19N) mutants were incubated with GST or GST-RBD (A) to confirm specificity of GST-RBD for active RhoA. Lysates co-expressing wildtype RhoA (B), RhoA(Q63L) (C) or RhoA(F30L) (D) with vector control or FLAG-tagged wildtype BNIPXL and deletions were incubated with GST-RBD as described in 'Materials and Methods'. Bound proteins and whole cell lysate input was analyzed using anti-RhoA (first and third panel) or anti-FLAG for BNIPXL (fourth panel). Amido-black staining was used to ascertain equal loading of GST fusion proteins. The integrity of GST fusion proteins was previously affirmed by checking their migration profiles on Commassie-blue stained gels.

3.4. Investigating the effects of BNIPXL and RhoA *in vivo*

3.4.1. Loss of individual motifs within the BCH domain affects cell phenotype

We next asked whether the BNIPXL deletions had any visible effects on its ability to induce cell morphological changes. To determine this, FLAG-tagged BNIPXLβ deletions were transiently expressed in HeLa cells and observed using confocal fluroscence microscopy (**Figure 3.31**). These mutants did not induce any apparent cell shape change when compared to wild-type BNIPXL although they were expressed at a level comparable to wild type BNIPXL. However, the △2 deletion appears to induce subtle cell elongation when compared to untransfected cells in the vicnity. Generally, the cells presented a uniform cytosolic distribution similar to that exhibited by the WBCH construct **(Figure 3.18c)** which correlates with their deficiency in RhoA binding. These observations suggest that a full composite of BCH domain is not only necessary for RhoA association but also for the induction of BNIPXL-induced morphological changes. In addition, these results also indicate that cell morphological changes elicited by BNIPXL are independent of protein dimerization.

3.4.2. BNIPXL potentiates protrusive phenotype during RhoA downregulation but is inhibited by constitutive active RhoA pathway

To better understand the cellular effects of RhoA on BNIPXL, we examined MCF-7 cells co-expressing BNIPXL and RhoA dominant active or negative mutants (**Figure 3.32**). Confocal fluorescence microscopy revealed that cells expressing BNIPXLβ and wild-type or constitutive active RhoA typically exhibit similar phenotypes, presenting

BNIPXL:

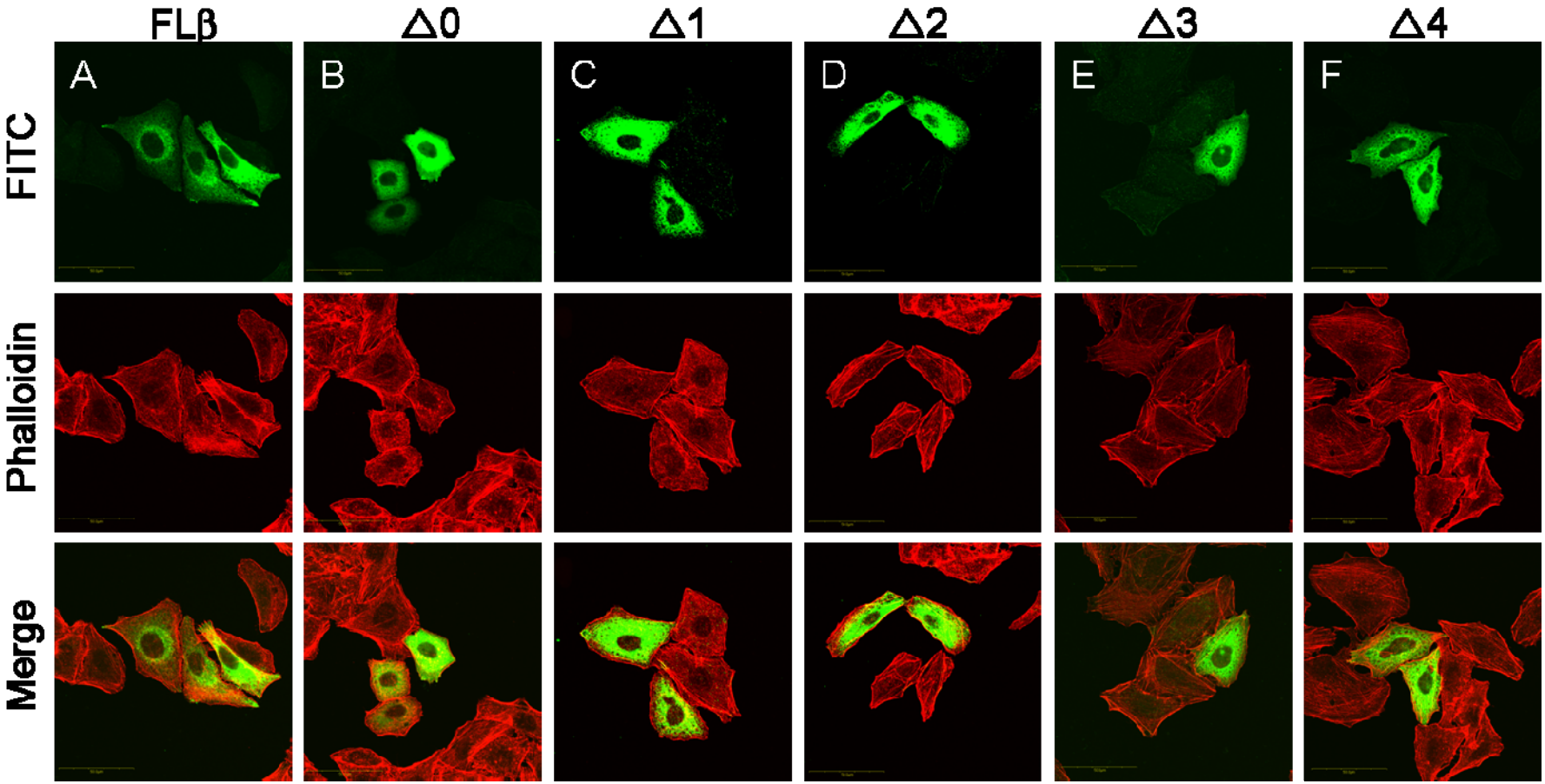

Figure 3.31. BNIPXL deletions do not induce any apparent cell shape change. (a-f) HeLa cells expressing FLAG-tagged BNIPXLβ deletion constructs was fixed, permeablized and stained with a mouse monoclonal anti-FLAG antibody followed by FITC-conjugated goat anti-mouse antibody. F-actin was detected using TRITC-conjugated phalloidin and visualized by confocal fluorescence microscopy. Scale bars, 50μm.

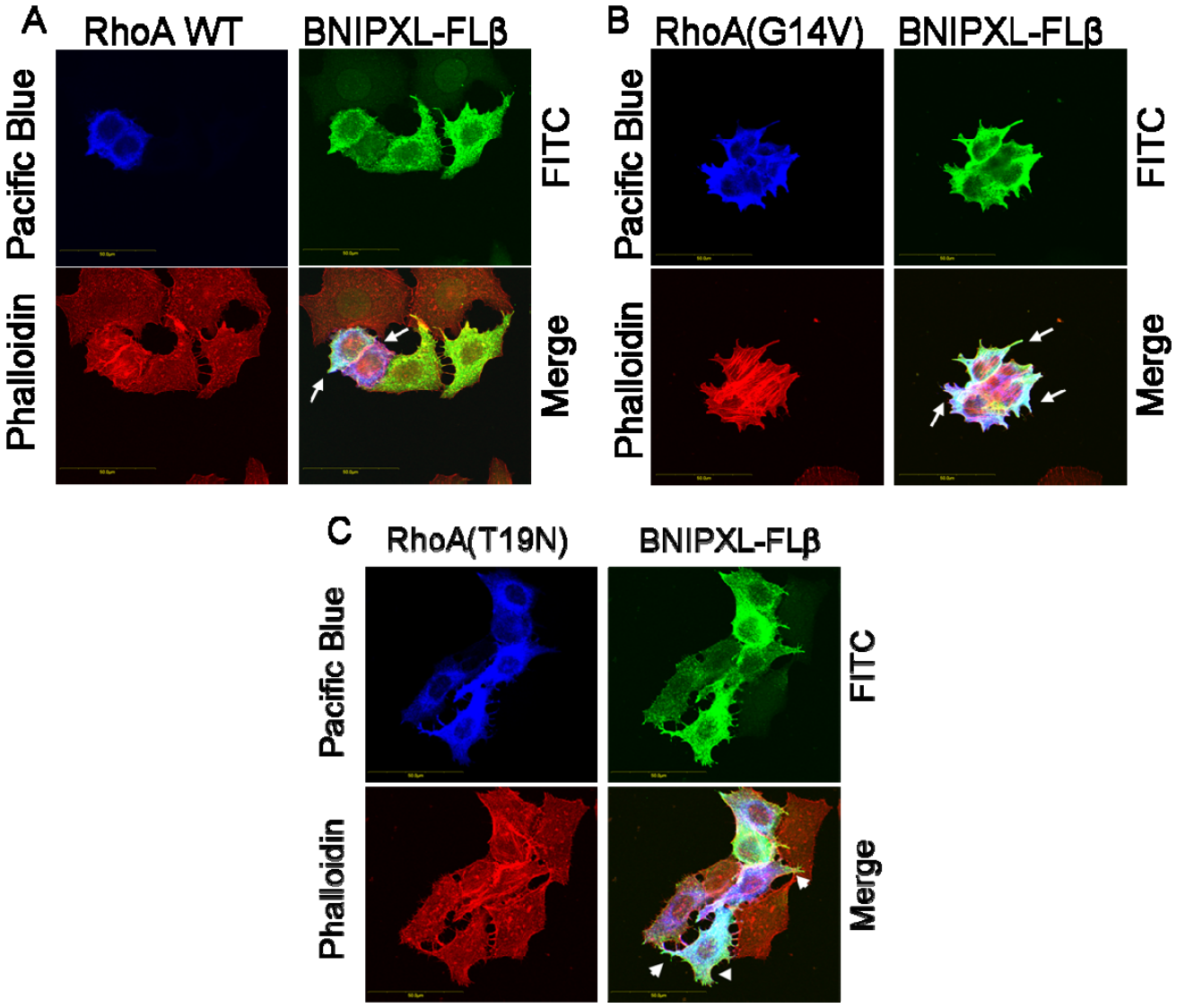
A
RhoA WT
BNIPXL-FLβ
Pacific Blue
FITC
Phalloidin
Merge
B
RhoA(G14V)
BNIPXL-FLβ
Pacific Blue
FITC
Phalloidin
Merge
C
RhoA(T19N)
BNIPXL-FLβ
Pacific Blue
FITC
Phalloidin
Merge

Figure 3.32. BNIPXL potentiates cell morphology associated with RhoA inactivation**.** (a-c) MCF-7 cells expressing FLAG-tagged BNIPXLβ and HA-tagged wild-type, dominant active (G14V) or negative (T19N) RhoA were fixed, permeabilized and stained using a mouse monoclonal anti-FLAG antibody and rabbit polyclonal anti-HA antibody followed by FITC-conjugated goat anti-mouse antibody and Pacific Blue-conjugated goat anti-rabbit antibody. F-actin was detected using TRITC-conjugated phalloidin and visualized by confocal fluorescent microscopy. Bottom right, merged image of overexpressed FLAG-tagged BNIPXLβ (green), HA-tagged RhoA (blue) and actin (red). Thin spikes (arrows) and filopodia-like extensions (arrowheads) are indicated. Scale bars, 50μm.

cell rounding and accompanying reduction in cell area with increase in actin stress fibers, as detected by the distinct phalloidin staining (**Figures 3.32a and 3.32b**). This was also observed in control cells expressing wild-type RhoA and RhoA(G14V) alone (**Figure 3.33**). Furthermore, when compared to singly transfected cells in the same field or RhoA controls, no extended protrusions or cell elongation was found although thin spikes were observed at their periphery (arrows). These observations are consistent with reports that constitutively active Rho induces a retracted cell shape (Buchsbaum *et al.,* 1996; Shang *et al.,* 2003). Furthermore, inactivation of Rho has been shown to be associated with the formation of protrusions at the cell periphery (Hirose *et al.,* 1998; Tatsis *et al.,* 1998; Shang *et al.,* 2003). Interestingly, cells co-expressing BNIPXLβ and dominant negative RhoA exhibit protrusions from the main cell body accompanied by more extensive filopodia-like extensions branching from the periphery of the proximal protrusions (**Figure 3.32c, arrowheads**). The drastic phenotype suggests that down-regulation of RhoA *in vivo* could enhance BNIPXL-induced cell morphological changes. Recent reports that siRNA-mediated knockdown of RhoA in MCF-7 results in cells exhibiting an elongated phenotype with large lamellipodia, a drastic reduction of cell to cell contact coupled with an enhanced migratory ability in this relatively non-motile cell line (Simpson *et al.,* 2004). These observations are consistent with our findings that BNIPXL can reduce active RhoA levels *in vitro*.

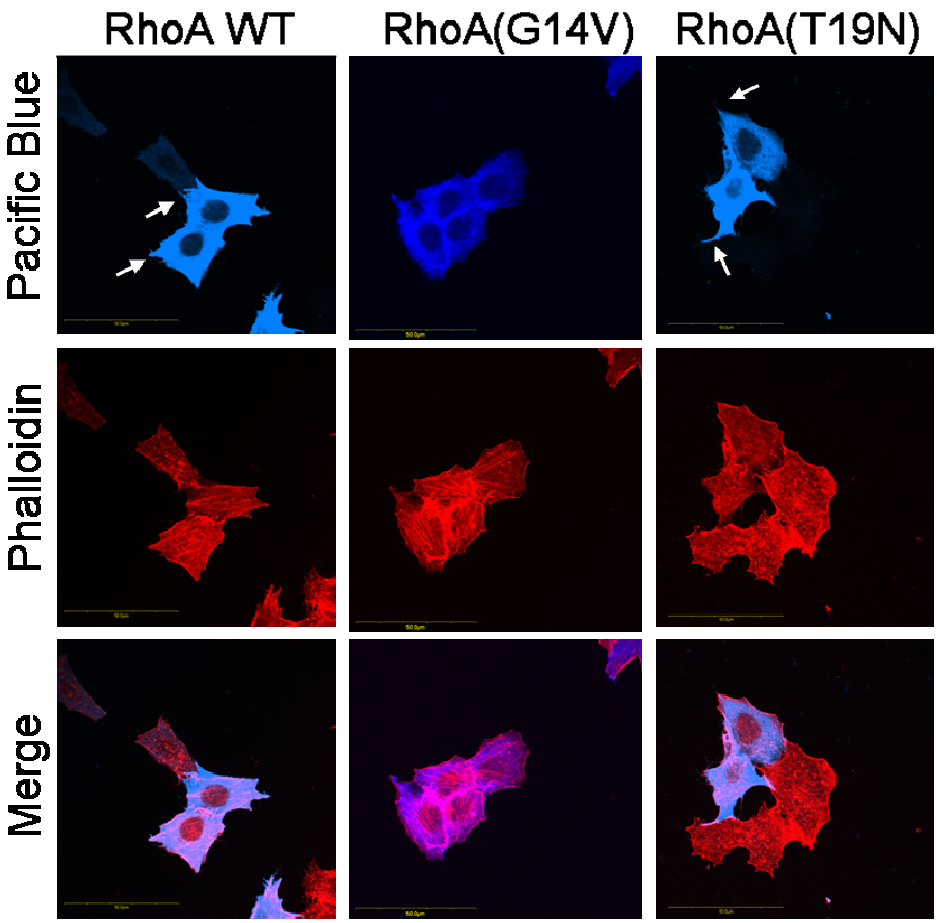

Figure 3.33. Expression of wild-type RhoA and mutants alone is not sufficient to induce drastic changes in cell morphology. MCF-7 cells expressing HA-tagged wild-type, dominant active (G14V) or negative (T19N) RhoA were fixed, permeabilized and stained using a rabbit polyclonal anti-HA antibody followed by Pacific Blue-conjugated goat anti-rabbit antibody. F-actin was detected using TRITC-conjugated phalloidin and visualized by confocal fluorescent microscopy. Bottom panel; merged image of HA-tagged RhoA (blue) and actin (red). Thin spikes (arrows) are indicated. Scale bars, 50μm.

3.4.3. A requirement for active Cdc42/Rac1 signaling pathways in BNIPXL-induced morphological changes

Our current observations coupled with the fact that Cdc42/Rac1 activation can induce cell protrusions led to the hypothesis that BNIPXL-induced cell shape changes may require the interplay of various Rho GTPase signaling. RhoA inactivation may require the concomitant activation of Cdc42/Rac1 signaling pathways or vice versa for coordination of cell dynamics required for cell shape changes (Sander *et al.,* 1999; Zondag *et al.,* 2000). To address the question if BNIPXL could indirectly cause the activation of Cdc42/Rac1 pathways, we examined the effect of the PAK-CRIB domain on BNIPXLβ-induced cell phenotype (**Figure 3.34**). This domain alone serves as a dominant negative mutant by sequestering all endogenous active Cdc42 and Rac1. This prevents activation of their downstream effectors, including PAK which mediates Cdc42 effect on morphological changes (Price *et al.,* 1998; Sells *et al.,* 1997; Kazuhiro *et al.,* 1997; Zhou *et al,,* 2005b). Interestingly, cells expressing both BNIPXLβ and the CRIB domain exhibited morphologies similar to that of the BNIPXL deletion mutants with well-defined cell borders and no cell elongation and membrane protrusions. This suggests that BNIPXL-induced phenotypes indeed require additional activation of the Cdc42/Rac effector pathways.

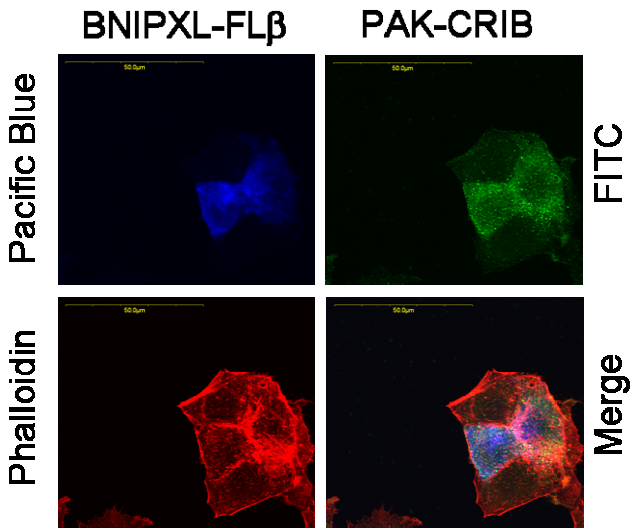

Figure 3.34. BNIPXL-induced cell morphological changes require involvement of Cdc/Rac1 effector pathways**.** MCF-7 cells expressing HA-tagged BNIPXLβ and FLAG-tagged PAK-CRIB were fixed, permeabilized and stained using a rabbit polyclonal anti-HA antibody and mouse monoclonal anti-FLAG antibody followed by FITC-conjugated goat anti-mouse antibody and Pacific Blue-conjugated goat anti-rabbit antibody. F-actin was detected using TRITC-conjugated phalloidin and visualized by confocal fluorescent microscopy. Bottom right, merged image of overexpressed HA-tagged BNIPXLβ (blue), FLAG-tagged PAK-CRIB (green) and actin (red). Scale bars, 50μm.

.

Discussion and Conclusions

4. Discussion and Conclusions

4.1. BNIPXL: a novel member of the BNIP-2 family in cell dynamics control

BNIPXL is a novel member of the BNIP-2 family that plays distinct roles in cell dynamics. Our current study provides insights into the structural and biochemical features of BNIPXL and their implications in RhoA-mediated cell shape changes. These findings highlight the functional significance of homologous BCH domains and the roles of the BNIP-2 family in Rho GTPase signaling pathways.

BNIPXL encompasses most of the prototypic BNIP-2 sequence at the C-terminus and based on bioinformatics analyses, the BNIPXL gene is encoded by 13 exons spanning ~86kbp at the human chromosome 9q21.2. The BNIPXL pre-mRNA undergoes alternative RNA splicing to produce two isoforms designated BNIPXLα and BNIPXLβ, indicating that different sub-populations of BNIPXL may target different proteins to direct diverse cellular events in a spatio-temporal manner. This is consistent with our previous findings that BNIP-S isoforms are functionally diverse with the full complement BCH domain being required for its pro-apoptotic effects whereas an incomplete BCH domain generated during RNA splicing became inert (Zhou *et al.,* 2002). Furthermore, several splice variants of the BPGAP family have also been identified and unlike the prototypic BPGAP1, co-workers demonstrate that BPGAP2 does not appear to cause extensive cell protrusions (Shang and Low, unpublished data). Sequence analyses indicate that the β isoforms of both BNIP-S and BNIPXL have truncated BCH domains towards the extreme C-terminus. Unlike BNIP-Sβ which is generated during intron splicing, BNIPXLβ is the result of an in-frame stop codon introduced after the exclusion of exons 11 and 12 at the C-terminus.

The expression profile of human and murine BNIPXL provides an indication of the diversity of BNIPXL function. Reverse-transcription PCR revealed that both BNIPXL isoforms were expressed in human brain, kidney and liver and in a panel of breast carcinoma cell lines. This indicates that both BNIPXL isoforms may participate in epithelial cell dynamics and tissue morphogenesis. This is consistent with our bioinformatics analysis which has identified an expressed sequence tag (EST) isolated from ovarian carcinoma encoding a putative BNIPXL splice variant lacking the C-terminal BCH domain (GenBank™ accession no. AU133997). In addition, the exclusive expression of the β isoform in the human embryonic epithelial cell line, HEK293T is intriguing. Perhaps, the differential BNIPXL expression may be due to the different cell type origins suggesting that BNIPXL may participate in embryonic development. This however, has yet to be determined.

Intriguingly, two recent publications demonstrate that BMCC1 (which shares 98.6% amino acid identity with BNIPXL at its C-terminus) is up-regulated in neuroblastoma patients with favourable prognoses (Machida *et al*., 2005; Ohira *et al*., 2005). The authors attribute the lower mortality rate to increased apoptosis in relation to increased BMCC1 expression. We have not been able to determine if BNIPXL is an isoform or if it is part of the larger BMCC1 due to the lack of suitable antibodies. Although our diagnostic RT-PCR seems to suggest that the region upstream of BNIPXL (~2.4kb) is expressed in both HEK293T and HeLa cells, we have not successfully cloned out the entire coding region (~8.0kb) of BMCC1 from these cell lines. Thus, it is still likely that this gene locus may generate several protein isoforms when translated.

Furthermore, the expression profile of BNIPXL in the mouse tissues is similar to that of BNIP-H/Caytaxin (Chew and Low, unpublished data), a protein whose loss-of-function is responsible for the Cayman ataxia, a form of neurological disorder (Bomar *et al.,* 2003). Together with phylogenetic analysis which indicates that the BCH domain of BNIPXL more closely resembles that of BNIP-H/Caytaxin, these results collectively suggest that BNIPXL may play important roles in neuronal cell morphogenesis.

4.1.1. Significance of the BNIPXL domain architecture and functional characterizaton

The conserved BCH domain at the C-terminus of BNIPXL distinguishes it as a member of the type I family together with BNIP-2, BNIP-S and BNIP-H. Previous studies demonstrate that distinct motifs within the BNIP-2 BCH domain mediate Cdc42 recruitment, catalytic activity and homo- and heterophilic interactions (Low et al., 1999; Low *et al*., 2000a; Low *et al*., 2000b; Zhou *et al.,* 2005a). Multiple sequence alignments of the type I BCH domains indicate the (288)EYV(290) Cdc42 binding motif is unique to BNIP-2 while the novel arginine finger (235)RRLRK(239) motif is conserved in BNIPXL and other members of the BNIP-2 family. The BNIP-2 dimerization (217)RRKMP(221) motif is highly conserved in BNIPXL and BNIP-H except the lysine residue which has been substituted with arginine in BNIPXL and BNIP-H to (650)RRRMP(654) and (241)RRRMP(245), respectively; while the corresponding sequence in BNIP-S (183)RAQVP(187) is less conserved.

Protein-protein interaction studies indicate that both BNIPXLα and BNIPXLβ can form homo- and heterophilic complexes with the same protein targets in this study thus,

the 23 amino acid truncation in the C-terminus of the BNIPXLβ BCH domain does not appear to affect homo- or heterophilic complex formation. However, we cannot rule out the possibility that *other* protein targets may bind BNIPXL isoforms differently. In addition, these findings are in line with previous work which demonstrates a role for the BCH domain in directing complex formation (Low *et al*., 2000a; Low *et al*., 2000b; Zhou *et al*., 2002; Shang *et al*., 2003). Our deletion studies did not successfully map the region of the BCH domain responsible for homophilic binding unlike that of BNIP-2 which is located in the proximal region of its BCH domain while studies in BNIP-S indicate that the lost of the C-terminus region in the β isoform abrogates homo- and heterophilic interactions. This suggests that the BCH domain of BNIPXL utilizes multiple motifs to direct homophilic associations.

Our earlier observations that the N-terminal BNIPXL fragments are prone to degradation indicates that this region of BNIPXL may be structurally less stable. Furthermore, full length BNIPXL migrated as a ~120 kDa band even though its expected size is ~80 kDa (**Figure 3.12**). This size disparity is augmented in fragments containing the N-terminus indicating that this region in BNIPXL may undergo post-translational modifications which serve to stabilize its conformation *in vivo*. This is consistent with our findings that the RhoA recruitment to the BNIPXL heterophilic complex is conformation-dependent and may involve post-translational modifications as discussed in **section 4.2.1**. This may also explain why several attempts to produce stable quantities of the full length GST-BNIPXL fusion proteins in *E. coli* were unsuccessful (data not shown). Thus, the yeast two-hybrid system was used to verify that BNIPXL mediates direct protein-protein interactions *in vivo*. Collectively, these findings indicate that the BNIPXL homophilic

motif may be employed in a manner dependent on its conformation or surrounding sequence.

Structurally, dimer formation may increase conformational stability by ensuring tighter interaction between the two subunits and the reduction of exposed hydrophobic surfaces. In addition, such complex formation may also exert allosteric influence on protein conformation thus regulating protein biochemical activity through structural adjustments of the active sites (Mei *et al.,* 2005). Molecular modeling of the BNIP-2 BCH domain using the Breakpoint cluster region homology (BH) domain of the p85α regulatory subunit of PI3K as a structural template indicates that the BCH domain adopts a conformation similar to that of the BH domain dimer (Low *et al.,* 2000a) while functional characterization demonstrates that the BNIP-2 BCH domain is a non-canonical GAP for Cdc42. This is consistent with recent findings which indicate that the BH domain functions as a GAP for Rab GTPases (Chamberlain *et al.,* 2004).

Biochemically, homo- and heterophilic interactions may represent a mechanism for modulating biochemical activity and intensity of cell response. For example, the presence of BNIP-2 and p50-RhoGAP results in mutual competition for Cdc42 binding *in vitro* in a nucleotide-independent manner (Low *et al.,* 1999). BNIP-Sα-induced pro-apoptotic events requires BCH domain-mediated homophilic interactions (Zhou *et al*., 2002) which is consistent with our recent findings which indicate that different pools of BNIP-S may work in concert to sequester p50-RhoGAP while promoting RhoA-mediated apoptosis (Zhou *et al.,* 2005b). Collectively, these corresponding structure-function relationships may provide insights into the functional roles of BNIPXL given that their BCH domains share ~45%-75% amino acid similarities (**Table 4**).

Previous studies indicate that BNIP-2, BNIP-S and BPGAP1 direct distinct cellular phenotypes that are directly attributed to the BCH domain (Zhou *et al.,* 2005a; Shang *et al*., 2003; Zhou *et al.,* 2002). We observed that BNIPXL expression induced cell elongation and was concentrated at the tips of these protrusions while the BCH domain was sufficient to elicit similar protrusions and distribution albeit without cell elongation. This suggests that BNIPXL-induced cell morphological changes in HeLa requires coordinate regulation and confirms the notion that homologous BCH domains can direct various aspects of cell dynamics.

In addition, the BCH domain-containing fragments of BNIPXL were localized in cytosolic punctate structures reminiscent of those observed with BNIP-2 (Zhou *et al.,* 2005a). The BCH domain appears to direct such cytosolic localization of BNIPXL and BNIP-2 as fragments lacking this domain exhibited a uniform cytosolic distribution. Thus, it is possible that these punctate structures represent membrane vesicles which direct the transport of BNIPXL and BNIP-2 to their sites of action at the leading edges of the membrane protrusions. These observations are consistent with sequence analyses which indicate that BNIPXL encompass most of the BNIP-2 sequence at its C-terminus with 66.9% amino acid identity between their BCH domains (**Figure 3.5**). However, unlike BNIP-2 which elicits drastic polarized cell elongation, with 'beads on a string' appearance along these extensions, BNIPXL exhibits more subtle cell elongation and protein distribution. Although, it is possible that the BNIPXL N-terminus may attenuate the drastic membrane protrusions observed with BNIP-2, this seems unlikely since removal of the N-terminus did not result in a more drastic morphology.

Alternatively, the unique structural motifs in the BNIPXL BCH domain may target different small GTPases to confer distinct phenotypes in cell morphogenesis. This is in line with our observations that deleting the individual regions within the BNIPXL BCH domain completely abrogates cell elongation and protrusions except the △2 mutant which appears to induce subtle cell elongation when compared to un-transfected cells. Similarly, co-workers have established that the full complement of the BCH domain of BNIP-Sα targets RhoA activation for cell rounding and apoptosis (Zhou *et al.,* 2005b) whereas BNIP-2 utilizes different motifs within its BCH domain to modulate the Cdc42 signaling pathway (Zhou *et al*., 2005a). In addition, sequence analyses indicate that the proximal region of the BNIPXL BCH domain (residues 615-644) resembles that of the Class I Rho-binding motif found in the RhoA effectors PKN, rhophilin and rhotekin (**Figure 3.21**). Co-workers have recently identified a similar motif in the BNIP-Sα BCH domain and its role in facilitating RhoA signaling pathways (Zhou *et al.,* 2005b). Here, we report that BNIPXL targets and inactivates RhoA instead and provide insights into the functional significance of this motif and its immediate regions in conferring distinct cellular effects for cell morphogenesis, as discussed below.

4.2. The role of BNIPXL in Rho GTPase signaling pathways

4.2.1. Significance of BNIPXL-RhoA associations

The striking structural similarities and morphological effects of BNIPXL and BNIP-2 collectively indicate that BNIPXL may associate with different members of the Rho family in mediating its cellular effects. Interestingly, unlike BNIP-2 which targets Cdc42, BNIPXL associates with RhoA and not Rac1 or Cdc42. Conversely, this binding to

RhoA was similar to that of BNIP-Sα (Zhou *et al.,* 2005b). Furthermore, both BNIPXLα and BNIPXLβ can associate with RhoA which may explain similar effects when expressed in HeLa cells. These findings are consistent with multiple sequence alignments (**Figure 3.6**) which indicates that the BNIP-2 (285)VPMEYVG(291) motif responsible for Cdc42 binding is absent from BNIPXL while both BNIPXL and BNIP-S appear to contain a Class I Rho-binding motif within their BCH domains. In line with these observations, the loss of RhoA binding to BNIPXL deletion mutants correlates with the attenuation of BNIPXL-induced cell morphological changes and indicates a functional link between RhoA and BNIPXL. In addition, our studies demonstrate that BNIPXL dimerization does not directly participate in cell shape changes as these deletion mutants retain their homo- and heterophilic interactions. However, we cannot exclude the possibility that dimerization may be necessary but not sufficient for BNIPXL function and that such interactions may play secondary regulatory roles in mediating other functions of BNIPXL.

Co-expression of BNIPXL and RhoA(T19N) in MCF-7 cells enhanced the BNIPXL-induced morphological changes with an increase in the number of filopodia-like protrusions extending from the cell periphery. These observations are consistent with Cdc42/Rac-mediated cell morphological changes and indicate that the expression of dominant negative RhoA may influence Ccdc42/Rac activation in parallel pathways leading to actin cytoskeleton remodelling. These findings are consistent with siRNA-mediated RhoA knockdown in MCF-7 cells which exhibit an elongated cell phenotype with large lamellipodia and an enhanced migratory ability (Simpson *et al.,* 2004) while a similar inhibition of RhoA in MDA-MB-231 cells reduced cell proliferation and invasiveness both *in vivo* and *in vitro* (Pille *et al*., 2005). In contrast, cells co-expressing

BNIPXL and RhoA(G14V) exhibited cell retraction coupled with increased stress fiber formation suggesting that constitutive RhoA activation can override BNIPXL-induced cell elongation and membrane protrusions.

To investigate the functional significance of BNIPXL-RhoA interactions, *in vitro* GTP/GDP loading assays were performed to determine if this association was nucleotide-dependent. Our findings that the BNIPXL BCH domain has higher affinity for GTPγS-RhoA than GDP-RhoA, unlike the RhoA effector ROCK, which only associates with the active GTP-bound form (Ishizaki *et al.,* 1997) indicates that the BCH domain can adopt conformations that aid the discrimination of subtle structural differences between the two nucleotide-bound states of the small GTPase. This binding profile is unique to BNIPXL and is unlike the BNIP-2 BCH domain which exhibits equal affinities for Cdc42 regardless of its nucleotide-binding status (Low *et al.,* 1999). Interestingly, full length BNIPXL failed to interact with RhoA *in vitro* suggesting that *in vivo* BNIPXL-RhoA interactions may involve post-translational modifications and/or a third partner. This is consistent with our direct binding assays which indicate that the CBCH fragment forms direct and strong interactions with RhoA while full-length BNIPXL-RhoA interactions are not readily detected. This suggests that the presence of the N-terminus in full-length BNIPXL may have an inhibitory effect on BNIPXL-RhoA interactions.

Furthermore, our deletion studies demonstrate that the Rho-binding motif is necessary but not sufficient for stable BNIPXL-RhoA interactions. We find that regions flanking this motif in the BCH domain contribute to BNIPXL-RhoA interactions possibly via allosteric interactions. We have confirmed that the loss of RhoA binding is not the result of a general perturbation of protein structure in the BNIPXL mutants since they

retained their ability to dimerize with wild-type BNIPXL *in vivo*. In view of recent reports that Rho effectors may utilize multiple motifs including their GTPase-binding domains (GBDs) to form contact points with regions outside the classical switch domains (Blumenstein and Ahmadian, 2004), we hypothesize that BNIPXL may utilize a similar strategy to ensure RhoA binding specificity. This is consistent with our current observations which suggest that allosteric sites in the BNIPXL BCH domain may act in concert with the Rho-binding motif to aid the discrimination of RhoA conformations associated with their respective nucleotide binding status. In addition, BNIPXL may undergo conformational changes *in vivo* that relieves restraints masking its RhoA recognition motif(s) in the BCH domain.

Disruption of autoinhibitory interactions is a common mechanism in Rho effector regulation as observed in ROCK (Amano *et al.,* 1997), mDia (Watanabe *et al.,* 1999) and Citron (Madaule *et al.,* 1998). More recently, a mechanism involving lipid modification of small GTPases has been implicated in the relief of auto-inhibitory, intramolecular interactions involving the BCH and GAP domains in p50-RhoGAP (Moskwa *et al.,* 2005). Similarly, BPGAP1 has been observed to adopt a similar conformation which regulates the functions of both its BCH and GAP domains (Shang and Low, unpublished data). We hypothesize that BNIPXL intermolecular interactions may instead play regulatory roles in other BNIPXL functions. To examine the functional significance of BNIPXL homo- and/or heterophilic complexes, it is necessary to first delineate the dimerization motif(s) responsible for these interactions and then examine their effects on BNIPXL-RhoA interactions.

Interestingly, our *in vivo* binding studies indicate that BNIPXL retains preferential binding to wild-type RhoA over RhoA(T19N). However, the BNIPXL-RhoA interactions are completely abolished with the RhoA(G14V) mutant (**Figure 3.27**). Although this may appear to contradict our previous *in vitro* results which demonstrate that BNIPXL associates with GTP-bound RhoA, these findings indicate the importance of the glycine residue in the P-loop motif for mediating nucleotide-dependent BNIPXL-RhoA interactions. The *in vitro* nucleotide-bound forms of RhoA closely resemble the *bona fide* conformations of the small GTPase while the RhoA dominant active and negative mutants exert their functions by modulating RhoA interactions with its regulatory factors. These mutants have amino acid substitutions in the RhoA P-loop (12)**G**DGAC**GKT**(19) motif which makes contact with a phosphate group of the bound nucleotide and coordinates a Mg^{2+} ion for stabilizing nucleotide binding. It is part of three distinct RhoA segments that border the nucleotide-binding site and participate in GTP/GDP discrimination (reviewed in Dvorsky and Ahmadian, 2004).

In addition, the P-loop region makes contact with the DH and GAP domains of RhoGEFs and RhoGAPs, respectively. Its interaction with the GAP domain facilitates RhoGAP recognition and discrimination of the RhoA nucleotide binding status while the insertion of DH domain residues in close proximity to the P-loop and the Mg^{2+}-binding area has been shown to promote nucleotide exchange by disrupting Mg^{2+}-ion coordination and favourable interactions for high affinity nucleotide binding (Worthylake *et al*., 2000; Buchwald *et al*., 2002; Rossman *et al*., 2002; Snyder *et al*., 2002). Thus, the substitution of glycine to valine at position 14 results in a GAP-insensistive RhoA mutant that abolishes its intrinsic and GAP-mediated GTPase activity (Lancaster *et al*., 1994; Ahmadian *et al*.,

1997) and results in the maintenance of a constitutively active state. Conversely, the substitution of threonine to asparagine at position 19 results in increased affinity for RhoGEFs, corresponding to impaired nucleotide exchange and decreased affinity for GTP (Seasholtz *et a*l., 1999). Thus, the dominant negative RhoA(T19N) mutant exerts its effects through RhoGEF sequestration and the subsequent inhibition of endogenous RhoA activation while the RhoA(G14V) mutant remains constitutively active as a result of impaired RhoGAP recognition.

In addition, we have also examined BNIPXL interactions with other constitutively active RhoA mutants to determine if the lack of binding with RhoA(G14V) is the result of the residue substitution or the active conformation of RhoA *per se*. The RhoA(F30L) and RhoA(Q63L) mutants have single amino acid substitutions in the switch I (residues 29-42) and switch II (residues 62-68) regions, respectively. While the RhoA(Q63L) is a RhoGAP insensitive mutant like RhoA(G14V), the RhoA(F30L) mutant is spontaneously activated independent of RhoGEF while retaining GAP-mediated GTPase activity. Interestingly, BNIPXL associates with RhoA(F30L) and not with RhoA(Q63L) suggesting that the RhoA glycine14 and/or glutamine63 residues may be important for BNIPXL-RhoA association (**Figure 3.28**). Alternatively, the BNIPXL BCH domain may function as a non-canonical GAP domain as observed with BNIP-2 (Low *et al*., 2000a).

Interestingly, these observations on RhoA binding to BNIPXL are analogous to that of BNIP-2 which exhibits diminished interaction with Cdc42(G12V) (Low *et al.,* 2000a) and is consistent with reports that demonstrate reduced RasGAP binding to the Ras(G12V) mutant (Krengel *et al*., 1990; Al-Mulla *et al*., 1999). Structurally, the Ras(G12V) mutation does not affect the overall Ras conformation but instead reduces the localized flexibility of

a polypeptide loop which participates in conformational changes associated with nucleotide binding and catalytic activity (Krengel *et al*., 1990; Tong *et al*., 1991; Franken *et al*., 1993). Furthermore, structural data from Cdc42(G12V) supports the argument that a mutation at position 12 does not alter the conformation of the GTPase structure *per se* (Rudolph *et al*., 1999). In light of this, the requirement for a glycine14 and/or glutamine63 for BNIPXL-RhoA association suggest that BNIPXL can discriminate localized RhoA conformational changes associated with nucleotide binding at its P-loop and Switch II regions in a manner similar to that of RhoGAPs.

Furthermore, a recent survey of the RhoA structural motifs indicate that the P-loop (residues 14-19) and Switch II (residues 62-68) regions may contribute to effector binding in addition to GAP and GEF recognition (reviewed in Dvorsky and Ahmadian, 2004). Collectively, these biochemical and cellular observations suggest that nucleotide-dependent BNIPXL-RhoA interactions may either interfere with RhoGEF-mediated guanine nucleotide exchange or hinder RhoA-effector recognition at different sites on the small GTPase thereby, downregulating RhoA pathways. In line with this hypothesis, *in vitro* Rho activity assays demonstrate that full-length BNIPXL could effectively reduce the levels of active wild-type RhoA *in vitro* whereas BNIPXL deletion mutants had no apparent effect. A similar reduction was observed for cells co-expressing BNIPXL and RhoA(F30L) albeit to a lesser extent.

4.2.2. BNIPXL-induced cell shape changes require coordinate modulation of Rho GTPase signaling pathways

Our findings that the PAK-CRIB domain which sequesters endogenous active Cdc42 can inhibit BNIPXL-induced cell morphological changes indicate a requirement for PAK activation downstream of Cdc42/Rac (**Figure 4.1**). Rho signaling pathways may exist in a hierarchical network, where the activation of one member can lead to the inactivation of another (Sander *et al.,* 1999; Zondag *et al.,* 2000). Alternatively, the activation of one member may be necessary to activate another (Kozma *et al.,* 1995; Nobes and Hall, 1995). Generally, actin cytoskeleton reorganization and cell motility are the result of coordinate Rac/Cdc42 and RhoA activities (Boshans *et al.,* 2000; Nobes and Hall, 1999; Noren *et al.,* 2000). Rac/Cdc42 activation is mainly associated with induction of protrusions and lamellipodia consistent with increased migratory potential while RhoA tends to increase cell adhesion and cell shape retraction. Although BNIPXL associates only with RhoA, it is possible that it may indirectly modulate the Cdc42/Rac signaling pathways, perhaps by targeting proteins like BNIP-2 to heterophilic complexes. Thus, BNIPXL may directly sequester cellular populations of active RhoA to reduce effector binding and activation while facilitating the activation of Cdc42/Rac pathways via its BCH domain to induce cell morphological changes. This is in line with findings that several proteins participate in novel modes of GTPase regulation. IQGAP1 is an atypical GAP-domain containing protein which inhibits the intrinsic Cdc42 GTPase activity (Brill *et al*., 1996; Hart *et al*., 1996; Ho *et al*., 1999) and positively regulates the Cdc42 pathway by stabilizing cellular populations of active Cdc42 to enhance filopodia induction and actin cytoskeleton

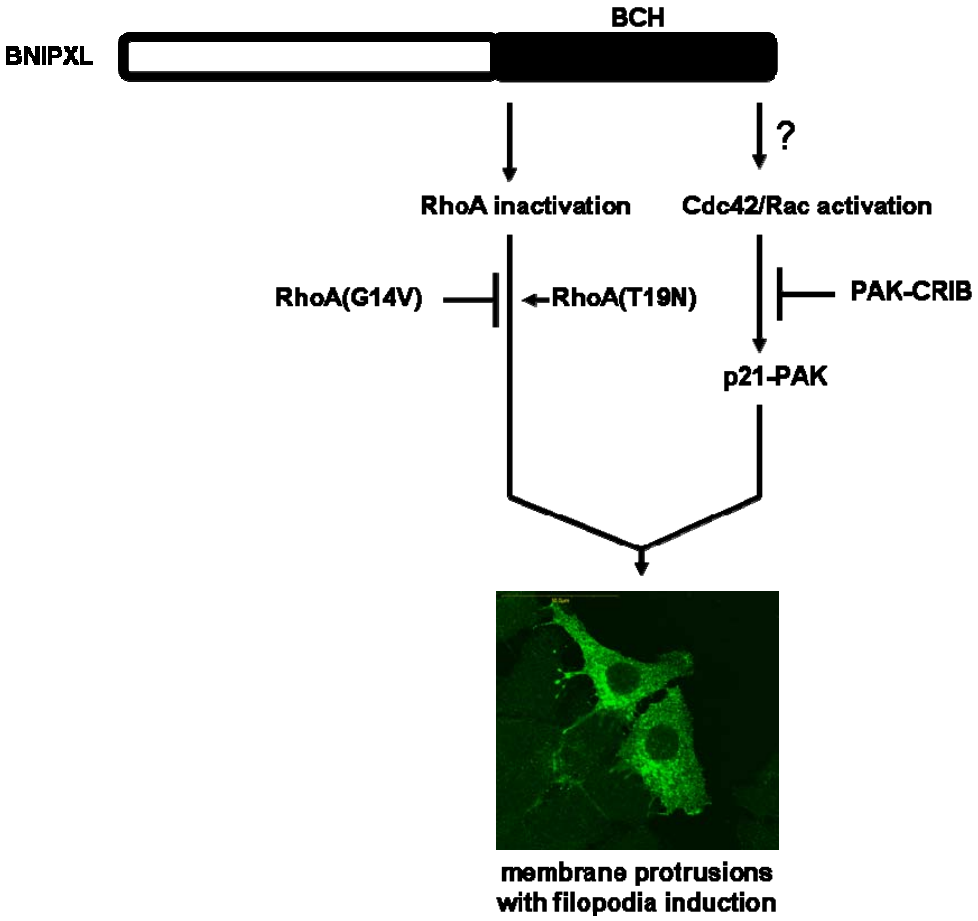

Figure 4.1. BNIPXL regulates cell shape determination through the Rho GTPase signaling pathways. The BNIPXL BCH domain directly facilitates RhoA downregulation resulting in membrane protrusions with filopodia induction. These morphological changes are enhanced with RhoA(T19N) and inhibited in the presence of RhoA(G14V) and the PAK-CRIB domain indicating that these cellular effects are likely to involve concomitant activation of Cdc42/Rac signaling pathways through an as yet unidentified interacting partner.

remodeling (Swart-Mataraza *et al*., 2002). More recently, IQGAP has been linked to microtubule dynamics via its recruitment to a complex with APC and CLIP-70 for coordinated regulation of the cytoskeleton reorganization during cell polarization and movement (Watanabe *et al*., 2004). In addition, recent work implicates the CDK inhibitor, $p27^{kip1}$ in modulating cell migration through Rac activation (McAllister *et al*., 2003) or by disrupting RhoGEF-mediated RhoA activation independent of its cell cycle functions (Besson *et al*., 2004). Furthermore, $p27^{kip1}$ has been demonstrated to associate with stathmin in regulating microtubule dynamics necessary for cell migration and invasion (reviewed in Iancu-Rubin and Atweh, 2005; Baldassarre *et al*., 2005).

4.3. Implications of BNIPXL-induced cell shape changes and its multi-motif BCH domain

Our current study has provided greater insights into the role of BCH domain-containing proteins in Rho signaling pathways and highlight the plasticity of the BCH domain in conferring distinct and novel mechanisms for cell morphogenesis by coupling different small GTPases to unique GTPase-binding motifs for actin cytoskeleton remodeling and cell shape changes. We demonstrate that BNIPXL functions differently from BNIP-2 and BNIP-S in mediating cell shape changes by directly promoting RhoA inactivation through its BCH domain. In light of this, BNIPXL might function as a scaffold which acts as a point of convergence for different Rho signaling pathways. Currently, there are several scaffold proteins that modulate Rho GTPase signaling pathways. For example, the class I RhoA effector Rhophilin-2, is a multi-domain protein that binds preferentially to GTP-bound RhoA but induces the loss of stress fibers through the concerted activities of

its resident domains. This indicates that Rhophilin-2 may promote F-actin turnover and limit stress fiber formation if RhoA activation intensity is below threshold levels (Peck *et al.,* 2002). In contrast, the Small Protein Effector of Cdc42 (SPECs) family proteins can sequester Cdc42 via their CRIB domains. This results in the inhibition of Cdc42-induced JNK activation and morphological changes indicating that SPECs may compete with Cdc42 effectors to promote the downregulation of Cdc42 pathways. In addition, SPECs may also modulate Cdc42 signaling by recruitment of additional protein partners to the SPEC-Cdc42 complex to direct alterations of normal Cdc42 signaling pathways for cytoskeleton reorganization (Pirone *et al.,* 2000).

Our most updated analyses indicate that in addition to the C-terminus BCH domain, BNIPXL contains a Walker A consensus (**G**XXXX**GK** (**T/S**) motif at its N-terminus (334)**G**PGWS**GKT**(341). This motif is characteristic of nucleotide binding proteins and is involved in positioning the triphosphate moiety of a bound nucleotide (Walker *et al.,* 1982). The P-loop is known to regulate the biochemical activities of several members of the Ras and Rab superfamily (Liang *et al.,* 2000; Li and Liang, 2001; Ding *et al.,* 2003; Zhu *et al.,* 2003) and downstream effectors such as B-Raf in a conformation dependent manner (Wan *et al.,* 2004). More recently, the P-loop motif has been implicated in coupling clathrin-mediated endocytosis with actin cytoskeleton organization (Guilherme *et al.,* 2004). The role of this Walker A motif remains to be further investigated. We note that the degradation profile of the N-terminus BNIPXL fragments indicate that a region close to the P-loop motif may exist in a hinge conformation that makes it structurally labile or sensitive toward proteases. Collectively, the unique structural features of BNIPXL

contribute to its distinct functions in cell morphogenesis and highlight the emergence of the BNIP-2 family as novel regulators of cell dynamics.

The use of dominant active and negative mutants has enabled the dissection of RhoA function in BNIPXL-induced cell shape changes. Although they represent a useful tool in functional characterization of downstream pathways, it is noted that the dominant negative mutants sequester upstream GEFs that may interact with multiple members of the Rho family thus blocking all endogenous Rho protein activation. Recent studies demonstrate that dominant negative Rac and Cdc42 mutants had aberrant effects on oncogenic Dbl-induced RhoA activation (Debreceni *et al.,* 2004). In view of this, a RhoGEF mutant that retained GTPase binding despite its impaired biochemical activity has enabled the specific inhibition of signaling pathways downstream of Rac activation (Debreceni *et al.,* 2004). The use of similar RhoA-specific GEF mutants should provide greater insights into the specific roles of the small GTPase in regulating diverse cellular events.

4.4. Conclusions and future work

In summary, we report the identification of a novel member of the BNIP-2 family, BNIPXL. BNIPXL is 769 amino-acid residues in length and encoded by a 13-exon gene mapped to human chromosome 9q21.2. It encompasses most of the prototypic BNIP-2 sequence at its distal carboxyl terminus. Interestingly, the BCH domain of BNIPXL resembles most closely to that of BNIP-H/Caytaxin, a protein whose loss-of-function is responsible for the Cayman ataxia, a form of neurological disorder. More recently, increased expression of an extended form of BNIPXL correlates to favorable prognosis in

childhood NBLs. *BNIPXL* undergoes alternative mRNA splicing within the BCH domain where removal of exons 11 and 12 introduces a premature stop codon that results in deletion of the last 36 amino acid residues for the β-isoform. Both isoforms are ubiquitously expressed in most human tissues and cell lines examined, except for the HEK293T cells that showed exclusive expression of only the β-isoform. Furthermore, mouse BNIPXL is highly expressed in the murine brain and neuronal cell lines. Through the BCH domain, BNIPXL associates with itself and other BCH-domain containing proteins. However, unlike BNIP-2, the BCH domain of BNIPXL associates specifically with RhoA but not Cdc42 or Rac1. It is sufficient to elicit membrane protrusions, potentiated only by co-expression of the dominant negative RhoA (T19N) but inhibited by co-expression of the PAK-CRIB domain that sequesters endogenous active Cdc42/Rac. Removal of the proximal region of the its BCH domain (residues 615-644) which resembles the Class I Rho-binding motifs as well as other regions abolished both RhoA binding and cell protrusions. This suggests that, unlike BNIP-S, a full composite of the BCH domain, probably via a conformation-dependent manner, is required for both RhoA binding and cell morphological changes. These results indicate that BNIPXL functions differently from BNIP-2 and BNIP-S in mediating cell shape changes by promoting RhoA inactivation via its BCH domain.

Our observations that BNIPXL can mediate cellular events through the coordination of resident motifs come amidst increasing evidence supporting an emerging notion that the BCH domain is an important signaling module integrating diverse small GTPase pathways into coherent cellular response. To fully understand the molecular mechanisms underlying the cellular effects observed with BNIPXL, future work involves

the identification of novel BNIPXL interacting partners using an established mass-spectrometry based proteomics approach. In addition, efforts to delineate the functions of the extended N-terminus will provide a better understanding of the roles of BNIPXL in modulating RhoA and Cdc42/Rac signaling pathways. Current structural data indicates that the RhoGAP domain adopts tertiary folds important for conformation-driven GTP hydrolysis. This raises the possibility that BNIPXL and other members of the BNIP-2 family may represent a novel class of non-canonical GAPs since their BCH domains are highly conserved and may adopt structurally similar conformations. Further investigations into the catalytic abilities of homologous BCH domains should provide a better understanding of the biochemical roles of the BNIP-2 family in Rho signaling. Future investigations will also determine if these BCH domains can modulate lipid signaling pathways based on their homology to the Sec14p lipid-binding domain (Zhou *et al.,* 2002; Aravind *et al.,* 1999). Recent work demonstrates the importance of the Sec14 homology domain in regulating cellular distribution and transforming activity of the Dbl family of exchange factors (Ueda *et al.,* 2004; Kostenko *et al.,* 2005) as well as conformation-dependent p50-RhoGAP activity (Moskwa *et al.,* 2005). This is in line with speculations that the Sec14 domain may bind PI-3,4,5-P_3 to regulate GAP activity via membrane recruitment and/or conformational changes (Krugmann *et al.,* 2002).

. Our current work has addressed some of the biochemical and cellular aspects of BNIPXL functions. Membrane protrusions and cell shape changes are precursors of cell movement. Thus, investigating the effects of BNIPXL in *in vitro* wound healing or cell migration assays will help elucidate the physiological roles of BNIPXL in cell dynamics. The use of appropriate cell lines stably expressing BNIPXL will greatly facilitate these

functional assays. Genetic model systems such as transgenic and knockout mouse represent *bona fide* models to better understand the biological roles of gene function during development and in disease progression. For example, ablation of p190-RhoGAP in mice has provided insights into the roles of RhoGAPs in Src-mediated adhesion signaling in neuronal morphogenesis (Brouns *et al*., 2000, Brouns *et al*., 2001) and in cell size (Sordella *et al*., 2002) and cell fate (Sordella *et al.,* 2003) determination downstream of insulin signaling during embryonic development. In addition, studies of transgenic mice overexpressing Ras and RhoA indicate their involvement in cell growth and cytoskeleton remodelling during cardiac myocyte development (Clerk and Sugden, 2000) while conditional Raf-1 gene knockouts have facilitated the dissection of its multiple roles in regulating cell movement and gene expression (Ehrenreiter *et al.,* 2005). Collectively, these reports have provided clearer understanding of the interplay of Ras and Rho signaling pathways *in vivo*.

The emergence of RNA-mediated interference (RNAi) technologies has provided excellent alternatives to transgenic mouse models for the study of gene function both *in vitro* and *in vivo*. RNAi mediated knockdown of BNIPXL expression will enable further characterization of its roles in cellular events. In addition, the progressive use of RNAi technologies in generating transgenic animal models is expected to facilitate tissue specific gene inactivation, thus overcoming the requirements for conditional knockouts in mice. (reviewed in Ristevsk, 2005). Co-workers have recently delineated the roles of RhoA and its effectors in convergence and extension (CE) movements during embryonic development in the zebrafish (Zhu *et al*., 2005). Functional knockdown of *RhoA* using morpholinos provides evidence linking CE movements to RhoA activation downstream of

Wnt signalling and independent of Wnt-mediated cell fate determination. The use of this established platform will provide a better understanding of the roles of BNIPXL during development (**Figure 4.2**).

In this work, we report the identification, isolation, characterization and functional analyses of a novel BCH domain-containing protein, BNIPXL. Our findings indicate that BNIPXL participates in cell morphogenesis by distinctly targeting RhoA unlike other members of the BNIP-2 family. These findings also highlight the plasticity of the BCH domain in conferring distinct mechanisms for cell morphogenesis by coupling different small GTPases to its unique GTPase-binding motifs, and possibly by targeting their immediate targets to the nearby region in a context-specific manner.

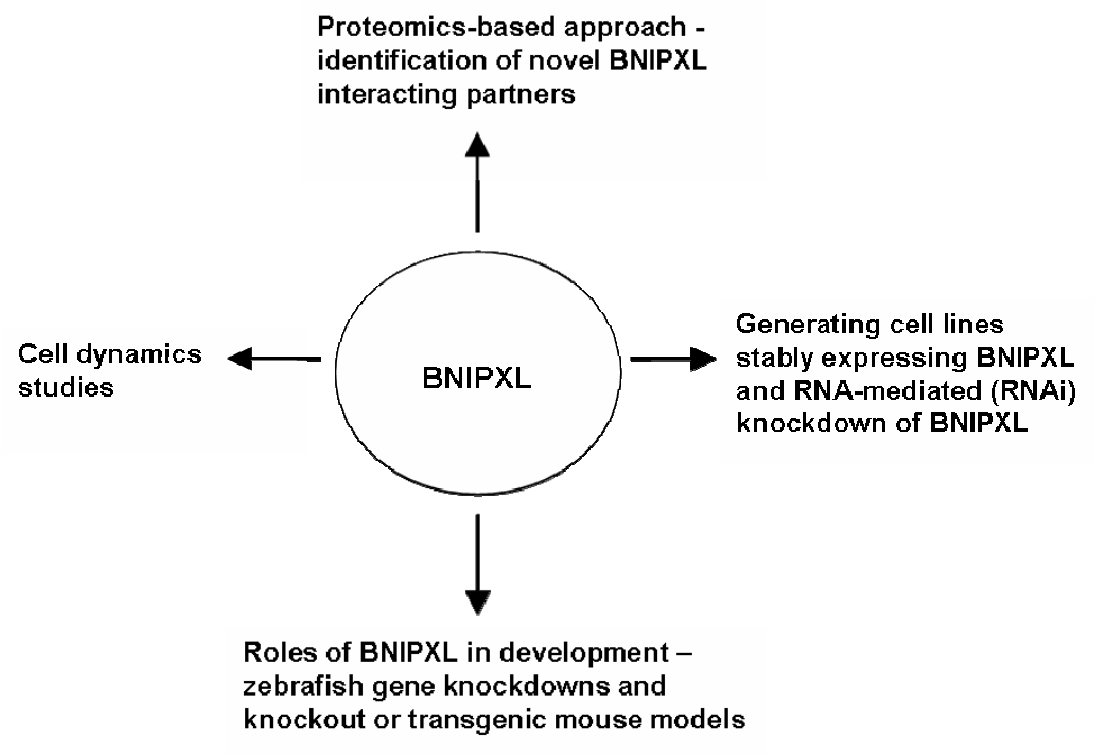

Figure 4.2. Schematic diagram illustrating all possible future work that should provide greater insights into the potential roles of BNIPXL in cell dynamics control, physiology and development.

References

5. References

Adra, C.N., Ko, J., Leonard, D., Wirth, L.J., Cerione, R.A. and Lim, B. (1993) Identification of a novel protein with GDP dissociation inhibitor activity for the ras-like proteins CDC42Hs and rac1. Genes Chromosomes Cancer, 8, 253-261

Adra, C.N., Manor, D., Ko, J.L., Zhu, S., Horiuchi, T., Van Aelst, L., Cerione, R.A. and Lim, B. (1997) RhoGDIgamma: A GDP-dissociation inhibitor for Rho proteins with preferential expression in brain and pancreas. Proc. Natl. Acad. Sci. USA 94, 4279-4284

Aghazadeh, B., Zhu, K., Kubiseski, T.J., Liu, G.A., Pawson, T., Zheng, Y. and Rosen, M.K. (1998) Structure and mutagenesis of the Dbl homology domain. Nat. Struct. Biol. 5, 1098-1107

Ahmadian, M.R., Stege, P., Scheffzek, K. and Wittinghofer, A. (1997) Confirmation of the arginine-finger hypothesis for the GAP-stimulated GTP hydrolysis reaction of Ras Nat. Struct. Biol. 4, 686-689

Ahmadian, M.R., Stege, P., Scheffzek, K., Wittinghofer, A. (1997) Confirmation of the arginine-finger hypothesis for the GAP-stimulated GTP-hydrolysis reaction of Ras. Nat. Struct. Biol. 4, 686-689

Ahmed, S., Kozma, R., Lee, J., Monfries, C., Harden, N. and Lim, L. (1991) The cysteine-rich domain of human proteins, neuronal chimaerin, protein kinase C and diaglycerol kinase binds zinc. Evidence for the involvement of a zinc-dependent strcture in phorbol ester binding. Biochem. J. 280, 233-241

Ahmed, S., Kozma, R., Monfries, C., Smith, P., Lim, H.H., Kozma, R., Ahmed, S., Vanniasingham, V., Leung, T. and Lim, L. (1990) Human brain n-chimaerin cDNA encodes a novel phorbol ester receptor. Biochem. J. 272, 767-773

Ahmed, S., Lee, J., Kozma, R., Best, A., Monfries, C. and Lim, L. (1993) A novel functional target for tumor-promoting phorbol esters and lysophosphatidic acid. The p21-rac-GTPase activating protein n-chimaerin. J. Biol. Chem. 268, 10709-10712

Ahmed, S., Lee, J., Wen, L.P., Zhao, Z., Ho, J., Best, A., Kozma, R. and Lim, L. (1994) Breakpoint cluster region gene product-related domain of n-chimaerin. Discrimination between Rac-binding and GTPase-activating residues by mutational analysis. J. Biol. Chem. 269, 17642-17648

Alam, M.R., Johnson, R.C., Darlington, D.N., Hand, T.A. Mains, R.E. and Eipper, B.A. (1997) Kalirin, a cytosolic protein with spectrin-like and GDP/GTP exchange factor-like domains that interacts with peptidylglycine alpha-amidating monooxygenase, an integral membrane peptide-processing enzyme. J. Biol. Chem. 272**,** 12667–12675.

Alberts, A.S., Bouquin, N., Johnston, L.H., Treisman, R. (1998) Analysis of RhoA-binding proteins reveals an interaction domain conserved in heterotrimeric G protein beta subunits and the yeast response regulator protein Skn7. J. Biol. Chem. 273, 8616– 8622

Al-Mulla, F., Milner-White, E. J., Going, J. J., and Birnie, G. D. (1999) Structural differences between valine-12 and aspartate-12 Ras proteins may modify carcinoma aggression. J. Pathol. 187**,** 433–438

Altschul, S.F., Madden, T.L., Schäffer, A.A., Zhang, J., Zhang, Z., Miller, W. and Lipman, D.J. (1997) Gapped BLAST and PSI-BLAST: a new generation of protein database search programs. Nucleic Acids Res. 25, 3389-3402

Amano, M., Chihara, K., Kimura, K., Fukata, Y., Nakamura, N., Matsuura, Y. and Kaibuchi, K. (1997) Formation of actin stress fibers and focal adhesions enhanced by Rho-kinase. Science 275, 1308-1211

Aravind, L., Neuwald, A.F. and Ponting, C.P. (1999) Sec14p-like domains in NF1 and Dbl-like proteins indicate lipid-regulation of Ras and Rho signaling. Curr. Biol. 9, R195-197

Arthur, W.T., Petch, L.A. and Burridge, K. (2000) Integrin engagement suppresses RhoA activity via a c-Src-dependent mechanism. Curr. Biol. 10, 719-722

Aspentrom, P. (2004) Integration of signaling pathways regulated by small GTPases and calcium. Biochim. Biophys. Act. 1742, 51-58

Assoian, R.K (1997) Anchorage-dependent cell cycle progression. J. Cell Biol. 136, 1-4

Assoian, R.K. and Schwartz, M.A. (2001) Integrins and cell proliferation; regulation of cyclin dependent kinases via cytoplasmic signaling pathways. J. Cell Sci. 114, 2553-2560
ataxia and ataxia/dystonia in the jittery mouse. Nat. Genet. 35, 264-269

Baldassare, J.J., Jarpe, M.B., Alferes, L., Raben, D.M. (1997) Nuclear translocation of RhoA mediates the mitogen-induced activation of phospholipase D involved in nuclear envelope signal transduction. J. Biol. Chem. 272, 4911-4914

Baldassarre, G., Belletti, B., Nicoloso, M.S., Schiappacassi, M., Vecchione, A., Spessotto, P., Morrione, A., Canzonieri, V. and Colombatti, A. (2005) $p27^{kip1}$-stathmin interaction influences sarcoma cell migration and invasion. Cancer Cell, 7, 51-63

Bankaitis, V.A., Aitken, J.R., Cleves, A.E. and Dowhan, W. (1990) An essential role for a phospholipid transfer protein in yeast Golgi function. Nature 347, 561–562

Barfod, E.T., Zheng, Y., Kuang, W.J., Hart, M.J., Evans, T., Cerione, R.A., Ashkenazi, A. (1993) Cloning and expression of a human CDC42 GTPase-activating protein reveals a functional SH3-binding domain. J. Biol. Chem. 268, 26059-26062

Barrett, T., Xiao, B., Dodson, E.J., Dodson, G., Ludbrook, S.B., Nurmahomed, K., Gamblin, S.J., Mussacchio, A., Smerdon, S.J. and Eccleston, J.F. (1997) The structure of the GTPase-activating domain from p50rhoGAP. Nature 385, 458-461

Bax, B. (1998) Domains of rasGAP and rhoGAP are related. Nature 392, 447-448

Belcredito, S., Brusadelli, A. and Maggi, A. (2000) Estrogens, apoptosis and cells of neural origin. J. Neurocyto. 29, 359-365

Belcredito, S., Vegeto, E., Brusadelli, A., Ghisletti, S., Mussi, P., Ciana, P. and Maggi, A. (2001) Estrogen neuroprotection: the involvement of the Bcl-2 binding protein BNIP-2. Brain Res. Rev. 37, 335-342

Bender, A. and Pringle, J.R. (1989) Multicopy suppression of the cdc24 budding defect in yeast by CDC42 and three newly identified genes including the ras-related gene RSR1. Proc. Natl. Acad. Sci. USA 86, 9976-9980

Bernards, A. (2003) GAPs galore! A survey of putative Ras superfamily GTPase activating proteins in man and Drosophila. Biochim. Biophys. Acta. 1603, 47-82

Bernards, A. and Settleman, J. (2004) GAP control: regulating the regulators of small GTPases. Trends Cell Biol. 14, 377-385

Bershadsky, A. (2004) Magic touch: how does cell-cell adhesion trigger actin assembly? Trends Cell Biol.14, 589-593

Besson, A., Gurian-West, M., Schmidt, A., Hall, A. and Roberts, J.M. (2004) $p27^{Kip1}$ modulates cell migration through the regulation of RhoA activation. Genes Dev. 18, 862-876

Bhattacharya, M., Babwah, A.V. and Ferguson, S.S.G. (2004) Small GTP-binding protein-coupled receptors. Biochem. Soc. Trans. 32, 1040-1044

Bi, F., Debreceni, B., Zhu, K., Salani, B., Eva, A. and Zheng, Y. (2001) Autoinhibition mechanism of proto-Dbl. Mol. Cell Biol. 21, 1463-1474

Billuart, P., Bienvenu, T., Ronce, N., des Portes, V., Vinet, M.C., Zemni, R., Roest Crollius, H., Carrie, A., Fauchereau, F., Cherry, M., Briault, S., Hamel, B., Fryns, J.P., Beldjord, C., Kahn, A., Moraine, C., Chelly, J. (1998) Oligophrenin-1 encodes a rhoGAP protein involved in X-linked mental retardation. Nature 392, 923-926

Billuart, P., Winter, C.G., Maresh, A., Zhao, X. and Luo, L. (2001) Regulating axon branch stability. the role of p190 RhoGAP in repressing a retraction signaling pathway. Cell 107, 195-207

Billuart, P., Winter, C.G., Maresh, A., Zhao, X. and Luo, L. (2001) Regulating axon branch stability: the role of p190 RhoGAP in repressing a retraction signaling pathway. Cell 107, 195-207

Birnboim, H.C. an Doly, J. (1979) A rapid alkaline extraction procedure for screening recombinant plasmid DNA. Nucleic Acids Res. 7, 1513-1523

Bishop, A.L. and Hall, A. (2000) Rho GTPases and their effector proteins. Biochem. J. 348, 241-255

Blangy, A., Vignal, E., Schmidt, S., Debant, A., Gauthier-Rouviere, C. and Fort. P. (2000) Trio controls Rac- and Cdc42-dependent cell structures through the direct activation of RhoG. J. Cell Sci. 113, 729-739

Blumenstein, L., and Ahmadian, M.R. (2004) Models of the cooperative mechanism for Rho-effector recognition: Implications for RhoA-mediated effector activation. J. Biol. Chem. 279, 53419-53426

Boettner, B. and van Aelst, L. (2002) The role of Rho GTPases in disease development. Gene 286, 155-174

Boivin, D. and Beliveau, R. (1995) Subcellular distribution and membrane association of Rho-related small GTP-binding proteins in kidney cortex. Am J. Physiol. 269, F180-F189

Bomar, J.M., Benke, P.J., Slattery, E.L., Puttagunta, R., Taylor, L.P., Seong, E., Nystuen, A., Chen, W., Albin, R.L., Patel, P.D., Kittles, R.A., Sheffield, V.C. and Burmeister, M. (2003) Mutations in a novel gene encoding a CRAL-TRIO domain cause human Cayman ataxia and ataxia/dystonia in the jittery mouse. Nat Genet. 35, 264-269

Bompard, G. and Caron, E. (2004) Regulation of WASP/WAVE proteins: making a long story short. J. Cell Biol. 166, 957-962

Bonner, A.E., Lemon, W.J., Devereux, T.R., Lubet, R.A. and You, M. (2004) Molecular profiling of mouse lung tumors: association with tumor progression, lung development and human lung adenocarcinomas. Oncogene, 23, 1166-1176

Boshans, R.L., Szanto, S., van Aelst, L., D'Souza-Schorey, C. (2000) ADP-ribosylation factor 6 regulates actin cytoskeleton remodeling in coordination with Rac1 and RhoA. Mol. Cell Biol. 20, 3685-3694

Bottazzi, M.E., Zhu, X., Bohmer, R.M. and Assoian, R.K. (1999) Regulation of p21cip1 expression by growth factors and the extracellular matrix reveals a role for transient ERK activity in G1 phase. J. Cell Biol. 146, 1255-1264

Boyartchuk, V.L., Ashby, M.N. and Rine, J. (1997) Modulation of Ras and a-factor function by carboxy-terminal proteolysis. Science 275, 1796-1800

Boyd, J. M., Malstrom, S., Subramaniam, T., Venkatesh, L. K., Schaeper, U., Elangovan, B., D'Sa-Eipper, C., and Chinnadurai, G. (1994) Adenovirus E1B 19 kDa and Bcl-2 proteins interact with a common set of cellular proteins. Cell, 79, 341-351

Briggs, M.W. and Sacks, D.B. (2003) IQGAP proteins are integral components of cytoskeleton regulation. EMBO Rep. 4, 571-574

Brill, S., Li, S., Lyman, C.W., Church, D.M., Wasmuth, J.J., Weissbach, L., Bernards, A. and Snijders, A.J. (1996) The ras GTPase-activating-protein-related human protein IQGAP2 harbors a potential actin binding domain and interacts with calmodulin and Rho family GTPases. Mol. Cell Biol. 16, 4869-4878

Brouns, M.R., Matheson, S.F. and Settleman, J. (2001) p190RhoGAP is the principal Src substrate in brain and regulates axon outgrowth, guidance and fasciculation. Nat. Cell Biol. 3, 361-367

Brouns, M.R., Matheson, S.F., Hu, K.Q., Delalle, I., Caviness, V.S., Silver, J., Bronson, R.T. and Settleman, J. (2000) The adhesion signaling molecule p190RhoGAP is required for morphogenetic processes in neural development. Development 127, 4891-4903

Brugnera, E., Haney, L., Grimsley, C., Lu, M., Walk, S.F., Tosello-Trampont, A.C., Macara, I.G., Madhani, H., Fink, G.R. and Ravichandran, K.S. (2002) Unconventional Rac-GEF activity is mediated through the dock180-ELMO complex. Nat. Cell Biol. 4, 574-582

Brunet, N., Morin, A. and Olofsson, B. (2002) RhoGDI-3 regulates RhoG and targets this protein to the Golgi complex through its unique N-terminal domain. Traffic, 3, 342-358

Bryan, B., Cai, Y., Wrighton, K., Wu, G., Feng, X., Liu, M. (2005) Ubiquitination of RhoA by Smurf1 promotes neurite outgrowth. FEBS Letts. 579, 1015-1019

Buchanan, F.G., Elliot, C.M., Gibbs, M and Exton, J.H. (2000) Translocation of the Rac1 guanine nucleotide exchange factor Tiam1 induced by platelet-derived growth factor and lysophosphatidic acid. J. Biol. Chem. 275, 9742-9748

Buchsbaum, R., Telliez, J.B., Goonesekera, S., Feig, L.A. (1996) The N-terminal pleckstrin, coiled-coil, and IQ domains of the exchange factor Ras-GRF act cooperatively to facilitate activation by calcium. Mol. Cell. Biol. 16, 4888-4896

Burbelo PD, Drechsel D and Hall A. (1995) A conserved binding motif defines numerous candidate target proteins for both Cdc42 and Rac GTPases. J. Biol. Chem. 270, 29071-29074.

Burridge, K. and Wennerberg, K. (2004) Rho and Rac take center stage. Cell 116 167-179

Buschwald, G., Friebel, A., Galan, J.E., Hardt, W.D., Wittinghofer, A., Scheffzek, K (2002) Structural basis for the reversible activation of a Rho protein by the bacterial toxin SopE. EMBO J. 21, 3286-3295

Bustelo, X.R. (2000) Regulatory and signaling properties of the Vav family. Mol. Cell Biol. 20, 1461-1477

Cabrera-Vera, T.M., Vanhauwe, J., Thomas, T.O., Medkova, M., Preininger, A., Mazzoni, M.R. and Hamm, H.E. (2003) Insights into G protein structure, function and regulation. Endocrine Rev. 24, 765-781

Caloca, M.J., Fernandez, N., Lewin, N.E., Ching, D., Modali, R., Blumberg, P.M. and Kazanietz, M.G. (1997) Beta2-chimaerin is a high affinity receptor for the phorbol ester tumor promoters. J. Biol. Chem. 272, 26488-26496

Cerione, R.A. and Zheng, Y. (1996) The Dbl family of oncogenes. Curr. Opin. Cell Biol. 8, 216-222

Chamberlain, M.D., Berry, T.R., Pastor, M.C. and Anderson, D.H. (2004) The p85α-subunit of phosphatidylinositol 3'-kinase binds to and stimulates the GTPase activity of Rab proteins J. Biol.Chem. 279, 48607-48614

Chang, L. and Goldman, R.D. (2004) Intermediate filaments mediate cytoskeletal crosstalk. Nat. Rev. Mol. Cell Biol. 5, 601-613

Cheng, L., Rossman, K.L., Mahon, G.M., Worthylake, D.K., Korus, M. and Sondek, J. (2002) RhoGEF specificity mutants implicate RhoA as a target for Dbs transforming activity. Mol. Cell Biol. 22, 6895-6905

Cherfils, J. and Chardin, P. (1999) GEFs: structural basis for their activation of small GTP-binding proteins. Trends Biochem. Sci. 24, 306-311

Cherfils, J. and Chardin, P. (1999) GEFs: Structural basis for their activation of small GTP-binding proteins. Trends Biochem. Sci. 24, 306-311

Choy, E., Chiu, V.K., Silletti, J., Feoktistov, M., Morimoto, T., Michaelson, D.,Ivanov, I.E., and Philips, M.R. (1999) Endomembrane trafficking of ras: the CAAX motif targets proteins to the ER and Golgi. Cell 98, 69-80

Chuang, T.H., Xu, X., Kaartinen, V., Heisterkamp, N., Groffen, J., Bokoch, G.M. (1995) Abr and Bcr are multifunctional regulators of the Rho GTP-binding protein family. Proc. Natl. Acad. Sci. USA 92, 10282-10286

Clarke, S. (1992) Protein isoprenylation and methylation at carboxyl-terminal cysteine residues. Annu. Rev. Biochem. 61, 355-386

Clerk, A. and Sugden, P.H. (2000) Small guanine nucleotide-binding proteins and myocardial hypertrophy. Circ Res. 86, 1019-1023

Coleman, M.L., Marshall, C.J. and Olson, M.F. (2004) Ras and Rho GTPases in G_1-phase cell-cycle regulation. Nat. Rev. Mol. Cell Biol. 5, 355-366

Colomer, V., Engelender, S., Sharp, A.H., Duan, K., Cooper, J.K., Lanahan, A., Lyford, G., Worley, P. and Ross, C.A. (1997) Huntingtin-associated protein 1 (HAP1) binds to a Trio-like polypeptide, with a rac1 guanine nucleotide exchange factor domain. Hum. Mol. Genet. 6**,** 1519–1525

Corbett, K.D and Alber, T. (2001) The many faces of Ras: recognition of small GTP-binding proteins. Trends Biochem. Sci. Vol. 26, 710-716

Cote, J.F. and Vuori, K. (2002) Identification of an evolutionarily conserved superfamily of DOCK180-related proteins with guanine nucleotide exchange activity. J Cell Sci. 115, 4901-4913

Crespo, P., Schuebel, K.E., Ostrom, A.A., Gutkind, J.S., Bustelo, X.R. (1997) Phosphotyrosine-dependent activation of Rac1- GDP/GTP exchange by the *vav* proto-oncogene product Nature, 385, 169-172

Cuff, J. A., Clamp, M. E., Siddiqui, A. S., Finlay, M. and Barton, G. J. (1998) JPred: A consensus secondary structure prediction server. Bioinformatics 14, 892-893

Dai, Q., Choy, E., Chiu, V., Romano, J., Silvka, S., Steitz, S.,Michaelis, S. and Philips, M.R. (1998) Mammalian prenylcysteine carboxyl methyltransferase is in the endoplasmic recticulum. J. Biol. Chem. 273, 15030-15034

Daly, R.J. (2004) Cortactin signalling and dynamic actin networks. Biochem J. 382, 13-25

Das, B., Shu, X., Day, G.J., Han, J., Krishna, U.M., Falck, J.R., and Broek, D. (2000) Control of intramolecular interactions between the pleckstrin homology and Dbl homology domains of Vav and Sos1 regulates Rac1 binding. J. Biol. Chem. 275, 15074-15081

Debant, A., Serra-Pages, C., Seipel, K., O'Brien, S., Tang, M., Park, S.H. and Streuli, M. (1996) The multidomain protein Trio binds the LAR transmembrane tyrosine phosphatase, contains a protein kinase domain, and has separate rac- specific and rho- specific guanine nucleotide exchange factor domains. Proc. Natl. Acad. Sci. USA 93, 5466–5471

Debreceni, B., Gao, Y., Guo, F., Zhu, K., Jia, B. And Zheng, Y. (2004) Mechanisms of guanine nucleotide exchange and Rac-mediated signaling revealed by a dominant negative Trio mutant. J. Biol. Chem. 279, 3777-3786

Denker, S.P and Barber, D.L. (2002) Cell migration requires both ion translocation and cytoskeletal anchoring by the Na-H exchanger NHE1. J. Cell Biol. 159, 1087-1096

Denker, S.P., Huang, D.C. Orlowski, J., Furthmayr, H. and Barber, D.L. (2000) Direct binding of the Na-H exchanger NHE1 to ERM proteins regulates the cortical cytoskeleton and cell shape independently of H^+ translocation. Mol. Cell, 6, 1425-1436

Diekmann, D., Brill, S., Garrett, M.D., Totty, N., Hsuan, J., Monfries, C., Hall, C., Lim, L. and Hall, A. (1991) *Bcr* encodes a GTPase-activating protein for p21rac. Nature 351, 400–402

Ding, J., Soule, G., Overmeyer, J.H. and Maltese, W.A. (2003) Tyrosine phosphorylation of the Rab24 GTPase in cultured mammalian cells. Biochim. Biophys. Res. Commun. 312, 670-675

Di-Poi, N., Faure, J., Grizot, S., Molnár, G., Pick, E. and Dagher, M. (2001) Mechanism of NAPDH oxidase activation by the Rac/Rho-GDI complex. Biochemistry, 40, 10014-10022

Dirac-Svejstrup, A.B., Sumizawa, T. and Pfeffer, S.R. (1997) Identification of a GDI displacement factor that releases endosomal Rab GTPases from Rab-GDO. EMBO J. 16, 465-472

Dransart, E., Morin, A., Cherfils, J. and Olofsson, B. (2005) Uncoupling of inhibitory and shuttling functions of Rho GDP dissociation inhibitors. J. Biol. Chem. 280, 4674-4683

Dubois, T., Paleotti, O., Mironov Jr., A.A, Fraisier, V., Stradal, T.E.B., De Matteis, M.A., Franco, M. and Chavrier, P. (2005) Golgi-localized GAP for Cdc42 functions downstream of ARF1 to control Arp2/3 complex and F-actin dynamics. Nat. Cell Biol. 7, 353-364

Dvorsky, R. and Ahmadian, M.R. (2004) Always look on the bright side of Rho: structural implications for a conserved intermolecular interface. EMBO Rep. 5, 1130-1136

Ehrenreiter, K., Piazzolla, D., Velamoor, V., Sobczak, I., Small, J.V., Takeda, J., Leung, T. and Baccarini, M. (2005) Raf-1 regulates Rho signaling and cell migration. J Cell Biol. 168, 955-964

Erickson, J.W., Zhang, C., Kahn, R.A., Evans, T. and Cerione, R.A. (1996) Mammalian Cdc42 is a Brefeldin A-sensitive component of the Golgi-apparatus. J. Biol. Chem. 271, 26850-26854

Erickson, J.W., Zhang, C., Kahn, R.A., Evans, T., and Cerione, R.A. (1996) Mammalian Cdc42 is a brefeldin A sensitive component of the Golgi apparatus. J. Biol. Chem. 271, 26850-26854

Etienne-Manneville, S. and Hall, A (2002) Rho GTPases in cell biology. Nature 420,629-635

Etienne-Manneville, S. and Hall, A. (2003) Cdc42 regulates GSK-3beta and adenomatous polyposis coli to control cell polarity. Nature 421, 753-756

Eva, A. and Aaronson, S.A. (1985) Isolation of a new human oncogene from a diffuse B-cell lymphoma. Nature 316, 273-275

Feig L.A. (1999) Tools of the trade: Use of dominant-inhibitory mutants of Ras-family GTPase. Nat. Cell Biol. 1, E25-27

Fidyk, N. J., and Cerione, R. A. (2002) Understanding the catalytic mechanism of GTPase-activating proteins: demonstration of the importance of switch domain stabilization in the stimulation of GTP hydrolysis. Biochemistry, 41**,** 15644-15653

Fields, S., and Song, O. K. (1989) A novel genetic system to detect protein-protein interactions. Nature 340, 245–246

Franken, S.M., Scheidig, A.J., Krengel, U., Rensland, H., Lautwein, A., Geyer, M., Scheffzek, K., Goody, R.S., Kalbitzer, H.R., Pai, E.F. and Wittinghofer, A. (1993) Three-dimensional structures and properties of a transforming and a nontransforming glycine-12 mutant of $p21^{H\text{-}ras}$ Biochemistry, 32, 8411-8420

Fritz, G., Just, I. and Kaina, B. (1999) Rho GTPases are over-expressed in human tumors. Int. J. Cancer, 81, 682-687

Fujisawa, K., Madaule, P., Ishizaki, T., Watanabe, G., Bito, H., Saito, Y., Hall, A. and Narumiya, S. (1998) Different regions of Rho determine Rho-selective binding of different classes of Rho target molecules. J. Biol. Chem. 273, 18943-18949

Fukumoto, Y., Kaibuchi, K., Hori, Y., Fujioka, H., Araki, S., Ueda, T., Kikuchi, A. and Takai, Y. (1990) Molecular cloning and characterization of a novel type of regulatory protein (GDi) for the rho proteins, ras p21-like small GTP-binding proteins. Oncogene, 5, 1321-1328

Furnari, F.B., Huang, H.J. and Cavenee, W.K. (1998) The phosphoinositol phosphatase activity of PTEN mediates a serum- sensitive G1 growth arrest in glioma cells Cancer Res. 58: 5002-5008.

Gamblin, S. J. and Smerdon, S. J. (1998) GTPase-activating proteins and their complexes. Curr. Opin. Struct. Biol. 8**,** 195-201

Garnier, M., Di Lorenzo, D., Albertini, A. And Maggi, A. (1997) Idenitification of estrogen-responsive genes in neuroblastoma SK-ER3 cells. J. Neurosci. 17, 4591-4599

Garrett, M.D., Self, A.J., van Oers, C. and Hall, A. (1989) Identification of distinct cytoplasmic targets for ras/R-ras and rho regulatory proteins. J. Biol. Chem. 264, 10–13

Gauthier-Rouviere, C., Vignal, E., Meriane, M., Roux, P., Montcourier, P., and Fort, P. (1998) RhoG GTPase controls a pathway that independently activates Rac1 and Cdc42Hs. Mol. Biol. Cell 9, 1379-1394

Gille, H. and Downward, J. (1999) Multiple Ras effector pathways contribute to G_1 cell cycle progression. J. Biol. Chem. 274, 22033-22040

Gjoerup, O., Lukas, J., Bartek, J. and Willumsen, B.M. (1998) Rac and Cdc42 are potent stimulators of E2F-dependent transcription capable of promoting retinoblastoma susceptibility gene product hyperphosphorylation. J. Biol. Chem. 273, 18812-18818

Glise, B. and Noselli, S (1997) Coupling of Jun amino-terminal kinase and Decapentaplegic signaling pathways in Drosophila morphogenesis. Genes Dev. 1738, 1738-1747

Golovanov, A.P., Chuang, T.H., DerMardirossian, C., Barsukov, I., Hawkins, D., Badii, R., Bokoch, G.M., Lian, L.Y. and Roberts, G.C. (2001a) Structure activity relationships in flexible protein domains: regulation of Rho GTPases by RhoGDI and D4 GDI. J. Mol. Biol. 305, 121-135

Golovanov, A.P., Hawkins, D., Barsukov, I., Badii, R., Bokoch, G.M., Lian, L.Y. and Roberts, G.C. (2001b) Structural consequences of site-directed mutagenesis in flexible

protein domains: NMR characterization of the L(55,56)S mutant of RhoGDI. Eur. J. Biochem. 268, 2253-2260

Gong, M.C., Iizuka, K., Nixon, G., Browne, J.P., Hall, A., Eccleston, J.F., Sugai, M., Kobayashi, S., Somlyo, A.V. and Somlyo, A.P. (1996) Role of guanine nucleotide-binding proteins-ras family or trimeric proteins or both in Ca^{2+} sensitization of smooth muscle. Proc Natl. Acad. Sci. USA 93, 1340-1345

Gosser, Y.Q., Nomanbhoy, T.K., Aghazadeh, B., Manor, D., Combs, C., Cerione, R.A. and Rosen, M.K. (1997) C-terminal binding domain of Rho GDP-dissociation inhibitor directs N-terminal inhibitory peptide to GTPases. Nature, 387, 814-819

Grabocka, E. and Wedegaertner, P.B. (2005) Functional consequences of $G\alpha_{13}$ mutations that disrupt interaction with p115RhoGEF. Oncogene, 24, 2155-2165

Graham, D.L., Eccleston, J.F., Lowe, P.N. (1999) The conserved arginine finger in rho-GTPase-activating protein is essential for efficient catalysis but not for complex formation with Rho.GDP and aluminium fluoride. Biochemistry 38, 985-991

Grizot, S., Faure, J., Fieschi, F.V., Vignais, Dagher, M. and Pebay-Peyroula, E. (2001) Crystal structure of the Rac-RhoGDI complex involved in NADPH oxidase oxidation. Biochemistry, 40, 10007-10013

Grosshans, J., Wenzl, C., Herz, H.M., Bartoszewski, S., Schnorrer, F., Vogt, N., Schwarz, H. and Muller H.A. (2005) RhoGEF2 and the formin Dia control the formation of the furrow canal by directed actin assembly during Drosophila cellularisation. Development 132, 1009-1020

Guilherme, A., Soriano, N.A., Bose, S., Holik, J., Bose, A., Pomerleau, D.P., Furcinitti, P., Leszyk, J., Corvera, S. and Czech, M.P. (2004) EHD2 and the novel EH domain binding

protein EHBP1 couple endocytosis to the actin cytoskeleton. J. Biol. Chem. 279, 10593-10605

Hall, A. (1998) Rho GTPases and the actin cytoskeleton. Science, 279, 509-514

Hames, B.D. (1998) An introduction to polyacrylamide gel electrophoresis. In: Gel Electrophoresis of Proteins - A Practical Approach. (Hames, B.D. and Rickwood, D., eds.). IRL Press, Oxford, pp. 1-86

Hancock, J.F., Paterson, H. and Marshall, C.J. (1990) A polybasic domain or palmitoylation is required in addition to the CAAX motif to localize $p21^{ras}$ to the plasma membrane. Cell, 63, 133-139

Hart, M.J., Callow, M.G., Souza, B. and Polakis, P. (1996) IQGAP1, a calmodulin-binding protein with a ras-GAP related domain, is a potential effector for CDC42Hs. EMBO J. 15, 2997-3005

Hart, M.J., Callow, M.G., Souza, B. and Polakis, P. (1996) IQGAP1, a calmodulin-binding protein with a rasGAP-related domain, is a potential effector for cdc42Hs. EMBO J. 15, 2997-3005

Hart, M.J., Eva, A., Evans, T., Aaronson, S.A., and Cerione, R.A. (1991) Catalysis of guanine nucleotide exchange on the CDC42Hs protein by the dbl oncogene product. Nature, 354, 311-314

Hart, M.J., Eva, A., Zangrilli, D., Aaronson, S.A., Evans, T., Cerione, R.A. and Zheng, Y. (1994) Cellular transformation and guanine nucleotide exchange activity are catalyzed by a common domain on the dbl oncogene product J. Biol. Chem. 269, 62-65

Hart, M.J., Jiang, X, Kozasa, T., Roscoe, W., Singer, W.D., Gilman, A.G., Sternweis, P.C. and Bollag, G. (1998) Direct stimulation of the guanine nucleotide exchange activity of p115RhoGEF by $G\alpha_{13}$. Science, 280, 2112-2114

Hart, M.J., Maru, Y., Leonard, D., Witte, O,N., Evans, T. and Cerione, R.A. (1992) A GDP dissociation inhibitor that serves as a GTPase inhibitor for the Ras-like protein CDC42Hs. Science, 258, 812-815

Hart, M.J., Sharma, S, elMasry, N., Qiu, R., McCabe, P., Polakis, P. and Bollag, G. (1996) Identification of a novel guanine nucleotide exchange factor for the Rho GTPase, J. Biol. Chem. 271, 25452-25458

Hill, C. S., Wynne, J. and Treisman, R. (1995) The Rho family GTPases RhoA, Rac1, and CDC42Hs regulate transcriptional activation by SRF. Cell 81, 1159-70

Hirose, M., Ishizaki, T., Watanabe, N., Uehata, M., Kranenburg, O., Moolenaar, W.H., Matsumura, F., Maekawa, M., Bito, H. and Narumiya, S. (1998) Molecular dissection of the Rho-associated protein kinase (p160ROCK)-regulated neurite remodeling in neuroblastoma N1E-115 cells. J. Cell Biol. 141, 1625-1636.

Ho, Y.D., Joyal, J.L., Li, Z. and Sacks, D.B. (1999) IQGAP1 integrates Ca^{2+}/calmodulin and Cdc42 signaling. J. Biol. Chem. 274, 464-470

Hoffman, G.R. and Cerione, R.A. (2000) Flipping the switch: the structural basis for signaling through the CRIB motif. Cell 102, 403-406

Hoffman, G.R. and Cerione, R.A.. (2004) Regulation of the RhoGTPases by RhoGDI. In: Molecular Biology Intelligence Unit: Rho GTPases (Symons, M., ed.), Landes Bioscience, pp. 32-45

Hoffman, G.R., Nassar, N. And Cerione, R.A. (2000) Structure of the Rho family GTP-binding protein Cdc42 in complex with the multifunctional regulator RhoGDI. Cell 100, 345-356

Hoffman, G.R., Nassar, N. and Cerione, R.A. (2000) Structure of the Rho family GTP-binding protein Cdc42 in complex with the multifunctional regulator RhoGDI. Cell, 100, 345-356

Hollinger, S. and Hepler, J.R. (2002) Cellular Regulation of RGS Proteins: Modulators and Integrators of G Protein Signaling. Pharmacol. Rev. 54, 527-559

Horii, Y., Beeler, J.F., Sakaguchi, K., Tachibana, M,, Miki, T. (1994) A novel oncogene, ost, encodes a guanine nucleotide exchange factor that potentially links Rho and Rac signaling pathways. EMBO J. 13, 4776-4786

Hu, K.Q. and Settleman, J. (1997) Tandem SH2 binding sites mediate the RasGAP-RhoGAP interaction: a conformational mechanism for SH3 domain regulation. EMBO J. 16, 473-483

Hunter, T. (2000) Signaling – 2000 and beyond. Cell, 100, 113-127

Iancu-Rubin, C. and Atweh, G.F. (2005) $p27^{kip1}$ and stathmin share the stage for the first time. Trends Cell Biol. 15, 346-348

Ihara, K., Muraguchi, S., Kato, M., Shimizu, T., Shirakawa, M., Kuroda, S., Kaibuchi, K. and Hakoshima, T. (1998) Crystal structure of human RhoA in a dominantly active form complexed with a GTP analogue. J. Biol Chem 273, 9656−9666

Ishizaki, T., Maekawa, M., Fujisawa, K., Okawa, K., Iwamatsu, A., Fujita, A., Watanabe, N., Sato, Y., Kakizuka, A., Morii, N. and Narumiya, S.(1996) The small GTP-binding

protein Rho binds to and activates a 160 kDa Ser/Thr protein kinase homologous to myotonic dystrophy kinase EMBO J. 15, 1885-1893

Ishizaki, T., Morishima, Y., Okamoto, M., Furuyashiki, T., Kato, T. and Narumiya, S. (2001) Coordination of microtubules and the actin cytoskeleton by the Rho effector mDia1. Nat. Cell Biol. 3, 8-14

Ishizaki, T., Naito, M., Fujisawa, K., Maekawa, M., Watanabe, N., Saito, Y. and Narumiya, S. (1997) p160ROCK, a Rho-associated coiled-coil forming protein kinase, works downstream of Rho and induces focal adhesions FEBS Letts. 404, 118-124

Isomura, M., Kikuchi, A., Ohga, N. and Takai, Y. (1991) Regulation of binding of rhoB p20 to membranes by its specific regulatory protein, GDP dissociation inhibitor. Oncogene 6, 119-124

Janmey, P.A. and Lindberg, U. (2004) Cytoskeletal regulation: rich in lipids. Nat. Rev. Mol. Cell Biol. 5, 658-666

Jenna, S., Hussain, N.K., Danek, E. I., Triki, I., Wasiak, S., McPherson, P.S. and Lamarche-Vane, N. (2002) The activity of the GTPase activating protein CdGAP, is regulated by the endocytic proten, intersectin. J. Biol. Chem. 277, 6366-6373

Johnstone, A. and Thorpe, R. (1987) Purification chains and fragments. In: Immunochemistry in Practice, 2nd edition. Boston: Blackwell Scientific Publications. 48-55.

Johnstone, C.N., Castellvi-Bel, S., Chang, L.M., Bessa, X., Nakagawa, H., harada, H., Sung, R.K., Pique, J.M., Castells, A. and Rustgi, A.K. (2004) ARHGAP9 is a novel member of the RHOGAP family related to ARHGAP1/CDC42GAP/p50RHOGAP: mutation and expression analyses in colorectal and breast cancers. 336, 59-71

Joyce, D., Bouzahzah, B., Fu, M., Albanese, C., D'Amico, M., Steer. J., Klein, J.U., Lee, R.J., Segall, J.E., Westwick, J.K., Der, C.J. and Pestell, R.G. (1999) Integration of Rac-dependent regulation of cyclin D1 trnascription through a nuclear factor-κB-dependent pathway. J. Biol. Chem. 274, 25245-25249

Karnoub, A.E. and Der, C.J. (2004) Rho family GTPases and cellular transformation. In: Molecular Biology Intelligence Unit: Rho GTPases (Symons, M., ed.), Landes Bioscience, pp. 163-177

Katzav, S., Cleveland, J.L., Heslop, H.E., and Pulido, D. (1991) Loss of the amino-terminal helix-loop-helix domain of the vav proto-oncogene activates its transforming potential. Mol. Cell Biol. 11, 1912-1920

Kazuhiro, A., Takeshi, N. and Michiyuki, M. (2004) Spatio-temporal regulation of Rac1 and Cdc42 activity during nerve growth factor-induced neurite outgrowth in PC12 cells. J. Biol. Chem. 279, 713– 719

Keep, N.H., Barnes, M. and Barsukov, I. (1997) A modulator of rho family G proteins, rhoGDI, binds these G proteins via an immunoglobulin-like domain and a flexible N-terminal arm. Structure, 5, 623-633

Khosravi-Far, R., Solski, P.A., Clark, G.J., Kinch, M.S. and Der, C.J. (1995) Activation of Rac1, RhoA, and mitogen-activated protein kinases is required for Ras transformation. Mol. Cell. Biol., 15, 6443-6453

Klebe, C., Prinz, H., Wittinghofer, A, and Goody, R.S. (1995) The kinetic mechanism of Ran - nucleotide exchange catalyzed by RCC1. Biochemistry 34, 12543-12552

Kosloff, M and Selinger, Z. (2001) Substrate assisted catalysis: application to G proteins. Trends Biochem. Sci. 26, 161-166

Kostenko, E.V., Mahon, G.M., Cheng, L. and Whitehead, I.P. (2005) The Sec14 Homology domain regulates the cellular distribution and transforming activity of the Rho-specific guanine nucleotide exchange factor Dbs. J. Biol. Chem. 280, 2807–2817

Kozasa, T., Jiang, X., Hart, M.J., Sternweis, P.M., Singer, W.D., Gilman, A.G., Bollag, G. and Sternweis, P.C. (1998) p115RhoGEF, a GTPase activating protein for $G\alpha_{12}$ and $G\alpha_{13}$ Science 280, 2109-2111

Kozma, R., Ahmed, S., Best, A. and Lim, L. (1995) The Ras-related protein Cdc42Hs and bradykinin promote formation of peripheral actin microspikes and filopodia in Swiss 3T3 fibroblasts. Mol Cell Biol. 15, 1942-1952

Kozma, S.C., Bogaard, M.E., Buser, K., Saurer, S.M., Bos, J.L., Groner, B. and Hynes, N.E. (1987) The human c-Kirsten ras gene is activated by a novel mutation in codon 13 in the breast carcinoma cell line MDA-MB-231. Nuclei Acids Res. 15, 5963-5971

Krengel, U., Schlichting, L., Scherer, A., Schumann, R., Frech, M., John, J., Kabsch, W., Pai, E. F., and Wittinghofer, A. (1990) Three-dimensional structures of H-ras p21 mutants: molecular basis for their inability to function as signal switch molecules. Cell 62, 539–548

Krugmann, S., Anderson, K.E., Ridley, S.H., Risso, N., McGregor, A., Coadwell, J., Davidson, K., Eguinoa, A., Ellson, C.D., Lipp, P., Manifava, M., Ktistakis, N., Painter, G., Thuring, J.W., Cooper, M.A., Lim, Z.Y., Holmes, A.B., Dove, S.K., Michell, R.H., Grewal, A., Nazarian, A., Erdjument-Bromage, H., Tempst, P,, Stephens, L.R. and Hawkins, P.T. (2002) Identification of ARAP3, a novel PI3K effector regulating both Arf and Rho GTPases, by selective capture on phosphoinositide affinity matrices. Mol. Cell, 9, 95-108

Kuroda, S., Fukata, M., Nakagawa, M., Fuji, K., Nakamura, T., Ookubo, T., Izawa, I., Nagase, T., Nomura, N., Tani, H., Shoji, I., Matsuura, Y., Yonehara, S. and Kaibuchi, K.

(1998) Role of IQGAP1, a target of the small GTPases Cdc42 and Rac1, in regulation of E-cadherin-mediated cell-cell adhesion. Science 281, 832-835

Lancaster, C.A., Taylor-Harris, P.M., Self, A.J., Brill, S., van Erp, H.E., Hall, A. (1994) Characterization of rhoGAP. A GTPase-activating protein for rho-related small GTPases. J. Biol. Chem. 269, 1137-1142

Lancaster, C.A., Taylor-Harris, P.M., Self, A.J., Brill, S., van Erp, H.E. and Hall, A. (1994) Characterization of RhoGAP, A GTPase-activating protein for rho-related small GTPases. J. Biol. Chem. 269, 1137-1142

Lee, M., Shen, B., Schwarzbauer, J.E., Ahn, J., Kwon, J. (2005) Connections between integrins and Rac GTPase pathways control gonad formation and function in C. elegans. Biochim Biophys Acta. 1723, 248-55

Leipe, D.D., Wolf, Y.I., Koonin, E.V. and Aravind, L. (2002) Classification and Evolution of P-loop GTPases and Related ATPases. J. Mol. Biol. 317, 41-72

Lelias, J.M., Adra, C.N., Wulf, G.M., Guillemot, J., Khagad, M., Caput, D. and Lim, B. (1993) cDNA cloning of a human mRNA preferentially expressed in hematopoietic cells and with homology to a GDP-dissociation inhibitor for the rho GTP-binding proteins. Proc. Natl. Acad. Sci. USA 90, 1479-1483

Lemmon, M.A. and Ferguson, K.M. (2000) Signal-dependent membrane targeting by pleckstrin homology (PH) domains. Biochem. J. 350, 1-18

Lenzen, C., Cool, R.H., Prinz, H., Kuhlmann, J. and Wittinghofer, A. (1998) Kinetic analysis by fluorescence of the interaction between Ras and the catalytic domain of the guanine nucleotide exchange factor Cdc25Mm. Biochemistry 20, 7420-7430

Leonard, D., Hart, M.J., Platko, J.V., Eva, A., Henzel, W., Evans, T. and Cerione, R.A. (1992) The identification and characterization of a GDP-dissociation inhibitor (GDI) for the CDC42Hs protein. J. Biol. Chem. 267, 22860-22868

Leonard, D.A., Lin, R., Cerione, R.A. and Manor, D. (1998) Biochemical studies of the mechanism of action of the Cdc42 GTPase-activating protein. J. Biol. Chem. 273, 16210-16215

Li, G. and Liang, Z. (2001) Phosphate-binding loop and Rab GTPase function: mutations at Ser29 and Ala30 of Rab5 lead to loss-of-function as well as gain-of-function phenotype. Biochem. J. 355, 681-689

Li, R., Zhang, B., Zheng, Y. (1997) Structural determinants required for the interaction between RhoA and the GTPase-activating domain of p190. J. Biol. Chem. 272, 32830-32835

Li, Z., Kim, S.H., Higgin, J.M., Brenner, M.B. and Sacks, D.B. (1999) IQGAP1 and calmodulin modulate E-cadherin function. J. Biol. Chem. 274, 37885-37892

Lian, L.Y., Barsukov, I., Golovanov, A.P., Hawkins, D.I., Badii, R., Sze, K.H., Keep, N.H., Bokoch, G.M. and Roberts, G.C. (2000) Mapping the binding site for the GTP-binding protein Rac-1 on its inhibitor RhoGDI-1. Structure Fold. Des. 8, 47-55

Liang, Z., Mather, T. and Li, G. (2000) GTPase mechanism and function: new insights from systematic mutational analysis of the phosphate-binding loop residue Ala30 of Rab5. Biochem. J. 346, 501-508

Lin, M. and van Golen, K.L. (2004) Rho-regulatory proteins in breast cancer motility and invasion. Breast Cancer Res. Treat. 84, 49-60

Lin, Q., Fuji, R.,Yang, W. and Cerione, R. (2003) RhoGDI is required for Cdc42-mediated cellular transformation. Curr. Biol. 13, 1469-1479

Lin, R., Cerione, R.A. and Manor, D. (1999) Specific contributions of the small GTPases Rho, Rac, and Cdc42 to Dbl transformation. J. Biol. Chem., 274, 23633-23641

Liu, H.W., Halayko, A.J., Fernandes, D.J., Harmon, G.S., McCauley, J.A., Kocieniewskii, P., McConville, J., Fu, Y., Forsythe, S.M., Koguti, P., Bellam, S., Dowel, M., Churchill, J., Lesso, H., Kassiri, K., Mitchell, R.W., Hershenson, M.B., Camoretti-Mercado, B. and Solway, J. (2003) The RhoA/Rho kinase pathway regulates nuclear localization of serum response factor. Am. J. Resp. Cell Mol. Biol. 29, 39-47

Liu, X., Wang, H., Eberstadt, M., Schnuchel, A., Olejniczak, E.T., Meadows, R.P., Schkeryantz, J.M., Janowick, D.A., Harlan, J.E., Harris, E.A., et. al., (1998) NMR structure and mutagenesis of the N-terminal Dbl homology domain of the nucleotide exchange factor Trio. Cell, 95, 269-277

Longenecker, K.L., Zhang, B., Derewenda, U., Sheffield, P.J., Dauter, Z., Parsons, J.T., Zheng, Y. and Derewenda. Z.S. (2000) Structure of the BH domain from graf and its implications for Rho GTPase recognition. J. Biol. Chem. 275, 38605-38610

Low, B.C., Lim, Y.P., Lim, J., Wong, E.S. and Guy, G.R. (1999) Tyrosine phosphorylation of the Bcl-2-associated protein BNIP-2 by fibroblast growth factor receptor-1 prevents its binding to Cdc42GAP and Cdc42. J. Biol Chem. 274, 33123-33130

Low, B.C., Seow, K.T. and Guy, G.R. (2000b) The BNIP-2 and Cdc42GAP homology domain of BNIP-2 mediates its homophilic association and heterophilic interaction with Cdc42GAP. J. Biol Chem. 275, 37742-33751

Low, B.C., Seow, K.T. and Guy, G.R. (2000a) Evidence for a novel Cdc42GAP domain at the carboxyl terminus of BNIP-2. J. Biol. Chem. 275, 37742– 37751.

Lu, W. and Mayer, B.J. (1999) Mechanism of activation of Pak1 kinase by membrane localization. Oncogene 18, 797-806

Lua, B.L. and Low, B.C. (2004) BPGAP1 interacts with cortactin and facilitates its translocation to cell periphery for enhanced cell migration. Mol Biol Cell. 15, 2873-2883

Lua, B.L. and Low, B.C. (2004) Filling the GAPs in cell dynamics control: BPGAP1 promotes cortactin translocation to the cell periphery for enhanced cell migration. Biochem Soc Trans. 32, 1110-1112

Lua, B.L. and Low, B.C. (2005a) Cortactin phosphorylation as a switch for actin cytoskeletal network and cell dynamics control. FEBS Lett. 579, 577-585

Lua, B.L. and Low, B.C. (2005b) Activation of EGF receptor endocytosis and ERK1/2 signaling by BPGAP1 requires direct interaction with EEN/endophilin II and a functional RhoGAP domain. J. Cell Sci. 118, 2707-2721

Luttrell, L.M. (2002) Activation and targeting of mitogen-activated protein kinases by G-protein-coupled receptors. Can. J. Physiol. Pharmacol. 80, 375-382

Madaule, P. and Axel, R. (1985) A novel ras-related gene family. Cell, 41, 31-40

Madaule, P., Eda, M., Watanabe, N., Fujisawa, K., Matsuoka, T., Bito, H., Ishizaki, T and Narumiya, S. (1998) Role of citron kinase as a target of the small GTPase Rho in cytokinesis. Nature 394, 491-494

Madaule, P., Furuyashiki, T., Reid, T., Ishizaki, T., Watanabe, G., Morii, N. and Narumiya, S. (1995) A novel partner for the GTP-bound forms of rho and rac. FEBS Lett. 377, 243-248

Maekawa, M., Ishizaki, T., Boku, S., Watanabe, N., Fujita, A., Iwamatsu, A., Obinata, T., Ohashi, K., Mizuno, K. and Narumiya, S. (1999) Signaling from Rho to the actin cytoskeleton through protein kinases ROCK and LIM-kinase. Science 285, 895-898

Malliri, A. and Collard, J.G. (2003) Role of Rho-family proteins in cell adhesion and cancer. Curr. Opin. Cell Biol. 15, 583-589

Mammoto, A., Huang, S., Moore, K., Oh, P. and Ingber, E. (2004) Role of RhoA, mDia and ROCK in cell-shape dependent control of the Skp2-p27kip1 pathway and the G1/S transistion. J. Biol. Chem. 279, 26323-26330

Manabe Ri, R., Kovalenko, M., Webb, D.J. and Horwitz, A.R. (2002) GIT1 functons in a motile, multi-molecular signaling complex that regulates protrusive acitivity and cell migration. J. Cell Sci. 115, 1479-1510

Manser, E., Huang, H-Y., Loo, T., Chen, X., Dong, J. and Leung, T. (1997) Expression of constitutively active αPAK reveals effects of the kinases and focal complexes. Mol. Cell. Biol. 17, 1129-1143

Mao, J., Yuan, H., Xie, W. and Wu, D. (1998) Guanine nucleotide exchange factor GEF115 specifically mediates activation of Rho and serum response factor by the G protein alpha subunit $G\alpha_{13}$. Proc. Natl. Acad. Sci. USA 95, 12973-12976

Marinissen, M.J. and Gutkind, J.S. (2001) G-protein-coupled receptors and signaling networks: emerging paradigms. Trends Pharmacol. Sci. 22, 368-376

Marinissen, M.J., Chiariello, M., Gutkind, J.S. (2001) Regulation of gene expression by the small GTPase Rho through the ERK6(p38-gamma) MAP kinase pathway. Genes.Dev. 15, 535-553

Masters, S.C. (2004) Co-immunoprecipitation from transfected cells. In Methods in Molecular Biology: Protein-protein interactions, methods and applications (Fu, H., ed.), pp337-350, Humana Press

McAllister, S.S., Becker-Hapak, M., Pintucci, G., Pagano, M. and Dowdy, S.F. (2003) Novel $p27^{kip1}$ C-terminal scatter domain mediates Rac-dependent cell migration independent of cell cycle arrest functions. Mol. Cell Biol. 23, 216-228

McGlade, J., Brunkhorst, B., Anderson, D., Mbamalu, G., Settleman, J., Dedhar, S., Rozakis-Adcock, M., Chen, L.B. and Pawson, T. (1993) The N-terminal region of GAP regulates cytoskeletal structure and cell adhesion. EMBO J. 12, 3073-3081

Meda. C., Vegeto, E., Pollio, G., Ciana, P., Patrone, C., Pellicciari, C., Maggi, A. (2000) Oestrogen prevention of neural cell death correlates with decreased expression of mRNA for the pro-apoptotic protein nip-2. J. Neuroendocrinol. 12, 1051-1059

Mei, G., Di Venere, A., Rosato, N. and Finazzi-Agro, A. (2005) The importance of being dimeric. FEBS J. 272, 16-27

Meller, N., Merlot, S. and Guda, C. (2005) CZH proteins: a new family of Rho-GEFs. J. Cell Sci. 118, 4937-4946

Mettouchi, A., Klein, S., Guo, W., Lopez-Lago, M., Lemichez, E., Westwick, J.K. and Giancotti, F.G. (2001) Integrin-specific activation of Rac controls progression through the G_1 phase of the cell cycle. Mol. Cell, 8, 115-127

Michaelson, D., Rush, M., Philips, M.R. (2004) Intracellular targeting of Rho family GTPases: implications of localization on function. In: Molecular Biology Intelligence Unit: Rho GTPases (Symons, M., ed.), Landes Bioscience, pp. 18-31

Michaelson, D., Silletti, J., Murphy, G., D'Eustachio, P., Rush, M., and Philips, M.R. (2001) Differential localization of Rho GTPases in live cells. Regulation by hypervariable regions and RhoGID binding. J. Cell Biol. 152, 111-126

Michaelson, D., Wasif, A., Chiu, V.K., Bergo, M., Silletti, J., Wright, L., Young, S.G. and Philips, M. (2005) Postprenylation CAAX processing is required for proper localization of Ras but not Rho GTPases. Mol. Cell Biol. 16, 1606-1616

Michiels, F., Stam, J.C., Hordijk, P.L., van der Kammen, R.A., Ruuls-Van Stalle, L., Feltkamp, C.A. and Collard, J.G. (1997) Regulated membrane localization of Tiam1, mediated by the NH_2-terminal pleckstrin homology domain, is required for Rac-dependent membrane ruffling and c-Jun NH_2-terminal kinase activation. J. Cell Biol. 137, 387-398

Milburn, M.V., Tong, L., deVos, A.M., Brunger, A., Yamaizumi, Z., Nishimura, S. and Kim, S.H. (1990) Molecular switch for signal transduction: structural difference between active and inactive forms of protooncogenic ras proteins. Science 247, 939-945

Miller, J. and Stagljar, I. (2004) Using the yeast-two hybrid system to identify interacting proteins. In Methods in Molecular Biology: Protein-protein interactions, methods and applications (Fu, H., ed.), pp247-262, Humana Press

Miyashita, T. (2004) Confocal microscopy for intracellular co-localization of proteins. In Methods in Molecular Biology: Protein-protein interactions, methods and applications (Fu, H., ed.), pp399-410, Humana Press

Moolenaar, W.H., van Meeteren, L.A. and Giepmans, B.N.G. (2004) The ins and outs of lysophosphatidic acid signaling. BioEssays 26, 870-881

Moon, S.Y., Zheng, Y. (2003) Rho GTPase-activating proteins in cell regulation. Trends Cell Biol. 13, 13-22

Morreale, A.,Venkatesan, M., Mott, H.R., Owen, D., Nietlispach, D., Lowe, P.N., and Laue, E.D. (2000) Structure of Cdc42 bound to the GTPase binding domain of PAK. Nat. Struct. Biol. 7, 384-388

Moskwa, P., Paclet, M., Dagher, M. and Ligeti, E. (2005) Autoinhibition of p50 Rho GTPase-activating Protein (GAP) is released by prenylated small GTPases J. Biol. Chem. 280, 6716–6720

Mura, Y., Kikuchi, A., Musha, T., Kuroda, S., Yaku, H., Sasaki, T. and Takai, Y. (1993) Regulation of morphology by rho p21 and its inhibitory GDP/GTP exchange protein (rhoGDI) in Swiss 3T3 cells. J. Biol. Chem. 268, 510-515

Murphy, C., Saffrich, R., Grummt, M., Gournier, H., Rybin, V., Rubino, M., Auvinen, P., Lutcke, A., Parton, R.G. and Zerial, M. (1996) Endosome dynamics regulated by a Rho protein. Nature, 384, 427-432

Musacchio, A., Cantley, L.C., Harrison, S.C. (1996) Crystal structure of breakpoint cluster region-homology domain from phosphoinositides 3-kinase p85 alpha subunit. Proc. Natl. Acad. Sci. USA 93, 14373-14378

Nagase, T., Ishikawa, K., Nakajima, D., Ohira M., Seki, N., Miyajima, N., Tanaka, A., Kotani, H., Nomura, N. and Ohara, O. (1997) Prediction of the coding sequences of unidentified human genes. VII. The complete sequences of 100 new cDNA clones from brain which can code for large proteins in vitro. DNA Res. 4, 141-150

Nassar, N., Hoffman, G. R., Manor, D., Clardy, J. C., and Cerione, R. A. (1998) Structures of Cdc42 bound to the active and catalytically compromised forms of Cdc42GAP. Nat. Struct. Biol. 5, 1047-1052

Nimnual, A.S., Taylor, L.J. and Bar-Sagi, D. (2003) Redox-dependent downregulation of Rho by Rac. Nat. Cell Biol. 5, 236-241

Nimnual, A.S., Yatsula, B.A., Bar-Sagi, D. (1998) Coupling of Ras and Rac guanosine triphosphates through the Ras exchanger Sos. Science 279, 560-563

Nobes, C.D. and Hall, A. (1995) Rho, rac and Cdc42 GTPases regulate the assembly of multimolecular focal complexes associated with actin stress fibers, lamellipodia and filopodia. Cell, 81, 53-62

Nobes, C.D. and Hall, A. (1995) Rho, rac and cdc42 GTPases: regulators of actin structures, cell adhesion and motility. Biochem. Soc. Trans. 23, 456– 459

Nobes, C.D. and Hall, A. (1999) Rho GTPases control polarity, protrusion and adhesion during cell movement. J. Cell Biol. 144, 1235-1244

Noda, M., Yasuda-Fukazawa, C., Moriishi, K., Kato, T., Okuda, T., Kurokawa, K.and Takuwa, Y. (1995) Involvement of rho in GTPγS-induced enhancement of phosphorylation of 20kDa myosin light chain in vascular smooth muscle cells: inhibition of phosphatase activity. FEBS Lett. 367, 246-250

Nomanbhoy, T.K. and Cerione, R.A. (1996) Characterization of the interaction between RhoGDI and Cdc42Hs using fluorescence spectroscopy. J. Biol. Chem. 271, 10004-10009

Nomanbhoy, T.K., Erickson, J.W., Cerione, R.A. (1999) Kinetics of Cdc42 membrane extraction by Rho-GDI monitored by real-time fluorescence resonance energy transfer. Biochemistry, 38, 1744-1750

Noren, N.K., Liu, B.P., Burridge, K. and Kreft, B. (2000) p120 catenin regulates the actin cytoskeleton via Rho family GTPases. J. Cell Biol. 150, 567-580

O'Bryan, J.P., Mohney, R. P. and Oldham, C. E. (2001) Mitogenesis and endocytosis: What's at the INTERSECTIoN ? Oncogene 20, 6300-6308

Oberneier, A., Ahmed, S., Manser, E., Yen, S.C., Hall, C. and Lim, L. (1998) PAK promotes morphological changes by acting downstream of Rac. EMBO J. 17, 4328-4339

Ohira, M., Oba, S., Nakamura, Y., Hirata, T., Ishii, S. and Nakagawara, A. (2005) A review of DNA microarray analysis of human neuroblastomas. Cancer Letts. 228, 5-11

Olofsson, B. (1999) Rho Guanine Dissociation Inhibitors: Pivotal molecules in cellular signaling. Cell. Signal. 11, 545-554

Olson, M.F., Pasteris, N.G., Gorski, J.L. and Hall, A. (1996) Faciogenital dysplasia protein [FGD1] and Vav, two related proteins required for normal embryonic development, are upstream regulators of Rho GTPases. Curr. Biol. 6, 1628-1633

Ozonoff, S. (1999) Cognitive impairment in neurofibromatosis type 1. Am. J Med. Genet., 89, 45-52

Paduch, M., Jelen, F. and Otlewski, J. (2001) Structure of small G proteins and their regulators. Acta Biochim. Polonica 48, 829-850

Page, K., Li, J., Hodge, J.A., Liu, P.T., Vanden Hoek, T.L., Becker, L.B., Pestell, R.G., Rosner, M.R. and Hershenson, M.B. (1999) Characterization of a Rac1 signaling pathways to cyclin D1 expression in airway smooth muscle cells. J. Biol. Chem. 274, 22065-22071

Palazzo, A.F., Cook., T.A., Alberts, A.S. and Gundersen, G.G. (2001) mDia mediates Rho-regulated formation and orientation of stable microtubules. Nat. Cell Biol. 3, 723-729

Pawson, T and Scott, J.D. (1997) Signaling through scaffold anchoring and adaptor proteins Science 278: 2075-2080.

Pawson, T. (2004) Specificity in signal transduction: from phosphotyrosine-SH2 domain interactions to complex cellular systems. Cell, 116, 191-203

Pawson, T. and Nash, P. (2000) Protein-protein interactions define specificity in signal transduction. Genes Dev. 14, 1027-1047

Pawson, T. and Nash, P. (2003) Assembly of cell regulatory systems through protein interaction domains. Science, 300, 445-452

Pawson, T. and Saxton, T.M. (1999) Signaling networks – do all roads lead to the same genes. Cell, 97, 675-678

Pawson, T., Raina, M. and Nash, P. (2002) Interaction domains: from simple binding events to complex cellular behaviour. FEBS Lett. 513, 2-10

Peck, J., Douglas, G., Wu, C.H., Burbelo, P.D. (2002) Human RhoGAP domain-containing proteins: structure, function and evolutionary relationships. FEBS Letts. 528, 27-34

Peck, J.W., Oberst, M., Bouker, K.B., Bowden, E. and Burbelo, P.D. (2002) The RhoA-binding protein, Rhophilin-2, Regulates Actin Cytoskeleton Organization. J. Biol. Chem. 277, 43924-43932.

Perona, R., Esteve, P., Jimenez, B., Ballestero, R.P. and Cajal, S.R. (1993) Tumorigenic activity of *rho* genes from *Aplysia californica*. Oncogene, 8, 1285-1292

Pfeffer, S. and Aivazian, D. (2004) Targeting Rab GTPases to distinct membrane compartments. Nat. Rev. Mol. Cell Biol. 5, 886-896

Pille, J.Y., Denoyelle, C., Varet, J., Bertrand, J.R., Soria, J., Opolon, P., Lu, H., Pritchard, L.L., Vannier, J.P., Malvy, C., Soria, C. and Li, H. (2005) Anti-RhoA and anti-RhoC siRNAs inhibit the proliferation and invasiveness of MDA-MB-231 breast cancer cells in vitro and in vivo. Mol. Ther. 11, 267-274

Pirone, D.M., Fukuhara, S., Gutkind, J.S. and Burbelo, P.D. (2000) SPECs, Small Binding Proteins for Cdc42. J. Biol. Chem. 275, 30, 22650-22656

Platko, J.V., Leonard, D.A., Adra, C.N., Shaw, R.J., Cerione, R. A. and Lim, B. (1995) A single residue can modify target-binding affinity and activity of the functional domain of the Rho-subfamily GDP dissociation inhibitors. Proc. Natl.Acad. Sci. USA 92, 2974-2978

Pollard, T.D., Blancholn, L., and Mullins, R.D. (2000) Molecular mechanisms controlling actin filament dynamics in non-muscle cells. Annu. Rev. Biophys. Biomol. Struct. 29, 545-576

Ponting, C.P., Schultz, J., Milpetz, F. and Bork, P. (1999) SMART: Identification and annotation of domains from signaling and extracellular protein sequences. Nucleic Acids Res.27, 229-232

Price, L.S., Langeslag, M., ten Klooster, J.P., Hordijk, P.L., Jalink, K. and Collard, J.G. (2003) Calcium signaling regulates translocation and activation of Rac. J. Biol. Chem. 278, 39413-39421

Price, L.S., Leng, J., Schwartz, M.A. and Bokoch, G.M. (1998) Activation of Rac and Cdc42 by integrins mediates cell spreading. Mol. Biol. Cell 9, 1863– 1871

Pruyne, D. and Bretscher, A. (2000) Polarization of cell growth in yeast. I. Establishment and maintenance of polarity states. J. Cell Sci. 113, 365-375

Qin, W., Hu, J., Guo, M., Xu, J., Li, J., Yao, G., Zhou, X., Jiang, H., Zhang, P., Shen, L., Wan, D. and Gu, J. (2003) BNIPL-2, a novel homologue of BNIP-2, interacts with Bcl-2 and Cdc42GAP in apoptosis. Biochem. Biophys. Res. Commun. 308, 379-385

Raftopoulou, M. and Hall, A. (2004) Cell migration: Rho GTPases lead the way. Dev. Biol. 265, 23-32

Rebecchi, M.J. and Scarlata, S. (1998) Pleckstrin homology domains: A common fold with diverse functions. Annu. Rev. Biophys. Biomol. Struct. 27, 503-528

Reinstein, J., Schlichting, I., Frech, M., Goody, R.S. and Wittinghofer, A**.** (1991) p21 with a phenylalanine 28-leucine mutation reacts normally with the GTPase-activating protein GAP but nevertheless has transforming properties. J. Biol. Chem. 266, 17700-17706

Ren, X.R., Du, Q.S., Huang, Y.Z., Ao, S., Lin, M. and Xiong, W. (2001) Regulation of CDC42 GTPase by praline-rich tyrosin kinase 2 interacting with PSGAP, a novel pleckstrin homology and Src homology 3 domain containing RhoGAP protein. J. Cell Biol. 152, 971-984

Revenu, C., Athman, R., Robine, S. and Louvard, D. (2004) The co-workers of actin filaments: from cell structures to signals. Nat. Rev. Mol. Cell Biol. 5, 1-12

Ridley, A. (2004) Rho proteins and cancer. Breast Cancer Res. Treat. 84, 13-19

Ridley, A.J. (2001) Rho family proteins: coordinating cell responses. Trends Cell Biol. 11, 471-477

Ridley, A.J. and Hall, A. (1992) The small GTP-binding protein rho regulates the assembly of focal adhesions and actin stress fibers in response to growth factors. Cell, 70, 389-399

Ridley, A.J., Paterson, H.F., Johnston, C.L., Diekmann, D. and Hall, A. (1992) The small GTP-binding protein rac regulates growth factor-induced membrane ruffling. Cell, 70, 401-410

Ridley, A.J., Self, A.J., Kasmi, F., Paterson, H.F., Hall, A., Marshall, C.J., Ellis, C. (1993) rho family GTPase activating proteins p190, bcr and rhoGAP show distinct specificities in vitro and in vivo. EMBO J. 12, 515-5160

Riento, K.and Ridley, A.J. (2003) ROCKS: multifunctional kinases in cell behaviour. Nat. Rev. Mol. Cell Biol. 4, 446-456

Ristevski, S. (2005) Making better transgenic models: conditional, temporal, and spatial approaches. Mol. Biotechnol. 29, 153-163

Rittinger, K., Taylor, W.R., Smerdon, S.J. and Gamblin, S.J. (1998) Support for shared ancestry of GAPs. Nature 392, 448-449

Rittinger, K., Walker, P.A., Eccleston, J.F., Nurmahomed, K., Owen, D., Laue, E., Gamblin, S.J. and Smerdon, S.J. (1997a) Crystal structure of a small G protein in complex with the GTPase-activating protein rhoGAP. Nature 388, 693-697

Rittinger, K., Walker, P.A., Eccleston, J.F., Smerdon, S.J., Gamblin, S.J., (1997b) Structure at 1.65 A of RhoA and its GTPase-activating protein in complex with a transition-state analogue. Nature 389, 758-762

Rogers, S.L., Wiedemann, U., Hacker, U., Turck, C. and Vale, R.D. (2004) Drosophila RhoGEF2 associates with microtubule plus ends in an EB1-dependent manner. Curr. Biol. 14, 1827-1833

Ron, D., Graziani, G., Aaronson, S.A., and Eva, A. (1989) The N-terminal region of proto-dbl down regulates its transforming activity. Oncogene 4, 1067-1072

Ron, D., Zannini, M., Lewis, M., Wickner, R.B., Hunt, L.T., Graziani, G., Tronick, S.R., Aaronson, S.A. and Eva, A. (1991) A region of proto-dbl essential for its transforming activity shows sequence similarity to a yeast cell cycle gene, CDC24, and the human breakpoint cluster gene, bcr. New Biol. 3, 372-379

Roof, R.W., Haskell, M.D., Dukes, B.D., Sherman, N., Kinter, M. and Parsons, S.J. (1998) Phosphotyrosine (p-Tyr)-dependent and independent mechanisms of p190 RhoGAP-p120 RasGAP interaction: Tyr1105 of p190, a substrate for c-Src, is the sole p-Tyr mediator of complex formation. Mol. Cell Biol. 18, 7052-7063

Rossman, K.L., Der, C.J. and Sondek, J. (2005) GEF means go: turning on Rho GTPases with guanine nucleotide-exchange factors. Nature Rev. Mol. Cell Biol. 6, 167-180

Rossman, K.L., Worthylake, D.K., Snyder, J.T., Siderovski, D.P., Campbell, S.L., Sondek, J. (2002) A crystallographic view of interactions between Dbs and Cdc42: PH-domain assisted guanine nucleotide exchange. EMBO J. 21, 1315-1326

Rossman, K.L., Worthylake, D.K., Snyder, J.T., Siderovski, D.P., Campbell, S.L. and Sondek, J. (2002) A crystallographic view of interactions between Dbs and Cdc42, PH domain-assisted guanine nucleotide exchange EMBO J. 21, 1315-1326

Rudolph, M.G., Wittinghofer, A. and Vetter, I.R. (1999) Nucleotide binding to the G12V-mutant of Cdc42 investigated by X-ray diffraction and fluorescence spectroscopy: Two different nucleotide states in one crystal. Protein Sci. 8, 778-787

Sagi, S.A., Seasholtz, T.M., Kobiashvili, M., Wilson, B.A., Toksoz, D. and Brown, J.H. (2001) Physical and Functional Interactions of $G\alpha_q$ with Rho and Its Exchange Factors. J. Biol. Chem. 276, 15445-15452

Sah, V.P., Seasholtz, T.M., Sagi, S.A. and Heller-Brown, J. (2000) The role of Rho ins G protein coupled receptor signal transduction. Annu. Rev. Pharmcol. Toxicol. 40, 459-489

Sahai, E., Alberts, A.S. and Treisman, R. (1998) RhoA effector mutants reveal distinct effector pathways for cytoskeletal reorganization, SRF activation and transformation. EMBO J. 17, 1350-1361

Sahai, E., Ishizaki, T, Narumiya, S. and Treisman, R. (1999) Transformation mediated by RhoA requires activity of ROCK kinases. Curr. Biol. 9, 136-145

Sambrook, J., and Russell, D.W. (2001). Molecular Cloning: A Laboratory Manual, 3rd ed., Cold Spring Harbor, NY: Cold Spring Harbor Press.

Sander, E.E., ten Klooster, J.P., van Delft, S., van der Kammen, R.A., Collard, J.G. (1999) Rac downregulates Rho activity: Reciprocal balance between both GTPases determines cellular morphology and migratory behavior. J. Cell Biol. 147, 1009–1022

Saraste, M., Sibbald, P.R., Wittinghofer, A (1990) The P-loop--a common motif in ATP- and GTP-binding proteins. Trends Biochem. Sci. 15, 430, 130-134

Sasaki, T. and Takai, Y., (1998) The Rho small G protein family-GDI system as a temporal and spatial determinant for cytoskeletal control. Biochem. Biophys. Res. Commun. 245, 641-645

Scheffzek, K., Ahmadian, M.R., Wittinghofer, A. (1998) GTPase-activating proteins: helping hands to complement an active site. Trends Biochem. Sci. 23, 257-262

Scheffzek, K., Stephan, I., Jensen, O.N., Illenberger, D. and Gierschik, P.(2000) The Rac-RhoGDI complex and the structural basis for the regulation of Rho proteins by RhoGDI. Nat. Struct. Biol. 7, 122-126

Scherle, P., Behrens, T. and Staudt, L.M. (1993) Ly-GDI, a GDP-dissociation inhibitory of the RhoA GTP-binding protein, is expressed preferentially in lymphocytes. Proc. Natl. Acad. Sci. USA 90, 7568-7572

Schmidt, A. and Hall, A., (2002) Guanine nucleotide exchange factors for Rho GTPases: turning on the switch. Genes Dev. 16, 1587-1609

Schmidt, W.K., Tam, A., Fujimura-Kamada, K. and Michaelis, S. (1998) Endoplasmic recticulum membrane localization of Rce1p and Ste24p, yeast proteases involved in carboxyl-terminal CAAX protein processing and amino-terminal a-factor cleavage. Proc. Natl. Acad. Sci. USA 95, 11175-11180

Schwartz, M.A. (2004) Rho signaling at a glance. J.Cell Sci. 117, 5457-5458

Seasholtz, T.M., Majumdar, M. and Brown, J.H. (1999) Rho as a mediator of G protein-coupled receptor signaling. Mol. Pharmacol. 55, 949-956

Sells, M.A., Knaus, U.G., Bagrodia, S., Ambrose, D.M., Bokoch, G.M. and Chernoff, J. (1997) Human p21-activated kinase (Pak1) regulates actin organization in mammalian cells. Curr. Biol. 7, 202–210

Settleman, J., Albright, C.F., Foster, L.C. and Weinberg, R.A. (1992) Association between GTPase activators for Rho and Ras families. Nature, 359, 153-154

Sha, B., Phillips, S.E., Bankaitis, V.A. and Luo, M. (1998) Crystal structure of the Saccharomyces cerevisiae phosphatidylinositol- transfer protein. Nature 391, 506–510

Shang, X., Zhou, Y.T. and Low, B.C. (2003) Concerted regulation of cell dynamics by BNIP-2 and Cdc42GAP homology/Sec14p-like, proline-rich, and GTPase-activating protein domains of a novel Rho GTPase-activating protein, BPGAP1. J. Biol Chem. 278, 45903-45914

Shaw, R.J., Henry, M., Solomon, F. and Jacks, T. (1998) RhoA-dependent phosphorylation and relocalization of ERM proteins into apical membrane/actin protrusions in fibroblasts. Mol. Biol. Cell 9, 403-419

Sheaff, R.J., Groudine, M., Gordon, M., Roberts, J.M. and Clurman, B.E. (1997) Cyclin E-CDK2 is a regulator of p27Kip1. Genes. Dev. 11, 1464-1478

Shen, L., Hu, J., Lu, H., Wu, M., Qin, W., Wan, D., Li, Y. and Gu, J. (2003) The apoptosis-associated protein BNIPL interacts with two cell proliferation-related proteins, MIF and GFER. FEBS Letts. 540, 86-90

Sherr, C.J. and Roberts, J.M. (1999) CDK inhibitors: positive and negative regulators of G_1-phase progression. Genes Dev. 13, 1501-1512

Shimizu,Y., Thumkeo, D., Keel, J., Ishizaki, T., Oshima, H., Oshima, M., Noda, Y., Matsumura, F., Taketo, M.M. and Narumiya, S. (2005) ROCK-I regulates closure of the eyelids and ventral body wall by inducing assembly of actomyosin bundles. J Cell Biol., 168, 941-953

Simpson, K.J., Dugan, A.S. and Mercurio, A.M. (2004) Functional analysis of the contribution of RhoA and RhoC GTPases to invasive breast carcinoma. Cancer Res. 64, 8694-8701

Snyder, J.T., Worthylake, D.K., Rossman, K.L., Betts, L., Pruitt, W.M., Siderovski, D.P., Der, C.J. and Sondek, J. (2002) Structural basis for the selective activation of Rho GTPases by Dbl exchange factors. Nat. Struct. Biol. 9, 468-475

Soisson, S.M., Nimnual, A.S., Uy, M., Bar-Sagi, D., and Kuriyan, J. (1998) Crystal structure of the Dbl and pleckstrin homology domains from the human Son of sevenless protein. Cell, 95, 259-268

Sordella, R., Classon, M., Hu, K.Q., Matheson, S.F., Brouns, M.R., Fine, B., Zhang, L., Takami, H., Yamada, Y. and Settleman, J. (2002) Modulation of CREB activity by the Rho GTPase regulates cell and organism size during mouse embryonic development. Dev Cell. 2, 553-65

Sordella, R., Jiang, W., Chen, G.C., Curto, M. and Settleman, J. (2003) Modulation of Rho GTPase signaling regulates a switch between adipogenesis and myogenesis. Cell, 113, 147-158

Swart-Mataraza, J.M., Li., Z. And Sacks, D.B. (2002) IQGAP1 is a component of Cdc42 signaling in the cytoskeleton. J. Biol. Chem. 277, 24753-24763

Symons, M. and Settleman, J. (2000) Rho family GTPases: more than simple switches. Trends Cell Biol. 10, 415-419

Takai, Y., Sasaki, T. and Matozaki, T. (2001) Small GTP-binding proteins. Physio. Rev. 81, 153-208

Takaishi, K., Kikuchi, A., Kuroda, S., Kotani, K., Sasaki, T. and Takai, Y. (1993) Involvement of rho p21 and its inhibitory GDP/GTP exchange protein (rhoGDI) in cell motility. Mol. Cell Biol. 13, 72-79

Takaishi, K., Sasaki, T, Kameyama, T., Tsukita, S., Tsukita, S. and Takai, Y. (1995) Translocation of activated Rho from the cytoplasm to membrane ruffling area, cell-cell adhesion sites and cleavage furrows. Oncogene, 11, 39-48

Tassabehji, M., Strachan, T., Sharland, M., Colley, A., Donnai, D., Harris, R. and Thakker, N. (1993) Tandem duplication within a neurofibromatosis type 1 (NF1) gene exon in a family with features of Watson syndrome and Noonan syndrome. Am. J. Hum. Genet. 53, 90–95.

Tatsis, N., Lannigan, D.A. and Macara, I.G. (1998) The function of the p190 Rho GTPase-activating protein is controlled by its N-terminal GTP binding domain. J. Biol. Chem. 273, 34631-34638

Tong, L., de Vos, A.M., Milburn, M.V., Kim, S.H. (1991) Crystal structures at 2.2 Å resolution of the catalytic domains of normal ras protein and an oncogenic mutant complexed with GDP. J. Mol. Biol. 217, 503-516

Tran Quang C., Gautreau, A., Arpin, M. and Treisman, R. (2000) Ezrin function is required for ROCK-mediated fibroblast transformation by the Net and Dbl oncogenes. EMBO J. 19, 4565-4576

Ueda, S., Kataoka, T., Satoh, T. (2004) Role of the Sec14-like domain of Dbl family exchange factors in the regulation of Rho family GTPases in different subcellular sites. Cell. Signal. 16, 899–906

Ueda, T., Kikuchi, A., Ohga, N., Yamamoto, J. and Takai, Y. (1990) Purification and characterization from bovine cytosol of a novel regulatory protein inhibiting the dissociation of GDP from and the subsequent binding of GTP to rhoB p20, a ras p21-like GTP-binding proteins. J. Biol. Chem. 265, 9373-9380

Upadhyaya, M., Maynard, J., Osborn, M. and Harper, P.S. (1997) Six novel mutations in the neurofibromatosis type 1 (NF1) gene. Hum. Mutat. 10, 248–250.

van Aelst, L., Joneson, T. and Bar-Sagi, D. (1996) Identification of a novel Rac1-interacting protein involved in membrane ruffling. EMBO J. 15, 3778-3786

van Leeuwen, F.N., van der Kammen, R.A., Habets, G.G. and Collard, J.G. (1995) Oncogenic activity of Tiam1 and Rac1 in NIH3T3 cells. Oncogene 11, 2215-2221

Vanni.C., Parodi, A., Mancini, P., Visco, V., Ottaviano, C., Torrisi, M.R. and & Eva, A. (2004) Phosphorylation-independent membrane relocalization of ezrin following association with Dbl *in vivo*. Oncogene 23, 4098-4106

Vegeto, E., Pollio, G., Pellicciari, C. and Maggi, A. (1999) Estrogen and progesterone induction of survival of monoblastoid cells undergoing TNF-α-induced apoptosis. FASEB J. 13, 793-803

Venter, J.C., Adams, M.D., Myers, E.W. et. al., (2001) The sequence of the human genome. Science 291, 1304-1351

Vetter, I.R. and Wittinghofer, A. (2001) The guanine nucleotide-binding switch in three dimensions Science 294, 1299-1304

Vidal, A., Millard, S.S., Miller, J.P. and Koff, A. (2002) Rho activity can alter the translation of p27 mRNA and is important for Ras^{V12} induced transformation in a manner dependent on p27 status. J. Biol. Chem. 277, 16433-16440

Vikis, H.G. and Guan, K.L. (2004) Gluthathione-S-transferase-fusion based assays for studying protein-protein interactions. In Methods in Molecular Biology: Protein-protein interactions, methods and applications (Fu, H., ed.), pp.175-186, Humana Press

Walker, J.E., Saraste, M., Runswick, M. J. & Gay, N. J. (1982). Distantly related sequences in the alpha- and beta-subunits of ATP synthase, myosin, kinases and other ATP-requiring enzymes and a common nucleotide binding fold. EMBO J. 1, 945-951

Wan, P.T., Garnett, M.J., Roe, S.M., Lee, S., Niculescu-Duvaz, D., Good, V.M., Jones, C.M., Marshall, C.J., Springer, C.J., Barford, D. and Marais, R. (2004) Mechanism of activation of the RAF-ERK signaling pathway by oncogenic mutations of B-RAF. Cell, 116, 855-867

Wang, H, Zhang, Y., Ozdamar, B., Ogunjimi, A.A., Alexandrova, E., Thomsen, G.H. and Wrana, J.L. (2003) Regulation of cell polarity and protrusion formation by trageting RhoA for degradation. Science 302, 1775-1779

Watanabe, N., Kato, T., Fujita, A., Ishizaki, T. and Narumiya, S. (1999) Cooperation between mDia1 and ROCK in Rho-induced actin reorganization. Nat. Cell Biol. 1, 136-143

Watanabe, N., Madaule, P., Reid, T., Ishizaki, T., Watanabe, G., Kakizuka, A., Saito, Y., Nakao, K., Jockusch, B.M. and Narumiya, S. (1998) p140mDia, a mammalian homolog of Drosophila diaphanous, is a target protein for Rho small GTPase and is a ligand for profilin. EMBO J. 16, 3044-3056

Watanabe, T., Noritake, J. and Kaibuchi, K. (2005) Regulation of microtubules in cell migration. Trends Cell Biol. 15, 76-83

Watanabe, T., Wang, S., Noritake, J., Sato, K., Fukata, M., Takefuji, M., Nakagawa, M., Izumi, N., Akiyama, T. and Kaibuchi, K. (2004) Interaction with IQGAP1 Links APC to Rac1, Cdc42, and Actin Filaments during Cell Polarization and Migration. Dev. Cell, 7, 871-883

Wear, M.A. and Cooper, J.A. (2004) Capping protein: new insights into mechanism and regulation. Trends Biochem. Sci. 29, 418-428

Wei, Y., Zhang, Y., Derewenda, U., Liu, X., Minor, W., Nakamot,o R.K., Somlyo, A.V., Somlyo, A.P. and Derewenda, Z.S. (1997) Crystal structure of RhoA-GDP and its functional implications. Nat. Struct. Biol. 4, 699-703

Welsh, C.F. (2004) Rho GTPases as key transducers of proliferative signals in G_1 cell cycle regulation. Breast Cancer Res. Treat. 84, 33-42

Welsh, C.F., Roovers, K., Villanueva, J., Liu, Y., Schwartz, M.A. and Assoian, R.K. (2001) Timing of cyclin D1 expression within G_1 phase is controlled by Rho. Nat. Cell Biol. 3, 950-957

Westwick, J.K., Lambert, Q.T., Clark, G.J., Symons, M., Van Aelst, L., Pestell, R.G. and Der, C.J. (1997) Rac regulation of transformation, gene expression and actin organization by multiple, PAK-independent pathways. Mol. Cell Biol. 17, 1329-1335

White, R. and O'Connell, P. (1991) Identification and characterization of the gene for neurofibromatosis type 1. Curr. Opin. Genet. Dev. 1, 15–19

Whitehead, I. P., Zohn, I.E., Der, C.J. (2001) RhoGTPase-dependent transformation by G protein-coupled receptors. Oncogene 20, 1547-1555

Whitehead, I.P., Campbell, S., Rossman, K.L. and Der, C.J. (1997) Dbl family proteins. Biochim. Biophys. Acta. 1332, F1-F23

Whitehead, I.P., Kirk, H., Kay, R. (1995) Retroviral transduction and oncogenic selection of a cDNA encoding Dbs, a homolog of the Dbl guanine nucleotide exchange factor. Oncogene, 10, 713-721

Whitehead, I.P., Lambert, Q.T., Glaven, J.A., Abe, K., Rossman, K.L., Mahon, G.M., Trzaskos, J.M., Kay, R., Campbell, S.L. and Der, C.J. (1999) Dependence of Dbl and Dbs transformation on MEK and NF-kappaB activation. Mol. Cell Biol. 19, 7759-7770

Wittinghofer, A (2000) The functioning of molecular switches in three dimensions. In GTPases (Vol. 24) (Hall, A., ed.), pp244-310, Oxford University Press.

Wittinghofer, A and Pai, E.F. (1991) The structure of Ras protein: a model for a universal molecular switch. Trends Biochem. Sci. 16, 382-387

Worthylake, D.K., Rossman, K.L. and Sondek, J. (2000) Crystal structure of Rac1 in complex with the guanine nucleotide exchange region of Tiam1. Nature, 408, 682-688

Wu, Y. and Horvitz, H.R. (1998) C. elegans phagocytosis and cell migration protein CED-5 is similar to human DOCK180. Nature 392, 501-504

Xiao, J.H., Davidson, I., Matthes, H., Garnier, J. and Chambon, P. (1991) Cloning, expression, and transcriptional properties of the human enhancer factor TEF-1. Cell 65, 551-568

Xie, L., Qin, W., He, X., Shu, H., Yao, G., Wan, D. and Gu, J. (2004) Differential gene expression in human hepatocellular carcinoma Hep3B cells induced by apoptosis-related gene *BNIPL-2*. World J. Gastroenterol. 10, 1286-1291

Yamashita, T., and Tohyama, M. (2003) The p75 receptor acts as a displacement factor that releases Rho from Rho-GDI. Nat. Neurosci. 6, 461-467

Yamochi, W., Tanaka, K., Nonaka, H., Maeda, A., Musha, T. and Takai, Y. (1994) Growth site localization of RhoI small GTP-binding protein and its involvement in bud formation in *Saccharomyces cerevisiae*. J. Cell Sci. 125, 1077-1093

Yang, D., Yu, J., Luo, Z., Carthy, C.M., Wilson, J.E., Liu, Z. and McManus, B.M. (1999) Identification of five differentially expressed genes in coxsackievirus B3-infected mouse heart. Cir. Res. 84, 704-712

Zajchowski, D.A., Bartholdi, M.F., Gong, Y., Webster, L., Liu, H., Munishkin, A., Beauheim, C., Harvey, S., Ethier, S.P. and Johnson, P.H. (2004) Identification of gene expression profiles that predict the aggressive behaviour of breast cancer cells. Cancer Res., 61, 5168-5178

Zalcman, G., Closson, V. and Camonis, J. (1996) Rho-GDI-3 is a new GDP dissociation inhibitor (GDI). Identification of a noncytosolic GDI protein interacting with the small GTP-binding proteins RhoB and RhoG. J. Biol. Chem. 271, 30366-30374

Zarrinpar, A., Bhattacharyya, R.P. and Lim, W.A. (2003) The structure and function of proline recognition domains, Science's STKE, 179, RE8

Zhang, B., Yang, L., Zheng, Y. (2005) Novel intermediate of Rac GTPase activation by guanine nucleotide exchange factor. Biochim. Biophys. Res. Commun. 331, 413-421

Zhang, F. L. and Casey, P.J. (1996) Protein prenylation: molecular mechanisms and functional consequences. Annu. Rev. Biochem. 65, 241-269

Zhang, H.M., Yanagawa, B., Cheung, P., Luo, H., Yuan, J., Chau, D., Wang, A., Bohunek, L., Wilson, J.E., McManus, B.M. and Yang, D. (2001) Nip21 gene expression reduces coxsackievirus B3 replication by promoting apoptotic cell death via a mitochondria-depedent pathway. Cir. Res. 90, 1251-1258

Zhang, L. Deng, M., Parthasarathy, R., Wang, L., Mongan, M., Molkentin, J.D., Zheng, Y. and Xia, Y. (2005) MEKK1 transduces activin signals in keratinocytes to induce stress fiber formation and migration. Mol. Cell. Biol. 25, 60-65

Zhang, L., Wang, W., Hayashi, Y., Jester, J.V., Birk, D.E., Gao, M., Liu, C., Kao, W.W., Karin, M. and Xia, Y. (2003) A role for MEK kinase 1 in TGF-β/activin-induced epithelium movement and embryonic eyelid closure. EMBO J. 22, 4443–4454.

Zhao, Z. and Manser, E. (2005) PAKs and other Rho-associated kinases – effectors with surprisingly diverse mechanisms of regulation Biochem. J. 386, 201-214

Zheng, Y., Bagrodia, S. and Cerione, R.A. (1994) Activation of phosphoinositide 3-kinase activity by Cdc42Hs binding to p85. J. Biol Chem. 269, 18727-18730

Zheng, Y., Fischer, D.J., Santos, M.F., Tigyi, G., Pasteris, N.G., Gorski, J.L. and Xu, Y. (1996) The faciogenital dysplasia gene product FGD1 functions as a Cdc42Hs- specific guanine-nucleotide exchange factor. J. Biol. Chem. 271, 33169-33172

Zheng, Y., Hart, M.J., Shinjo, K., Evans, T., Bender, A. and Cerione, R.A. (1993) Biochemical comparisons of the Saccharomyces cerevisiae Bem2 and Bem3 proteins. Delineation of a limit Cdc42 GTPase-activating protein domain. J. Biol. Chem. 268, 24629–24634

Zheng, Y., Hart, M.J., Shinjo, K., Evans, T., Bender, A. and Cerione, R.A. (1993) Biochemical comparisions of the Saaccharomyces cerevisiae Bem2 and Bem3 proteins.

Delineation of a limit Cdc42 GTPase-activating protein domain. J. Biol. Chem. 268, 24629-24634

Zhou, Y.T., Guy, G.R. and Low, B.C. (2005a) BNIP-2 induces cell elongation and membrane protrusions by interacting with Cdc42 via a unique Cdc42-binding motif within its BNIP-2 and Cdc42GAP homology domain. Exp Cell Res. 303, 263-274

Zhou, Y.T., Guy, G.R. and Low, B.C. (2005b) BNIP-Salpha induces cell rounding and apoptosis by displacing p50RhoGAP and facilitating RhoA activation via its unique motifs in the BNIP-2 and Cdc42GAP homology domain. Oncogene, *In Press*.

Zhou, Y.T., Soh, U.J., Shang, X., Guy, G.R. and Low, B.C. (2002) The BNIP-2 and Cdc42GAP homology/Sec14p-like domain of BNIP-Salpha is a novel apoptosis-inducing sequence. J Biol Chem. 277, 7483-7492

Zhu, G., Liu, J., Terzyan, S., Zhai, P., Li, G., Zhang, X.C. (2003) High resolution crystal structures of human Rab5a and five mutants with substitutions in the catalytically important phosphate-binding loop. J. Biol. Chem. 278, 2452-2460

Zhu, S., Liu, L., Korzh, V., Gong, Z. and Low, B.C. (2005) RhoA acts downstream of Wnt5 and Wnt11 to regulate convergence and extension movements by involving effectors Rho Kinase and Diaphanous: use of zebrafish as an in vivo model for GTPase signaling. Cell. Signal. 18, 359-372

Zondag, G.C., Evers, E.E., ten Klooster, J.P., Janssen, L., van der Kammen, R.A., Collard, J.G. (2000) Oncogenic Ras downregulates Rac activity, which leads to increased Rho activity and epithelial-mesenchymal transition. J. Cell Biol. 149, 775-782

Appendices

LOCUS AY439213 2491 bp mRNA linear PRI 09-DEC-2003
DEFINITION Homo sapiens BNIPXL-alpha (BNIPXL) mRNA, complete cds, alternatively spliced.
ACCESSION AY439213
VERSION AY439213.1 GI:38259612
KEYWORDS .
SOURCE Homo sapiens (human)
ORGANISM Homo sapiens
Eukaryota; Metazoa; Chordata; Craniata; Vertebrata; Euteleostomi; Mammalia; Eutheria; Euarchontoglires; Primates; Catarrhini; Hominidae; Homo.
REFERENCE 1 (bases 1 to 2491)
AUTHORS Soh,J.K.U., Zhou,Y.T. and Low,B.C.
TITLE BNIPXL, an extra long member of the BNIP-2 family
JOURNAL Unpublished
REFERENCE 2 (bases 1 to 2491)
AUTHORS Soh,J.K.U., Zhou,Y.T. and Low,B.C.
TITLE Direct Submission
JOURNAL Submitted (16-OCT-2003) Department of Biological Sciences, National University of Singapore, Blk. S2, 14 Science Drive 4, Singapore 117543, Singapore
FEATURES Location/Qualifiers
source 1..2491
/organism="Homo sapiens"
/mol_type="mRNA"
/db_xref="taxon:9606"
/chromosome="9"
/map="9q21.31"
/tissue_type="brain; kidney"
gene 1..2491
/gene="BNIPXL"
CDS 163..2472
/gene="BNIPXL"
/note="BNIP-2 family; extra long; alternatively spliced"
/codon_start=1
/product="BNIPXL-alpha"
/protein_id="AAR15150.1"
/db_xref="GI:38259613"
/translation="MSKLTLSEGHPETPVDGDLGKQDICSSEASWGDFEYDVMGQNID
EDLLREPEHFLYGGDPPLEEDSLKQSLAPYTPPFDLSYITEPAQSAETIEEAGSPEDE
SLGCRAAEIVLSALPDRRSEGNQAETKNRLPGSQLAVLHIREDPESVYLPVGAGSNIL
SPSNVDWEVETDNSDLPAGGDIGPPNGASKEISELEEEKTIPTKEPEQIKSEYKEERC
TEKNEDRHALHMDYILVNREENSHSKPETCEERESIAELELYVGSKETGLQGTQLASF
PDTCQPASLNERKGLSAEKMSSKSDTRSSFESPAQDQSWMFLGHSEVGDPSLDARDSG
PGWSGKTVEPFSELGLGEGPQLQILEEMKPLESLALEEASGPVSQSQKSKSRGRAGPD
AVTHDNEWEMLSPQPVQKNMIPDTEMEEETEFLELGTRISRPNGLLSEDVGMDIPFEE
GVLSPSAADMRPEPPNSLDLNDTHPRRIKLTAPNINLSLDQSEGSILSDDNLDSPDEI
DINVDELDTPDEADSFEYTGHEDPTATKDSGQESESIPEYTAEEEREDNRLWRTVVIG
DQEQRIDMKVIEPYRRVISHGGLRGYYGDGLNAIIVFAACFLPDSSRADYHYVMENLF
LYVISTLELMVAEDYMIVYLNGATPRRRMPGLGWMKKCYQMIDRRLRKNLKSFIIVHP
SWFIRTILAVTRPFISSKFSSKIKYVNSLSELSGLIPMDCIHIPESIIKLDEELREAS
EAAKTSCLYNDPEMSSMEKDIDLKLKEKP"
misc_feature 1891..2340
/gene="BNIPXL"
/note="Region: sec14p-like lipid-binding domain"
misc_feature 1909..2364
/gene="BNIPXL"

```
                     /note="Region: sec14p-like domain"
     misc_feature    1960..2394
                     /gene="BNIPXL"
                     /note="Bnip2 and Cdc42GAP-like domain; Region: BCH domain"
ORIGIN
        1 gctttgtttg atggtgatcc acatttatcc acagagaatc ctgccttggt tcctgatgct
       61 ttgctagcct cagacacttg tctggatata agcgaagctg cctttgacca cagtttcagc
      121 gatgcctcag gtctcaacac atccacggga acaatagatg acatgagtaa actgacatta
      181 tccgaaggcc atccggaaac gccagttgat ggggacctag ggaagcaaga tatctgctca
      241 tctgaagcct cgtggggtga ttttgaatat gatgtaatgg gccagaatat cgatgaagat
      301 ttactgagag agcctgaaca cttcctgtat ggtggtgacc ctccctttgga ggaagattct
      361 ctgaagcagt cgctggcacc gtacacacct ccctttgatt tgtcttatat cacagaacct
      421 gcccagagtg ctgaaacaat agaggaagct gggtctccag aggatgaatc tctgggatgc
      481 agagcagcag agatagtgct ttctgcactt cctgatcgaa gaagtgaggg aaaccaggct
      541 gagaccaaaa acagactgcc tggatcccag ctggctgtgc tgcatattcg tgaagaccct
      601 gagtccgttt atttgccggt aggagcaggc tccaacattt tgtctccatc aaacgttgac
      661 tgggaagtag aaacagataa ttctgattta ccagcaggtg gagacatagg accaccaaat
      721 ggtgccagca aggaaatatc agaattggaa gaagaaaaaa caattcctac caaagagcct
      781 gagcagataa aatcagaata caaggaagaa agatgtacag agaagaatga agatcgtcat
      841 gcactacaca tggattacat acttgtaaac cgtgaagaaa attcacactc aaagccagag
      901 acctgtgaag aaagagaaag catagctgaa ttagaattgt atgtaggttc caaagaaaca
      961 gggctgcagg gaactcagtt agcaagcttc ccagacacat gtcagccagc ctccttaaat
     1021 gaaagaaaag gtctctctgc agagaaaatg tcttctaaaa gcgatacgag atcatctttt
     1081 gaaagccctg cacaagacca gagttggatg ttcttgggcc atagtgaggt tggtgatcca
     1141 tcactggatg ccagggactc agggcctggg tggtccggca agactgtgga gccgttctct
     1201 gaactcggct tgggtgaggg tccccagctg cagattctgg aagaaatgaa gcctctagaa
     1261 tctttagcac tagaggaagc ctctggtcca gtcagccaat cacagaagag taagagccga
     1321 ggcagggctg gcccggatgc agttacccat gacaatgaat gggaaatgct ttcaccacag
     1381 cctgttcaga aaaacatgat ccctgacacg gaaatggagg aggagacaga gttccttgag
     1441 ctcggaacca ggatatcaag accaaatgga ctactgtcag aggatgtagg aatggacatc
     1501 ccctttgaag agggcgtgct gagtcccagt gctgcagaca tgaggcctga acctcctaat
     1561 tctctggatc ttaatgacac tcatcctcgg agaatcaagc tcacagcccc aaatatcaat
     1621 ctttctctgg accaaagtga aggatctatt ctctctgatg ataacttgga cagcccagat
     1681 gaaattgaca tcaatgtgga tgaacttgat acccccgatg aagcagattc ttttgagtac
     1741 actggccatg aagatcccac agccaccaaa gattctggcc aagagtcaga gtctattcca
     1801 gaatatacgg ccgaagagga acgggaggac aaccggcttt ggaggacagt ggtcattgga
     1861 gaccaagagc agcgcattga catgaaggtc atcgagccct acaggagagt catttctcac
     1921 ggaggactta gaggatacta tggggacggt ctaaatgcca tcattgtgtt tgccgcctgt
     1981 tttctgccag acagcagtcg ggcggattac cactatgtca tggaaaatct tttcctatat
     2041 gtaataagta ctttagagtt gatggtagct gaagactata tgattgtgta cttgaatggt
     2101 gcaacccaa gaaggaggat gccagggcta ggctggatga agaaatgcta ccagatgatt
     2161 gacagacggt tgaggaagaa tttgaaatca ttcatcattg ttcatccatc ttggttcatc
     2221 agaacaatcc ttgctgtgac acgacctttt ataagttcaa aattcagcag taaaattaaa
     2281 tatgtcaata gcttatcaga actcagtggg ctgatcccaa tggattgcat ccacattcca
     2341 gagagcatca tcaaactgga tgaagaactg agggaagcat cagaggcagc taaaactagc
     2401 tgcctttaca atgatccaga aatgtcttct atggagaagg atattgactt gaagctgaaa
     2461 gaaaagcctt agttggccat gctggaagaa g
//
```

LOCUS AY439214 2405 bp mRNA linear PRI 09-DEC-2003
DEFINITION Homo sapiens BNIPXL-beta (BNIPXL) mRNA, complete cds, alternatively spliced.
ACCESSION AY439214
VERSION AY439214.1 GI:38259614
KEYWORDS .
SOURCE Homo sapiens (human)
ORGANISM Homo sapiens
Eukaryota; Metazoa; Chordata; Craniata; Vertebrata; Euteleostomi; Mammalia; Eutheria; Euarchontoglires; Primates; Catarrhini; Hominidae; Homo.
REFERENCE 1 (bases 1 to 2405)
AUTHORS Soh,J.K.U., Zhou,Y.T. and Low,B.C.
TITLE BNIPXL, an extra long member of the BNIP-2 family
JOURNAL Unpublished
REFERENCE 2 (bases 1 to 2405)
AUTHORS Soh,J.K.U., Zhou,Y.T. and Low,B.C.
TITLE Direct Submission
JOURNAL Submitted (16-OCT-2003) Department of Biological Sciences, National University of Singapore, Blk. S2, 14 Science Drive 4, Singapore 117543, Singapore
FEATURES Location/Qualifiers
source 1..2405
/organism="Homo sapiens"
/mol_type="mRNA"
/db_xref="taxon:9606"
/chromosome="9"
/map="9q21.31"
/tissue_type="brain; kidney"
gene 1..2405
/gene="BNIPXL"
CDS 163..2361
/gene="BNIPXL"
/note="BNIP-2 family; extra long; alternatively spliced"
/codon_start=1
/product="BNIPXL-beta"
/protein_id="AAR15151.1"
/db_xref="GI:38259615"
/translation="MSKLTLSEGHPETPVDGDLGKQDICSSEASWGDFEYDVMGQNID
EDLLREPEHFLYGGDPPLEEDSLKQSLAPYTPPFDLSYITEPAQSAETIEEAGSPEDE
SLGCRAAEIVLSALPDRRSEGNQAETKNRLPGSQLAVLHIREDPESVYLPVGAGSNIL
SPSNVDWEVETDNSDLPAGGDIGPPNGASKEISELEEEKTIPTKEPEQIKSEYKEERC
TEKNEDRHALHMDYILVNREENSHSKPETCEERESIAELELYVGSKETGLQGTQLASF
PDTCQPASLNERKGLSAEKMSSKSDTRSSFESPAQDQSWMFLGHSEVGDPSLDARDSG
PGWSGKTVEPFSELGLGEGPQLQILEEMKPLESLALEEASGPVSQSQKSKSRGRAGPD
AVTHDNEWEMLSPQPVQKNMIPDTEMEEETEFLELGTRISRPNGLLSEDVGMDIPFEE
GVLSPSAADMRPEPPNSLDLNDTHPRRIKLTAPNINLSLDQSEGSILSDDNLDSPDEI
DINVDELDTPDEADSFEYTGHEDPTATKDSGQESESIPEYTAEEEREDNRLWRTVVIG
DQEQRIDMKVIEPYRRVISHGGLRGYYGDGLNAIIVFAACFLPDSSRADYHYVMENLF
LYVISTLELMVAEDYMIVYLNGATPRRRMPGLGWMKKCYQMIDRRLRKNLKSFIIVHP
SWFIRTILAVTRPFISSKFSSKIKYVNSLSELSGLIPMDCIHIPESIIKY"
misc_feature 1891..2340
/gene="BNIPXL"
/note="Region: sec14p-like lipid-binding domain"
misc_feature 1909..2334
/gene="BNIPXL"

```
                     /note="Region: sec14p-like domain"
     misc_feature    1960..2355
                     /gene="BNIPXL"
                     /note="Bnip2 and Cdc42GAP-like domain; Region: truncated
                     BCH domain"
ORIGIN
        1 gctttgtttg atggtgatcc acatttatcc acagagaatc ctgccttggt tcctgatgct
       61 ttgctagcct cagacacttg tctggatata agcgaagctg cctttgacca cagtttcagc
      121 gatgcctcag gtctcaacac atccacggga acaatagatg acatgagtaa actgacatta
      181 tccgaaggcc atccggaaac gccagttgat ggggacctag ggaagcaaga tatctgctca
      241 tctgaagcct cgtggggtga ttttgaatat gatgtaatgg gccagaatat cgatgaagat
      301 ttactgagag agcctgaaca cttcctgtat ggtggtgacc ctcctttgga ggaagattct
      361 ctgaagcagt cgctggcacc gtacacacct ccctttgatt tgtcttatat cacagaacct
      421 gcccagagtg ctgaaacaat agaggaagct gggtctccag aggatgaatc tctgggatgc
      481 agagcagcag agatagtgct ttctgcactt cctgatcgaa gaagtgaggg aaaccaggct
      541 gagaccaaaa acagactgcc tggatcccag ctggctgtgc tgcatattcg tgaagaccct
      601 gagtccgttt atttgccggt aggagcaggc tccaacattt tgtctccatc aaacgttgac
      661 tgggaagtag aaacagataa ttctgattta ccagcaggtg gagacatagg accaccaaat
      721 ggtgccagca aggaaatatc agaattggaa gaagaaaaaa caattcctac caaagagcct
      781 gagcagataa aatcagaata caaggaagaa agatgtacag agaagaatga agatcgtcat
      841 gcactacaca tggattacat acttgtaaac cgtgaagaaa attcacactc aaagccagag
      901 acctgtgaag aaagagaaag catagctgaa ttagaattgt atgtaggttc caaagaaaca
      961 gggctgcagg gaactcagtt agcaagcttc ccagacacat gtcagccagc ctccttaaat
     1021 gaaagaaaag gtctctctgc agagaaaatg tcttctaaaa gcgatacgag atcatctttt
     1081 gaaagccctg cacaagacca gagttggatg ttcttgggcc atagtgaggt tggtgatcca
     1141 tcactggatg ccagggactc agggcctggg tggtccggca agactgtgga gccgttctct
     1201 gaactcggct tgggtgaggg tccccagctg cagattctgg aagaaatgaa gcctctagaa
     1261 tctttagcac tagaggaagc ctctggtcca gtcagccaat cacagaagag taagagccga
     1321 ggcagggctg gcccggatgc agttacccat gacaatgaat gggaaatgct ttcaccacag
     1381 cctgttcaga aaaacatgat ccctgacacg gaaatggagg aggagacaga gttccttgag
     1441 ctcggaacca ggatatcaag accaaatgga ctactgtcag aggatgtagg aatggacatc
     1501 ccctttgaag agggcgtgct gagtcccagt gctgcagaca tgaggcctga acctcctaat
     1561 tctctggatc ttaatgacac tcatcctcgg agaatcaagc tcacagcccc aaatatcaat
     1621 ctttctctgg accaaagtga aggatctatt ctctctgatg ataacttgga cagcccagat
     1681 gaaattgaca tcaatgtgga tgaacttgat acccccgatg aagcagattc ttttgagtac
     1741 actggccatg aagatcccac agccaccaaa gattctggcc aagagtcaga gtctattcca
     1801 gaatatacgg ccgaagagga acgggaggac aaccggcttt ggaggacagt ggtcattgga
     1861 gaccaagagc agcgcattga catgaaggtc atcgagccct acaggagagt catttctcac
     1921 ggaggactta gaggatacta tggggacggt ctaaatgcca tcattgtgtt tgccgcctgt
     1981 tttctgccag acagcagtcg ggcggattac cactatgtca tggaaaatct tttcctatat
     2041 gtaataagta ctttagagtt gatggtagct gaagactata tgattgtgta cttgaatggt
     2101 gcaaccccaa gaaggaggat gccagggcta ggctggatga agaaatgcta ccagatgatt
     2161 gacagacggt tgaggaagaa tttgaaatca ttcatcattg ttcatccatc ttggttcatc
     2221 agaacaatcc ttgctgtgac acgacctttt ataagttcaa aattcagcag taaaattaaa
     2281 tatgtcaata gcttatcaga actcagtggg ctgatcccaa tggattgcat ccacattcca
     2341 gagagcatca tcaaatattg acttgaagct gaaagaaaag ccttagttgg ccatgctgga
     2401 agaag
//
```

Appendix II: Primer pairs used in semi-quantitative RT PCR

	Oligonucleotide sequence
*Human BNIPXL (full length)	Forward: 5'-CCG CTC GAG ATG AGT AAA CTG ACA TTA TCC G-3' Reverse: 5'-ATA AGA ATG CGG CCG CCT TCT TCC AGC ATG GCC AAC TAA GGC-3'
*Human BNIPXL (BCH domain)	Forward: 5'-CCG CTC GAG ATC ATT GTG TTT GCC GCC TG-3' Reverse: 5'-ATA AGA ATG CGG CCG CTC ATT TAG CTG CCT CTG ATG CTT CCC TCA G-3'
Mouse BNIPXL (full length)	Forward: 5'-ATG AGT AAG CTG ACT CTA TCG-3' Reverse: 5'-CCT CCT CCA GCA GGC CAG CTA CGG CTT-3'
Rat BNIPXL (full length)	Forward: 5'-ATG AGT AAG TTG ACT CTA TCG-3' Reverse: 5'-TCC TCC CGC AGG CCA TTA GGG CTT-3'

*Human BNIPXL primers have *Xho*I (forward) and *Not*I (reverse) restriction sites incorporated at the respective 5' ends.